THE UNIVERSITY OF ALBERTA

CONDITIONAL SIMULATION AND KRIGING AS AN AID TO OIL SANDS DEVELOPMENT : AN APPLICATION IN PART OF THE ATHABASCA DEPOSIT

by

© ROUSSOS-GEORGIOS DIMITRAKOPOULOS

A THESIS
SUBMITTED TO THE FACULTY OF GRADUATE STUDIES AND RESEARCH
IN PARTIAL FULFILMENT OF THE REQUIREMENTS FOR THE DEGREE
OF MASTER OF SCIENCE

DEPARTMENT OF GEOLOGY

EDMONTON, ALBERTA
FALL, 1985

THE UNIVERSITY OF ALBERTA

RELEASE FORM

NAME OF AUTHOR ROUSSOS-GEORGIOS DIMITRAKOPOULOS

TITLE OF THESIS CONDITIONAL SIMULATION AND KRIGING AS AN AID TO OIL SANDS DEVELOPMENT : AN APPLICATION IN PART OF THE ATHABASCA DEPOSIT

DEGREE FOR WHICH THESIS WAS PRESENTED MASTER OF SCIENCE

YEAR THIS DEGREE GRANTED FALL, 1985

Permission is hereby granted to THE UNIVERSITY OF ALBERTA LIBRARY to reproduce single copies of this thesis and to lend or sell such copies for private, scholarly or scientific research purposes only.

The author reserves other publication rights, and neither the thesis nor extensive extracts from it may be printed or otherwise reproduced without the author's written permission.

(SIGNED) R. Dimitrakopoulos

PERMANENT ADDRESS:

14 Komotinis str.
ATHENS 11526
GREECE

DATED September 16 1985

THE UNIVERSITY OF ALBERTA

FACULTY OF GRADUATE STUDIES AND RESEARCH

The undersigned certify that they have read, and recommend to the Faculty of Graduate Studies and Research, for acceptance, a thesis entitled CONDITIONAL SIMULATION AND KRIGING AS AN AID TO OIL SANDS DEVELOPMENT : AN APPLICATION IN PART OF THE ATHABASCA DEPOSIT submitted by ROUSSOS-GEORGIOS DIMITRAKOPOULOS in partial fulfilment of the requirements for the degree of MASTER OF SCIENCE.

C.D. Williams

Supervisor

Wayne H.

Frank W. Schwartz

Date Sept. 14 1985

ABSTRACT

Geostatistical modelling of reservoir variability in the Athabasca oil-sands deposit prior to either surface or *in-situ* mining can provide valuable information to guide the extraction process. Geological and engineering characteristics (variables) such as elevations of bitumen-saturated and waste (barren) zones, percentage bitumen saturation, porosity and permeability have a controlling effect on recovery methods.

Each geological variable is considered to be a particular realization of a random function defined within a geological domain. This function can be inferred from available data (boreholes) under the hypothesis of stationarity. Other realizations (models) of the same random function can then be generated using the technique of conditional simulation, which is a combination of kriging and simulated correlated variables. The statistical models of geological variables so produced are in conformity with the histogram, variogram and actual data values, and most importantly, they mimic spatial variability between sampled locations.

The key factor in geological applications of geostatistics is the translation of geological reality into mathematical abstraction. Each random statistical function is a function of the physical processes which produced the deposit, which processes in turn varied in both space and time. The deposit under study has been divided into seven

domains based on the best available geological model, and different random functions established for each variable in each domain.

Three-dimensional models describing the *in-situ* fluctuation of elevations and bitumen saturations were produced and stored as grids having 30 m horizontal and 1 m vertical resolution.

In addition, minimum variance (kriged) three-dimensional models of the same variables were constructed, stored and in-place reserve calculation was performed. These models were produced on two scales.

The large scale model covered an area of 337 km^2 on a grid of 600 m horizontal and 3 m vertical resolution. This model covered the total study area. The estimated reserves in place were calculated at 1.81 billion m^3 (11.36 billion bbl).

The small scale model covered a control area of 5.7 km^2 on a grid of 30 m horizontal and 1 m vertical resolution. The estimated in place reserves were 65.72 million m^3 (413.40 million bbl).

All constructed models can be used to examine and test various implications of the extraction process.

ACKNOWLEDGEMENTS

I would like to thank all those who directly and indirectly helped me to carry out this study. In particular, I wish to thank my supervisor, Dr. G. D. Williams, for his support, encouragement and guidelines; my co-supervisor, Prof. W. H. Griffin, who undertook the difficult task of teaching me some of the intricacies of the theory of regionalized variables as well as upgrading my computer programming skills.

I am also grateful to the Academy of Athens for supporting my studies with a small but very important scholarship; the Alberta Research Council - Alberta Geological Survey for providing me with a research grant. More specifically I would like to thank Dr. G. Mossop of the Alberta Research Council who provided considerable support through his interest on the project, as did his colleague Mr. P. Flach, who provided me with cooperation and very helpful advice on the sedimentologic and stratigraphic aspects of the Athabasca oil sands. I would also like to thank the Alberta Oil Sands Technology and Research Authority for substantially supporting my studies with a much needed and greatly appreciated scholarship.

Many thanks are also in order for the Department of Mineral Engineering and particularly to its Chairman L. R. Plitt who provided me with research and computer funds when I needed them.

Special thanks to G. MacCallum for providing acces to the data used in this study.

Dr. A. Journel and Mr. G. Luster of the Applied Earth Sciences Department, Stanford University very kindly permitted me to use their basic non-conditional simulation subroutines as well as provided me with advice on various aspects of simulation.

I am also indebted to Dr. K. Muehlenbachs for both financial and personal support at very difficult times as well as giving me the opportunity to work with him in the area of stable isotopes.

I also wish to thank my parents who provided the encouragement to undertake this study in Canada. Thanks also to my colleague, Rudy Strobl for his friendship and for helping a quite incompetent draftsman like myself. Finally, I will always be grateful to Tricia Mahon, a good and loyal friend who, in addition to being a remarkable typist which was very handy, is probably the main reason I survived two endless and vicious Canadian winters.

Table of Contents

Chapter Page

1. INTRODUCTION 1
   - 1.1 Objectives and Plan of the Project 5
   - 1.2 Previous Geostatistical Applications in the Athabasca Deposit 6
   - 1.3 The Current Modelling Philosophy 8
2. GEOLOGY OF THE ATHABASCA OIL SANDS 12
   - 2.1 Previous Work 13
   - 2.2 Regional Geology 16
   - 2.3 Stratigraphy and Depositional Environments of the McMurray Formation 20
   - 2.4 Features of the McMurray Formation within the Study Area and Delineation of the Geological Domains 24
3. THEORETICAL APPROACH TO MODELLING OF OIL DEPOSITS ..35
   - 3.1 Random Functions, Random Variables and Regionalized Variables 39
   - 3.2 Stationarity, Moments and Ergodicity 41
   - 3.3 Stochastic Structure of a Random Function and Corresponding Properties. 44
     - 3.3.1 Construction of the model variogram of a regionalized phenomenon. 45
     - 3.3.2 Robustness of the model variogram. 48
   - 3.4 Estimation Using Kriging. 49
     - 3.4.1 Remarks on the kriging system of equations. 52
     - 3.4.2 The estimation error and its distribution. 54
   - 3.5 Generation of Stochastic Fields. 55
     - 3.5.1 Simulation in one-dimension. 56

3.5.2 Simulation in three-dimensions using the turning bands method. 60

3.5.3 Remarks on the turning bands method 62

3.6 Conditional Simulation 66

4. DATA ANALYSIS AND DATA-BASE CONSTRUCTION 70

4.1 Data Evaluation 72

4.2 Simple Statistics as a Test for Homogeneity ...73

4.2.1 Data statistics in the control area 84

5. STRUCTURAL ANALYSIS OF THE ATHABASCA OIL-SANDS 92

5.1 Variography within the Large Area 93

5.1.1 Variogram evaluation on the basis of the geology of the McMurray Formation ..116

5.1.2 Fitting variogram models 117

5.2 Variography in the Small Area 123

5.2.1 Geological evaluation of the experimental variograms 130

5.2.2 Fitting the variogram models 131

5.2.3 Surface variograms in the small area ...135

5.3 Comparison of the Fitted Variograms to Known Models 143

6. MINIMUM VARIANCE MODELS 145

6.1 Modelling of the Large Area 145

6.2 Modelling of the Small Area 153

7. CONDITIONALLY SIMULATED MODELS 167

7.1 Simulation of the Surfaces 167

7.2 Non-Conditional Simulation of the Pay Zones ..169

7.2.1 Evaluation of the simulated fields 181

7.3 Conditioning of the Simulated Pay Zones 189

8. PRELIMINARY EVALUATION OF THE IN-PLACE RESERVES ...203

8.1 Definitions 203
8.2 Evaluation of the Large Area 204
8.3 Evaluation of the Small Area 213
8.4 Remarks on the Reserves Estimation 228
9. CONCLUSIONS AND SUGGESTIONS 232
9.1 The use of Conditional Simulation 232
9.2 The Improvement of Geostatistical Models 233
9.3 Future Applications and Development of Geostatistics 234
REFERENCES 236
APPENDIX 1. REGULARIZATION OF SAMPLE SIZE 245
APPENDIX 2. THE OILSAND SYSTEM 248

List of Figures

Figure 1.1: (a) Lower Cretaceous heavy oil deposits of Alberta and study area location; (b) schematic cross-section of the Western Canadian sedimentary basin..11

Figure 2.1: Correlation chart of the heavy-oil-bearing strata of the Western Canadian sedimentary basin......18

Figure 2.2: Schematic representation of outcropping facies of the McMurray Formation 21

Figure 2.3: Structure contours on the Devonian unconformity surface...................................27

Figure 2.4: Isopach of the McMurray Formation 28

Figure 2.5: Isopach of zone 1 29

Figure 2.6: Structure contours on the top of the McMurray Formation................................. 30

Figure 2.7: Surface topography in the study area..........31

Figure 2.8: Distribution of boreholes within the study area (large area) and control area (small area).......32

Figure 2.9: Stratigraphic cross-section of the McMurray Formation. Correlation and delineation of the six identified zones from well to well using gamma ray and resistivity logs 33

Figure 2.10: Stratigraphic cross-section of the McMurray Formation. Correlation and delineation of the six identified zones from well to well using gamma ray and resistivity logs 34

Figure 3.1: (a) Grouping of irregularly spaced data for experimental variogram calculation (b) Comparison of real, estimated and simulated profiles 47

Figure 3.2: The turning bands method......................63

Figure 4.1: Histograms of oil saturation according to the first classification in zones 1 (top) and 2 (bottom)..74

Figure 4.2: Histogram of oil saturation according to the first classification in zone 3.......................75

Figure 4.3: Stratigraphic cross-section A-A' of the McMurray Formation in the study area. Note that the delineation of the different zones is according to the second classification.............................77

Figure 4.4: Stratigraphic cross-section B-B' of the McMurray Formation in the study area. Note that the delineation of the different zones is according to the second classification.............................78

Figure 4.5: Histograms of oil saturation according to the second classification in zones 1 (top) and 2 (bottom)..79

Figure 4.6: Histograms of oil saturation according to the second classification in zones 3 (top) and 4 (bottom)..80

Figure 4.7: Histograms of oil saturation according to the second classification in zones 5 (top) and 6 (bottom)..81

Figure 4.8: Histogram of oil saturation according to the second classification in zone 7......................82

Figure 4.9: Histogram of oil saturation within the small area of zones 1 (top) and 2 (bottom).................86

Figure 4.10: Histogram of oil saturation within the small are of zones 3 (top) and 4 (bottom)............87

Figure 4.11: Histogram of oil saturation within the small area of zones 5 (top) and 6 (bottom)............88

Figure 4.12: Histogram of oil saturation within the small are of zone 7..................................89

Figure 5.1: Experimental variograms of oil saturation in zone 1, large area, in the E-W (top) and NE-SW (bottom) directions..................................95

Figure 5.2: Experimental variograms of oil saturation in zone 1, large area, in the N-S (top) and NW-SE (bottom) directions..................................96

Figure 5.3: Experimental and model variograms of oil saturatuon in zone 1, large area; average horizontal (top) and vertical (bottom) 97

Figure 5.4: Experimental variograms of oil saturation in zone 2, large area, in the E-W (top) and NE-SW (bottom) directions..................................98

Figure 5.5: Experimental variograms of oil saturation in zone 2, large area, in the N-S (top) and NW-SE (bottom) directions..................................99

Figure 5.6: Experimental and model variograms of oil saturation in zone 2, large area; average horizontal (top) and vertical (bottom) 100

Figure 5.7: Experimental variograms of oil saturation in zone 3, large area, in the E-W (top) and NE-SW (bottom) directions.................................101

Figure 5.8: Experimental variograms of oil saturation in zone 3, large area, in the N-S (top) and NW-SE (bottom) directions.................................102

Figure 5.9: Experimental and model variograms of oil saturation in zone 3, large area; average horizontal (top) and vertical (bottom) 103

Figure 5.10: Experimental variograms of oil saturation in zone 4, large area, in the E-W (top) and NE-SW (bottom) directions.................................104

Figure 5.11: Experimental variograms of oil saturation in zone 4, large area, in the N-S (top) and NW-SE (bottom) directions.................................105

Figure 5.12: Experimental and model variograms of oil saturation in zone 4, large area; average horizontal (top) and vertical (bottom) 106

Figure 5.13: Experimental variograms of oil saturation in zone 5, large area, in the E-W (top) and NE-SW (bottom) directions.................................107

Figure 5.14: Experimental variograms of oil saturation in zone 5, large area, in the N-S (top) and NW-SE (bottom) directions.................................108

Figure 5.15: Experimental and model variograms of oil saturation in zone 5, large area; average horizontal (top) and vertical (bottom) 109

Figure 5.16: Experimental variograms of oil saturation in zone 6, large area, in the E-W (top) and NE-SW (bottom) directions.................................110

Figure 5.17: Experimental variograms of oil saturation in zone 6, large area, in the N-S (top) and NW-SE (bottom) directions. 111

Figure 5.18: Experimental and model variograms of oil saturation in zone 6, large area; average horizontal (top) and vertical (bottom). 112

Figure 5.19: Experimental variograms of oil saturation in zone 7, large area, in the E-W (top) and NE-SW (bottom) directions......................................113

Figure 5.20: Experimental variograms of oil saturation in zone 7, large area, in the N-S (top) and NW-SE (bottom) directions......................................114

Figure 5.21: Experimental and model variograms of oil saturation in zone 7, large area; average horizontal (top) and vertical (bottom)..........................115

Figure 5.22: Experimental and model variograms of oil saturation in zone 1, small area; average horizontal (top) and vertical (bottom) 124

Figure 5.23: Experimental and model variograms of oil saturation in zone 2, small area; average horizontal (top) and vertical (bottom) 125

Figure 5.24: Experimental and model variograms of oil saturation in zone 3, small area; average horizontal (top) and vertical (bottom) 126

Figure 5.25: Experimental and model variograms of oil saturation in zone 4, small area; average horizontal (top) and vertical (bottom) 127

Figure 5.26: Experimental and model variograms of oil saturation in zone 5, small area; average horizontal (top) and vertical (bottom) 128

Figure 5.27: Experimental and model variograms of oil saturation in zone 6, small area; average horizontal (top) and vertical (bottom) 129

Figure 5.28: Experimental and model variograms of the topographic surface (top) and top of zone 1 (bottom)...137

Figure 5.29: Experimental and model variograms of the top of zone 2 (top) and top of zone 3 (bottom).......138

Figure 5.30: Experimental and model variograms of the top of zone 4 (top) and top of zone 5 (bottom).......139

Figure 5.31: Experimental and model variograms of the top of zone 6 (top) and top of zone 7 (bottom).......140

Figure 5.32: Experimental and model variograms of the bottom of zone 7.....................................141

Figure 6.1: First cross-section of the grade model of the large area.....................................147

Figure 6.2: Error map of the first cross-section. 148

Figure 6.3: Second cross-section of the grade model of the large area 149

Figure 6.4: Error map of the second cross-section 150

Figure 6.5: Third cross-section of the grade model of the large area 151

Figure 6.6: Error map of the third cross-section 152

Figure 6.7: First cross-section of the grade model of pay zone 1 in the small area 155

Figure 6.8: Error map of the first cross-section of pay zone 1 156

Figure 6.9: Second cross-section of the grade model of pay zone 1 in the small area 157

Figure 6.10: Error map of the second cross-section of pay zone 1 158

Figure 6.11: First cross-section of the grade model of pay zone 2 in the small area 159

Figure 6.12: Error map of the first cross-section of pay zone 2 160

Figure 6.13: Second cross-section of the grade model of pay zone 2 in the small area 161

Figure 6.14: Error map of the second cross-section of pay zone 2 162

Figure 6.15: First cross-section of the grade model of pay zone 3 in the small area 163

Figure 6.16: Error map of the first cross-section of pay zone 3 164

Figure 6.17: Second cross-section of the grade model of pay zone 3 in the small area 165

Figure 6.18: Error map of the second cross-section of pay zone 3 166

Figure 7.1: Variograms of the two-dimensional simulated field (top) and conditionally simulated surface topography (bottom)....................................170

Figure 7.2: Variograms of the conditionally simulated tops of zone 1 (top) and zone 2 (bottom).............171

Figure 7.3: Variograms of the conditionally simulated tops of zone 3 (top) and zone 4 (bottom).............172

Figure 7.4: Variograms of the conditionally simulated tops of zone 5 (top) and zone 6 (bottom).............173

Figure 7.5: Variograms of the conditionally simulated top of zone 7 (top) and bottom of zone 7 (bottom)....174

Figure 7.6: Simulated model of the topographic surface in the small area....................................175

Figure 7.7: Conditionally simulated model of the topographic surface in the small area................176

Figure 7.8: Minimum variance model of the topographic surface in the small area...........................177

Figure 7.9: Minimum curvature model of the topographic surface in the small area............................178

Figure 7.10: Horizontal (top) and vertical (bottom) variograms of the simulated oil saturation in pay zone 1...182

Figure 7.11: Horizontal (top) and vertical (bottom) variograms of the simulated oil saturation in pay zone 2...183

Figure 7.12: Horizontal (top) and vertical (bottom) variograms of the simulated oil saturation in pay zone 3...184

Figure 7.13: Horizontal (top) and vertical (bottom) variograms of the conditionally simulated oil saturation in pay zone 1..............................185

Figure 7.14: Horizontal (top) and vertical (bottom) variograms of the conditionally simulated oil saturation in pay zone 2..............................186

Figure 7.15: Horizontal (top) and vertical (bottom) variograms of the conditionally simulated oil saturation in pay zone 3..............................187

Figure 7.16: First cross-section of the conditionally simulated pay zone 1...................................191

Figure 7.17: Pay zone 1. First cross-section of the small area model using conditionally simulated boundaries and kriged grades..........................192

Figure 7.18: Second cross-section of the conditionally simulated pay zone 1...................................193

Figure 7.19: Pay zone 1. Second cross-section of the small area model using conditionally simulated boundaries and kriged grades..........................194

Figure 7.20: First cross-section of the conditionally simulated pay zone 2...................................195

Figure 7.21: Pay zone 2. First cross-section of the small area model using conditionally simulated boundaries and kriged grades........................196

Figure 7.22: Second cross-section of the conditionally simulated pay zone 2.................................197

Figure 7.23: Pay zone 2. Second cross-section of the small area model using conditionally simulated boundaries and kriged grades........................198

Figure 7.24: First cross-section of the conditionally simulated pay zone 3.................................199

Figure 7.25: Pay zone 3. First cross-section of the small area model using conditionally simulated boundaries and kriged grades........................200

Figure 7.26: Second cross-section of the conditionally simulated pay zone 3.................................201

Figure 7.27: Pay zone 3. Second cross-section of the small area model using conditionally simulated boundaries and kriged grades........................202

Figure 8.1: Isopach of the overburden in the large area...207

Figure 8.2: Isopach of pay zone 1 in the large area......208

Figure 8.3: Isopach of barren zone 1 in the large area...209

Figure 8.4: Isopach of pay zone 2 in the large area......210

Figure 8.5: Isopach of barren zone 2 in the large area ..211

Figure 8.6: Isopach of pay zone 3 in the large area 212

Figure 8.7: Minimum variance isopach of the overburden in the small area...................................216

Figure 8.8: Conditionally simulated isopach of the overburden in the small area.........................217

Figure 8.9: Minimum variance isopach of pay zone 1 in the small area.....................................218

Figure 8.10: Conditionally simulated isopach of pay zone 1 in the small area.................................219

Figure 8.11: Minimum variance isopach of barren zone 1 in the small area...................................220

Figure 8.12: Conditionally simulated isopach of barren zone 1 in the small area............................221

Figure 8.13: Minimum variance isopach of pay zone 2 in the small area.....................................222

Figure 8.14: Conditionally simulated isopach of pay zone 2 in the small area.................................223

Figure 8.15: Minimum variance isopach of barren zone 2 in the small area...................................224

Figure 8.16: Conditionally simulated isopach of barren zone 2 in the small area............................225

Figure 8.17: Minimum variance isopach of pay zone 3 in the small area.....................................226

Figure 8.18: Conditionally simulated isopach of pay zone 3 in the small area.................................227

Figure 8.19: Polygons drawn in section 6342600 m Northing..229

Figure 1: Histogram of the lengths of the original weight % oil samples...............................247

Figure 2: Flow-diagram of OILSAND (OS) system............250

List of Tables

Table 4.1: Summary statistics of the % bitumen for each zone in the large area..................................83

Table 4.2: Summary statistics of the % bitumen for each zone in the small area..................................90

Table 4.3: Summary statistics of the elevations of the zones tops and bottoms in the small area, and average thickness..................................91

Table 5.1: Summary of the weight % oil saturation average horizontal model variograms in the large area..................................120

Table 5.2: Summary of the weight % oil saturation vertical model variograms in the large area..........121

Table 5.3: Summary of the weight % oil saturation average horizontal model variograms in the small area..................................132

Table 5.4: Summary of the weight % oil saturation vertical model variograms in the small area..........133

Table 5.5: Summary of the zones tops and bottoms model variograms in the small area........................141

Table 7.1: Summary statistics of the conditionally simulated elevations of the zones tops and bottoms in the small area..................................179

Table 8.1: Area, perimeter, volume, and average thickness of the zones in the large area.............205

Table 8.2: Volumes, in-place bitumen and strip ratios of the pay zones in the large area......................206

Table 8.3: Area, perimeter, volume and average thickness of the zones in the small area......................214

Table 8.4: Volumes, in-place bitumem and stripping ratios of the pay zone in the small area.............215

Table 8.5: Volume, grade and error integration using the polygons of section 6342600 m Northing...............231

1. INTRODUCTION

An immense volume of heavy oil sands is present in five main areas in the Lower Cretaceous of the western Canadian sedimentary basin (Figure 1.1) and at shallow depths near the up-dip edge of the basin. These are the Peace River, Wabasca, Cold Lake, Lloydminster and Athabasca deposits. The Athabasca deposit is the largest and is one of the world's largest self-contained accumulations of hydrocarbons with estimated global reserves of 922 billion barrels (Outtrian and Evans, 1978), and is therefore at least 6 times larger than the giant oil field Ghawar of Saudia Arabia. Clearly, this incredible petroleum storage not only adds significant resources to the international energy supply but also, and more importantly, its efficient exploitation can lead Canada to energy self sufficiency and provide an ongoing basis for further economic growth.

In the Athabasca area almost 90 percent of the oil sands are too deeply buried to be considered potentially recoverable by established surface mining techniques. The characteristics of significance such as oil saturations, porosity, permeability, thickness, boundary locations and others, even within a small part of the deposit, lack homogeneity. Therefore, in both in-situ recovery and surface mining, advance analyses and geostatistical modelling are designed to investigate the distribution of these non-homogeneous characteristics and will provide the basis for more and profitable oil recovery. It is theoretically possible to obtain all the required resolution specific to a deposit or orebody through drillhole spacing of a few tenths of a metre, but the cost of such an operation is so staggering that it is most likely it will largely exceed any profits generated by eventual extraction of the oil or metal. Clearly, it is in the best interests of efficiency and profitability to search for probabilistic techniques which will assist in constructing a model by representing, as accurately as possible, the characteristics of the potential deposit by utilizing information from more widely-spaced drillholes. The model can then serve effectively as the basis for further development and successful exploitation.

The purpose of this study is to contribute to the development of the exploitation procedures of the Athabasca deposit by demonstrating the value of geostatistics in oil sands applications. (It is necessary to clarify, at this point, that the term 'geostatistics' is used throughout this study in its European sense of the 'Theory of Regionalized Variables', developed by Georges Matheron and co-workers at the Centre du Morphologie Mathematique at Fontainebleau, France.) This study will also discuss the philosophy behind geostatistics, how it must be applied in order to incorporate the available geological information (geological model) to the geostatistical model and thus produce more realistic and accurate models to represent, spatially, all the variables of relevance. Specifically, this study will deal with the technique of conditional simulation (Matheron, 1973; Journel, 1974a, 1974b).

Conditional simulation is the geostatistical method which, with given data from available control points, assigns simulated values of the characteristics of interest (regionalized variables) to a grid of points with the desired density so that the simulated variable, while reproducing the known information at the sample locations, also mimics faithfully the spatial variability between sample locations. This technique, which is a combination of kriging (objective analysis) and simulation of correlated variates, provides models of the characteristics under investigation in conformity with the histogram, spatial variability (variogram) and actual values at locations sampled.

The key factor in the conditional simulation technique is its maximum respect to the spatial quality variability (fluctuation), although one might ask what the difference might be if, instead, an estimation technique such as kriging was used. Kriging can certainly provide, under adequate geological control, the best minimum variance, linear and unbiased estimate (BLUE) of the mean. Means, however, are smoothed reality and spatial variability is lost. Accordingly, simulation and estimation have two different objectives. In the case, for example, of the Athabasca oil sands development, kriging estimation can assign mean grade values in blocks and provide the model for the reserves estimation with a minimum known variance. However, only conditional simulation can reconstruct models which mimic reality, thus representing the fluctuations of the ore grade among mining units. It is the grade fluctuation as well as the means that control the efficiency of mining operations, be they extractive or in-situ. In addition to a numerical model of the spatial variability of grades the variabilities of boundaries of the mineralisation(s) are vital to rational exploitation. These boundaries can also be conditionally simulated to provide planners and operators with reliable 'what if' tools.

Conditional simulation models representing characteristics of an oil sand deposit can also be of value to in-situ recovery schemes. A three dimensional model, for example, representing the variability of permeability (from core data) can reveal possible paths that the steam of a steam injection will most likely follow.

One must never forget, however, that any conditional simulation model can mimic reliably the real case only insofar as the geological hypothesis and the data on which it is based are accurate portrayals. It must be continually recognized that both the subjectivity of the geological interpretation, which is the basis for the model and guides the geostatistical analysis, as well as the quality of the data, will determine the numerical resolution of the model.

1.1 Objectives and Plan of the Project

The primary objective of this study is to simulate variables, such as upper and lower elevations of ore intervals, and oil saturations (grade) using the conditional simulation technique as well as to estimate reserves in place using the technique of kriging (objective analysis) in a specific part of the Athabasca oil sand deposit (Twp. 94-96, Rge. 11-12 W4M). This study specifically includes (a) geological and geostatistical analysis (variogram estimation) of all pertinent variables in the deposit in order to define geologically its boundaries and match the statistical model to the geological model; (b) in-place reserves estimation and error analysis of the estimation of (a); (c) conditional simulation in three dimensions of the deposit boundaries, and oil saturation based on the model established in (a). The specific plan of work was as follows:

1. The geologically homogeneous oil sand zones within the above-noted area were defined, correlated and numerically mapped.

2. The bitumen percentage from core for each zone was identified and individual bitumen percentage statistics were estimated. These statistics were then measured against known models (Grasley, 1982).

3. Using the statistics derived in point #2, bitumen percentage values were estimated together with associated estimation error and a block model of the deposit was

created. Individual block dimensions were 3 m vertical and 600 m horizontal. Global bitumen percentages in-place were estimated.

4. A higher resolution block model for a 5.7 km^2 sub-area (control area) was constructed to test the statistics used in point #3. Bitumen percentages were estimated and the estimation error was calculated. Individual blocks were 1 m vertical and 30 m horizontal.

5. The positions of the geological boundaries in the control area were conditionally simulated and the results were used to illustrate the interaction between the variabilities of boundary positions and estimated grade.

6. The in-place bitumen percentages for the sub-area in point #4 were then conditionally simulated.

7. Point #6 was integrated and compared with point #3 for cross-validation of the mean using the methods in point #2 for validation of variability.

1.2 Previous Geostatistical Applications in the Athabasca Deposit

Applications of the theory of regionalized variables in the Athabasca and other oil sand accumulations are very limited in the current geostatistical literature. In addition, the existing studies (Zwicky, 1975, 1979; Dowd and Royle, 1977) deal primarily with the first step of any geostatistical study which is the structure of the regionalized variables chosen (variogram estimation).

Zwicky's (1975,1979) work, in particular, deals with the estimation of variograms such as 'pay thickness', 'reject thickness', 'grade' and an economic parameter called 'quality factor' in a section of the Athabasca oil sands. In his first paper (Zwicky, 1975), the characteristics selected as regionalized variables were used to determine whether the data density was sufficient to locate the major ore bodies and estimate global reserves. In his second paper, (Zwicky, 1979), the significance of the variograms was discussed and examples given.

Dowd and Royle (1977) discuss the construction, analyses and verification of variogram models (geostatistical structural analysis) of regionalized variables such as 'percent saturated weight of oil', 'percent saturated weight of water', 'percent saturated weight of solids' and 'minimum porosity' in a section of the Athabasca oil sands. Their paper concludes with a short discussion of the estimation of in place reserves in the area.

Dowd and Royle (1977) demonstrate a different conceptual approach in terms of applied geostatistics from that used by Zwicky (1975, 1979). The difference consists in that the domains (or regions) within which the regionalized variable(s) is distributed, are first defined by Dowd and Royle (1977). Accordingly, the investigated part of the deposit is divided into different zones in a vertical sense, giving to the estimated variograms a 'meaning' with respect to the way that these regions are selected. There is no indication, in Dowd and Royle's paper, however, on what the definition of these domains is based. It is apparent that if their definition is arbitrary or erratic with respect to the geological facts, so the concluded geostatistical analysis will be misleading.

From the oil industry, the only private report on geostatistics available to us is that of Grasley (1982). Like earlier studies, this study also dealt with variogram estimation of the regionalized variable, 'weight percent oil' in a part of the Athabasca oil sands. Grasley (1982) indicated that the definition and delineation of different domains are controlled by the geological process leading to their formation. More importantly, Grasley's work clearly indicates that the application of geostatistical analyses is basically a problem in geology.

1.3 The Current Modelling Philosophy

In the geostatistical context, a variable distributed within pre-defined space (geometric field, Matheron, 1963) is said to be 'regionalized'. In the same context, this variable has a fundamental property in that its values in different locations are not independent (as in classical statistics) but are correlated, and this correlation is a function of distance. Such a variable is usually a characteristic of a certain phenomenon, such as oil saturation is, for example, a characteristic of an oil deposit. It becomes apparent than an intermingling of the same characteristics from different phenomena could only lead to an erroneous conclusion. Therefore, it is of primary importance, particularly in cases of marked lack of homogeneity of the characteristics of the deposit under development, to investigate the possibility of coexistance of independent phenomena and, should they exist, to distinguish and accordingly use them in geostatistical analysis.

A deposit of almost ideal lack of homogeneity is the Athabasca oil sands; the distribution, configuration and oil saturation of the individual bitumen accumulations within the host McMurray Formation are controlled by the grain size distribution, permeability and porosity in the host sediment. Furthermore, these parameters are direct functions of the different depositional environments and facies of the McMurray sediments. Thus, any geostatistical analysis of the characteristics of the Athabasca oil sands must be based on a geological interpretation of the depositional setting of the McMurray Formation (geological model) which will ultimately serve as the basis for defining and delineating the different geological domains within which the selected regionalized variables must be examined.

It is important to conclude this chapter by reiterating that the subjectivity of the geological interpretation has to be introduced to the geostatistical model and unfortunately, there is no statistical probability theory which can finally evaluate such an interpretation. Our only indication of mixing of different depositional environments can sometimes be determined by the bimodal shape of a simple histogram of the variable examined. In conclusion, good geological control is the basis for a robust geostatistical model but it is only successful in-situ recovery and mining that can ultimately verify the accuracy of the model.

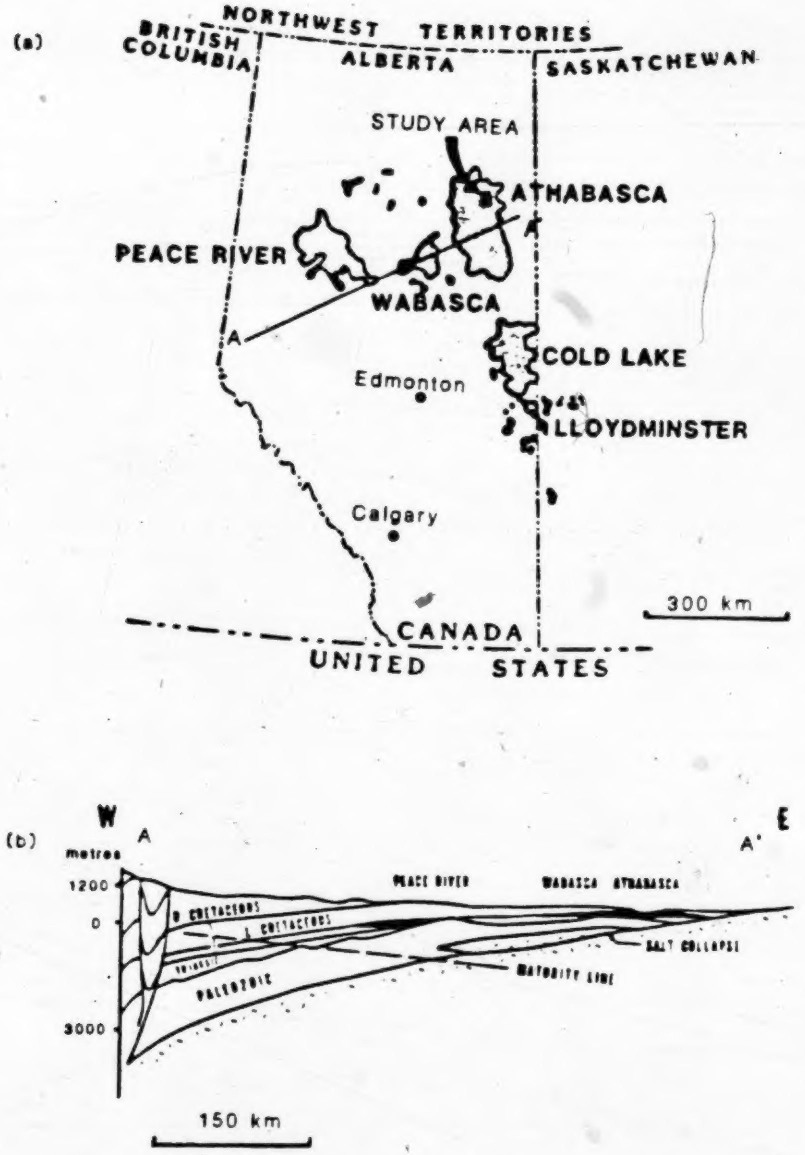
(a)
NORTHWEST TERRITORIES
BRITISH COLUMBIA
ALBERTA
SASKATCHEWAN
STUDY AREA
ATHABASCA
A'
PEACE RIVER
WABASCA
A
COLD LAKE
Edmonton
LLOYDMINSTER
Calgary
300 km
CANADA
UNITED STATES
(b)
W
A
E
A'
metres
1200
0
3000
PEACE RIVER
WABASCA ATHABASCA
U CRETACEOUS
L CRETACEOUS
TRIASSIC
PALEOZOIC
SALT COLLAPSE
MATURITY LINE
150 km

Figure 1.1 (a) Lower Cretaceous heavy oil deposits of Alberta and study area location; (b) schematic cross-section of the Western Canadian sedimentary basin (adapted from Demaison, 1977).

2. GEOLOGY OF THE ATHABASCA OIL SANDS

The Athabasca oil sands are located in the northeastern part of Alberta, adjacent to the valley of the Athabasca River. They cover an area of 26,000 square kilometres (Twp. 77-102, Rge. 6-21 W4M) and crop out in the valleys of the Athabasca River and its tributaries north of the town of Fort McMurray. The heavy bitumens (API gravities 8° - 10°, viscosity 10^6 centipoise at 10° C) are trapped within the sediments of the McMurray Formation which were deposited during Early Cretaceous (Aptian-Albian) time.

The McMurray Formation comprises 35 to 70 m of uncemented quartz sand and associated shale. It demonstrates high porosities (20-30 percent) and permeabilities (up to 5,000 milidarcies) as well as high bitumen saturations (commonly 10-18 weigh percent oil). Very little post-depositional textural change is present in the McMurray sediments indicating that porosity/permeability patterns in the reservoir can be viewed as direct functions of the sedimentary facies distribution (Mossop, 1980) and thus, the depositional setting controls the bitumen saturations and distribution. The study area (Figure 1.1) of this project is a section of the surface mineable region of the Athabasca deposit and extends over an area of about 140 km^2 (Twp. 64-66, Rge. 11-12 W4M).

2.1 Previous Work

Since 1788, when Peter Pond saw and reported on the bitumen-bearing sands outcropping along the Athabasca River, the Athabasca oil sands have been the subject of continual investigation and, at times, of vigorous controversy.

An extensive presentation and discussion of the work related to several aspects of the Athabasca oil sands geology up to 1965 can be found in Conybeare (1966). The list of earlier studies and their contributions can be completed with a bibliography in Carrigy (1962). For this reason, we will mainly concentrate on the researchers and their conclusions during the past two decades.

For historical reasons, we would like to mention the geological information given by Richardson (in Franklin, 1828), who believed the oil sands were of Devonian age. The McMurray Formation, however, was later defined, described and correlated with the lower Luscar Formation of west-central Alberta by McLearn (1917).

The most comprehensive survey of the geology of the McMurray area is that of Carrigy (1959a), in which there is a full account of the stratigraphy and depositional context as well as a formal designation of the type sections. Subsequent work is founded upon this report, including petrology (Carrigy, 1959b, 1962, 1963a, 1963b, 1966), heavy mineral assemblages and provenance (Carrigy, 1963a, 1963b, 1966), sedimentary structures (Carrigy, 1963a, 1967) and depositional environments (Carrigy, 1971, 1973).

The recognition, during the last decade, of the importance of the depositional setting of the McMurray sediments on the control of the bitumen saturation and distribution led to detailed facies studies and reconstruction of depositional processes. Most of the results are contained in Mossop (1976, 1978, 1980a, 1980b), Flach (1977), Mossop and Flach (1978, 1983, 1984), James (1977), James and Oliver (1978), Nelson and Glaister (1978), Stewart and MacCallum (1978), Stewart (1981), and Rennie (1983, 1984). There is, however, some controversy about the depositional interpretation of the McMurray Formation and particularly the middle part of it, with the above investigations suggesting environments from fluvial to estuarine to deltaic. Trace fossil studies (Pemberton *et al.*, 1982) do not seem to resolve the situation, but they suggest the influence of salt water on the upper parts of the formation.

Structural aspects of the Cretaceous strata in the McMurray area are discussed and described in detail by Martin and Jamin (1963) and Vigrass (1968). These authors, as well as Stewart (1963), describe the paleogeomorphology and recent structure of the sub-Cretaceous unconformity at the top of the Devonian limestones, underlying the McMurray sediments.

In addition to the studies on the geology of the McMurray Formation, the question of scientific interest which many researchers attempted to answer was, and for some still is, 'where did the bitumen come from?' The answers given to this problem can be formulated as follows: (a) escape through fissures from Devonian reservoirs (Link, 1951; Sproule, 1951); (b) in-situ formation from organic material deposited with the sand (Hume, 1951; Corbett, 1955) or the associated argillaceous sediments (Montgomery et al., 1974); (c) derivation from materials leached from soils to the reservoir and conversion to heavy hydrocarbons (Hodgson and Hitchon, 1965); (d) up-dip migration of light oils from the deeper parts of the basin and subsequent alteration to heavy bitumen (Vigrass, 1968; Hitchon, 1963; Gussow, 1956). Geochemical investigations of the heavy oils and correlation with oils from other deposits within the basin (Deroo et al., 1977, Derro et al., 1974) strongly support the last theory. The same studies, as well as Jardine (1974), demonstrate biodegradation to be the main factor in their alteration after migration/entrapment.

Finally, reserves estimation studies using traditional techniques (isopachs etc.) have been attempted, either globally or locally. Pow et al. (1963) estimate that the Athabasca deposit contains 626 billion barrels. Stewart (1963) estimates that it contains 560 billion barrels. Currently, the in-place reserves are estimated at 922 billion barrels (Outtrian and Evans, 1978).

Local estimation studies, particularly in the northern part of the Athabasca deposit (Gregoire Lake area), were undertaken by Benthin and Orgnero (1977) and Steinmetz

(1976) who applied a Monte Carlo method to produce and predict the probability distribution of total thickness values.

2.2 Regional Geology

The Athabasca oil sands deposit is located in the Lower Cretaceous sediments of the up-dip edge of the Western Canadian sedimentary basin which occupies Alberta and part of British Columbia. Under the Plains, the basin appears as a nearly featureless, gently west-dipping homocline (Figure 1b), classified as 'foreland basin' (Halbouty et al., 1970; Klemme, 1975) or 'foredeep basin' (Bally, 1975). This homocline is locally warped by the mild deformation of the Peace River Arch (Stelck, 1975) with which the Athabasca deposit is associated (Demaison, 1977).

The Lower Cretaceous strata of the basin represent most of the epoch, and all stages are presented with the exception of the Neocomian (Rudkin, 1964). These strata are divided into the Mannville Group in which the oil sand deposits occur (Figure 2.1), and include at the top the lower part of the Colorado Group. They are divided from the Upper Cretaceous sediments by the Base of Fish Scales lithologic marker.

The Mannville Group is divided into two units with time-rock significance (Williams, 1960, 1963; Rudkin, 1964). The Lower Mannville is primarily a basal fill deposit and the Upper Mannville, an equally divided marine/non-marine clastic sequence. In late Jurassic time, Western Canada was uplifted and the Jurassic Sea was expelled (Williams and Stelck, 1975). A long period of non-deposition and erosion followed which resulted in the development of gently undulating erosional surfaces mainly on the Upper Paleozoic carbonates and shales until Early Cretaceous time when non-marine clastic sedimentation occurred. Two sources for these sediments existed. In the west, the Nelson and Cassiar-Omineca batholiths, emplaced during the late Jurassic, continued their uplift during early Cretaceous time, providing a western source of detrital sediments. At the same time the Canadian Shield provided an eastern source of sediments. These sediments, which were mainly sands filling in most of the irregularities on the erosional surface, represent dominantly fluvial environments with the exception of marine shales occurring in northern Alberta, where the early Cretaceous Arctic or Boreal Sea transgressed into the area. The end of the Lower Mannville depositional episode was marked by deposition of the marine Wabiskaw and Bluesky sands by the advancing Boreal Sea. Continuation of subsidence allowed the Boreal Sea to advance further into northern and central Alberta, forming a tongue of marine shales represented today by the Clearwater and Spirit River Formations. At the end of Mannville time, further transgression of both Gulfian and Boreal Seas resulted

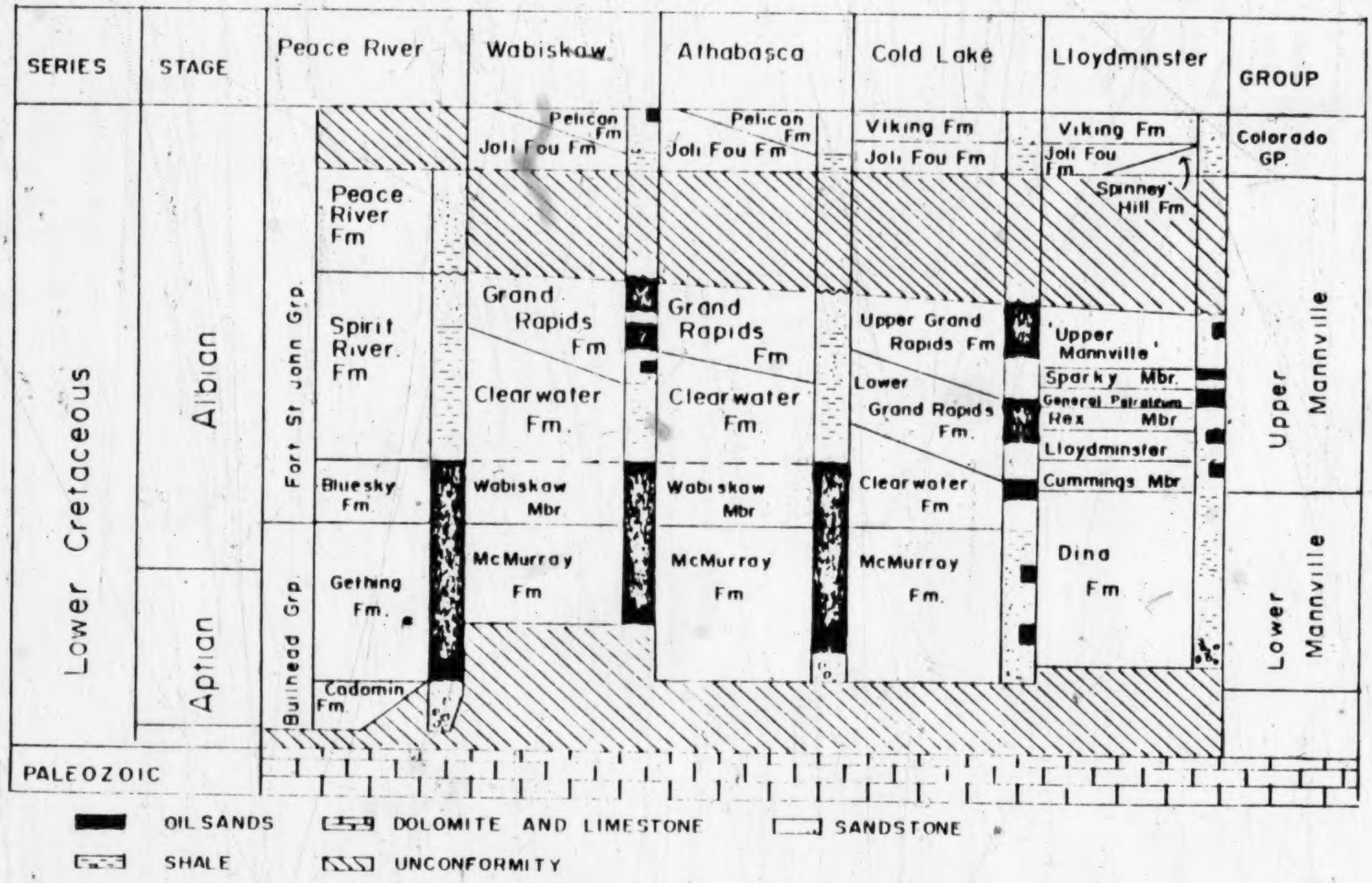
SERIES
STAGE
Peace River
Wabiskaw
Athabasca
Cold Lake
Lloydminster
GROUP
Lower Cretaceous
Albian
Aptian
PALEOZOIC
Fort St John Grp.
Bullhead Grp.
Peace River Fm
Spirit River Fm
Bluesky Fm
Gething Fm.
Cadomin Fm.
Pelican Fm
Joli Fou Fm
Grand Rapids Fm
Clearwater Fm.
Wabiskaw Mbr
McMurray Fm
Viking Fm
Upper Grand Rapids Fm
Lower Grand Rapids Fm.
Clearwater Fm
McMurray Fm.
Spinney Hill Fm
'Upper Mannville'
Sparky Mbr.
General Petroleum
Rex Mbr
Lloydminster
Cummings Mbr
Dina Fm
Colorado GP.
Upper Mannville
Lower Mannville
OIL SANDS
DOLOMITE AND LIMESTONE
SANDSTONE
SHALE
UNCONFORMITY

Figure 2.1 Correlation chart of the heavy-oil-bearing strata of the Western Canadian sedimentary basin.

6

in the formation of an epicontinental ocean in which the predominantly shaly Upper Cretaceous sediments were laid down.

In many of the coarser-grained sediments giant heavy oil deposits occur near the margin of the basin in the Peace River, Wabasca, Cold Lake, Lloydminster and Athabasca areas (Figure 2.1). Similar factors which led to their formation are: (a) the presence of adequate volumes of thermally-mature organic-rich rocks, such as the argillaceous sediments within the Cretaceous, predominantly within the Mannville Group, in deeper parts of the basin (Deroo et al., 1974, 1977); (b) a widespread regional cap, mostly marine shales, such as the Clearwater and Spirit River Formations, which restrained vertical fluid escaping from the underlying permeable and porous sediments and led fluid laterally to the edge of the basin; (c) the regional gently-dipping homocline structure of the basin, a favourable feature in enhancing up-dip fluid migration, in combination with both stratigraphic traps and local reversals of the slope near the margin of the basin (Demaison, 1977); (d) subsequent to the entrapment, alteration, including mainly biodegradation as well as water-washing, inorganic oxidation and secondary migration/deasphalting (Deroo et al., 1974, 1977).

2.3 Stratigraphy and Depositional Environments of the McMurray Formation

Informally, the McMurray Formation in the Athabasca area, is divided into three members (Carrigy, 1971, 1973; Flach, 1977; Mossop and Flach, 1983) which are depicted in Figure 2.2. The lower member, consisting of poorly sorted sands, conglomerate, clay breccias, dark grey organic shales, silts and coals (Carrigy, 1973; Flach, 1977; Mossop, 1978b; James and Oliver, 1978) extends over a limited area, lying unconformably on the undulating eroded Devonian limestones. It is acknowledged in most studies to be of fluvial origin (Carrigy, 1971; Jardine, 1974; Flach, 1977; Stewart, 1981) but Rennie (1983, 1984) intepreted it as a delta marsh deposit with early fluvial remnants in places.

The middle member, fully described in outcrops and mine face exposures (Mossop and Flach, 1983), exhibits two main facies. In the lower part, it consists of thick-bedded sand characterized by large-scale trough cross-sets, averaging 1 m in thickness, of moderately to well-sorted, fine grained quartz with some shale components in the form of interclastic breccias. This facies has a sharp erosional base, but at the top it transitionally grades into and interdigitates with the beds at the base of the overlying epsilon cross-stratified facies. Sets of epsilon cross-stratified facies average 15 m in thickness with the surfaces dipping an average 10°. The sloping strata

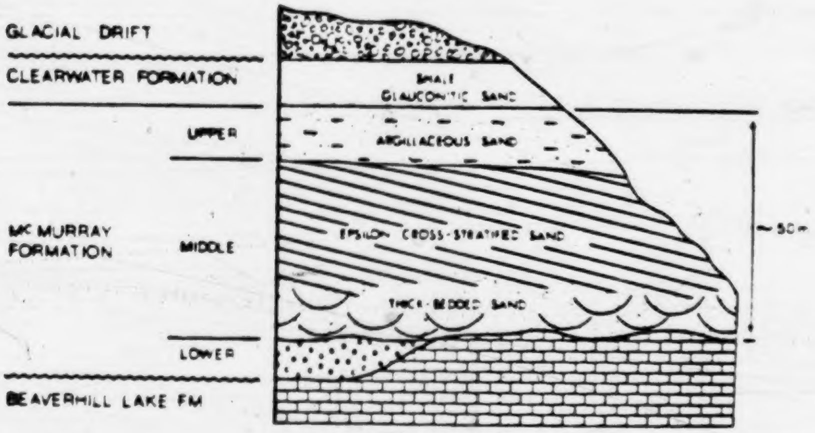
GLACIAL DRIFT
CLEARWATER FORMATION
SHALE
GLAUCONITIC SAND
UPPER
ARGILLACEOUS SAND
McMURRAY FORMATION
MIDDLE
EPSILON CROSS-STRATIFIED SAND
~50m
THICK-BEDDED SAND
LOWER
BEAVERHILL LAKE FM

Figure 2.2 Schematic representation of outcropping facies of the McMurray Formation (adapted from Mossop and Flach, 1983)

consist of decimetre-to metre-thick beds of fine to very fine-grained sand, separated by partings of argillaceous silt 2-5 cm thick which increase in abundance towards the top of the set. Tabular clay-walled burrows exist mostly in the upper part of the epsilon cross-sets, decreasing in abundance towards the bases (Pemberton et al., 1983).

The depositional environment of this middle member on the basis of its scoured base, its upward-fining character, the upward decrease in the scale of the cross-bedding, and the continuity from the thick bedded sands into the epsilon-cross strata, indicating the synchronous nature of the facies and paleocurrent directions, is intepreted as lateral accretion deposits of very deep sinuous channels. Particularly, the thick-bedded sand facies represents sedimentation by large bed forms deep in the channel while the epsilon cross-strata resulted from the lateral accretion of the point bar of the same channel. In the epsilon cross-strata, the sand beds are interpreted as having been deposited during flood stages and the shale from suspended load fall-out during times of low discharge (see Mossop and Flach, 1983 for details).

The same facies are also recognizable in the subsurface with the addition of mud dominated ones, which generally do not crop out. Subsurface control indicates that these shaly and interbedded sandstone-shale sequences, up to 30 metres thick and laterally very extensive, exist adjacent to channel deposits. These fine grained sediments are thought to have been deposited in shallow, long-standing lakes and brackish bays which existed contemporaneously with large meandering channels (see Flach and Mossop, 1985 for detailed discussion).

A sequence of horizontally bedded sands and muds above the dipping epsilon cross-strata of the middle member constitutes the upper member. It varies in thickness from 15 to 30 metres and is composed of bioturbated, argillaceous sands and shales. Lithologies of these facies are consistent with floodplain deposition, with coals marking development of swamps, and ironstones denoting relative stillstands in sedimentation (Mossop and Flach, 1983). Marine influence is present in this upper member; particularly in the subsurface and especially in the northern part, upward-coarsening units are interpreted as offshore marine bars. Further north and also at the top of the unit, open marine conditions and glauconite is present (Flach and Mossop, 1985).

The interpretation of the depostional setting of the middle and upper members of the McMurray Formation is controversial. Carrigy (1971, 1973) envisioned the units as the forset and topset beds of a Gilbert-type delta, building into a standing body of brackish water. Flach and Mossop (1985) however, point out that the formation is not 'deltaic', for it demonstrates an upward-fining character grading from fluvial at the base to marine at the top. This is unlike a progradational delta complex, which is upward-coarsening, from marine at the base to continental at the top. The same authors also note that the gradual aggradation of the existing channel system is not in agreement with the required channel system progradation into the standing water body of Carrigy's models.

The other interpretation of the middle and upper members is that of 'estuarine' (Stewart and MacCallum, 1978; Stewart, 1981; Rennie, 1983, 1984). Flach and Mossop (1985) reject this interpretation.

An extensive discussion of the subsurface facies of the McMurray and their interpretation can be found in Flach and Mossop (1985). The results of this study, briefly discussed above, will constitute the geological model for our study for it provides the most realistic and well-documented interpretation of the depositional environments of the formation.

2.4 Features of the McMurray Formation within the Study Area and Delineation of the Geological Domains

In the study area, the McMurray Formation consists of about 70 m of oil saturated sands and shales. These sand and shales overlie the sub-Cretaceous unconformity surface, the topography of which is depicted in Figure 2.3. Evident in Figure 2.3 are local structural highs and lows due to post-unconformity collapse of Devonian limestones. This collapse was the result of the partial solution of the underlying the Devonian salt beds in the Elk Point Evaporites (Carrigy, 1971; Stewart, 1963). Similar features on the Devonian surface can be identified in figure 2.4, which presents an isopach map of the McMurray Formation.

The lower member of the formation exists only in parts of the area, and particularly in structural lows. The middle and upper members exist over the whole study area, although in the southeastern part, the upper member is partly removed by erosion (Figure 2.5). The present structure of the McMurray top as well as the surface topography are depicted in figures 2.6 and 2.7 respectively.

Within the study area, and on the basis of the depositional environments already discussed, six different zones (geological domains) were identified using geophysical logs from 306 wells (Figure 2.8). These geological domains are shown in cross sections in figures 2.9 and 2.10, using the Clearwater Formation as a datum.

The lower McMurray, occurring only in part of the area, is divided into three zones. The lowest (zone 6) includes the water-bearing sands below the oil/water contact of the reservoir, the shaly facies and conglomerates with very low oil saturation in places. The reason that these facies are mixed is that all are of no economic interest and further division would only increase computational time. Zone 5 includes oil saturated channels and adjacent overbank muds and where it exists, its average thickness is 8 to 10 metres. Major oil sand bodies appear to exist in this zone. The upper shaly phases of the lower McMurray are included in zone 4 which, in places, also includes shaly phases of the very lower part of the middle member, below thick, oil saturated sands. The reason for this mixing is the same as for zone 6.

The middle McMurray facies (thickness 30-40 m), deep channels and the associated muds and abandoned channels are included in zone 3, where the main ore body appears to exist.

Zone 2 includes the non-marine facies of the upper member. It averages a thickness of 15 - 25 metres and scattered bitumen accumulations appear to exist. The marine facies, offshore bars and open marine deposits of the upper member are included in zone 1. In Figure 2.5, an isopach of zone 1, a bay-like invasion of the sea in the northern part of the area marks the beginning of the transgression of the Boreal Sea. In the southeast part of the area, as can be seen from the same figure, the sediments of zone 1 have been eroded .

The identified tops and bottoms of the 5 selected zones, after they have been traced in individual boreholes, as well as the surface elevations, were entered in the computer and three-dimensional grids were produced representing the six different domains into which the study area was at first divided.

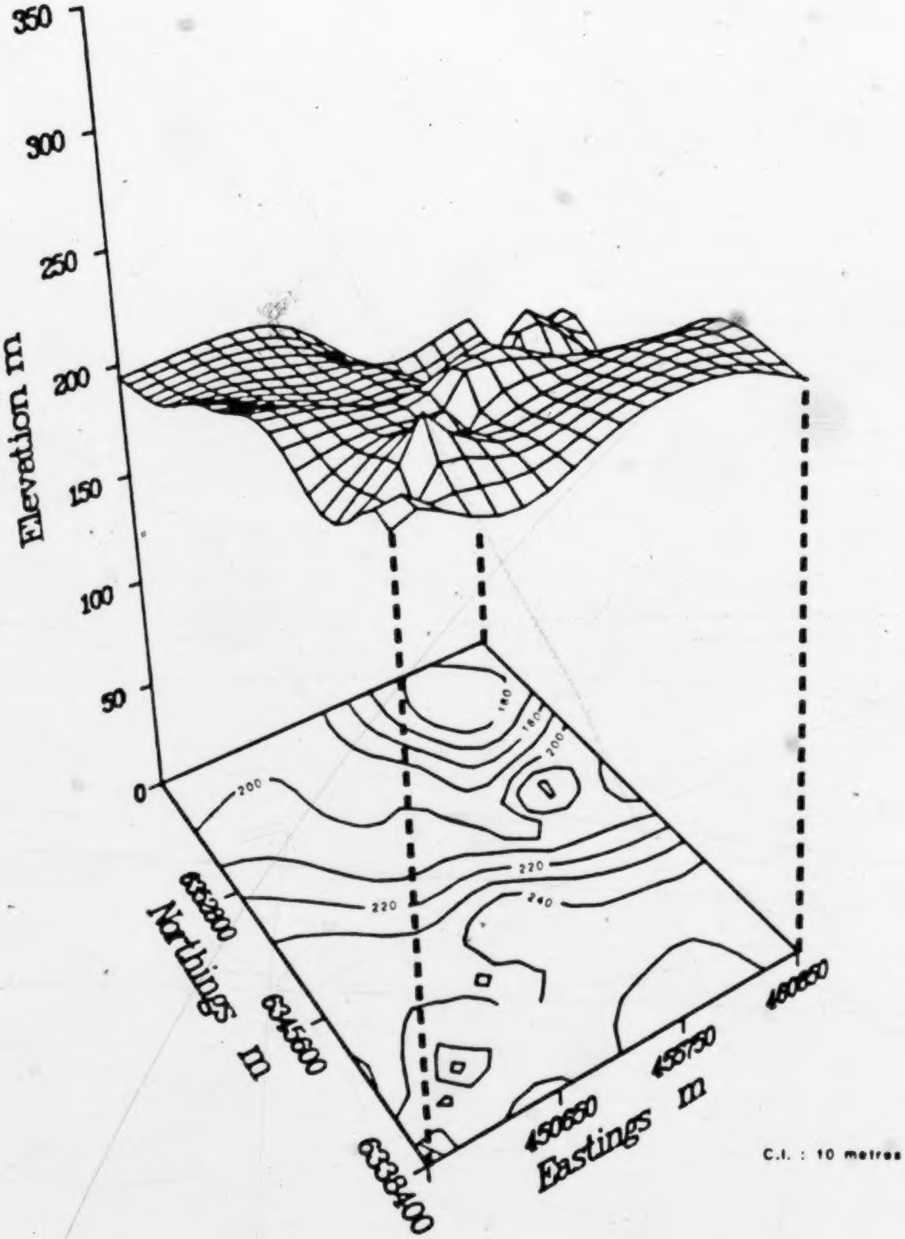

Figure 2.3 Structure contours on the Devonian unconformity surface.

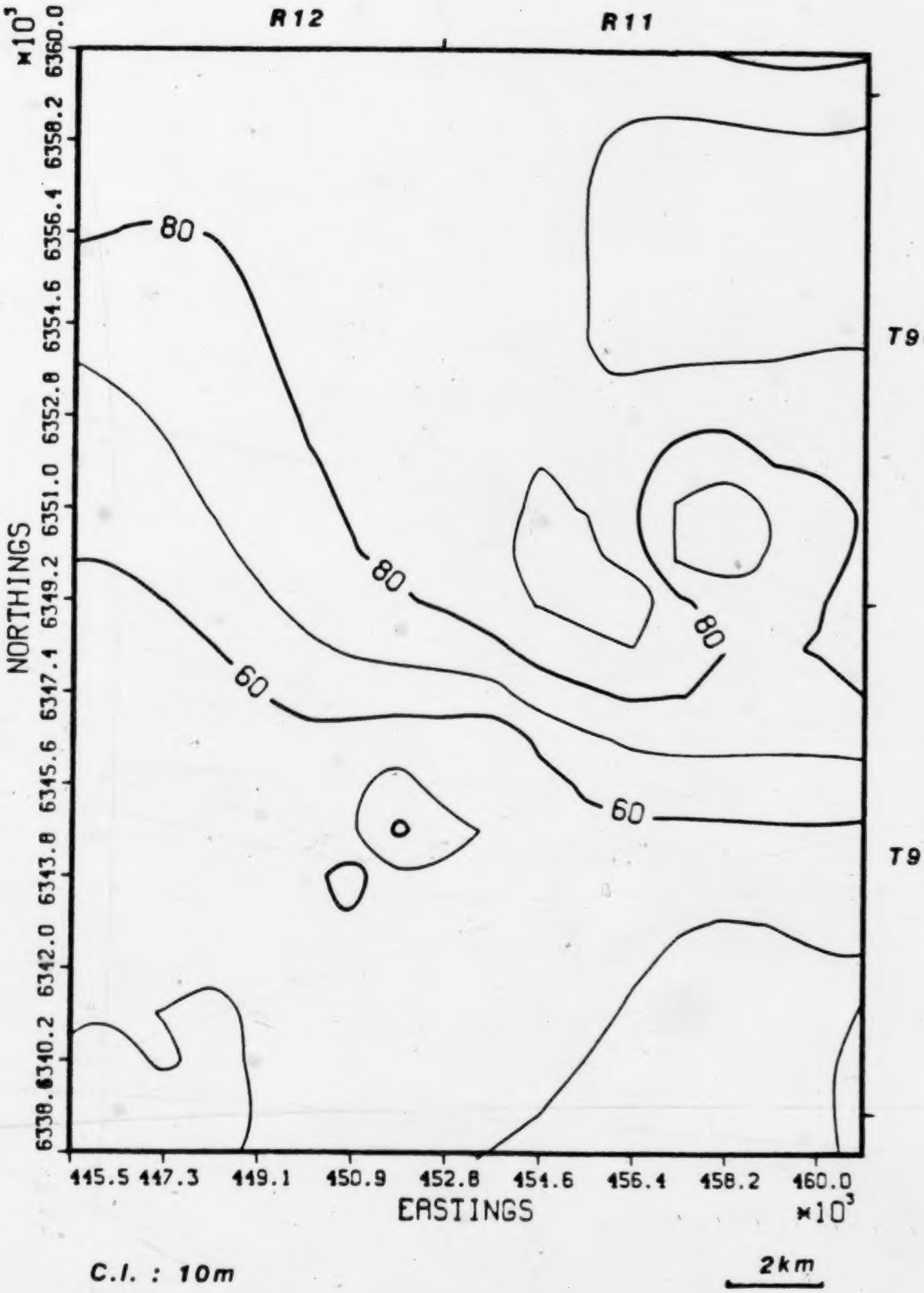
R12
R11
T96
T95
80
80
80
60
60
NORTHINGS
×10³
6360.0
6358.2
6356.4
6354.6
6352.8
6351.0
6349.2
6347.4
6345.6
6343.8
6342.0
6340.2
6338.4
445.5
447.3
449.1
450.9
452.8
454.6
456.4
458.2
460.0
EASTINGS
×10³
C.I. : 10m
2km

Figure 2.4 Isopach of the McMurray Formation.

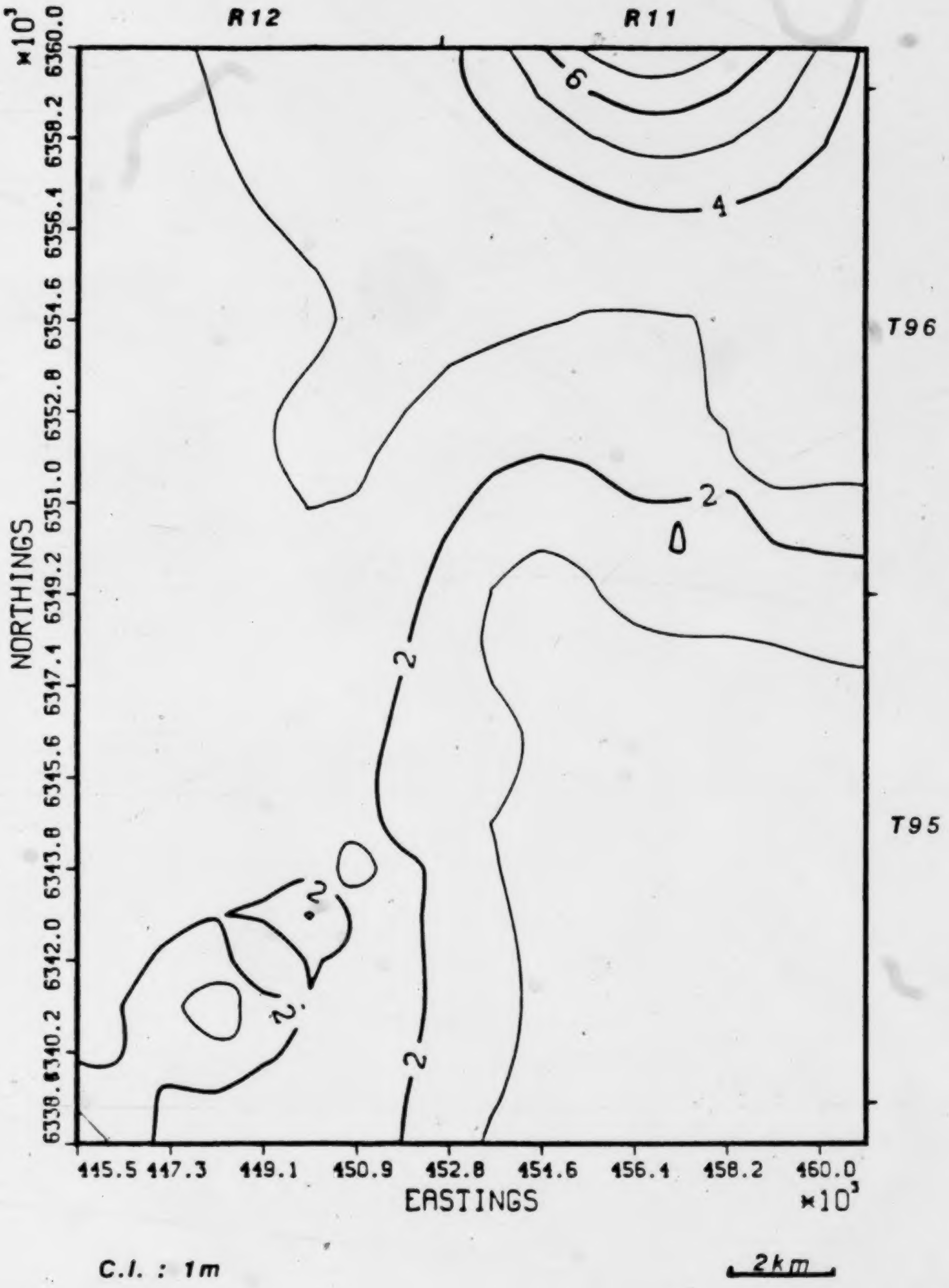
R12
R11
T96
T95
6
4
2
2
2
2
2
NORTHINGS
×10³
6360.0
6358.2
6356.4
6354.6
6354
6352.8
6351.0
6349.2
6347.4
6345.6
6343.8
6342.0
6340.2
6338.6
EASTINGS
×10³
445.5
447.3
449.1
450.9
452.8
454.6
456.4
458.2
460.0
C.I. : 1m
2km

Figure 2.5 Isopach of zone 1.

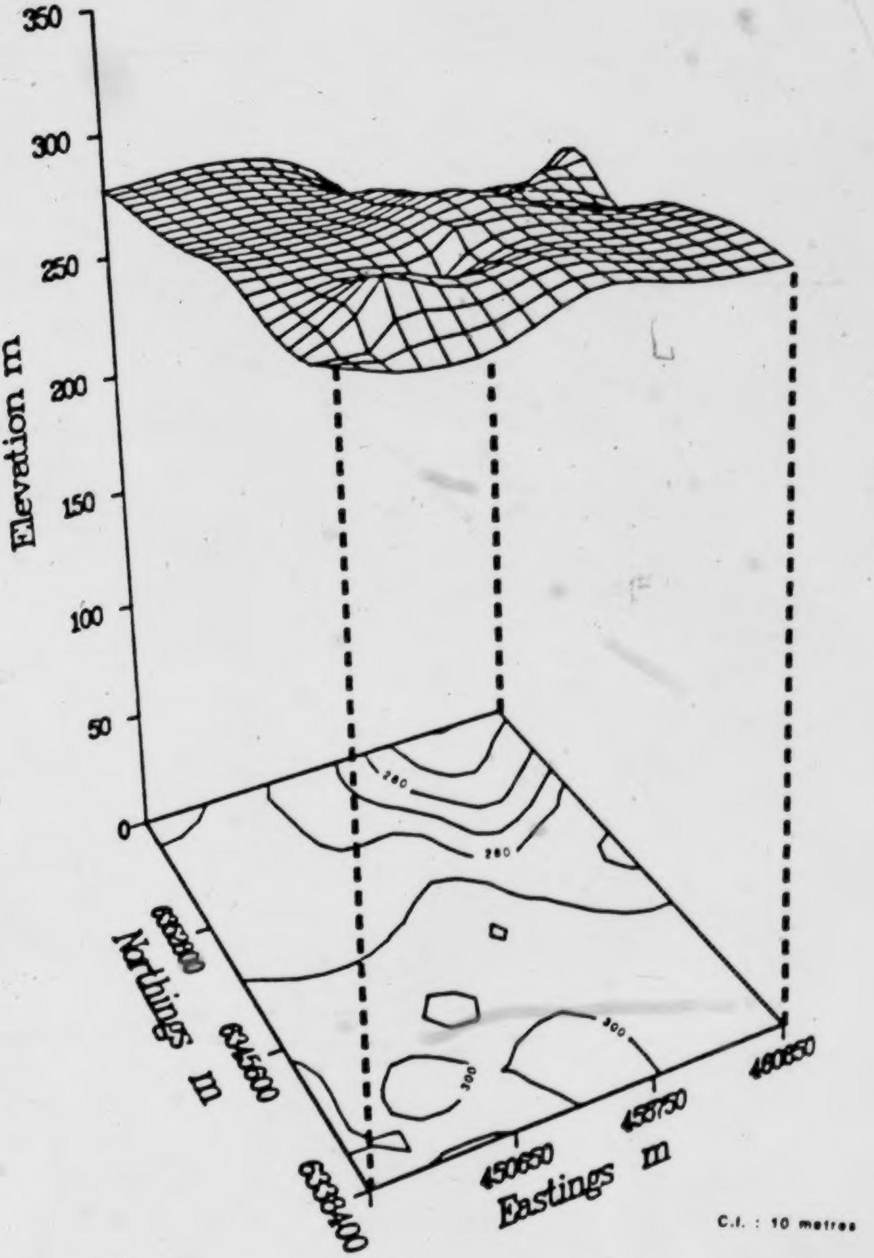

Figure 2.6 Structure contours on the top of the McMurray Formation.

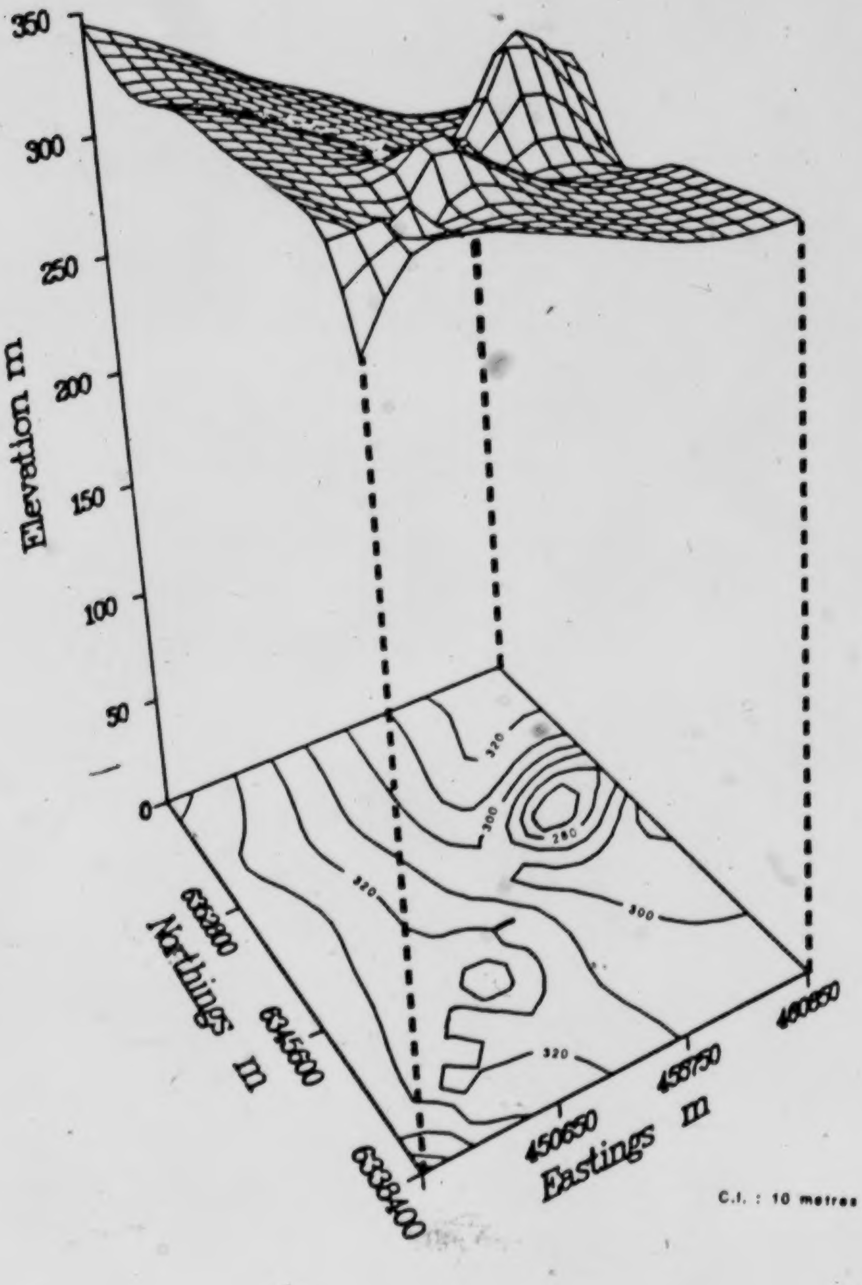

Figure 2.7 Surface topography.

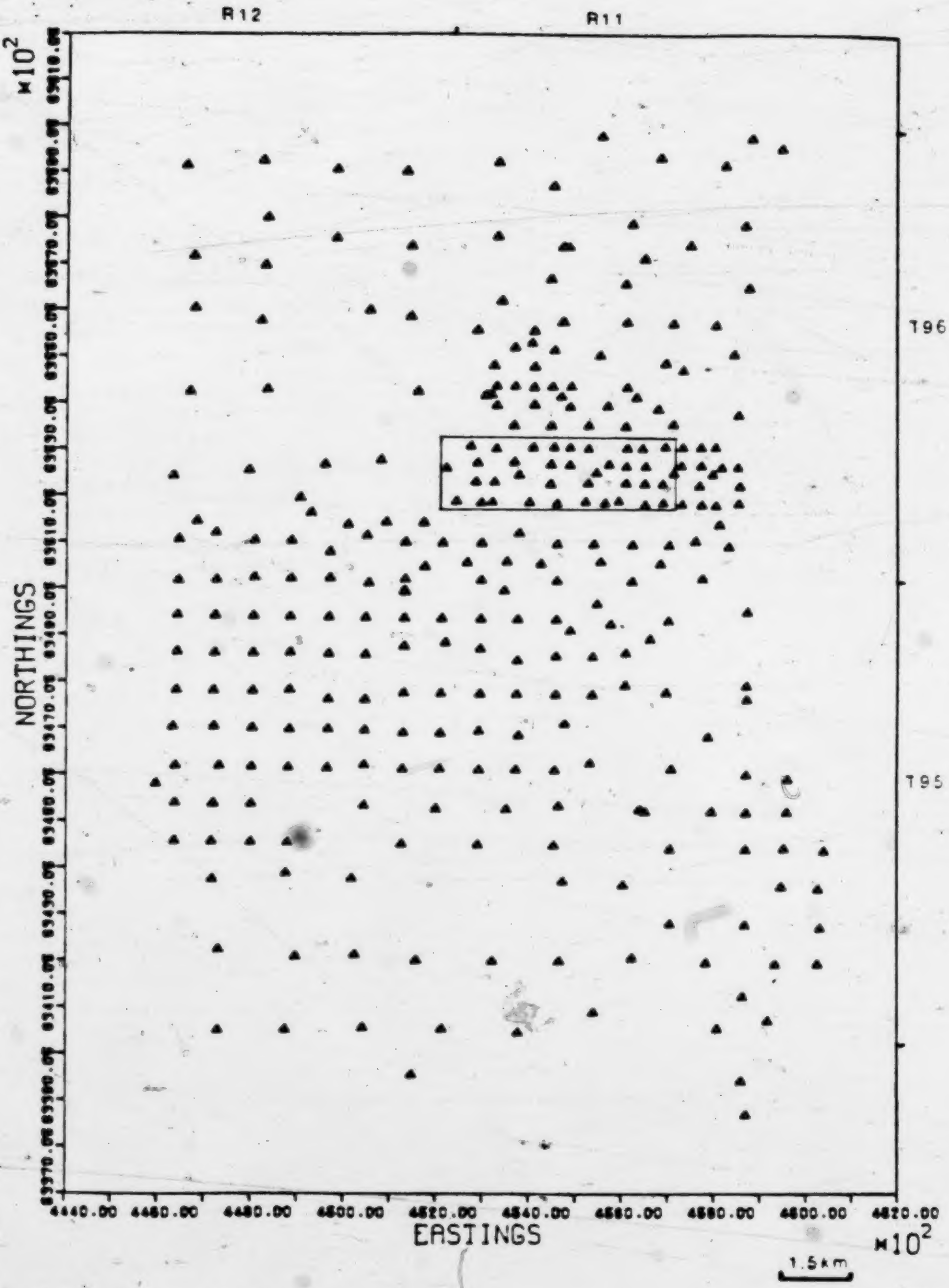
R12
R11
T96
T95
NORTHINGS
x10^2
63370.00
63390.00
63410.00
63430.00
63450.00
63470.00
63490.00
63510.00
63530.00
63550.00
63570.00
63590.00
63610.00
4440.00
4460.00
4480.00
4500.00
4520.00
4540.00
4560.00
4580.00
4600.00
4620.00
EASTINGS
x10^2
1.5km

Figure 2.8 Distribution of boreholes within the study area (large area) and control area (small area).

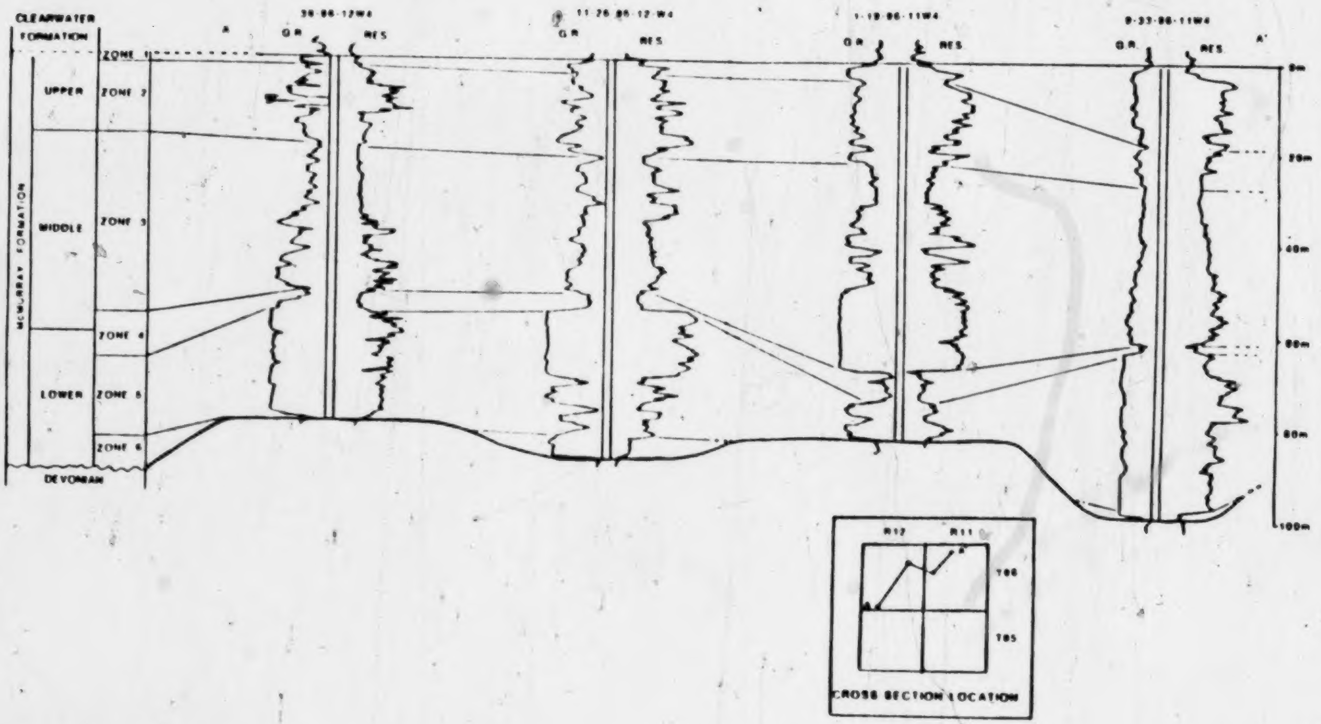
CLEARWATER FORMATION
MCMURRAY FORMATION
UPPER
MIDDLE
LOWER
DEVONIAN
ZONE 1
ZONE 2
ZONE 3
ZONE 4
ZONE 5
ZONE 6
A
36-86-12W4
G.R.
RES
11-26-86-12-W4
G.R.
RES
1-19-86-11W4
G.R.
RES
9-33-86-11W4
G.R.
RES
A'
0m
20m
40m
60m
80m
100m
R12
R11
T86
T85
CROSS SECTION LOCATION

Figure 2.9 Stratigraphic cross-section of the McMurray Formation. Correlation and delineation of the six identified zones from well to well using gamma ray and resistivity logs.

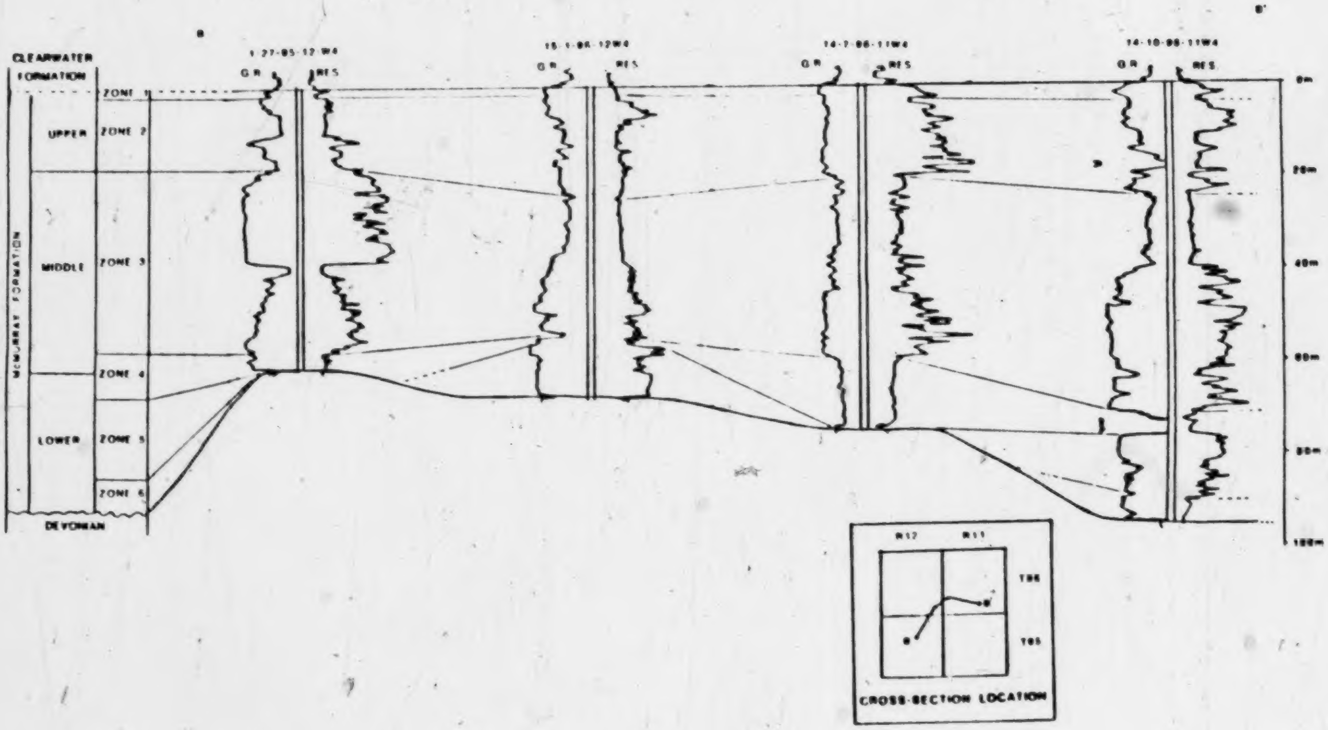
B
B'
CLEARWATER FORMATION
MCMURRAY FORMATION
UPPER
MIDDLE
LOWER
DEVONIAN
ZONE 1
ZONE 2
ZONE 3
ZONE 4
ZONE 5
ZONE 6
1-27-85-12-W4
15-1-86-12W4
14-7-86-11W4
14-10-86-11W4
G R
RES
0m
20m
40m
60m
80m
100m
R12
R11
T86
T85
CROSS-SECTION LOCATION

Figure 2.10 Stratigraphic cross-section of the McMurray Formation. Correlation and delineation of the six identified zones from well to well using gamma ray and resistivity logs.

3. THEORETICAL APPROACH TO MODELLING OF OIL DEPOSITS

Determinism and indeterminism are two well-known, diametrically opposed philosophical schools of thought, reflecting different methodologies which attempt to quantitatively describe natural phenomena, including geological phenomena. These two methodologies can be identified in scientific attempts to search for and mathematically formulate relationships or laws governing past and current geological processes and events as well as assaying the nature and variability of geological features.

This study deals with the formulation of the nature and variability of geological features of oil deposits. In such a case a deterministic approach would use a polynomial or a differential equation in order to fit a line or a surface which will approximate a set of observations. Such an approach, however, has conceptual deficiencies. It is virtually independent of the nature of the phenomena it attempts to describe, because it assumes complete independence or randomness of the observations. In an indeterministic (stochastic) approach, the stochastic structure of the data set is used in order to describe or assess the spatial variability of the geological feature examined.

Note the following idealized example. Imagine that we have a rectangle which is divided into a number of equal-sized smaller rectangles. One person is then placed in the center of each of these smaller rectangles and then, for a set period of time, each person arbitrarily distributes bitumen about their respective rectangles. When the set period of time has elapsed, a small, single sample is taken from each small rectangle. From that resulting set of data an attempt is made to deduce the spatial distribution of the bitumen. The characteristic of this data set is that all samples are completely independent of each other and thus our only choice is to proceed by inference, using a deterministic method. The argument would be valid if we were to use, on a smaller scale, samples from one of the small rectangles because the bitumen was 'thrown' in the area arbitrarily. The question which we will try now to answer is how the above arbitrarily constructed oil deposit represents the real case or, in other words, can an oil deposit adequately be represented by a deterministic model.

An oil deposit formation is a combination of independent physical processes in time and space. These processes include burial of organic rich sediments, maturation of organic matter, migration, entrapment and accumulation of migrating hydrocarbons and, in some cases, post-entrapment alterations. As an end result of these processes, it should be apparent that an oil deposit is not a random phenomenon.

The configuration and the distribution and fluctuation in space of the characteristics of a hydrocarbon accumulation depend upon the trapping situation and the properties and spatial distributions of the rock bodies which host the hydrocarbons. The properties of the reservoir rocks are themselves a result of their depositional setting, post-depositional diagenetic alterations and structural deformation. As a result, the characteristics of a reservoir and their spatial distribution and variability are not random, certainly not on a macroscopic scale. However, on a microscopic scale, randomness may exist as a result of local variable conditions.

In comparing a real oil reservoir with the artificial one we constructed earlier, we can distinguish two main differences: (i) In the real case the reservoir is a result of the same or related sequence(s) of physical processes, while in the artificial reservoir the processes involved in the construction (i.e. the different people distributing bitumen in each rectangle) are independent. (ii) Within a part of the real deposit, where local microconditions exist, the oil saturations are not independent since they are governed by the same or related micro-conditions. In the example reservoir, within one of the small rectangles, oil saturations are arbitrary and completely independent.

As a conclusion to this comparison it is apparent that our artificially created oil deposit, while ideal for a deterministic approach for modelling is far from the real case. In reality, observations of a characteristic at different locations over the deposit are not independent but correlated, due to the genetic uniformity of the deposit. This correlation is a function of the locations of the observations, and it constitutes the stochastic structure of the observations. As a consequence a deterministic approach would be appropriate only in the cases in which the observations are located adequately far from each other so that no correlation between them appears to exist.

In terms of mathematical formulation, the stochastic approach considers a characteristic of a deposit as a realization of a random function. This realization can be inferred or other realizations can be constructed using the first two moments of the random function.

The mathematical background of stochastic processes and random functions was developed over the last 60 years. The basic theory was pioneered by Kolmogorov (1931), Khinchin (1934), Wiener (1950), Doob (1953), Slutski (1960) and Yaglom (1962). In the physical sciences, classic work from Matern (1960) in forestry and Gandin (1965) in meteorology is well known.

In geosciences and particularly in modelling and evaluation of mineral deposits, stochastic processes were introduced by Matheron during the 60's. The theory has been adapted and expanded to the particular needs of the field and it is known as the 'theory of regionalized variables' (Matheron 1963a, 1963b, 1965, 1967, 1969, 1972, 1973; Journel 1974a, 1974b; Journel and Huijbregts, 1978; David, 1977). It has also been termed geostatistics. The basic concepts of geostatistics as they are considered in this study will be explained in the following paragraphs.

3.1 Random Functions, Random Variables and Regionalized Variables

Let an arbitrary set of k points x_1, x_2, ..., x_k in R^n (n-dimensional space) be set T. A random function of an argument x in T is function Z(x), whose values are random variables. In other words, a random function is a family of random variables $Z(x_1)$, $Z(x_2)$, ..., $Z(x_k)$ corresponding to points x_1, x_2, ..., x_k of the set T.

A random function is specified, (i) if for each point x in T the distribution function of the quality $Z(x_i)$:

$$Fx_i(z_i)=\mathrm{Prob}\{Z(x_i)< z_i\} \qquad (3.1.1)$$

is given and (ii) if the distribution function of the k-dimensional random variable:

$$Fx_1,x_2,\ldots,x_k(z_1,z_2,\ldots,z_k)= \mathrm{Prob}\{Z(x_1)<z_1,\ Z(x_2)<z_2,\ \ldots,\ Z(x_k)<z_k\} \qquad (3.1.2)$$

is given.

The distribution function (3.1.2) must satisfy the conditions of symmetry and compatibility. The converse is also true. That is, any system of distribution functions (3.1.2) satisfying the above conditions can be regarded as defining a random function on T. Different and more sophisticated definitions of random functions also exist. These will not be mentioned since they are outside the scope of this study.

A random variable is the function that assigns specific numerical value at point x in T, according to a certain probability distribution. Each numerical value assigned by the random variable at x is a particular realization of the random variable.

A regionalized variable is a simple function $z(x)$ which takes a value at every point x in R^3. This function possesses the following characteristics. First, it is distributed within physically homogeneous space. Second, it is additive. Third, it may be locally erratic and random but it has a mean structural aspect which can be represented as a function. In relation to random functions and random variables, a set of regionalized variables $z(x)$ can be considered as a particular realization of a set of random variables $\{Z(x), \forall x \in R^3\}$, which set is a random function $Z(x)$.

In a physical context we may consider the variable say, oil saturation of an oil deposit. This variable is a regionalized variable since (i) it is distributed in three dimensional physically bounded space, (ii) it has a mean structural aspect (correlation), and (iii) it is additive. Let us consider now the oil saturation $z(x_1)=13\%$ at point x_1 of the reservoir. This particular oil saturation $z(x_1)$ can be considered as a particular realization of the random variable $Z(x_1)$ defined at point x_1. Consequently the oil saturations at all points x_1, x_2, ...,x_n which constitute the reservoir are particular realizations of the set of random variables $\{Z(x_1), Z(x_2), \ldots, Z(x_n)\}$, or as whole, the oil saturation of the deposit is one realization of the random function $Z(x)$.

In an operational sense, the probabilistic interpretation of a regionalized variable as one realization of a random function has the advantage that one, as we shall see, can construct other realizations of the same random function. However, from one realization (i.e. one deposit) it is impossible to infer all or part of the probability law which defines the underlying random function. Thus, certain assumptions must be made. These assumptions are included in the hypothesis of stationarity, which we will further explain.

3.2 Stationarity, Moments and Ergodicity

A random function $Z(x)$ will be called stationary if all the distribution functions (3.1.2) defining $Z(x_i)$ remain the same when the whole set of points $x_1, x_2, \ldots, x_K$ is shifted by a vector h:

$$F_{x_1,x_2,\ldots,x_K}(x_1,x_2,\ldots,x_K)= F_{x_1+h,x_2+h,\ldots,x+h}(x_1,x_2,\ldots,x_K) \qquad (3.2.1)$$

for any $x_1, x_2, \ldots, x_K$ and h.

This means that every one-dimensional distribution function (3.1.1) does not depend on the position x_i $(i=1,2,\ldots,k)$ and that the multi-dimensional distribution functions (3.1.2) can only depend on the separation vector

h. This property is known as strict stationarity.

The physical meaning of stationarity is that within a geologically homogeneous zone of, for example, an oil deposit, the oil saturations at different locations do not depend on their position, but rather on their separation distance. In addition, it implies that the regionalized variable, oil saturation in our example, repeats itself within the space of the homogeneous zone. This repetition provides the equivalent of many realizations of the random function (oil saturation here) permitting a certain amount of inference.

In geostatistics, only part of the distribution law of the underlying random function is used (linear geostatistics). More precisely the first and second-order moments.

The first-order moment of the distribution function of the random function $Z(x)$ if it exists is:

$$E\{Z(x)\}=m(x) \tag{3.2.2}$$

where $m(x)$ is a function of x.

The second-order moments of a random variable $Z(x)$ considered in geostatistics are:

(i) The *a priori* variance of $Z(x)$, defined when it exists, the second-order moment about $m(x)$:

$$\mathrm{Var}\{Z(x)\}=E\{[Z(x)-m(x)]^2\} \tag{3.2.3}$$

which is also a function of x.

(iii) The covariance. If two random variables $Z(x_1)$ and $Z(x_2)$ have variances defined at points x_1 and x_2 they also have a covariance defined as:

$$C(x_1,x_2)=E\{[Z(x_1)-m(x_1)][Z(x_2)-m(x_2)]\} \tag{3.2.4}$$

which is a function of x_1 and x_2.

(iii) The variogram, defined as :

$$2\gamma(x_1,x_2)=Var\{Z(x_1)-Z(x_2)\} \tag{3.2.5}$$

is also a function of x_1 and x_2. The function $\gamma(x_1,x_2)$ is called the semi-variogram. Usually the term variogram is used for both functions.

In linear geostatistics, it is important that the above moments exist and that they can be approximated from a sufficiently large number of uniquely located samples.

A random function $Z(x)$ is said to be stationary of second-order if (i) the first moment exists and it does not depend on x:

$$E\{Z(x)\}=m \ , \forall x \in R^n \tag{3.2.6}$$

and (ii) for each pair of random variables $Z(x)$ and $Z(x+h)$ the covariance exist and depends on the distance vector h:

$$C(h)=E\{Z(x)Z(x+h)\}-m^2 \ , \forall x \in R^n \tag{3.2.7}$$

This also implies that the variogram exist and it is:

$$\gamma(h)=C(0)-C(h) \tag{3.2.8}$$

Because, however, the *a priori* variance and the covariance do not always exist in many physical phenomena the second order stationarity hypothesis or weak stationarity is reduced to the intrinsic hypothesis.

Accordingly, a random function Z(X) is said to be intrinsic if (i) its first moment exists and depends on x:

$$E\{Z(x)\}=m \ , \forall \ x \in R^n \quad (3.2.9)$$

and (ii) the increment [Z(x+h)-Z(x)] has, for all possible vectors h, a finite variance which does not depend on x:

$$Var\{Z(x+h)-Z(x)\}=E\{[Z(x+h)-Z(x)]^2\}=2\gamma(h) \ , \forall \ x \in R^n \quad (3.2.10)$$

It is apparent that second order stationarity implies the intrinsic hypothesis but the converse is not true.

Ergodicity or better the ergodic theorem allows us, in practice, to approximate from a sufficiently large number of observations the first and second order moments of a stationarity random function Z(x).

3.3 Stochastic Structure of a Random Function and Corresponding Properties.

The stochastic structure of a stationary random function Z(x) is expressed and described by the second order moments of the stationary random function, namely the covariance and variogram (or semi-variogram), as defined in the previous paragraph.

The properties, behavior and theoretical variogram models are extensively presented and discussed by Journel and Huijbregts (1978, p.148-235) and thus are not presented here. Only the construction and fitting of variograms is discussed in the next two paragraphs.

3.3.1 Construction of the model variogram of a regionalized phenomenon.

There are two stages in the construction of the model variogram of a regionalized phenomenon. The first involves the calculation of the experimental variogram from the available set of data. The second is the fitting of the appropriate model variogram to the experimental one.

In the first stage, the experimental variogram $\gamma^*(h)$ is calculated using the formula:

$$\gamma^*(h)=1/2N\ \Sigma_{i=1}^{N}[z(x+h)-z(x)]^2$$

(3.3.4.1)

where, N is number of pairs separated by distance h, z(x) the value of the regionalized phenomenon at point x, z(x+h) the value of the regionalized phenomenon at point x+h.

The number of pairs N for each distance h must be sufficiently large for the estimated value of $\gamma^*(h)$ to be reliable. 50 pairs or more are usually considered sufficient.

Using formula (3.3.4.1), an experimental variogram can be calculated for one or more directions. It is also apparent that the data must be on a regular grid. If this does not hold true, as in most cases in real life, classification of data in groups is required. In such a case

(Figure 3.3a), data are grouped and the distance h is averaged for each group. The grouping is made on the basis of the parameters, the angle of tolerance and the distance of tolerance as can be seen in figure 3.3a. The experimental variogram from irregularly spaced data is an average one, the larger the angle and distance of tolerance, the smoother it becomes. The only criterion for setting the above parameters is a sufficiently large number of pairs N for each distance h.

A model variogram is next fitted to the experimental points (or curve). Depending on the configuration of the experimental variogram, one or more theoretical model variograms are fitted. The fit is usually done by choosing the appropriate sill(s) and range(s) of the theoretical model(s) to be used. The model better representing the experimental points is finally considered as the model variogram of the regionalized phenomenon. It must be pointed out that choosing the 'best' model variogram is subjective, intuitive proceadure and can not be mathematically defined.

The most important aspect in calculating a variogram is the volume (support) of the samples in use. This volume can influence the variogram calculation in two ways. The first is the shape of the experimental curve, which can be very misleading if the support among samples varies significantly. Accordingly, samples must have the same size. If not, as usually the case is, they must be regularized (Appendix I) over the same support.

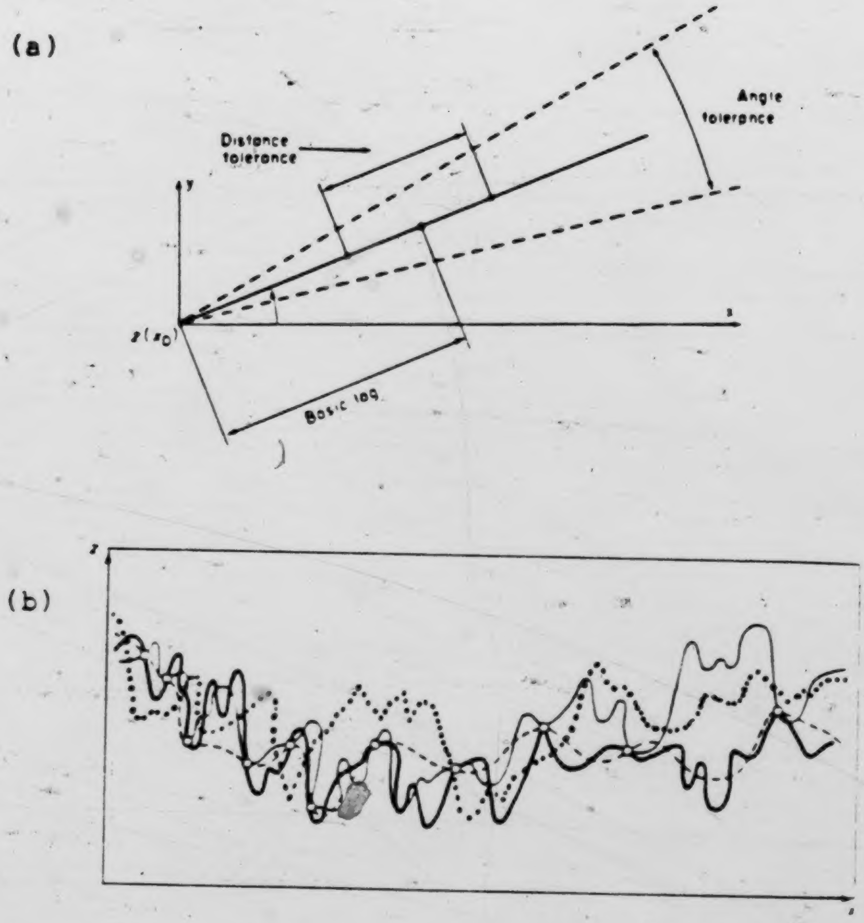
(a)
Angle tolerance
Distance tolerance
y
x
z(x0)
Basic lag
(b)
z
x

Figure 3.1 (a) Grouping of irregularly spaced data for experimental variogram calculation (adapted after Journel and Huijbregts, 1978, p.223). (b) Comparison of real, estimated and simulated profiles. ——, reality; ----, kriging; ...., simulation; ——, conditional simulation; oooo, conditioning data (modified after Journel and Huijbregts, 1978, p.494)

The second influence of the sample volume on the behavior of the experimental variogram is that as the support increases, the sill of the variogram decreases and the range increases. This indicates the need for transformation of the variogram constructed on samples of some volume to the equivalent point variogram, i.e. the variogram which corresponds to samples with point support.

3.3.2 Robustness of the model variogram.

From a statistical point of view, it is difficult to evaluate a model variogram. This is due to the fact that there is no technique available which would enable us to put confidence intervals on the variogram model. The only test is to exclude some data from the available data set and then try to estimate them using different variogram models. The model which produces values closest to the real ones can then be considered as the most appropriate.

From a physical point of view, a model variogram can be qualitatively evaluated on the basis of available geological information. The most robust model is then the one which more clearly represents geological reality. One significant improvement can be considered if distance is not measured in its euclidian sense but rather in its natural, geological sense. For example, in a meanderic stream channel, the distance between points on the channel is not measured by the straight line which connects them but by the distance measured parallel to the meandering shape of the channel.

3.4 Estimation Using Kriging.

Let $z(x_i)$ where $i=1,2,\ldots,n$ be a set of values from a realization of a second order stationary random function $Z(x)$ at points x_1, x_2, ..., x_n. The question is how $z_0(x)$ at point x_0 can be estimated or interpolated using the available data $z(x_i)$ and the stochastic structure of the underlying random function. The theory developed to solve this problem within the limits of linear geostatistics is known as the theory of kriging or objective analysis. This theory, which will be briefly described below, can provide the best mean linear unbiased estimate (BLUE) $z^*(x_0)$ for $z(x_0)$.

The value to be estimated, can be expressed as a linear function of the known values as follows:

$$z^*(x_0)=\lambda_1 z(x_1)+\lambda_2 z(x_2)+\ldots+\lambda_n z(x_n)$$

or

$$z^*(x_0)=\Sigma_{i=1}^{n}\lambda_i z(x_i) \qquad (3.4.1)$$

It is obvious from this equation that the estimator $z^*(x_0)$ is a mean and λ_1, λ_2, ..., λ_n are weighing factors for each $z(x_i)$. Just as the values $z(x_i)$ are considered particular realizations of a set of random variables $Z(x_i)$ at points x_i, the estimated value $z^*(x_0)$ is one realization of a random variable $Z^*(x_0)$ at point x_0. Note that the quantity $[z(x_0)-z^*(x_0)]=r(x_0)$, or estimation error, is also a particular realization of the random variable $R(x_0)$ at point x_0.

A linear estimator can be defined terms of random variables as follows:

$$Z_K^*(x_0)=\Sigma_{i=1}^{n}\lambda_i Z(x_i)$$

(3.4.2)

In order for this estimator to be unbiased, the following condition must be valid:

$$E\{Z(x_0)-Z_K^*(x_0)\}=0$$

(3.4.3)

This means that the mean estimation error is zero. Following equation (3.4.3.), we conclude:

$$\Sigma_{i=1}^{n}\lambda_i=1$$

(3.4.4)

Equation (3.4.4) is known as the 'non-bias condition' and it implies that the sum of all the weight factors is equal to 1.

In order for the estimator $Z^*(x_0)$ to be best, the estimation variance or error variance σ_K^2 must be minimal. That is:

$$Var\{Z(x_0)-Z^*(x_0)\}=\sigma_K^2=minimum$$

or

$$\sigma_K^2=E\{[Z(x_0)-Z^*(x_0)]^2\}=minimum$$

(3.4.5)

Using the standard Lagrangian technique, equation (3.4.5) is valid, under the condition imposed by equation (3.4.4), only when:

$$\Sigma_{i=1}^{n}\lambda_i C_{ij}+\mu=C_{i0} \quad , \forall \ i=1,2,\ldots,n$$

(3.4.6)

where μ is the Lagrange parameter, C_{ij} the covariance between points x_i and x_j, and C_{i0} is the covariance between points x_i and x_0.

Equations (3.4.4) and (3.4.6) constitute a system of n+1 equations with n+1 unknowns which is called the kriging system. The complete developement of the kriging equations is given by David (1977, p.237-242).

The kriging system can also be expressed in terms of the variogram function $\gamma(h)$ as follows:

$$\Sigma_{j=1}^{n}\lambda_j\gamma_{ij}+\mu=\gamma_{i0} \;,\; \forall\; i=1,2,\ldots,n$$
$$\Sigma_{j=1}^{n}\lambda_j=1 \qquad (3.4.7)$$

This system is also valid if the corresponding random function is only intrinsic.

The corresponding minimum estimation variance or kriging variance is then:

$$\sigma_K^2=1-\Sigma_{i=1}^{n}\lambda_i C_{i0}+\mu \qquad (3.4.8)$$

or

$$\sigma_K^2=\Sigma_{i=1}^{n}\lambda_i\gamma_{i0}+\mu \qquad (3.4.9)$$

The kriging system of equations can be expressed in matrix form as:

$$[K][\lambda]=[M]$$

from which:

$$[\lambda]=[K]^{-1}[M]$$

and

$\sigma_K^2 = 1 - [\lambda]'[M]$

where $[\lambda]'$ the transpose matrix of $[\lambda]$

It also is:

$$[\lambda] = \begin{bmatrix} \lambda_1 \\ \lambda_2 \\ \cdot \\ \cdot \\ \cdot \\ \lambda_n \\ \mu \end{bmatrix} \qquad [M] = \begin{bmatrix} C_{10} \\ C_{10} \\ \cdot \\ \cdot \\ \cdot \\ C_{n0} \\ 1 \end{bmatrix}$$

and

$$[K] = \begin{bmatrix} C_{11} & C_{12} & \dots & C_{1n} & 1 \\ C_{21} & C_{12} & \dots & C_{1n} & 1 \\ \cdot & \cdot & \dots & \cdot & 1 \\ \cdot & \cdot & \dots & \cdot & 1 \\ \cdot & \cdot & \dots & \cdot & 1 \\ C_{n1} & C_{n2} & \dots & C_{1n} & 1 \\ 1 & 1 & \dots & 1 & 0 \end{bmatrix}$$

Note that [K] is a symmetric matrix with a major diagonal.

3.4.1 Remarks on the kriging system of equations.

We have already discussed how the covariance function of a second-order stationary random function is positive definite. As a consequence, the covariance matrix [K] is strictly positive definite and it has a strictly positive determinant. This results in the fact that the kriging system always has an unique solution.

A consequence of the existence and uniqueness of the solution of the kriging system is that the kriging variance is non-negative. Kriging is not only an unbiased estimator, it also constitutes an exact interpolator. This means that the kriging system reproduces the actual data points and the corresponding kriging variance is zero. This is simply because of the fact that estimation of a data point assigns a weighting factor of one to the data point.

For distances greater than the range of the variogram or the covariance function used by the kriging system, the estimates are equal to the arithmetic mean of the available data.

The nature of the kriging estimates, i.e. minimum variance weighted averages of the available data, results in the fact that kriging estimates are smoother than the data. Thus they cannot claim to completely restore the spatial variability of the corresponding regionalized phenomenon.

The kriging system, as it has been developed in the previous paragraph, makes use of normalized variograms or covariance functions with respect to the *a priori* variance of the corresponding random function. As a result, the kriging variance in equations (3.4.13) and (3.4.14) is also normalized with respect to the *a priori* variance.

Another assumption of the previous paragraph is that the data as well as the estimators are expressed on a point support (punctual kriging). It is very common, however, that the available data are not defined on a point support and that the estimates must be defined over a particular volume (block estimation). In this case, the kriging system and the kriging variance can be properly modified and expressed with respect to the support of the data and blocks to be estimated.

The kriging equations can also be properly adapted in the case where the corresponding random function is only intrinsic (i.e. drift or trend exists). This type of kriging is termed 'unbiased kriging of order k' or 'universal kriging' and it represents the general case, where both random and deterministic components exist.

3.4.2 The estimation error and its distribution.

We have already defined the estimation error at point x_0 as a realization of the random variable $[Z(x_0)-Z^*(x_0)]= R(x_0)$ at point x_0. If the kriging estimation deals with a second-order stationary random function, the errors at the estimated points x_j where $j=1,2,...,n$ can be considered as a realization of a second-order stationary random function $R(x_0)$, which is characterized by its distribution:

$$F(u)=\mathrm{Prob}\{R(x)<u\}$$

Since $R(x)$ is second-order stationary, it is possible calculate the probability that the error will fall within any interval $[a,b]$:

$$\mathrm{Prob}\{a\leq R(x)\leq b\}=F(b)-F(a) \quad , \forall \; x$$

From the kriging conditions we have that:

(i) The first order moment (mean) of the distribution is:

$$E\{R(x)\}=m_e=0$$

(ii) The second order moment (variance) of the distribution is:

$$Var\{R(x)\}=E\{[R(x)]^2\}-m_e^2=\sigma_e^2=\text{min. and constant} \ , \forall\ x$$

The above equations define a standard two-parameter distribution function, which we can use, under assumptions, in order to put confidence intervals the magnitude of the estimation errors.

The most commonly used and most frequently occurring two-parameter distribution function of the estimation error is the normal distribution (Journel and Huijbregts, 1978, p.50). Accordingly, the normal confidence interval $[m_e \pm 2\sigma_e]$ of classical statistics containing approximately 95% of the observed errors is a good criterion for evaluating the quality of the estimation. It must, however, be noted that experience indicates that a Gaussian distribution function underestimates very small and very large errors, indicating that the real distribution function of an estimation error has usually a slightly more pronounced mode and larger tails than the Gaussian one.

3.5 Generation of Stochastic Fields.

Let Z(x) be a second-order stationary random function in R^n with known and finite first and second order moments. It is possible to generate (simulate) n-dimensional fields that have the same mean, variance and stochastic structure with Z(x). These simulated fields are then considered as different realizations of $Z(x)$ in R^n.

Several techniques have been developed for simulation of n-dimensional stochastic fields. Jenkins and Watts (1968) considered moving averages (on different geometric configurations) which describe a field with a Poisson distribution. Rodriguez-Itrube and Mejia (1974a, 1974b) used simulated orthogonal random measures with a variance density which meets the spectrum measure of the imposed covariance. Matheron (1973) used a technique which consists of one-dimensional simulations on lines that turns in n-dimensional space, known as the 'turning bands method'. This last technique has been more widely used in geostatistics because it is considered as relatively simple and efficient as well as reasonable in terms of computer time (Journel, 1974b). The classical Monte Carlo simulation technique has also been used, however it generates fields with only one specific stochastic structure which is that of pure nugget effect. In the following two sections, the 'turning bands method' in R^3 will be examined.

3.5.1 Simulation in one-dimension.

Let $T(t_i)$ be a series of independent random variables located at discrete intervals at points $i-k,\ldots,i,\ldots,i+k$. These independent random variables have the same uniform distribution, mean (expectation) of zero and variance of σ^2.

Another set of random variables $Y(t_i)$, can be defined if we consider the moving average process with weighting function f(k) as follows:

$$Y(t_i)=\Sigma_{-\infty}^{+\infty} f(k)T(t_i+k) \qquad (3.5.1.1)$$

Since $Y(t_i)$ are products of simple weighted sums of independent random variables, their distribution function, according to the Central Limit Theorem, will tend towards a normal distribution. The first order moment will be:

$$\begin{aligned}E\{Y(t_i)\}&=E\{\Sigma_{-\infty}^{+\infty} f(k)T(t_i)\}\\ &=\Sigma_{-\infty}^{+\infty} f(k)E\{T(t_i+k)\\ &=\Sigma_{-\infty}^{+\infty} f(k)E\{T(t_i+k)\\ &=\Sigma_{-\infty}^{+\infty} f(k)m\\ &=0\ ,\ \forall\ t_i\end{aligned}$$

The covariance for every pair of random variables $\{Y(t_i+k),\ Y(t_i+j+h)\}$ will be:

$$\begin{aligned}C_d^j(h)&=E\{Y(t_i+k)Y(t_i+j+h)\}-m^2\\ &=E\{Y(t_i+k)Y(t_i+j+h)\}\\ &=E\{(\Sigma_{-\infty}^{+\infty} f(k)T(t_i+k))\Sigma_{-\infty}^{+\infty} f(k)T(t_i+j+h))\}\\ &=\Sigma_{-\infty}^{+\infty} f(k)\Sigma_{-\infty}^{+\infty} f(k)E\{T(t_i+k)T(t_i+j+h)\}\end{aligned}$$

Since $T(t_i+k)$ and $T(t_i+j+k)$ are independent, the expectation of their product will be zero, unless $t_i+k=t_i+j+h$ or $k=j+h$. In the last case, $E\{[T(t_i+k)]^2\}=\sigma^2$. Accordingly, the covariance $C_d^j(h)$ will be:

$$C_d^j(h)=\sigma^2\Sigma_{-\infty}^{+\infty} f(k)f(k-h) \qquad (3.5.1.2)$$

Thus the set of random variables $Y(t_i)$ has an expectation of zero and a defined covariance function which depends on h. Consequently, it can be considered as a second-order stationary one-dimensional random function Y(t).

The continuous version of the random Y(t) function can also be defined as:

$$Y(u)=\int_{-\infty}^{+\infty} f(u+r)T(r)dr \tag{3.5.1.3}$$

where T(r)dr is a stationary random measure with a Dirac covariance measure (Journel, 1974a, 1974b), an example of which is the differential form of Brownian motion.

The corresponding covariance is:

$$C'(h)=\int_{-\infty}^{+\infty} f(u)f(u+h)du \tag{3.5.1.4}$$

which indicates that C'(h) is the convolution product of the function f(u) and its transpose f(-u).

It is obvious that from a set of realizations of a set of independent random functions, it is possible to produce one-dimensional realizations of a random function with a particular covariance function if the weighting function f(u) corresponding to this covariance can be determined.

According to the Bochner's theorem of harmonic analysis, a covariance function can be expressed as a Fourier transform. Accordingly, C'(h) can be expressed as $\mathcal{F}[C'(h)]$. Following the property that a Fourier transform of a convolution of a function and its transpose is the product of the Fourier transform of the function and itself, we have:

$$\mathcal{F}[C'(h)]=\mathcal{F}[f(u)*f(-u)]=[\mathcal{F}(f(u))]^2$$

Finding the inverse Fourier transform of the above, the weighting function f(u) can be calculated for every C'(h).

Practically, calculation of f(u) requires heavy Fourier transform calculations. For the three most common covariance or variogram models, spherical, exponential and Gaussian, the weighting functions have been calculated by Journel (1974a, 1974b).

For the spherical covariance or variogram it is:

$$f(u)=\sqrt{12K/a^3}\ ,\ \forall\ u \in [-a/2,a/2]$$

$$f(u)=0\ ,\ \text{otherwise;}$$

where a refers to the range of the spherical variogram and K is the desired variance of the simulated values. Verification of the above weighting function is relatively simple (Knudsen, 1981, p.15).

For the exponential model it is:

$$f(u)=2(\sqrt{K\lambda})(1-\lambda u)e^{-\lambda u}\ ,\ \forall\ u\geq 0$$

$$f(u)=0\ ,\ \text{otherwise;}$$

For the Gaussian covariance or variogram model, it is:

$$f(u)=(16K/a^3\sqrt{\pi})ue^{2u^2/a^2},\ \forall\ -\infty<u<+\infty$$

In simulating realizations of a one-dimensional, second-order stationary random function, the discreet covariance $C_d'(h)$ is calculated for every distance h. This creates a bias, which is expressed as $C_d'(h)-C'(h)$. One must ensure that the appropriate corrections are made so that $C'(0)=C_d'(0)$.

3.5.2 Simulation in three-dimensions using the turning bands method.

Let $Y(u_1)$ be a stationary second-order, one-dimensional random function with a zero mean ($E\{Y(u_1)\}=0$) and an one-dimensional covariance function $C_1(hu_1)$. A three-dimensional, second-order stationary random function can then be defined as follows:

$$Z_1(u_1,v_1,w_1)=Y(u_1),\ \forall \text{ point in } R^3 \qquad (3.5.2.1)$$

$Z_1(u_1,v_1,w_1)$ has an expectation of zero and a three-dimensional covariance as follows:

$$C_1=C_1(hu_1,hv_1,hw_1)=C'(hu_1) \qquad (3.4.2.2)$$

(u_1,v_1,w_1) is a three-dimensional unit system of orthogonal axis and hu_1, hv_1, hw_1 the projects of vector h on axis u_1, v_1, w_1 (Figure 3.4).

In order to generate a realization $z_s(x)$ at point x in R^3 of a three dimensional, second-order stationary random function $Z_s(x)$ with a given isotropic covariance function, the following must be considered.

On line L_1, corresponding to vector u_1, k realizations $y(u_1)$ of $Y(u_1)$ are simulated at points with spacing b. Perpendicular to L_1 k+1 planes are considered crossing L_1 at the midpoints between the simulated points on L1. Consequently a number of bands (slices) are defined by successive pairs of the planes considered. The thickness of each band is b, that is, equal to the spacing of the simulated points on L_1. It is apparent that one simulated realization of $Y(u_1)$ corresponds to each band. This simulated value is assigned to each point within the corresponding band (Figure 3.4).

Consider now a plane P_1 perpendicular to L_1. P_1 will be contained within a band and consequently at each point x_1 on P_1 a simulated realization of $Y(u_1)$ will correspond.

N lines L_i, $i=1,2,\ldots N$ corresponding to vectors u_1, u_2, ..., u_N are uniformly distributed over the unit sphere defined by (u_i, v_i, w_i). On each line L_1, L_2, ..., L_N, realizations of the random functions $Y(u_1)$, $Y(u_2)$ ..., $Y(u_N)$, with the N random functions being independent, are simulated at points with spacing b. It is apparent that point x_1 will not only belong to P_1 but also to planes P_2, P_3, ..., P_N perpendicular to L_1, L_2, ..., L_N respectively. Thus for each point x in R^3, there will be N different corresponding realizations $Y(u_i)=Z_i(x)$ (according to equation (3.5.2.1)).

The realization $z_s(x)$ then at point x of $Z_s(x)$ will be given by the equation (Journel and Huijbregts, 1978, p.499) as follows:

$$z_s(x)=1/\sqrt{N}\ \Sigma_{i=1}^{N} z_i(x) \qquad (3.5.2.3)$$

The covariance function corresponding to $Z_s(x)$ will be:

$$C(h)=E\{Z_s(x)Z_s(x+h)\}$$

When $N\to\infty$ we have:

$$C(h)=1/2\pi \int_{1/2\,\text{sphere unit}} C'(\langle h,u\rangle)du \tag{3.5.2.4}$$

where $\langle h,u\rangle$ will be the projection of vector h on axis u.

Equation (3.5.2.4) can be rewritten as follows:

$$C(h)=1/2\pi \int_0^{2\pi} d\theta \int_0^{\pi/2} C'(|h\cos\phi|)\sin\phi \, d\phi$$

Setting $t=|h\cos\phi|$, and integrating out ϕ, we have:

$$C(h)=1/h \int_0^h C'(t)\, dt \tag{3.5.2.5}$$

Taking the antiderivative of equation (3.5.2.5), we have:

$$C'(t)=\partial[hC(h)]/\partial h \tag{3.5.2.6}$$

According to Bochner's theorem $C'(t)$ as defined by equation (3.5.2.6) is a positive definite function in one dimension and accordingly it can be considered as a covariance function. Consequently the covariance of the one dimensional simulations required for the simulation of a three-dimensional stochastic field with covariance function C(h), is known.

The simulation method described in this section is termed the 'turning bands method' because the N lines and the corresponding bands can be deduced from each other by rotation in space.

3.5.3 Remarks on the turning bands method

In practice, the number N of required lines L_i is set to 15 (Journel, 1974a). These lines correspond to the lines joining the mid-points of the opposite edges of a regular

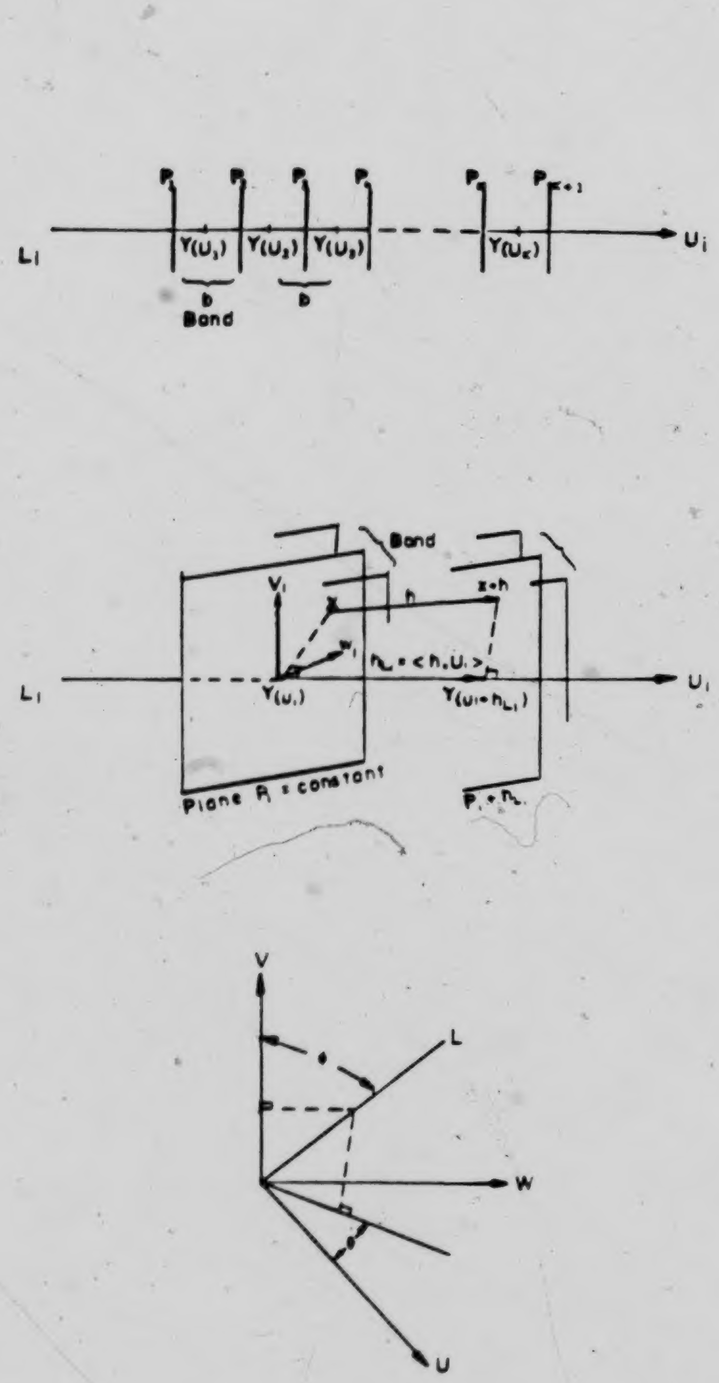
P1
P2
P3
P4
Pk
Pk+1
L1
Y(U1)
Y(U2)
Y(U3)
Y(Uk)
Ui
b
Band
b
Band
V1
x
h
x+h
W1
hL = <h,U1>
L1
Y(U1)
Y(U1+hL1)
U1
Plane P1 = constant
P1 + hL
V
L
W
U

Figure 3.2 The turning bands method (modified after Journel, 1974b).

icosahedron. Accordingly, equation (3.5.2.3) becomes:

$$z_s(x)=1/\sqrt{15}\ \Sigma_{i=1}^{15} z_i(x) \tag{3.5.3.1}$$

and the corresponding covariance is:

$$C^*(h)=1/15\ \Sigma_{i=1}^{15} C'(<h,u_i>) \tag{3.5.3.2}$$

Equation (3.5.3.2) is the icosahedron approximation of the covariance function C(h) given by equation (3.5.2.3). The difference between C(h) and $C^*(h)$ can be theoretically corrected on the basis of the geometric properties of the regular icosahedron (Journel, 1974a). In practice, this correction is omitted.

In equation (3.5.2.3), the sum $\Sigma_{i=1}^{n} z_i(x)$ is multiplied by $1/\sqrt{N}$. In this way, the *a priori* variance of $Z_s(x)$ is $C^*(0)$ (Journel and Huijbregts, 1978).

The random function $Z_s(x)$, according to the described theory, has an expectation $E\{Z_s(x)\}=0$ and accordingly the simulated stochastic field has a mean of zero. A constant m can be added to each simulated point producing a realization with a mean equals to m. If a strictly intrinsic field is to be simulated then to each point of the simulated realization of $Z_s(x)$ the drift m(x) is added.

In the case of simulation of an anisotropic stochastic field, two cases can be distinguished. If the field to be simulated is to be geometrically anisotropic, then, as in the case of kriging, the directional covariances (or variograms) are transformed to isotropic. Simulation is performed in an isotropic field and this field is transformed to geometrically anisotropic by simply scaling the corresponding three dimensional unit vectors.

In the case of zonal anisotropy, several fields are simulated. Each of these fields has a covariance function corresponding to one of the nested structures which constitute the covariance of the zonally anisotropic random function to be simulated. The simulated realizations are finally added at each point. The result is a realization of the zonally anisotropic random function.

Simulation of points in R^3 may be further developed in order to produce realizations on a volume support.

The physical meaning of the turning band method may also be considered. A deposit is envisioned as a result of many one dimensional physical processes. Accordingly, the three dimensional random function corresponding to the deposit is a result of many one dimensional random functions which correspond to the one dimensional physical processes. Apparently the three dimensional stochastic structure of the deposit will be a product of the one dimensional stochastic structures of the one dimensional physical processes.

In practice, many realizations of a random function Z(x) defining a physical phenomenon can be produced. The number of these realizations may be reduced by conditioning the simulated realization. That is, to 'force' somehow the simulated realizations to respect the available data. This procedure is called 'conditional simulation' and it can provide more realistic models of the spatial variability of a characteristic of a deposit.

3.6 Conditional Simulation

Let $z_0(x)$ be a true value of a regionalized variable at point x . From an available set of data, we can estimate the value $z^*_{OK}(x)$ using kriging. The following equation can be formed:

$$z_0(x)=z^*_{OK}(x)+[z_0(x)-z^*_{OK}(x)] \tag{3.6.1}$$

where $[z_0(x)-z^*_{OK}(x)]$ is the unknown kriging error. In terms of random functions, equation (3.6.1) becomes:

$$Z(x)=Z^*_K(x)+[Z(x)-Z^*_K(x)] \tag{3.6.2}$$

The kriging error has the property that it is orthogonal to (independent of) the kriging estimate (Journel and Huijbregts, 1978, p.496), as follows:

$$E\{Z^*_K(y)[Z(x)-Z^*_K(x)]\}=0 \quad , \forall \; x,y$$

This suggests that we can simulate realizations of the error $[Z(x)-Z^*_K(x)]$ and add them to $Z^*_K(x)$ since the real error is not known. This requires that the kriging error and the simulated error are isomorphic (i.e. can admit the same covariance).

If we consider a random function $Z_s(x)$ independent of $Z(x)$ but isomorphic to it, analogous kriging procedure leads to:

$$Z_s(x)=Z^*_{sK}(x)+[Z_s(x)-Z^*_{sK}(x)] \tag{3.6.3}$$

If realizations of $Z_s(x)$ are known, the estimation error $[Z_s(x)-Z^*_{sK}(x)]$ is also known, and since $Z_s(x)$ isomorphic to $Z(x)$, the corresponding errors are also isomorphic to each other.

We can now define a random function $Z_{cs}(x)$ isomorphic to $Z(x)$ as follows:

$$Z_{cs}(x)=Z^*_K(x)+[Z_s(x)-Z^*_{sK}(x)] \tag{3.6.4}$$

The defined random function $Z_{cs}(x)$ has the following properties:

i) It is isomorphic to $Z(x)$ in terms of the variogram function but not necessarily in terms of the covariance (Journel and Huijbregts, 1978, p.498).

ii) It has the same expectation with $Z(x)$. This follows as a consequence of the unbiased kriging estimator, as follows:

$$E\{Z(x)-Z^*_K(x)\}=0$$

or

$$E\{Z(x)\}=E\{Z^*_K(x)\}$$

and similarly:

$$E\{Z_s(x)\}=E\{Z^*_{sK}(x)\}$$

which entails to:

$$E\{Z_{cs}(x)\}=E\{Z^*_K(x)+[Z_s(x)-Z^*_{sK}(x)]\}=E\{Z(x)\}\ ,\ \forall x$$

iii) Simulated realizations of $Z_{cs}(x)$ are conditioned to the available data. This is because, at a data point x_α, there will be:

$$Z^*_K(x_\alpha)=Z(x_\alpha)$$

due to the exactness of kriging as interpolator. Also, for the same reason:

$$Z_s(x_\alpha)=Z^*_{sK}(x_\alpha)$$

or

$$[Z_s(x_\alpha)-Z^*_{sK}(x_\alpha)]=0$$

which, if substituted in equation (3.6.4), entails to:

$$Z_{cs}(x_\alpha)=Z(x_\alpha)$$

iv) The estimation variance of the conditional simulated values $Z_{cs}(x)$ is twice the kriging variance of the values $Z^*_K(x)$. This is because the estimation variance is:

$$E\{(Z(x)-Z_{cs}(x))^2\}=$$

$$E\{(Z(x)-Z^*_K(x)-[Z_s(x)-Z^*_{sK}(x)])^2\}=$$

$$E\{([Z(x)-Z^*_K(x)]-[Z_s(x)-Z^*_{sK}(x)])^2\}=$$

$$E\{[Z(x)-Z^*_K(x)]^2+[Z_s(x)-Z^*_{sK}(x)]^2$$

$$-2[Z(x)-Z^*_K(x)][Z_s(x)-Z^*_{sK}(x)]\}$$

which, taking into account the independence of the two kriging errors and their zero expectation, entails to:

$$E\{[Z(x)-Z^*_K(x)]^2\} + E\{[Z(x)-Z^*_K(x)]\}=$$

$$2E\{[Z(x)-Z^*_K(x)]^2\}=2\sigma_K^2$$

or

$$E\{[Z(x)-Z_{cs}(x)]^2\}=2\sigma_K^2$$

v) With respect to simulation models conditional simulation adds a accuracy by respecting the available data. The conditioning also produces more robust models because it adds local characteristics. It also, with respect to kriging models, is advantageous in its aspect that it respects, without substituting reality, the spatial variability of the regionalized phenomenon (Figure 3.3b).

4. DATA ANALYSIS AND DATA-BASE CONSTRUCTION

Two main sets of data were made available for this study. The first consisted of elevations of the top of the McMurray Formation, the Devonian unconformity, and the collar elevation from 306 vertical wells (Figure 2.9). The elevations were in metres from the mean sea level. Formation tops were picked from core. The location of each of the 306 wells, in both U.T.M. and D.L.S systems, was included in the same data set.

The second set of data consisted of 12,608 samples, corresponding to the weight percent oil saturation of the same number of intervals. The top and bottom of each interval, in metres from the collar elevation, was given. These intervals were not necessarily continuous and their thickness varied from 0.2 to 4 metres. All saturation measurements were from core analyses of 187 wells within the study area. For the rest of the wells of the study area, no information on bitumen saturation was available.

Because data accuracy is a requirement for realistic geostatistical modelling, the quality of the data provided for this study was carefully evaluated.

In the first data set, the elevations of the top and bottom of the McMurray Formation were cross-checked against the available geophysical logs of each well. No significant differences were found with the exception of a restricted number of wells (approximately 3%). In the case of significant differences, the elevations determined from logs were used. It must also be noted that in the location of the wells, an expected error of ±30 metres may exist. A similar, but smaller, error may also exist in the measurement of collar elevations.

In the second data set, extensive inaccuracies were detected. These inaccuracies consisted of overlapping successive intervals. In order to correct the problem, geophysical logs were used in a qualitative way. If the overlapping intervals were a rich one and a poor one in terms of oil content, the boundary between the two samples was preferably determined using resistivity and gamma-ray logs. If the two intervals were both rich or poor, the bottom of the first (top) interval was considered as the boundary. It is also interesting to note that in testing the bitumen content of some samples from the data set versus the bitumen content of the same intervals calculated from logs, the given data were found to usually indicate higher oil saturations. No modifications were, however, made in the data set.

To the data provided a third data set was added. This consists of the elevations of the tops and bottoms of the six zones, as defined in chapter two, for each of the 306 wells of the study area.

4.1 Data Evaluation

It is apparent that small inaccuracies in the first data set did not influence the modelling procedure. This is due to the fact that (i) the main oil-saturated zones were not very close to the top or the bottom of the McMurray Formation and (ii) possible inaccuracies in the collar elevation or the exact location of the wells are a part of reality .

The accuracy of the models produced was influenced, to a degree, by the apparent errors in the second data set, but the bias introduced by these errors was minimal after the corrections were made.

When the data on a regionalized variable are expressed over significantly different thicknesses, (or volumes) geostatistical treatment requires their averaging (regularization) over constant thickness (or volume). Accordingly, the raw data on weight percent oil saturation were transformed and expressed over samples of equal length of one metre.

The raw data in the second data set were substituted by the regularized samples (9,260). The regularization procedure, described in Appendix I, has smoothed the raw data, but since the length of the regularized samples was almost equal to the average sample length (0.96 m), no bias was introduced.

The third data-set, composed of the tops of the different zones into which the McMurray Formation was divided, could be only evaluated in terms of the homogeneity of the zones it defined.

4.2 Simple Statistics as a Test for Homogeneity

The conceptual robustness in geostatistical modelling was based in this study, as already discussed, on the delineation of geological domains within which the bitumen was distributed. In chapter two, six zones were defined. These zones are geologically homogeneous as far as the depositional environment of each case was concerned. It was, however, necessary to statistically verify this homogeneity. If homogeneity was present, the frequency curve of the oil saturation in each zone will would be unimodal and it would tend towards one of the known and well defined frequency curves. If not, geology should provide a reasoning and a solution.

In figures 4.1, 4.2, 4.7 and 4.8, relative frequency histograms of the oil saturation of the six zones are plotted. The distribution in zones 1, 2 and 3 are bimodal, suggesting that the zones are considered homogeneous and that further division was required.

The bimodal shape of the histograms in zones 1, 2 and 3 was expected because of the existence in the same zone of both shaly facies with low bitumen saturations and sand bodies with high bitumen concentration.

If the definition of different geological domains was based on a detailed study of the sedimentary facies of the

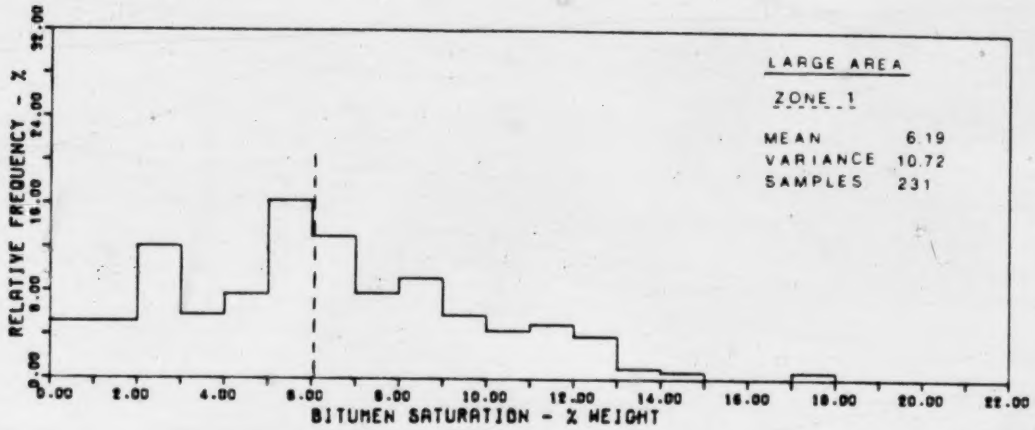

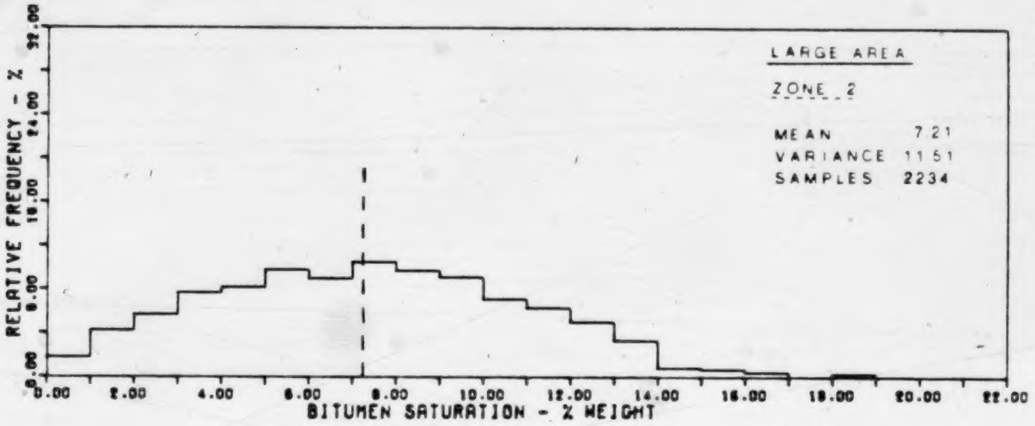

Figure 4.1 Histograms of oil saturation according to the first classification in zones 1 (top) and 2 (bottom).

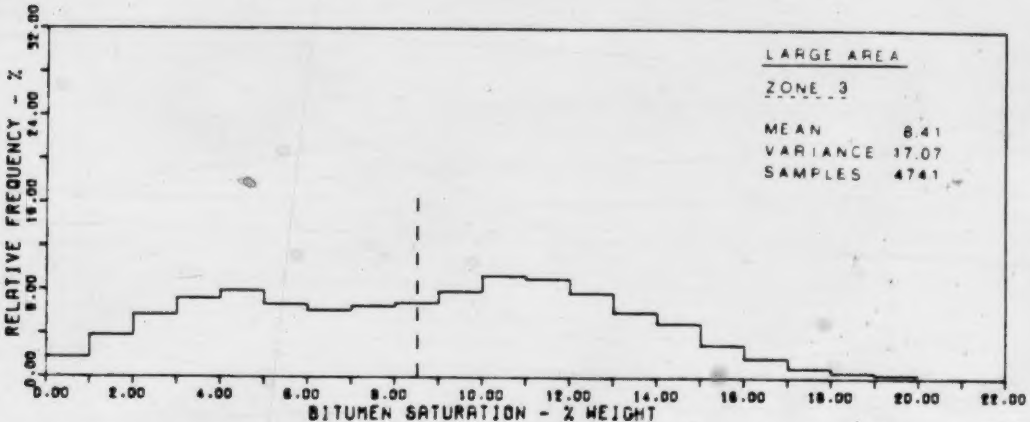

Figure 4.2 Histogram of oil saturation according to the first classification in zone 3.

of the McMurray Formation, homogeneity should be easily obtained. Since a detailed sedimentological analyses was not available, and was deyond the scope of this study, homogeneity was obtained to a reasonable extent on the basis of more engineering than geological criteria, as follows.

Large and rather continuous sand channels appear to exist in zone 3. Smaller and non-continuous sand bodies appear to be present in zone 2. This suggested that a new zone could be established between zones 2 and 3 which would include shaly facies at the top of zone 3 and the bottom of zone 2. Also, shaly facies at the top of zone 2 were included in zone 1. As a result of this procedure, 7 zones were finally established (Figures 4.3 and 4.4).

The relative frequency histograms of each zone were plotted (Figures 4.5, 4.6, 4.7 and 4.8). All distributions after the second classification appear unimodal and, accordingly, each zone was considered statistically homogeneous. The frequency curves in zones 2, 4 and 6 (main oil saturated sand bodies) approximated normal distributions, but were skewed. The mean and variance of all distributions are given in Table 4.1.

From a geological point of view, the reclassification of the different domains may not completly reflect reality, but at least as far as the three main bitumen saturated zones are concerned, geological homogeneity continued to exist.

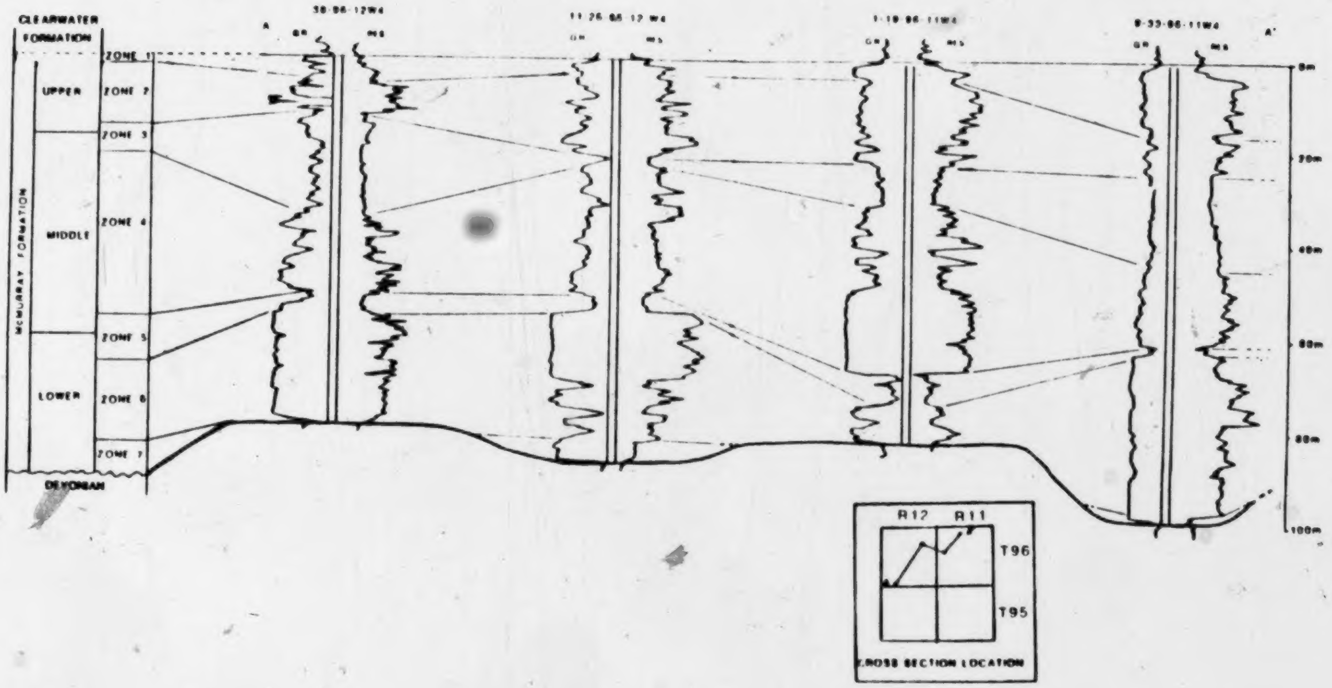
CLEARWATER FORMATION
MCMURRAY FORMATION
UPPER
MIDDLE
LOWER
ZONE 1
ZONE 2
ZONE 3
ZONE 4
ZONE 5
ZONE 6
ZONE 7
DEVONIAN
A
38-96-12W4
GR
MS
11-26-95-12 W4
GR
MS
1-19-96-11W4
GR
MS
9-33-96-11W4
GR
MS
A'
0m
20m
40m
60m
80m
100m
R12
R11
T96
T95
CROSS SECTION LOCATION

Figure 4.3 Stratigraphic cross-section A-A' of the McMurray Formation in the study area. Note that the delineation of the different zones is according to the second classifi cation.

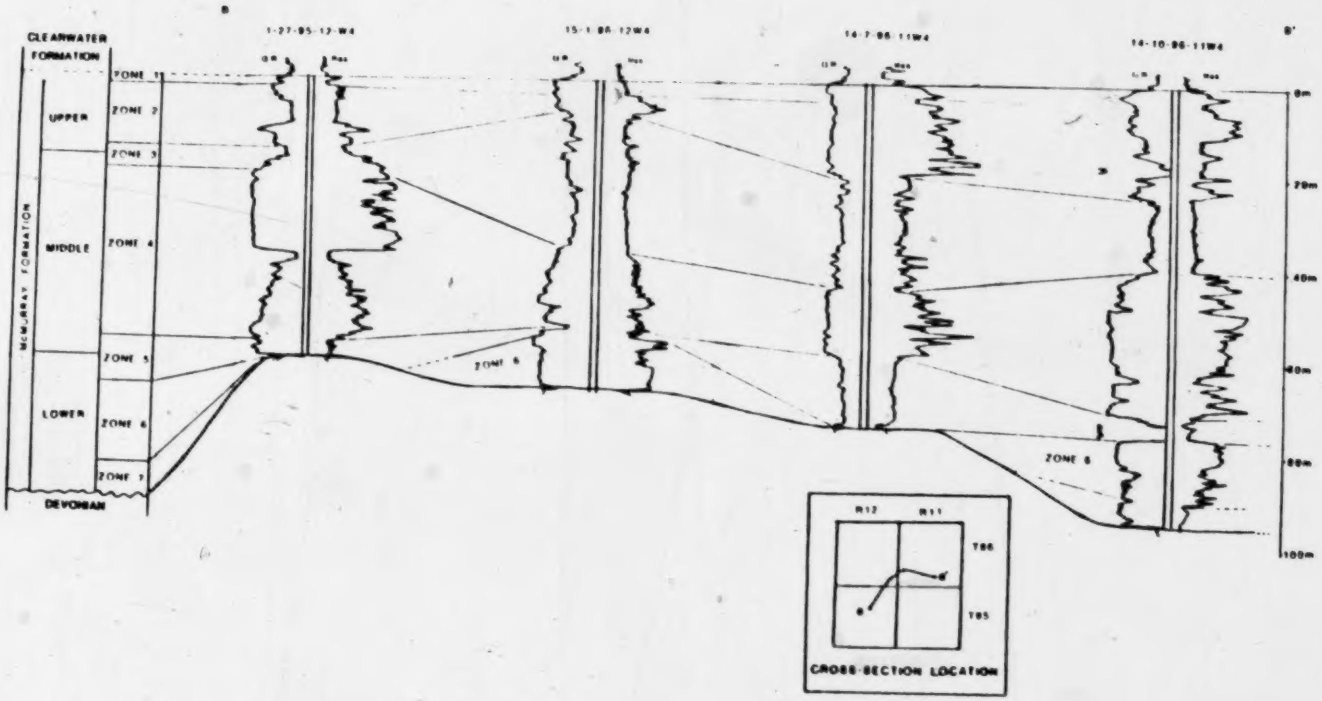
B
B'
1-27-95-12-W4
15-1-86-12W4
14-7-86-11W4
14-10-86-11W4
GR
Res
CLEARWATER FORMATION
MCMURRAY FORMATION
UPPER
MIDDLE
LOWER
DEVONIAN
ZONE 1
ZONE 2
ZONE 3
ZONE 4
ZONE 5
ZONE 6
ZONE 7
ZONE 8
0m
20m
40m
60m
80m
100m
R12
R11
T86
T85
CROSS-SECTION LOCATION

Figure 4.4 Stratigraphic cross-section B-B' of the McMurray Formation in the study area. Note that the delineation of the different zones is according to the second classification.

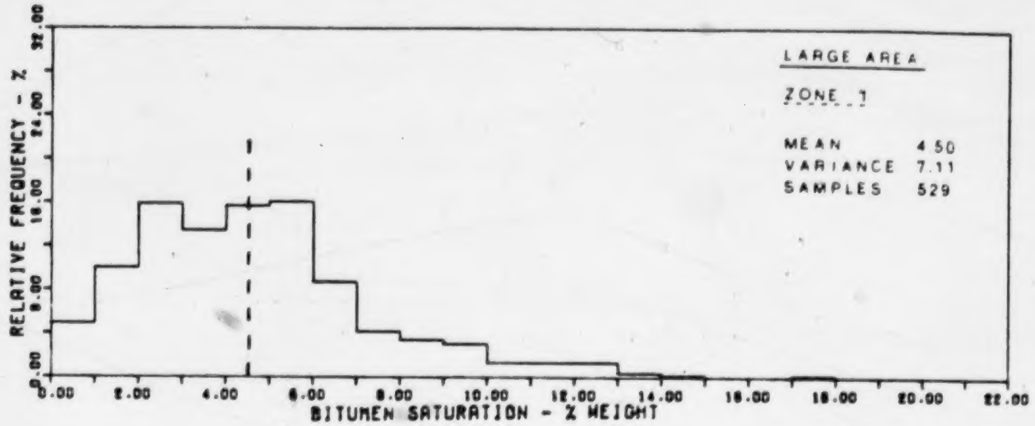

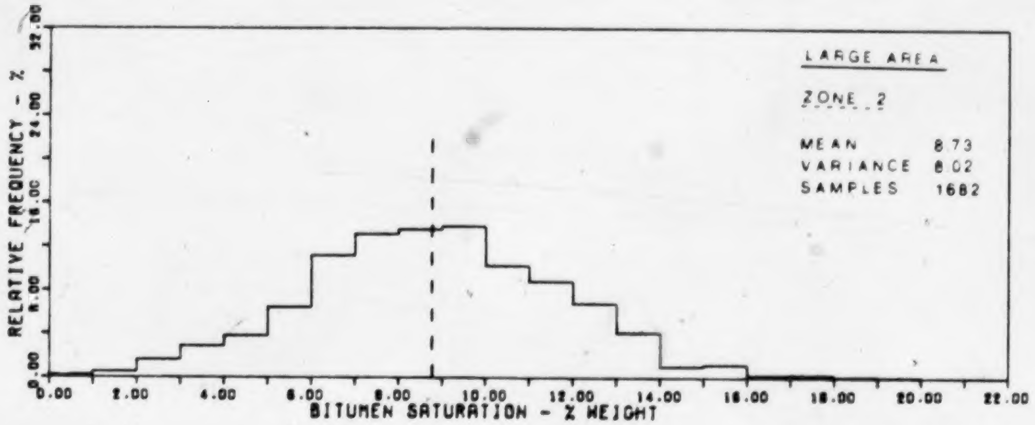

Figure 4.5 Histograms of oil saturation according to the second classification in zones 1 (top) and 2 (bottom).

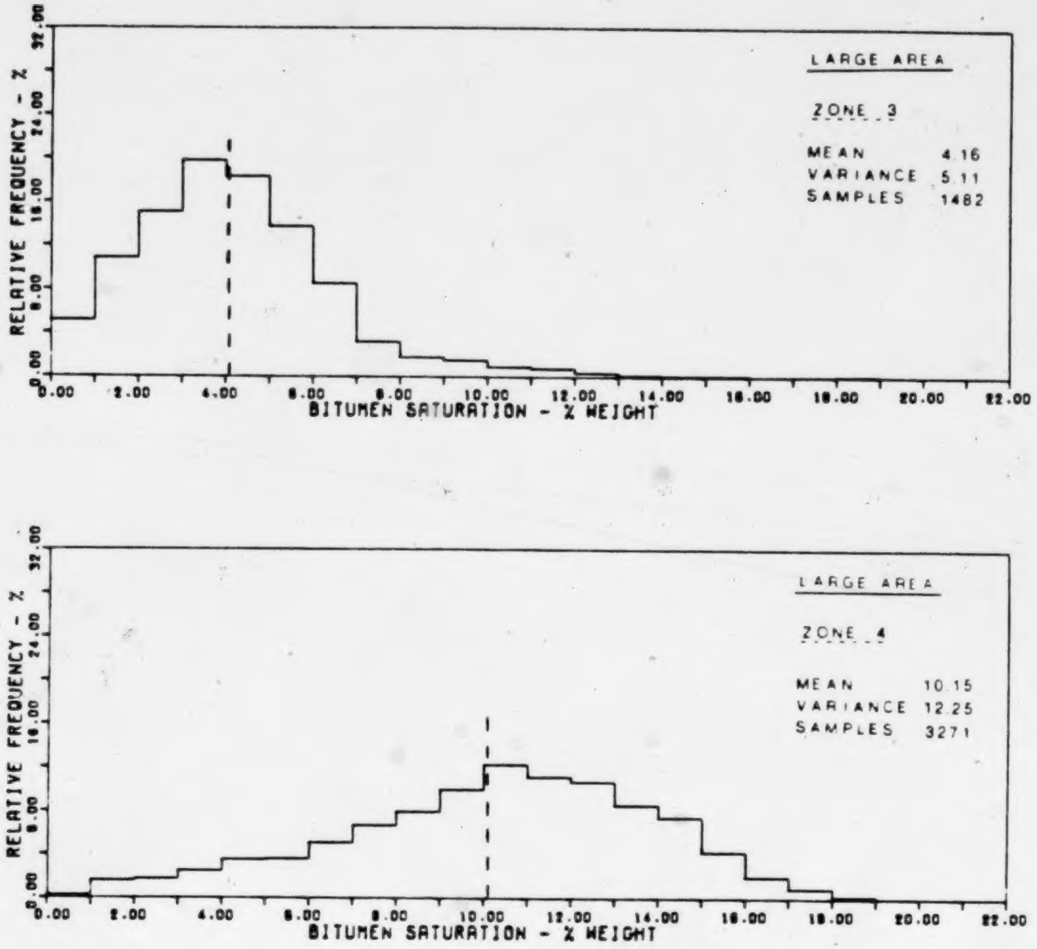

Figure 4.6 Histograms of oil saturation according to the second classification in zones 3 (top) and 4 (bottom).

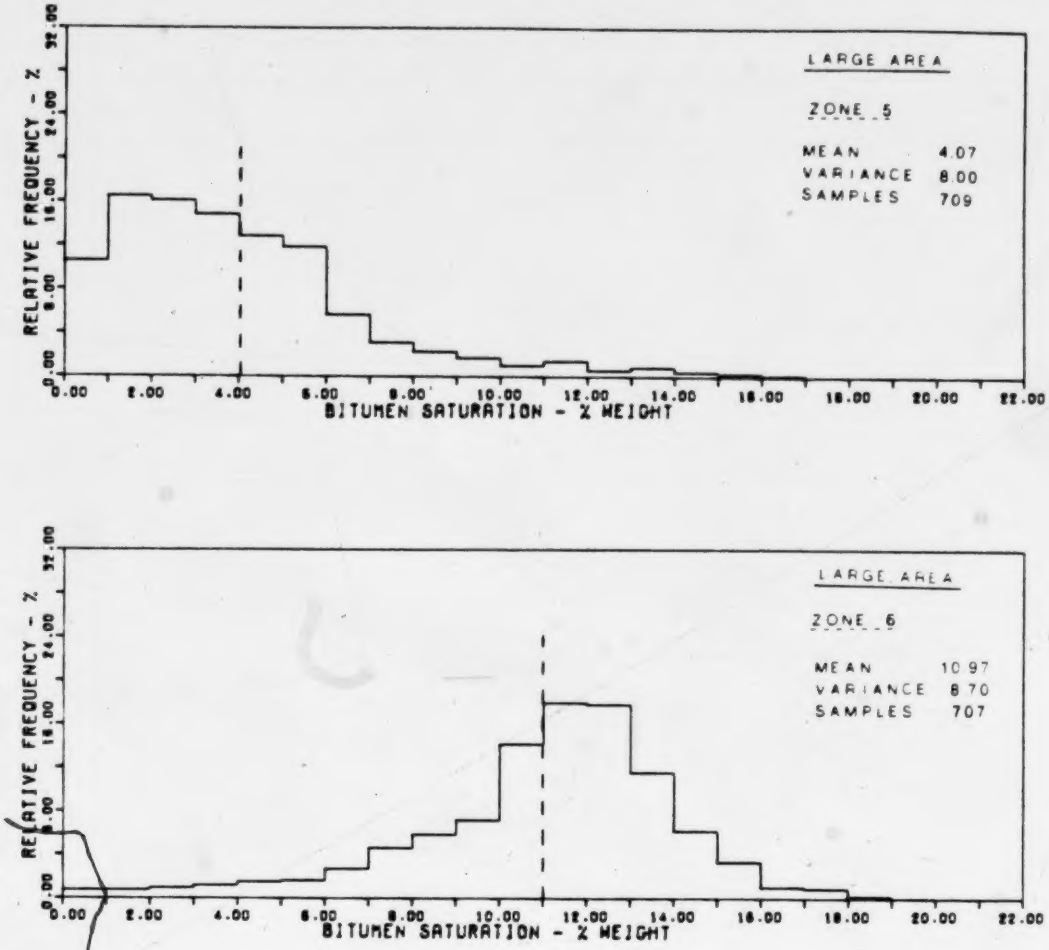

Figure 4.7 Histograms of oil saturation according to the second classification in zones 5 (top) and 6 (bottom). Note that zones 5 and 6 are the same as zones 4 and 5 of the first classification.

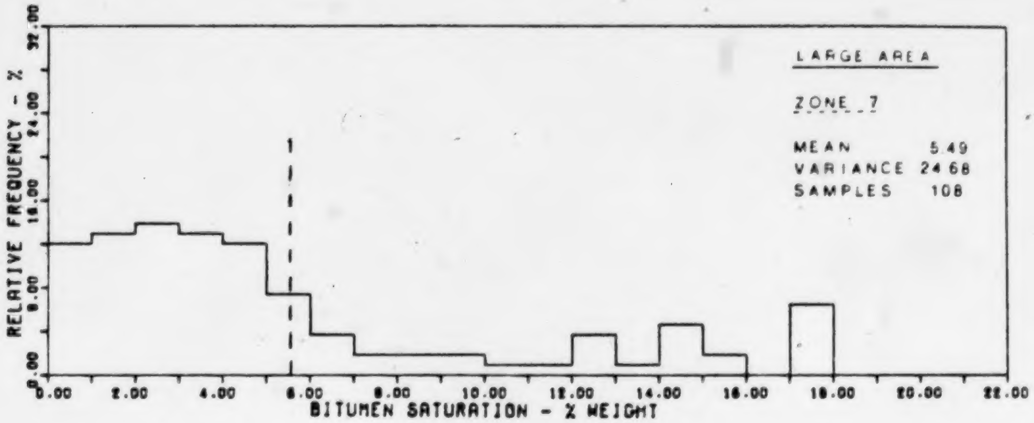

Figure 4.8 Histogram of oil saturation according to the second classification in zone 7. Note that zone 7 is the same as zone 6 of the initial classification.

TABLE 4.1 Summary statistics of the % bitumen for each zone in the large area.

Zone	Number of samples	Mean (weight %)	Variance (weight %)^2
1	529	4.50	7.11
2	1682	8.73	8.02
3	1482	4.16	5.11
4	3271	10.15	12.25
5	709	4.07	8.00
6	1604	10.97	8.70
7	108	5.49	24.68

In an operational sense, the new classification improved the establishment of the main 'ore'-bodies to be mined, while preserving their geological characteristics.

The third set of data was modified according to the new classification.

4.2.1 Data statistics in the control area

Within the study area, a control area of approximately 5.7 square kilometres was selected for detailed geostatistical reconstruction. This control area (Figure 2.9) included sections 7, 8 and 9 of Twp 96, Rng 11 W4M. It included 33 wells with an average spacing of 400 metres and 1,720 regularized samples on oil saturation, of 1 metre length each, were available.

The control area will be referred to as the small area in comparison with the total study area which will be referred to as the large area.

The relative frequency histograms of the oil saturations of each zone within the small area are depicted in Figures 4.9, 4.10, 4.11 and 4.12. They indicate that all distributions are unimodal with the distributions of zones 2, 4 and 6 tending towards the normal curve. The same distributions are less skewed than their equivalents in the large area.

The mean, variance and number of samples for each zone of the small area are given in Table 4.2.

The mean and variance of the elevations of the tops and bottoms of each zone of the small area as well as the average thickness are given in Table 4.3.

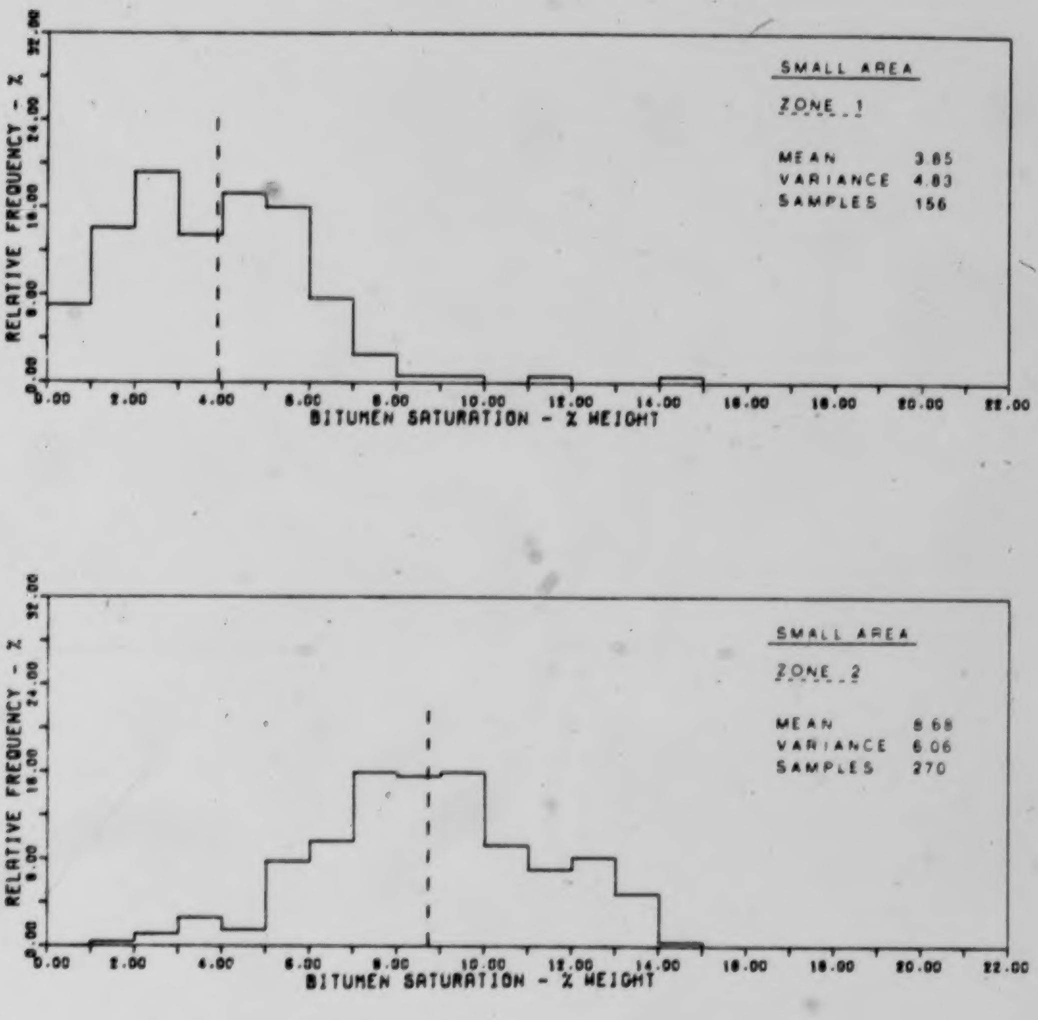

Figure 4.9 Histogram of oil saturation within the small area of zones 1 (top) and 2 (bottom).

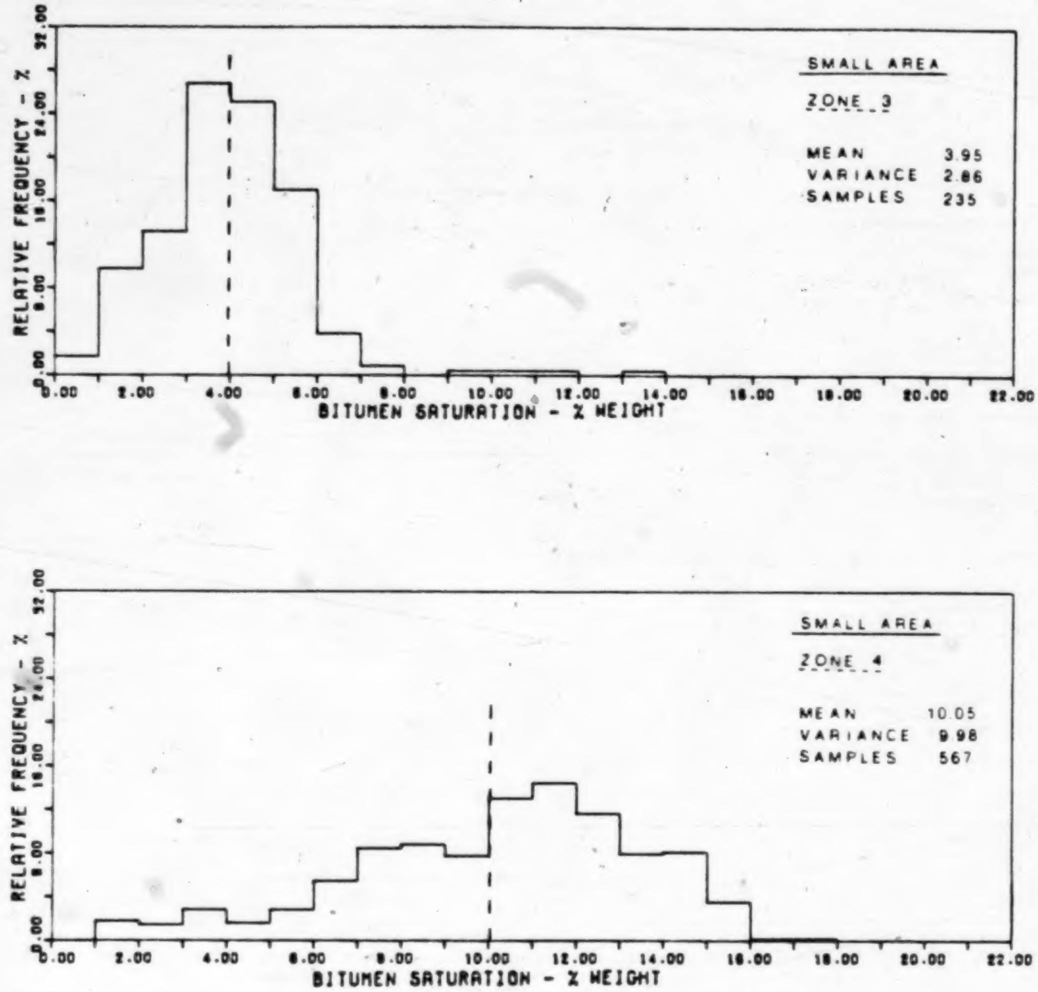

Figure 4.10 Histogram of oil saturation within the small are of zones 3 (top) and 4 (bottom).

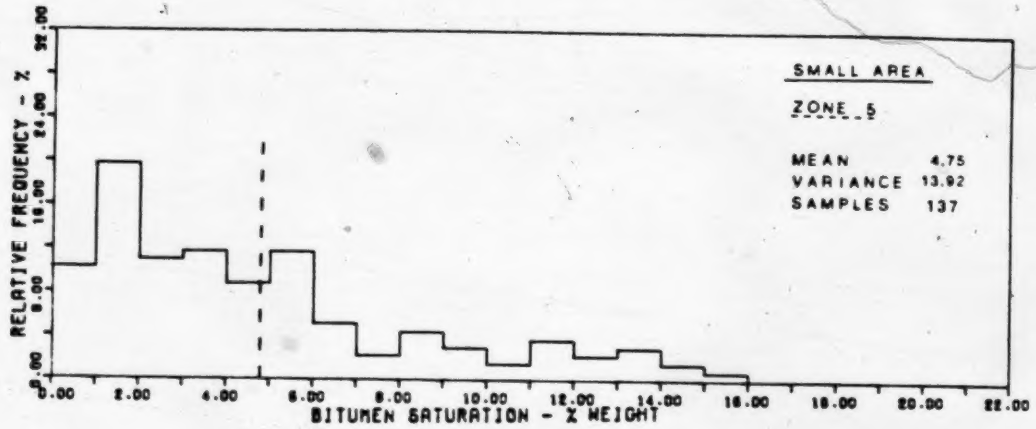

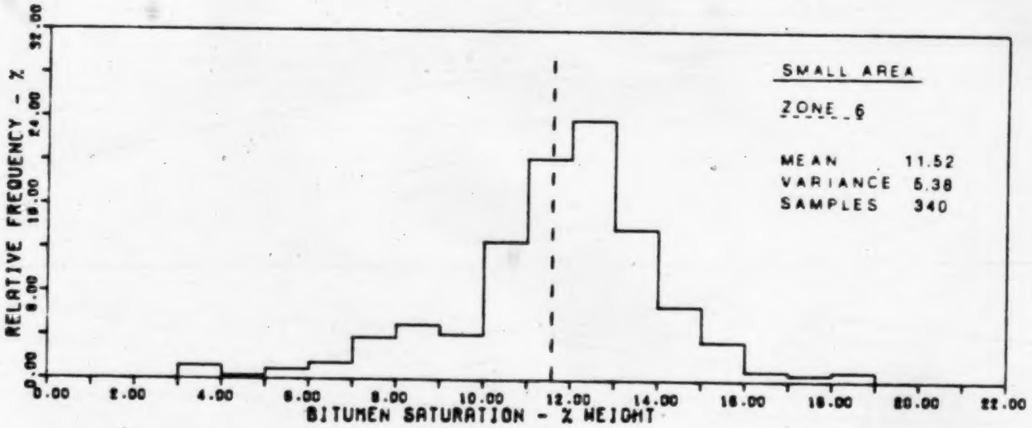

Figure 4.11 Histogram of oil saturation within the small area of zones 5 (top) and 6 (bottom).

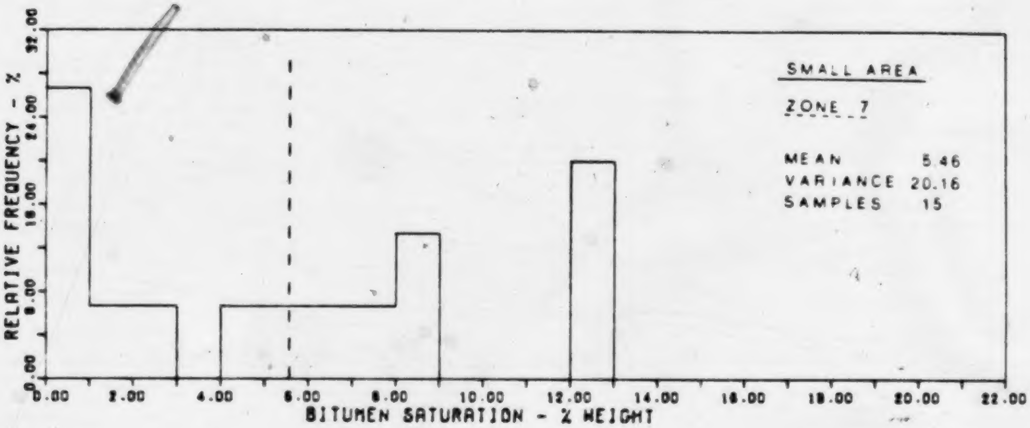

Figure 4.12 Histogram of oil saturation within the small are of zone 7.

TABLE 4.2 Summary statistics of the % bitumen for each zone in the small area.

Zone	Number of samples	Mean (weight %)	Variance (weight %)^2
1	156	3.85	4.83
2	270	8.68	6.06
3	235	3.95	2.86
4	567	10.05	9.98
5	137	4.75	13.92
6	340	11.52	5.38
7	15	5.46	20.16

TABLE 4.3 Summary statistics of the elevations of the zones tops and bottoms in the small area, and average thickness.

Zone	Number of samples	Mean (m)	Variance (m)^2	Average thickness (m)
Surface	33	293.9	67.08	
				7.6
1-top	33	286.3	40.52	
				14.0
2-top	33	272.0	50.96	
				11.3
3-top	33	260.7	109.50	
				9.1
4-top	33	251.6	150.30	
				25.9
5-top	33	226.4	178.70	
				10.7
6-top	33	215.7	150.80	
				19.1
7-top	33	196.6	118.20	
				2.7
7-bottom	33	193.9	85.19	

5. STRUCTURAL ANALYSIS OF THE ATHABASCA OIL-SANDS

Structural analysis in geostatistical terminology is considered to be the mathematical modelling of the stochastic structure of the regionalized phenomenon under study using variogram models.

The geological characteristics analysed in this study, were the weight percent oil saturation and elevations of top and bottom of each of the 7 zones in the McMurray Formation. These characteristics are regionalized variables because they possess the following properties: they are distributed within geologically defined and bounded domains; they are additive; they are locally erratic and random but have a mean, functionally representable structural aspect.

Structural analysis (variography) was performed in both the large area (total study area) and the small area (control area).

All variograms of oil saturation were calculated on the same sample support (length of 1 metre). Because the support was very small, with respect to resolution distances, all experimental variograms were considered as point variograms, and were plotted in a normalized form using the variance of each sample set as the *a priori* variance. In each zone, experimental variograms of the oil saturation were calculated in the horizontal directions east-west northeast-southwest, north-south, northwest-southeast. The average horizontal and vertical variograms of each zone were also calculated. Average variograms were calculated for the elevations of the tops of each zone.

5.1 Variography within the Large Area

The available wells in the large area were not on a regular grid. Accordingly, directional horizontal experimental variograms were calculated by grouping the data as discussed in Chapter Three. The basic lag used was 600 metres. The angle of tolerance was set to 25° and the distance of tolerance equal to the basic lag. Vertical variograms were calculated using a basic lag of 1 metre.

The number of pairs for each point of the experimental variograms ranged from 500 to 12,000 and thus the variograms were considered as very reliable.

In zone 1, directional horizontal variograms (Figures 5.1. and 5.2) had approximate ranges of 2000 metres in the E-W and NE-SW directions. In the N-S and NW-SE directions, ranges were approximately 1500 metres. The vertical variogram (Figure 5.3 bottom) had a range of 5 metres. Fluctuation of the experimental curves around their sill, particularly in the N-S and NW-SE, indicate rather discontinuous sand bodies. The bitumen content of these sand bodies is low (mean weight percent oil 3.85).

In zone 2, directional horizontal variograms (Figures 5.4 and 5.5) appear as pure nugget effects. This is due to the fact that the existing oil saturated sand bodies have dimensions smaller than the minimum spacing (400 m) of the wells in the area and accordingly, they were not detected.

The vertical variogram (Figure 5.6 bottom) had a range of approximately 12 metres. The sand bodies in zone 2 are of small dimensions (less than 400 m) but they have relativelly high oil content (meam weight percent bitumen 8.68).

Zone 3 represents a barren zone. The existing bituminous sands are erratic, very restricted in extend and their oil content very low (mean weight percent oil 3.95). The directional horizontal variograms (Figure 5.7 and 5.8) exhibited ranges from less than 500 m to 1500 m and the vertical (Figure 5.9 bottom) approximately 14 metres.

In zone 4, directional variograms exhibited ranges of 1200 metres in the N-E and NE-SW directions as well as 1600 metres and 2000 metres in the directions N-S and NW-SE respectively (Figure 5.10 and 5.11). The vertical variogram of this zone (Figure 5.12 bottom) had a range of 13 metres. Directional variograms also indicated a better continuity in the N-S and NE-SW directions. This together with the high mean oil saturation (10.05) reveal that zone 4 represents a main 'ore'-body.

Zone 5 represents a barren zone. Directional variograms (Figure 5.13 and 5.14)indicated no apparent structure. The vertical variogram (Figure 5.15 bottom) exhibited a range of 6 metres.

In zone 6, directional variograms (Figure 5.16 and 5.17) reached their sill in 1200 metres, 1000 metres, 1600 metres and 2000 metres in the directions E-W, NE-SW, N-S and NW-SE respectively. The same variograms became unstable at

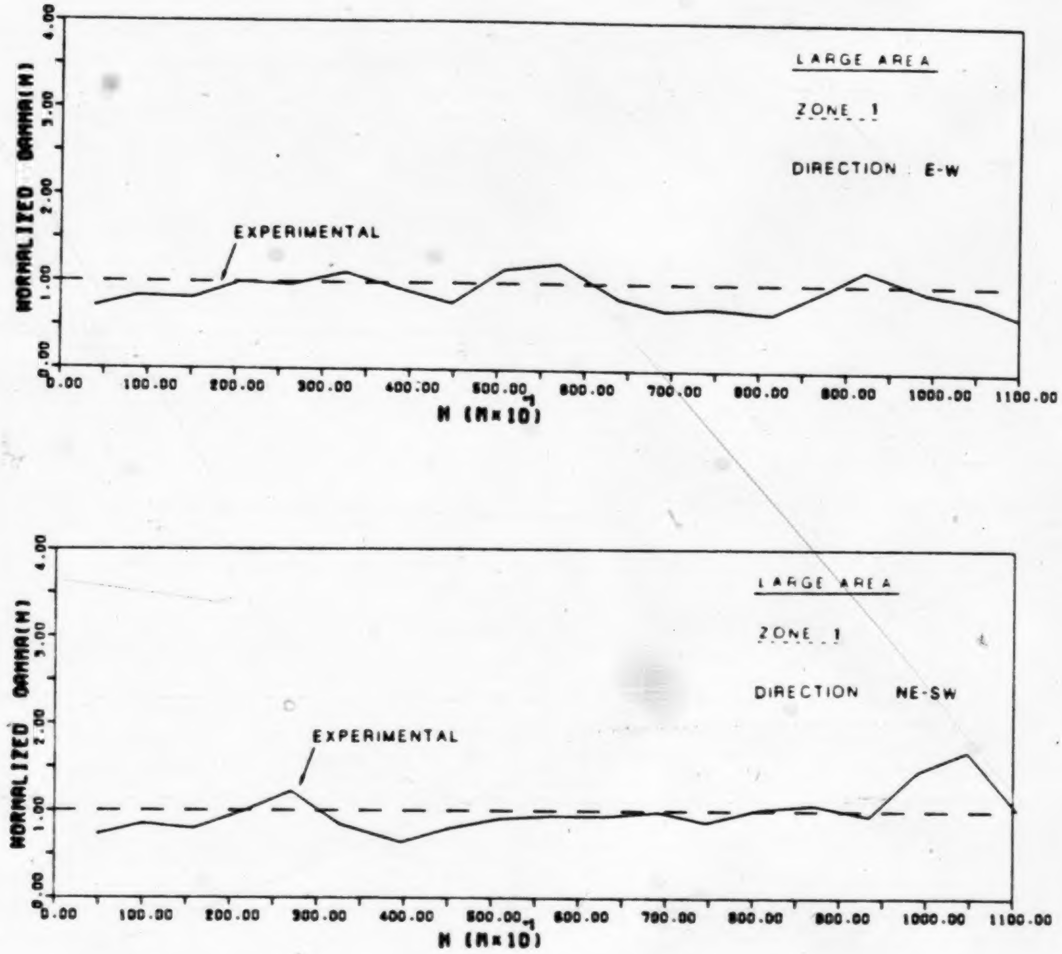

Figure 5.1 Experimental variograms of oil saturation in zone 1, large area, in the E-W (top) and NE-SW (bottom) directions.

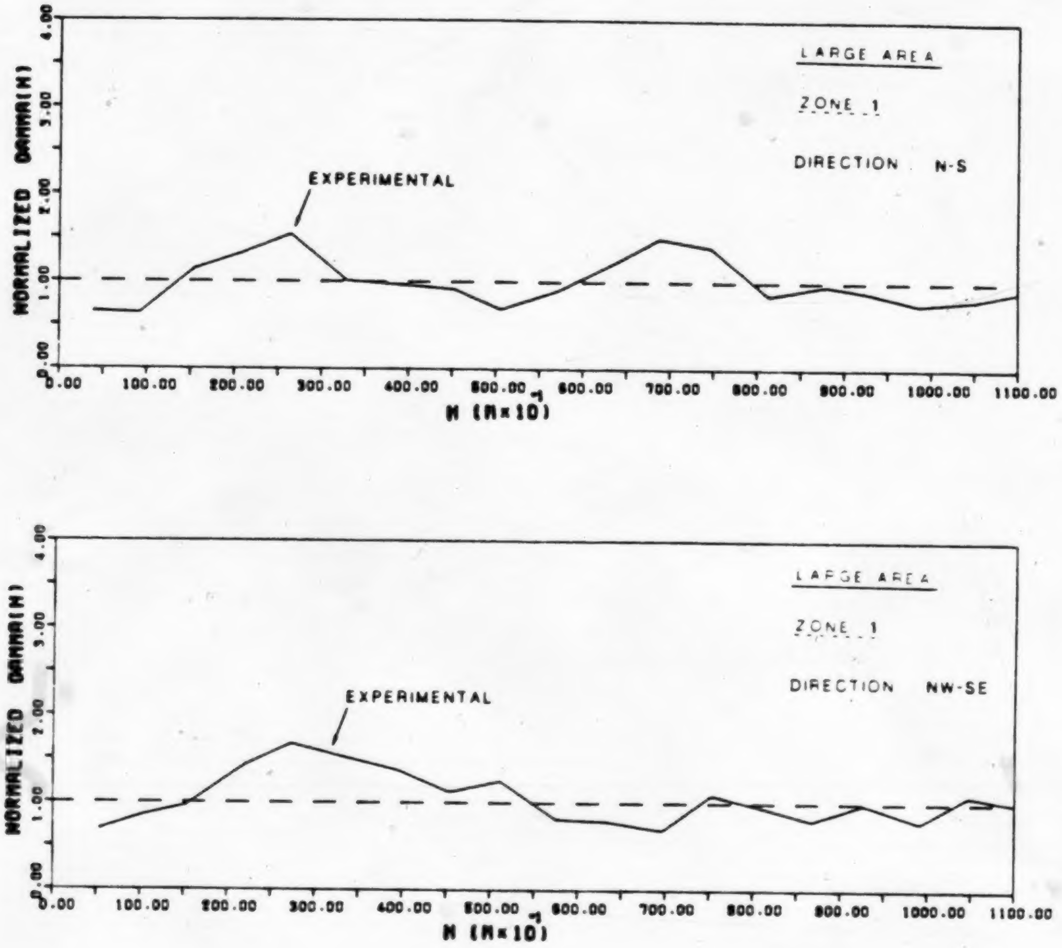

Figure 5.2 Experimental variograms of oil saturation in zone 1, large area, in the N-S (top) and NW-SE (bottom) directions.

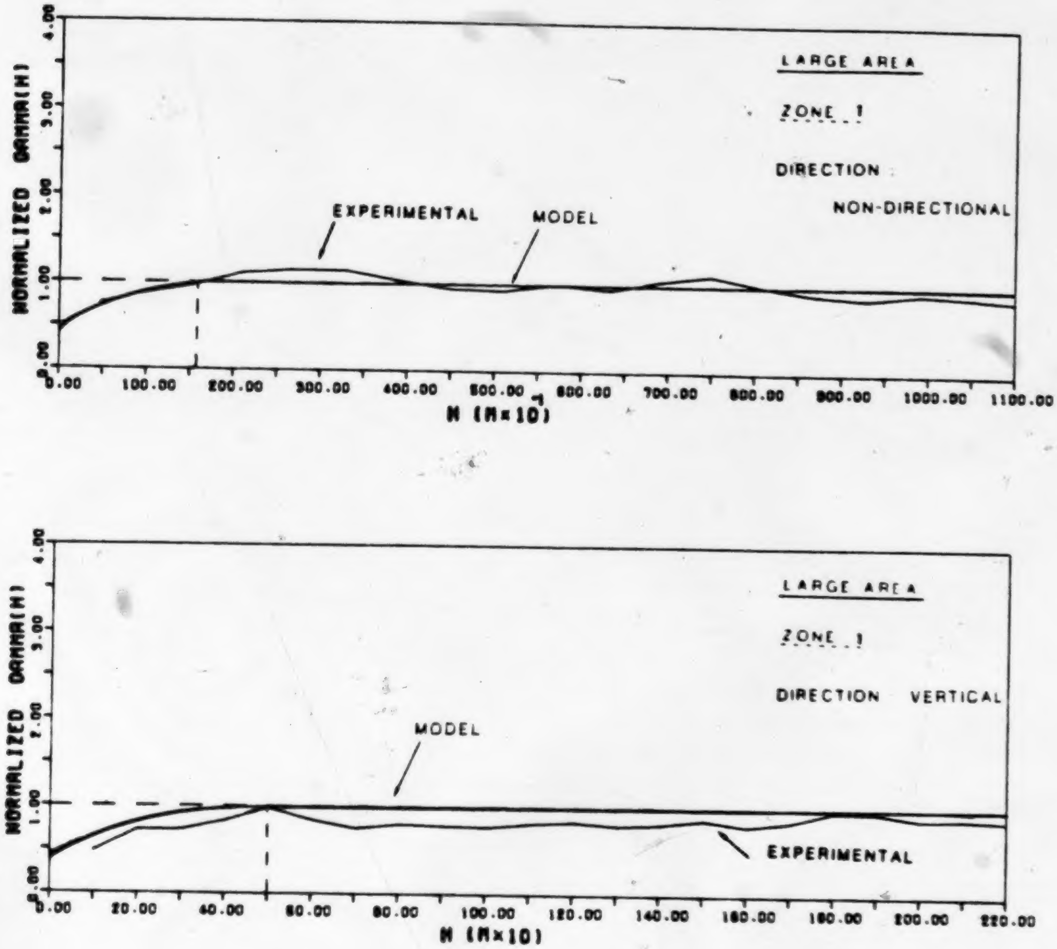

Figure 5.3 Experimental and model variograms of oil saturation in zone 1, large area; average horizontal (top) and vertical (bottom).

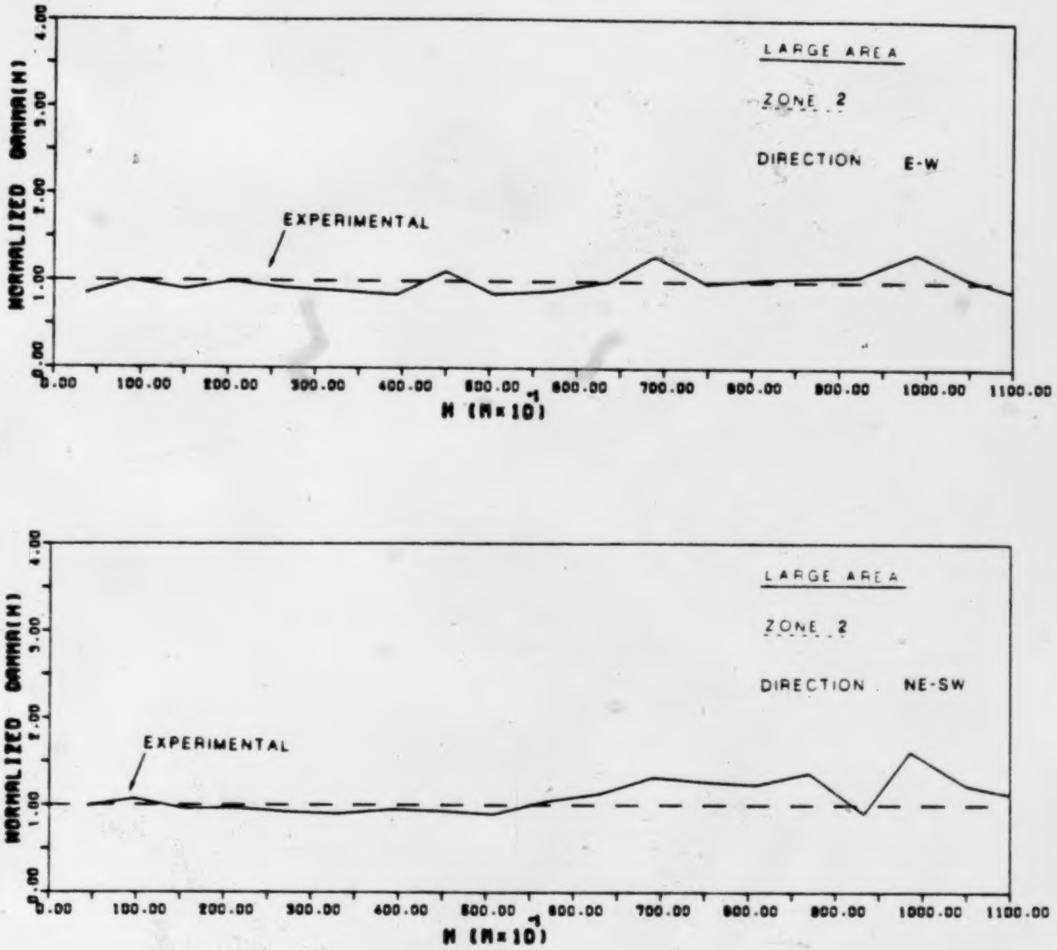

Figure 5.4 Experimental variograms of oil saturation in zone 2, large area, in the E-W (top) and NE-SW (bottom) directions.

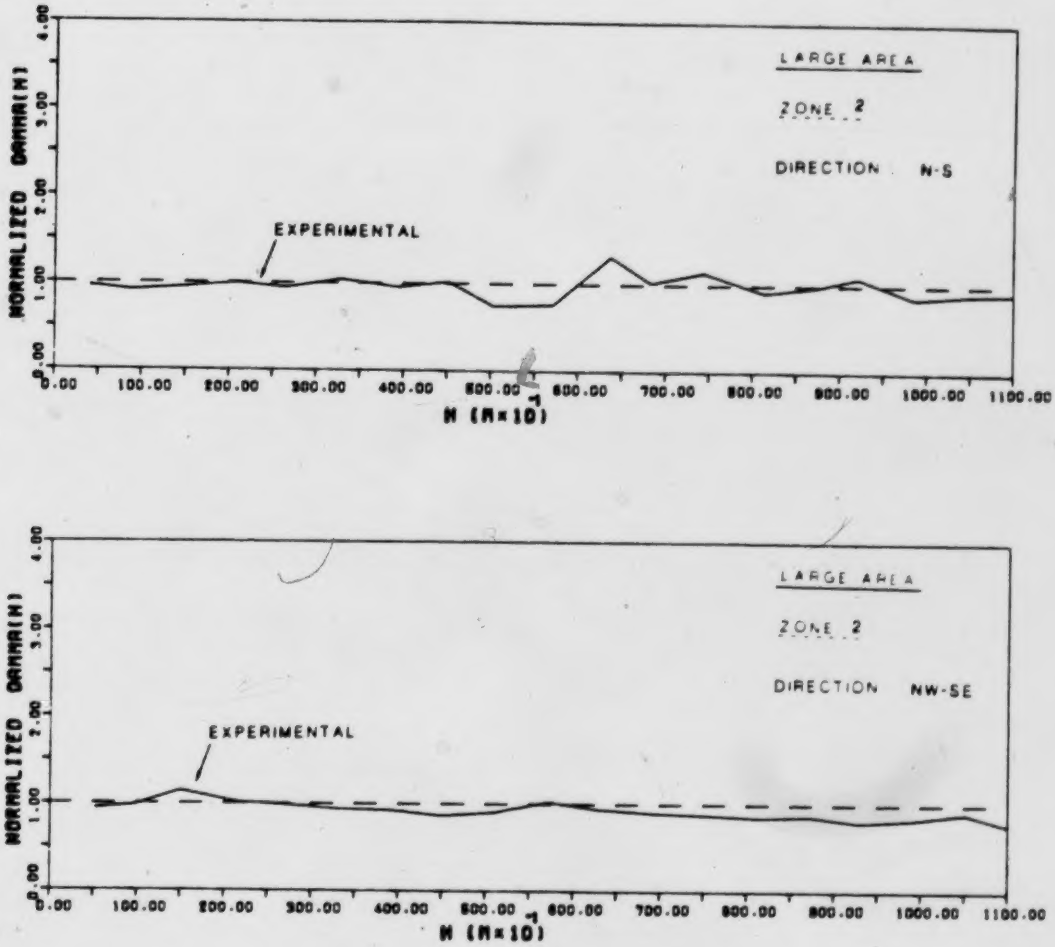

Figure 5.5 Experimental variograms of oil saturation in zone 2, large area, in the N-S (top) and NW-SE (bottom) directions.

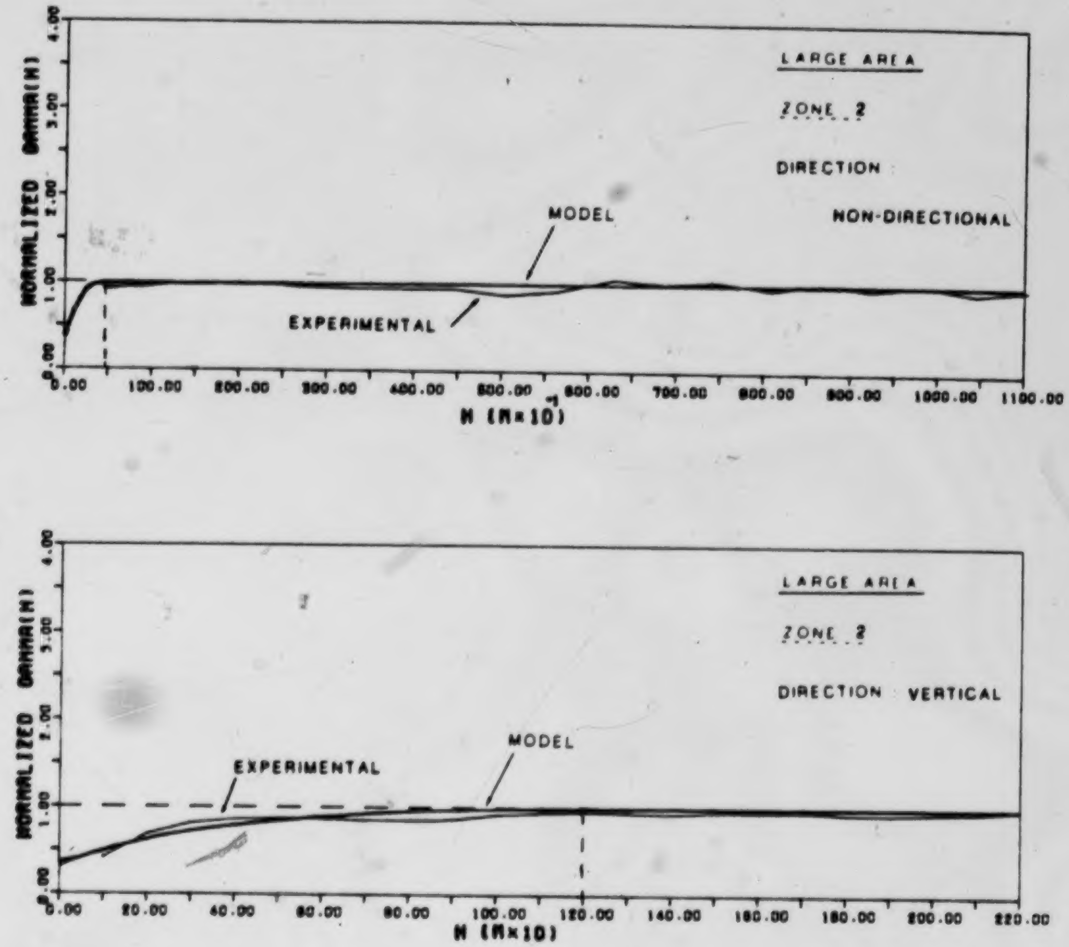

Figure 5.6 Experimental and model variograms of oil saturation in zone 2, large area; average horizontal (top) and vertical (bottom).

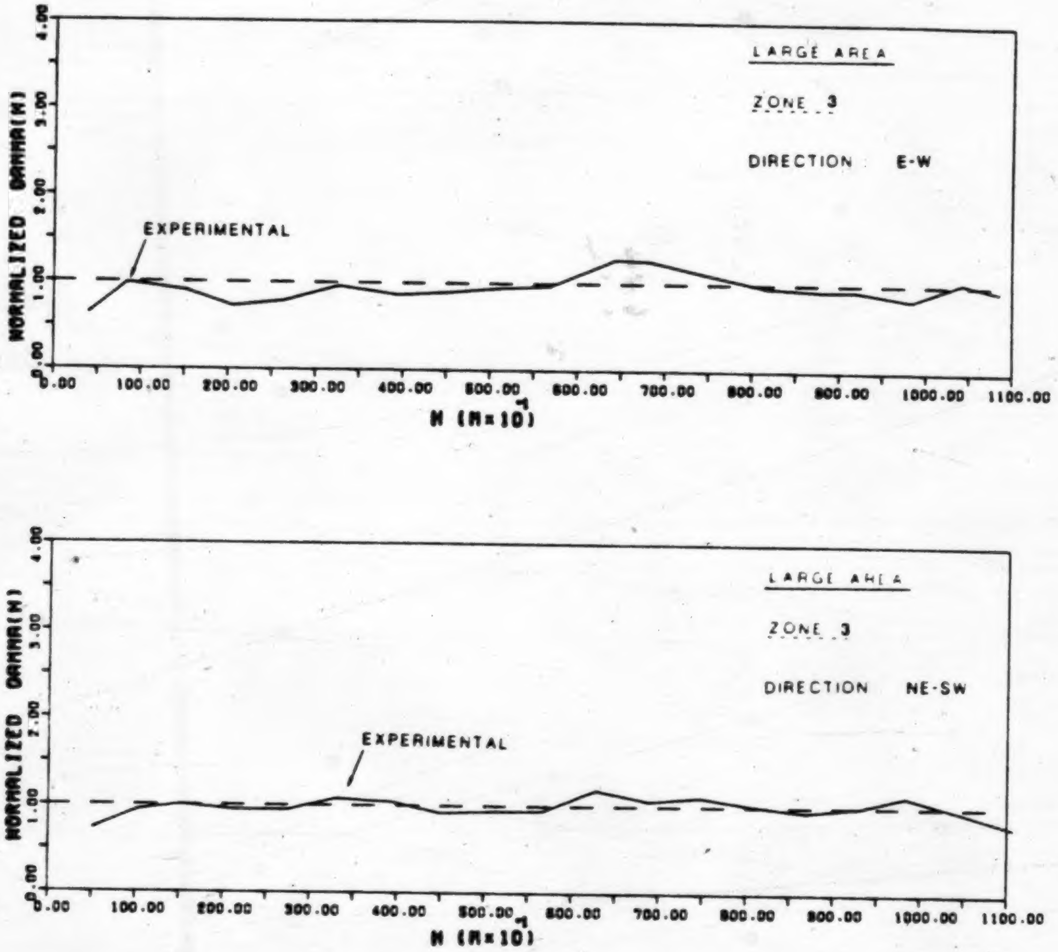

Figure 5.7 Experimental variograms of oil saturation in zone 3, large area, in the E-W (top) and NE-SW (bottom) directions.

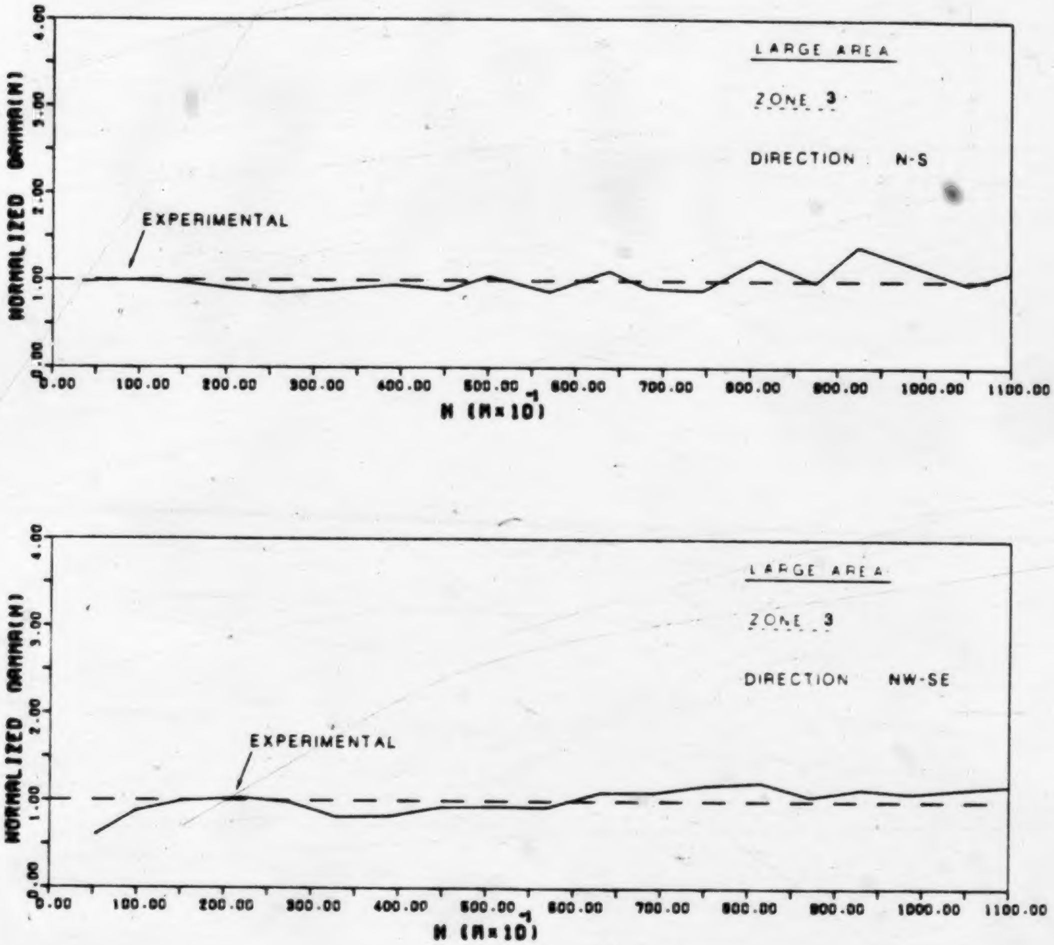

Figure 5.8 Experimental variograms of oil saturation in zone 3, large area, in the N-S (top) and NW-SE (bottom) directions.

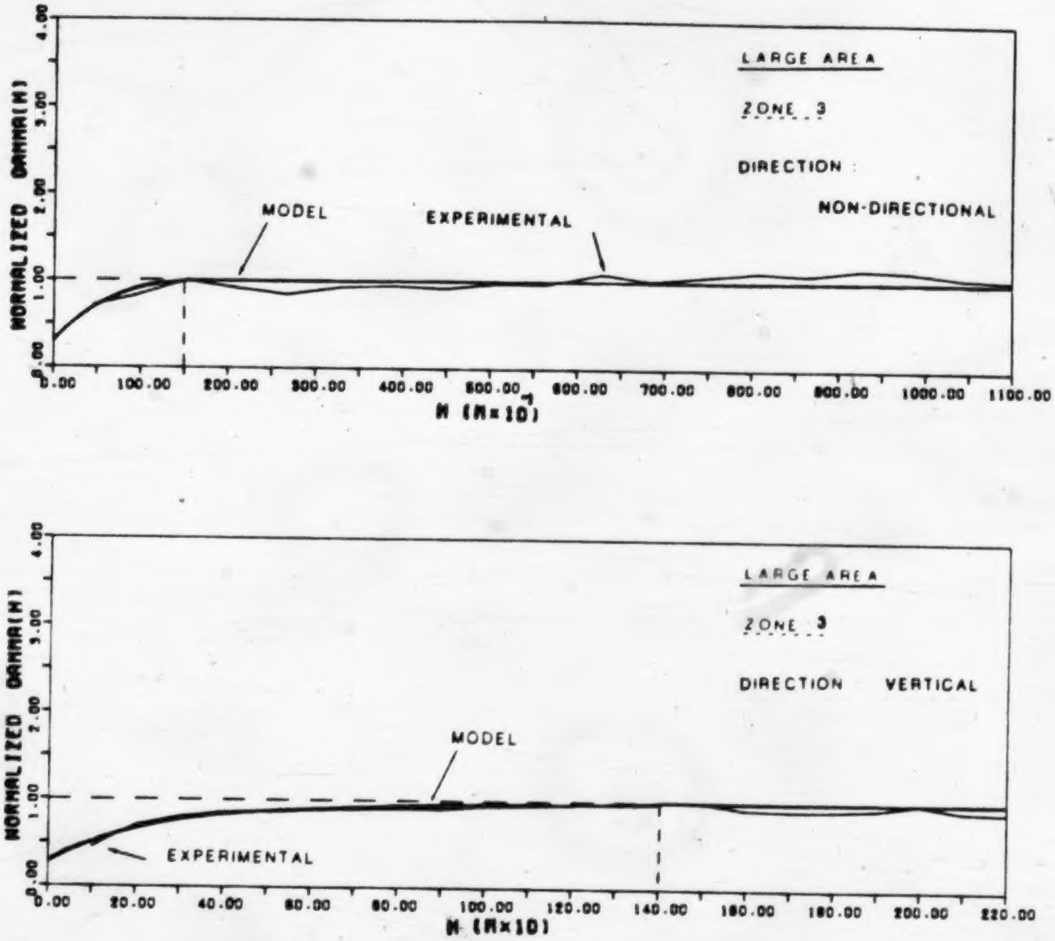

Figure 5.9 Experimental and model variograms of oil saturation in zone 3, large area; average horizontal (top) and vertical (bottom).

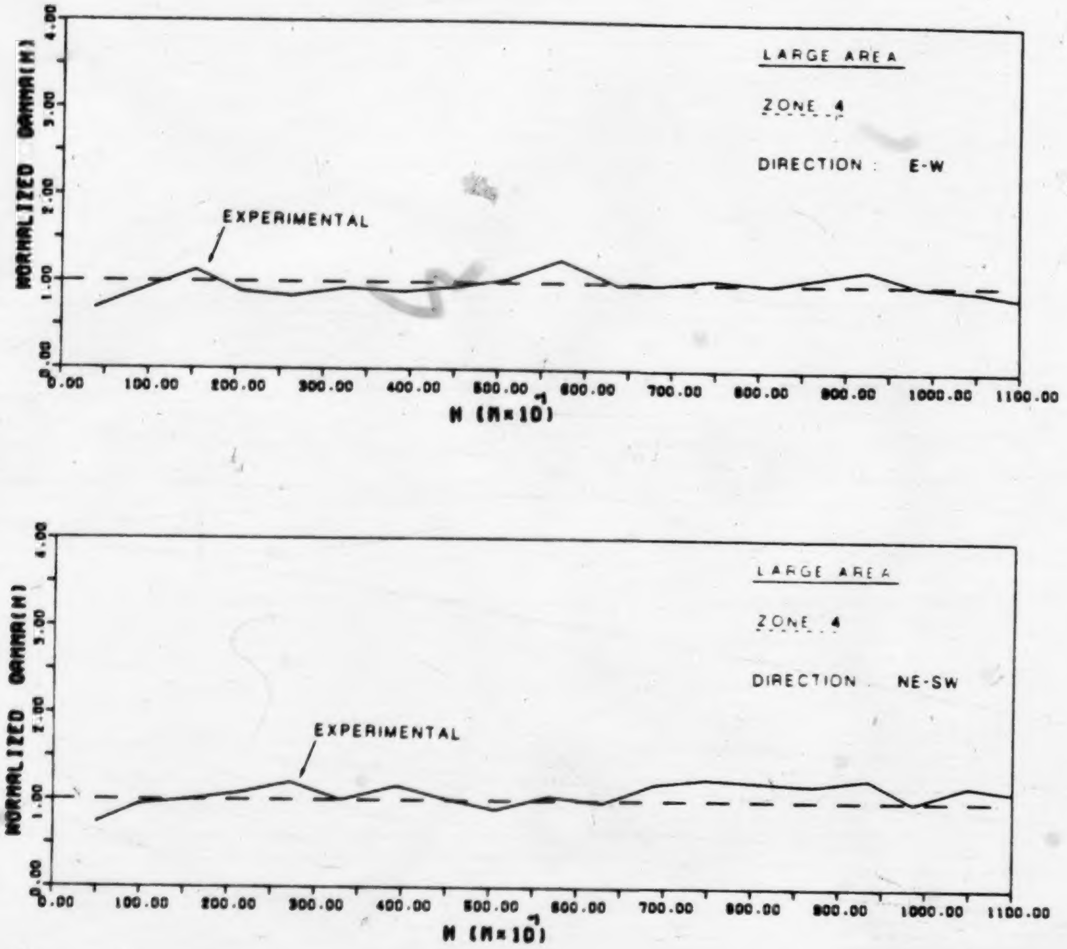

Figure 5.10 Experimental variograms of oil saturation in zone 4, large area, in the E-W (top) and NE-SW (bottom) directions.

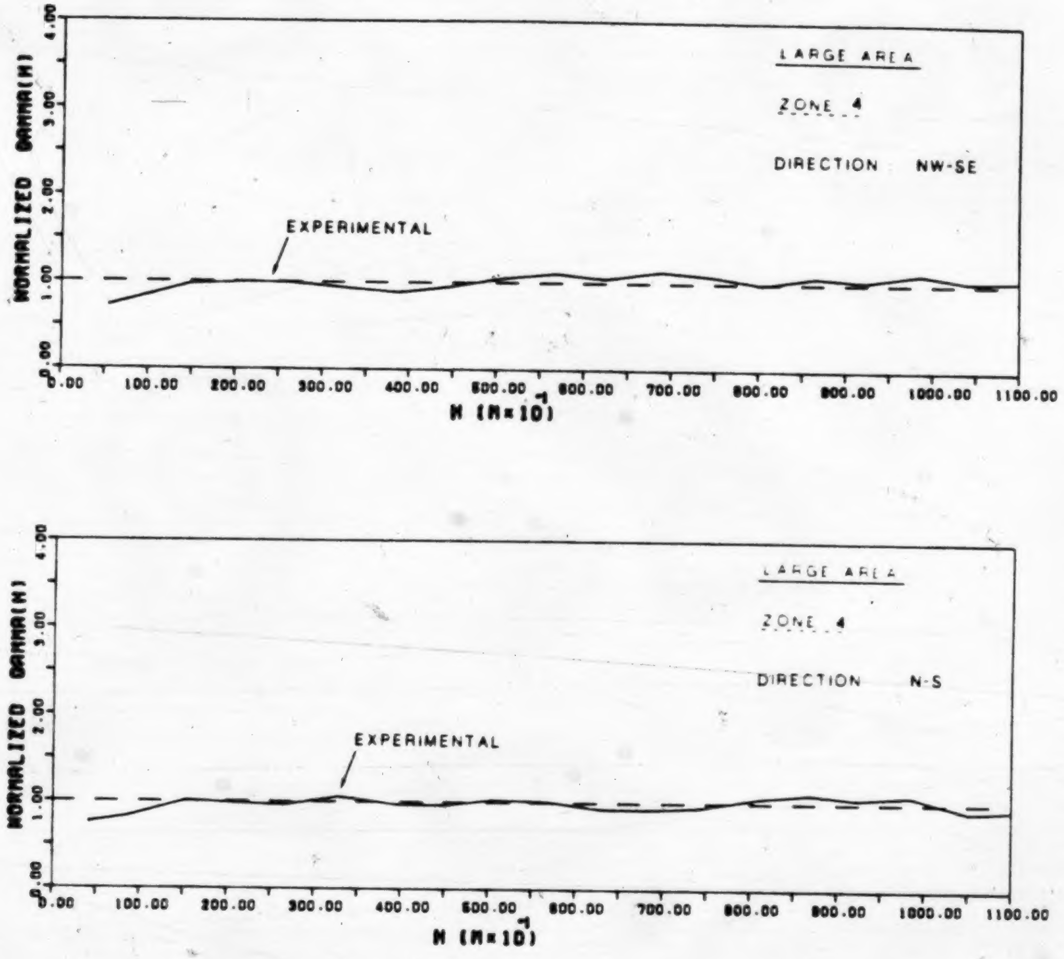

Figure 5.11 Experimental variograms of oil saturation in zone 4, large area, in the N-S (top) and NW-SE (bottom) directions.

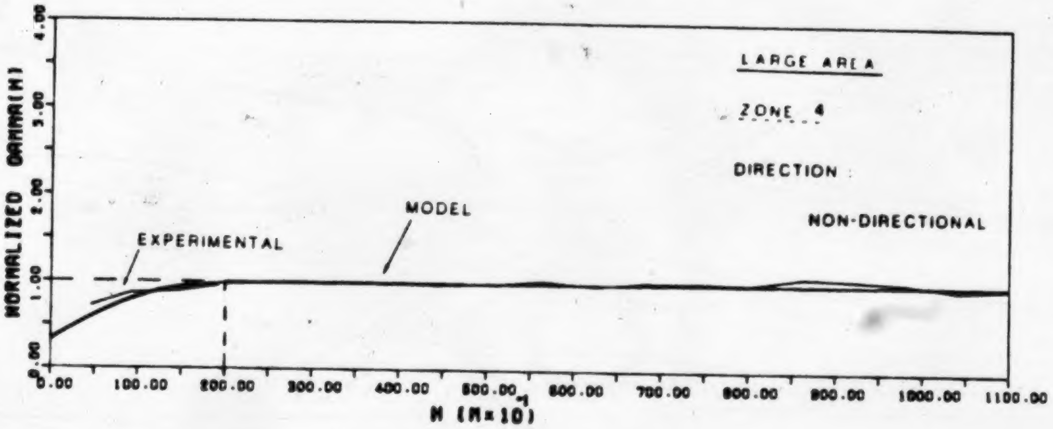

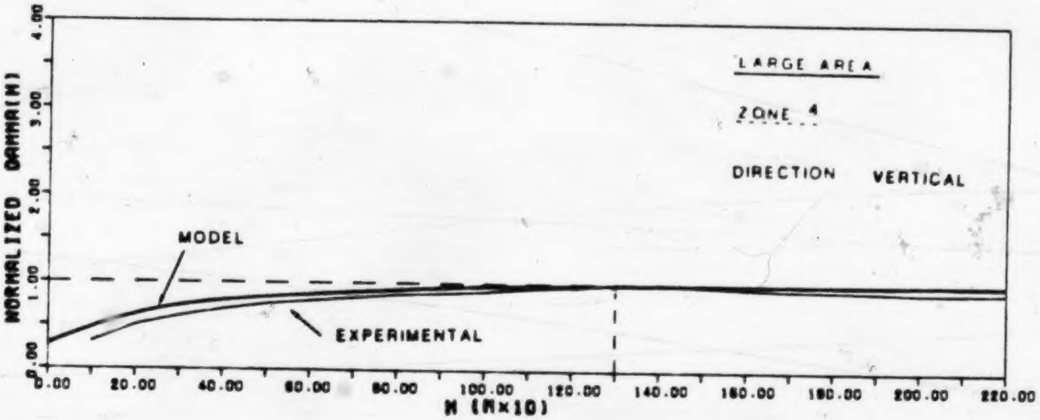

Figure 5.12 Experimental and model variograms of oil saturation in zone 4, large area; average horizontal (top) and vertical (bottom).

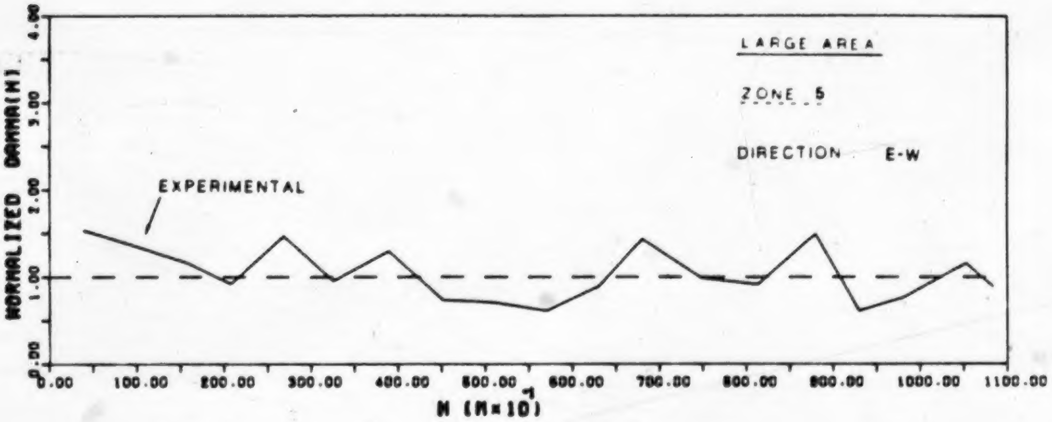

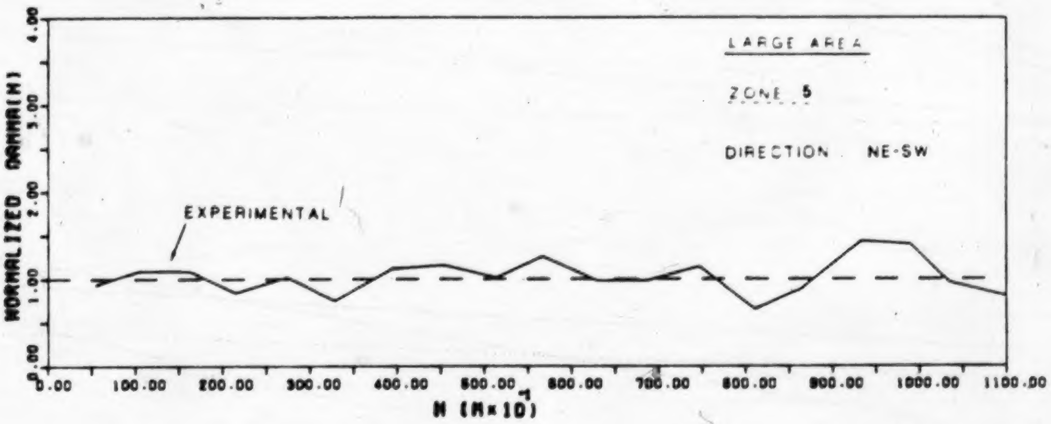

Figure 5.13 Experimental variograms of oil saturation in zone 5, large area, in the E-W (top) and NE-SW (bottom) directions.

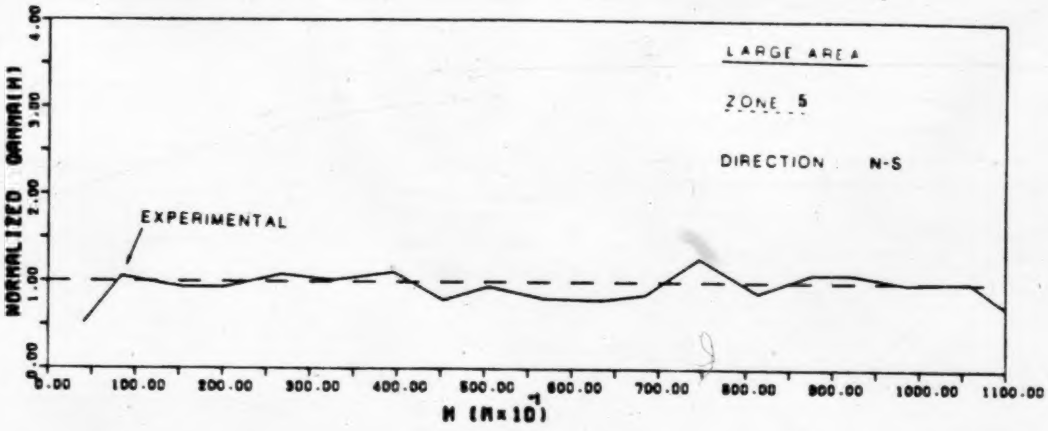

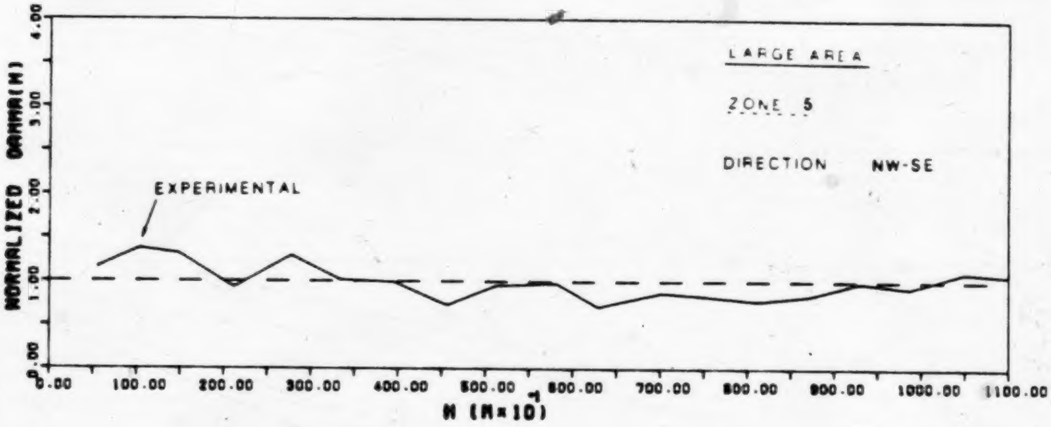

Figure 5.14 Experimental variograms of oil saturation in zone 5, large area, in the N-S (top) and NW-SE (bottom) directions.

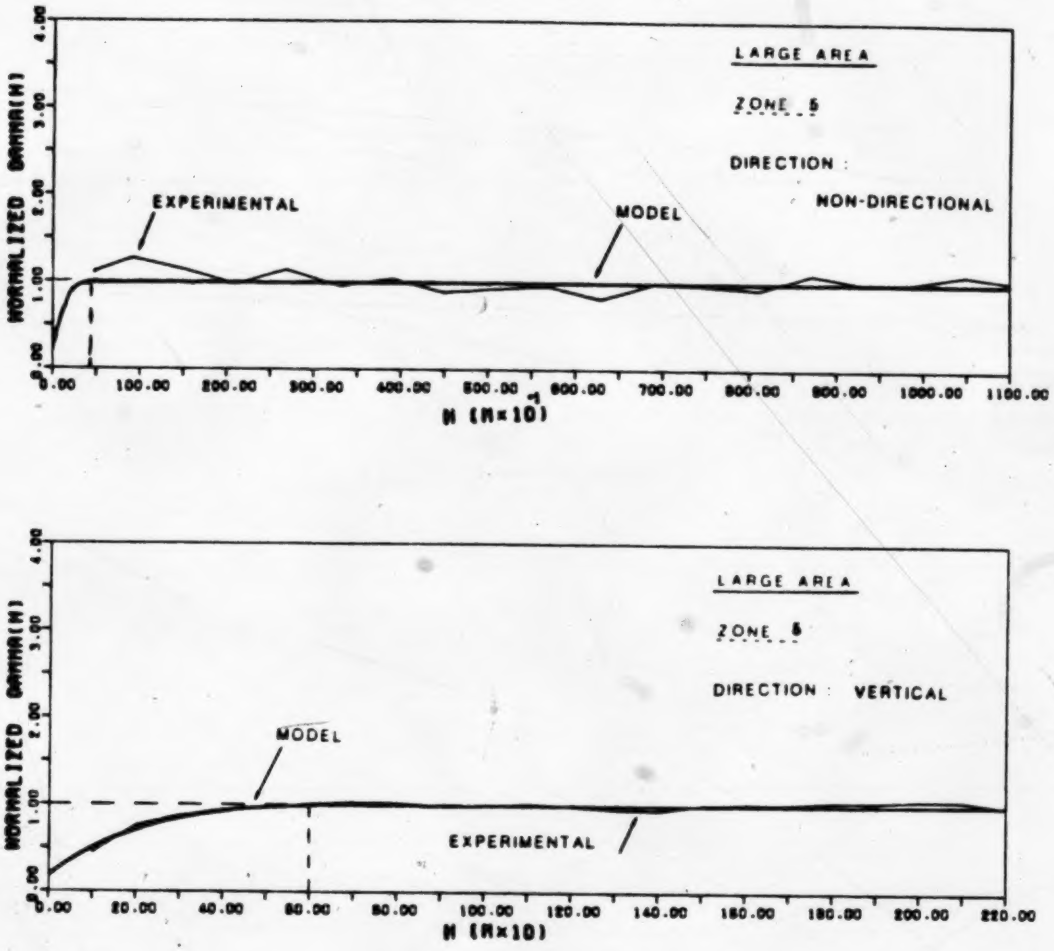

Figure 5.15 Experimental and model variograms of oil saturation zone 5, large area; average horizontal (top) and vertical (bottom).

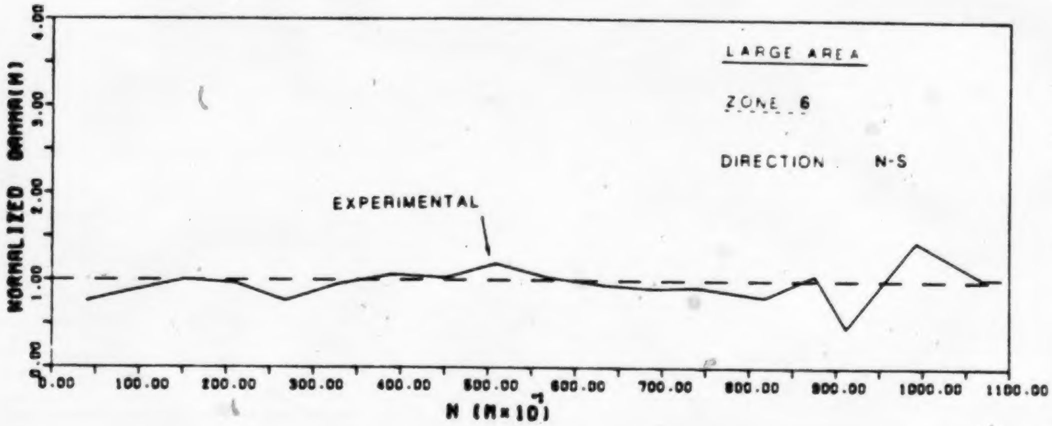

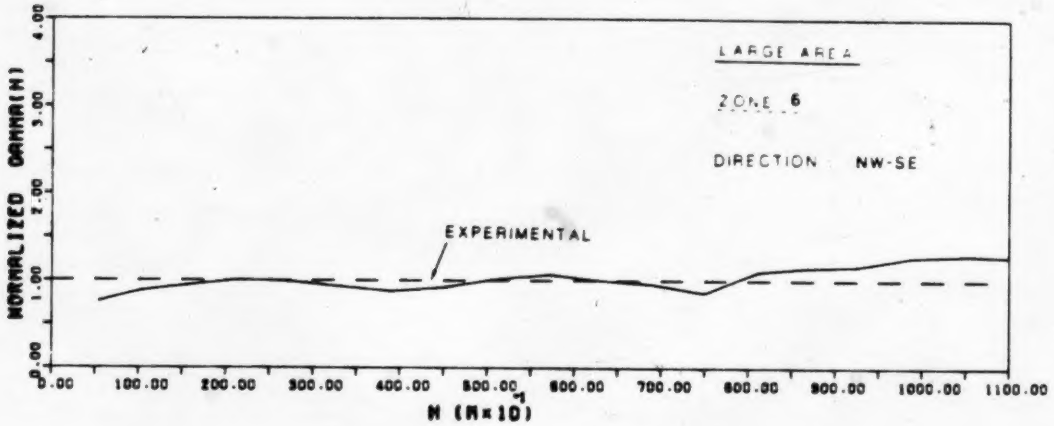

Figure 5.16 Experimental variograms of oil saturation in zone 6, large area, in the E-W (top) and NE-SW (bottom) directions.

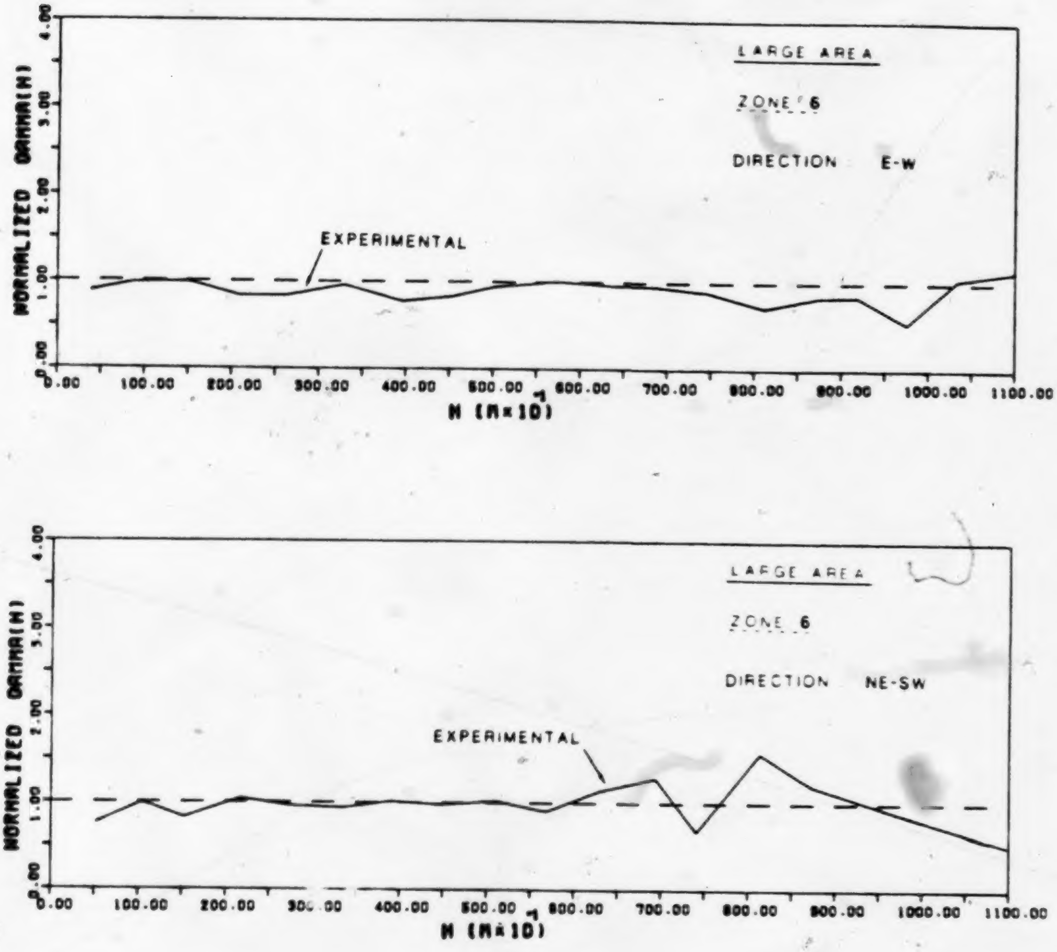

Figure 5.17 Experimental variograms of oil saturation in zone 6, large area, in the N-S (top) and NW-SE (bottom) directions.

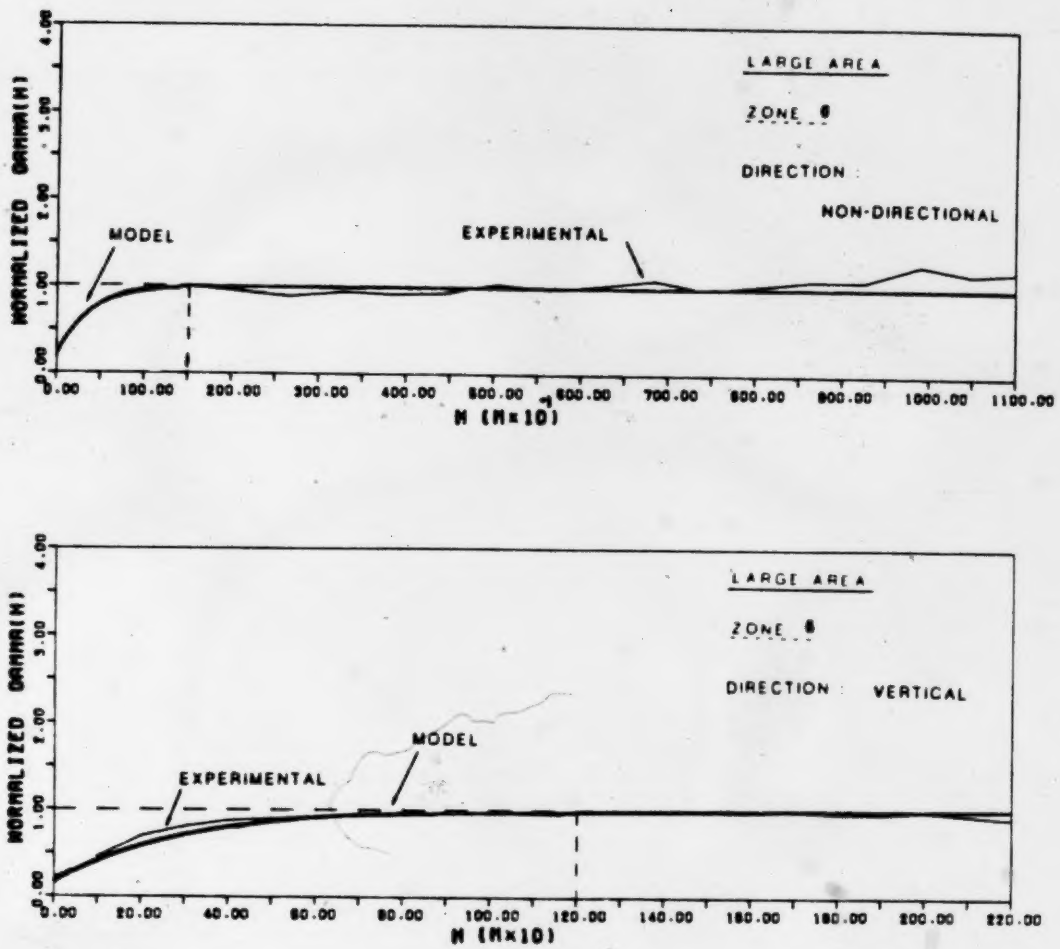

Figure 5.18 Experimental and model variograms of oil saturation in zone 6, large area; average horizontal (top) and vertical (bottom).

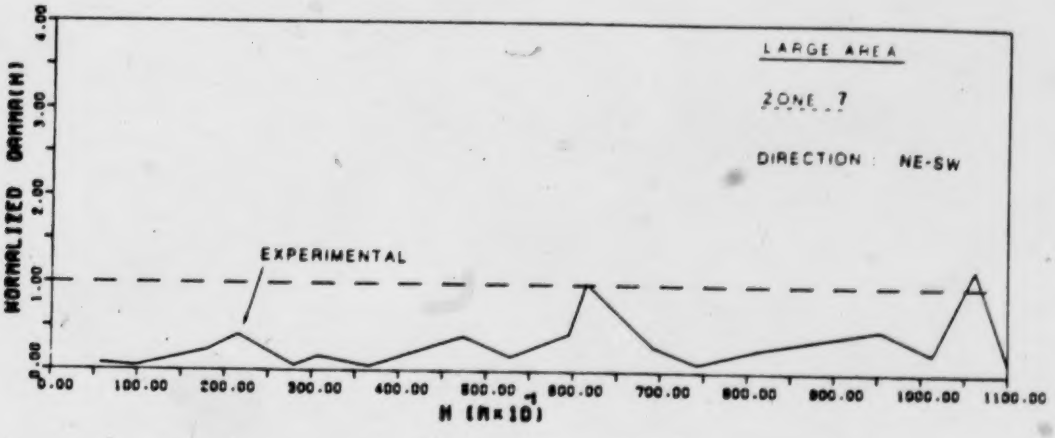

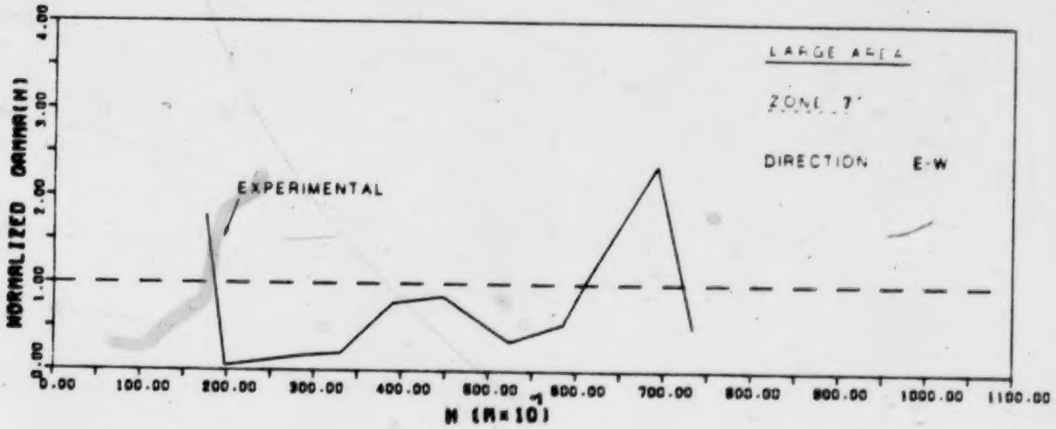

Figure 5.19 Experimental variograms of oil saturation in zone 7, large area, in the E-W (top) and NE-SW (bottom) directions.

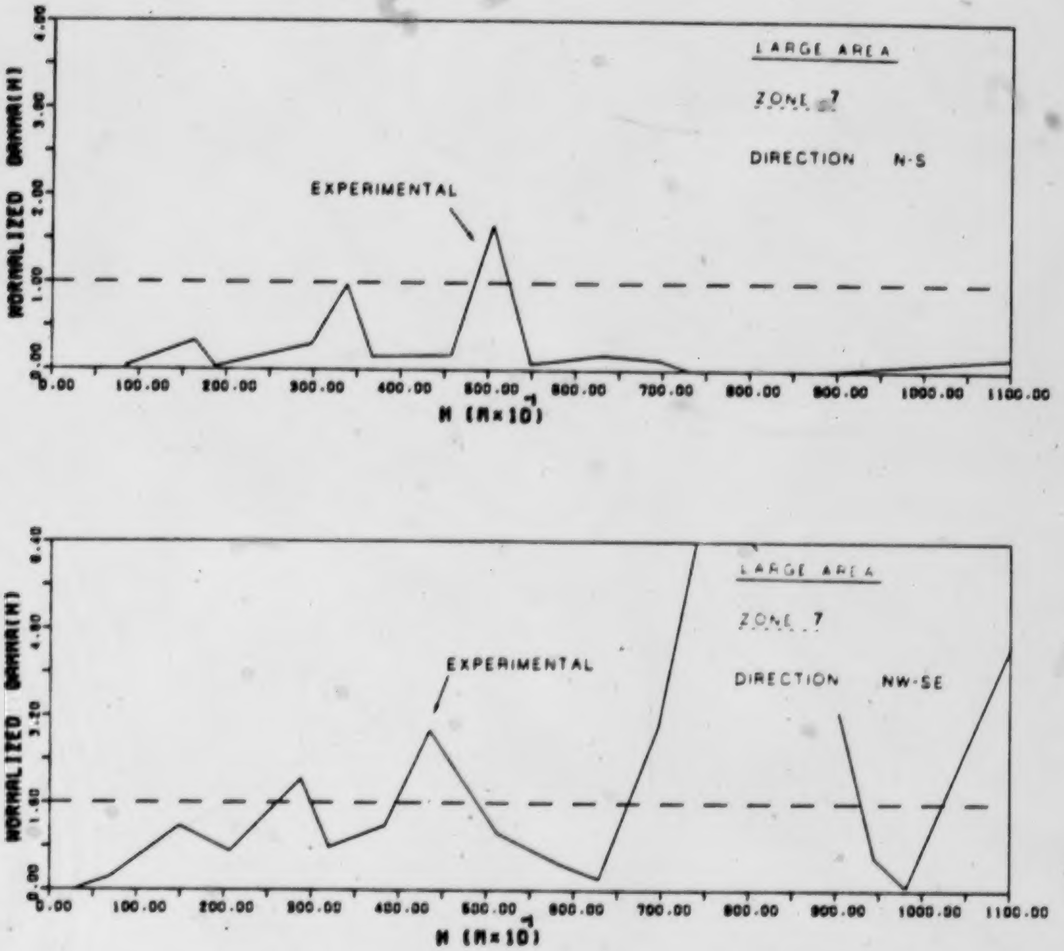

Figure 5.20 Experimental variograms of oil saturation in zone 7, large area, in the N-S (top) and NW-SE (bottom) directions.

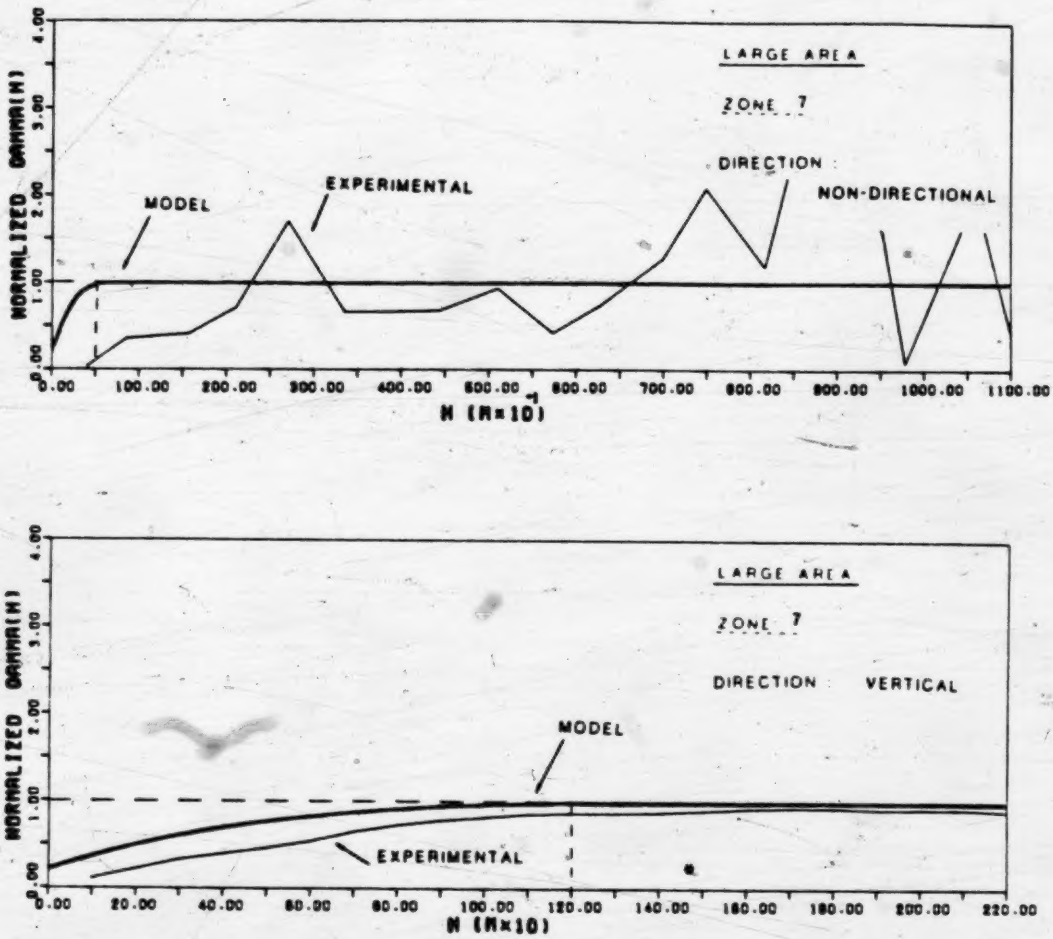

Figure 5.21 Experimental and model variograms of oil saturation in zone 7, large area; average horizontal (top) and vertical (bottom).

distances grater than 8 kilometres indicating local trends or discontinuities. The vertical variogram (Figure 5.18 bottom) had a range of 6 metres. Zone 6 represents a main oil saturated zone, because it is fairly continuous and it has high bitumen content (mean weight percent oil 11.52).

In zone 7, horizontal variograms (Figure 5.19 and 5.20) were very unstable. This was expected in zones characterized by complete lack of homogeneity. The vertical variogram (Figure 5.21 bottom) had a range of 12 metres. Zone 7 is a barren zone.

To summarize, zones 4 and 6 represent the main oil saturated zones while zone 2 contributes with some local, relatively small, 'pockets' of oil-sand.

5.1.1 Variogram evaluation on the basis of the geology of the McMurray Formation

Zones 1, 3, 5, and 7 can not be evaluated with any confidence because they lack geological homogeneity. On the contrary, one can qualitatively evaluate the variograms of zones 2, 4 and 6 as well as indicate the relationship between geology and variograms since these zones are homogeneous at least depositionally.

Accordingly, in zone 2, one can say that the experimental variograms do not contradict the geological model (flood plain deposition) since the existing structures are not detected for a drilling spacing of about to 400 metres.

In zone 4, the longer ranges in th N-S and NW-SE directions are in agreement with the N-S to NW-SE trend of the paleo-channels of the middle McMurray. The ranges in the E-W and NE-SW directions correspond to the width of the average meandrer belt of the paleo-channels. The range of the vertical variogram indicates that the thickness of the sand bodies is larger than 13 metres, which agrees with the interpretation of dip channel sedimentation of the middle McMurray facies. In conclusion, the experimental variograms of zone 4 are in agreement or adequately express the geology of the middle McMurray Formation.

In zone 6, as in zone 4, the ranges of the variograms in the N-S and NW-SE directions are longer and thus in agreement with the geological hypothesis that the fluvial paleo-channel system of the lower McMurray has a N-S to NW-SE trend. The vertical variogram indicates that the thickness of the paleochannels is at least 12 metres. Again, the variograms appear to be in agreement with the geology of the lower McMurray.

To summarize, experimental variograms of zones 2, 4 and 6 are considered to represent adequately geological reality.

5.1.2 Fitting variogram models

The stochastic structure of the oil saturation of each zone in the large area, was treated as geometrically anisotropic in two-dimensions. Accordingly, simple spherical variogram models with a nugget effect were fitted to the average horizontal and vertical experimental variograms of each zone. Note that the spherical variogram is the most commonly used model. The model variograms fitted are given below.

In zone 1, the average horizontal model was:

$$\gamma_1(h_i)=0.45+0.55[1.5(h_i/1600)-0.5(h_i/1600)^3] \, , \quad \forall \; h_i<1600 \text{ m}$$

and

$$\gamma_1(h_i)=1.0 \, , \; \forall \; h_i \geq 1600 \text{ m}$$

The vertical was:

$$\gamma_1(h_t)=0.45+0.55[1.5(h_t/5)-0.5(h_t/5)^3] \, , \; \forall \; h_t<5 \text{ m}$$

and

$$\gamma_1(h_t)=1.0 \, , \; \forall \; h_t \geq 5 \text{ m}$$

Note that for the estimation or simulation process, the horizontal and vertical distances must be scaled by k and 1/k respectively. After estimation or simulation is performed the scaling must be removed.

In zone 2, the average horizontal model was:

$$\gamma_2(h_i)=0.4+0.6[1.5(h_i/1100)-0.5(h_i/1100)^3] \, , \quad \forall \; h_i<1100 \text{ m}$$

and

$$\gamma_2(h_i)=1.0 \, , \; \forall \; h_i \geq 1100 \text{ m}$$

The vertical was:

$$\gamma_2(h_t)=0.4+0.6[1.5(h_t/12)-0.5(h_t/12)^3] \, , \; V \; h_t<12 \text{ m}$$

and

$$\gamma_2(h_t)=1.0 \, , \; \forall \; h_t \geq 12 \text{ m}$$

In zone 3, the average horizontal model was:

$$\gamma_3(h_i)=0.35+0.75[1.5(h_i/1100)-0.5(h_i/1100)^3] , \quad \forall\ h_i<1100 \text{ m}$$

and

$$\gamma_3(h_i)=1.0 , \forall\ h_i \geq 1100 \text{ m}$$

The vertical was:

$$\gamma_3(h_t)=0.35+0.75[1.5(h_t/14)-0.5(h_t/14)^3] , \forall\ h_t<14 \text{ m}$$

and

$$\gamma_3(h_t)=1.0 , \forall\ h_t \geq 14 \text{ m}$$

In zone 4, the average horizontal model was:

$$\gamma_4(h_i)=0.38+0.62[1.5(h_i/2000)-0.5(h_i/2000)^3] , \quad \forall\ h_i<2000 \text{ m}$$

and

$$\gamma_4(h_i)=1.0 , \forall\ h_i \geq 2000 \text{ m}$$

The vertical was:

$$\gamma_4(h_t)=0.38+0.72[1.5(h_t/13)-0.5(h_t/13)^3] , \forall\ h_t<13 \text{ m}$$

and

$$\gamma_4(h_t)=1.0 , \forall\ h_t \geq 13 \text{ m}$$

In zone 5, the average horizontal model was:

$$\gamma_5(h_i)=0.25+0.75[1.5(h_i/450)-0.5(h_i/450)^3] , \quad \forall\ h_i<450 \text{ m}$$

and

$$\gamma_5(h_i)=1.0 , \forall\ h_i \geq 450 \text{ m}$$

The vertical was:

$$\gamma_5(h_t)=0.25+0.75[1.5(h_t/6)-0.5(h_t/6)^3] , \forall\ h_t<6 \text{ m}$$

and

TABLE 5.1 **Summary of the weight % oil saturation average horizontal model variograms in the large area.**

Zone	**Normalized nugget effect (weight %)^2**	**Range (m)**	*A priori* Variance (weight %)^2
1	0.45	1600	7.11
2	0.40	1100	8.02
3	0.35	1100	5.11
4	0.38	2000	12.25
5	0.25	450	8.00
6	0.25	1100	8.70
7	0.25	500	24.68

TABLE 5.2 Summary of the weight % oil saturation vertical model variograms in the large area.

Zone	Normalized nugget effect (weight %)^2	Range (m)	*A priori* Variance (weight %)^2
1	0.45	5	7.11
2	0.40	12	8.02
3	0.35	14	5.11
4	0.38	13	12.25
5	0.25	6	8.00
6	0.25	12	8.70
7	0.25	12	24.68

$\gamma_5(h_t)=1.0 \ , \ \forall \ h_t \geq 6 \text{ m}$

In zone 6, the average horizontal model was:

$$\gamma_6(h_i)=0.25+0.75[1.5(h_i/1100)-0.5(h_i/1100)^3] \ , \quad \forall \ h_i<1100 \text{ m}$$

and

$$\gamma_6(h_i)=1.0 \ , \ \forall \ h_i \geq 1100 \text{ m}$$

The vertical was:

$$\gamma_6(h_t)=0.25+0.75[1.5(h_t/16)-0.5(h_t/16)^3] \ , \ \forall \ h_t<16 \text{ m}$$

and

$$\gamma_6(h_t)=1.0 \ , \ \forall \ h_t \geq 16 \text{ m}$$

In zone 7, the average horizontal model was:

$$\gamma_7(h_i)=0.25+0.75[1.5(h_i/500)-0.5(h_i/500)^3] \ , \quad \forall \ h_i<500 \text{ m}$$

and

$$\gamma_7(h_i)=1.0 \ , \ \forall \ h_i \geq 500 \text{ m}$$

The vertical was:

$$\gamma_7(h_t)=0.25+0.75[1.5(h_t/12)-0.5(h_t/12)^3] \ , \ \forall \ h_t<12 \text{ m}$$

and

$$\gamma_6(h_t)=1.0 \ , \ \forall \ h_t \geq 12 \text{ m}$$

The characteristics of the fitted variograms in the large area are summarized in Tables 5.1 and 5.2.

Note that variograms of the tops and bottoms of the zones in the large area were not calculated. This is because a 'minimum curvature' algorithm instead of kriging was used for the interpolation of the elevations.

5.2 Variography in the Small Area

As in the large area, the available wells within the small area were not on a regular grid. Accordingly, horizontal variograms were calculated by grouping the data. The basic lag was 300 metres, the distance of tolerance 150 metres and the angle of tolerance 25°. Average horizontal variograms were considered as very reliable since the number of pairs for each experimental point of the variograms was larger than 150. However, directional horizontal variograms were not considered as reliable (nunber of pairs less than 30) and were not included. The vertical variograms were calculated with a basic lag of 1 meter and were very reliable (number of pairs for experimental points larger than 110).

In zones 1, 2, 3 and 6, the average horizontal variograms appear as pure nugget effect. Apparently, the existing structures were not detected because they are of smaller dimensions than the drilling spacing. Vertical variograms of the same zones had ranges of 3, 3.5, 4 and 3 metres respectively.

In zone 4, the average horizontal variogram had a range of approximately 900 metres and the vertical had a range of 11 metres.

In zone 5, average horizontal variogram reached its sill at 600 metres and the vertical at 4.5 metres.

Due to the very small number of samples (15), variograms of zone 7 were not calculated.

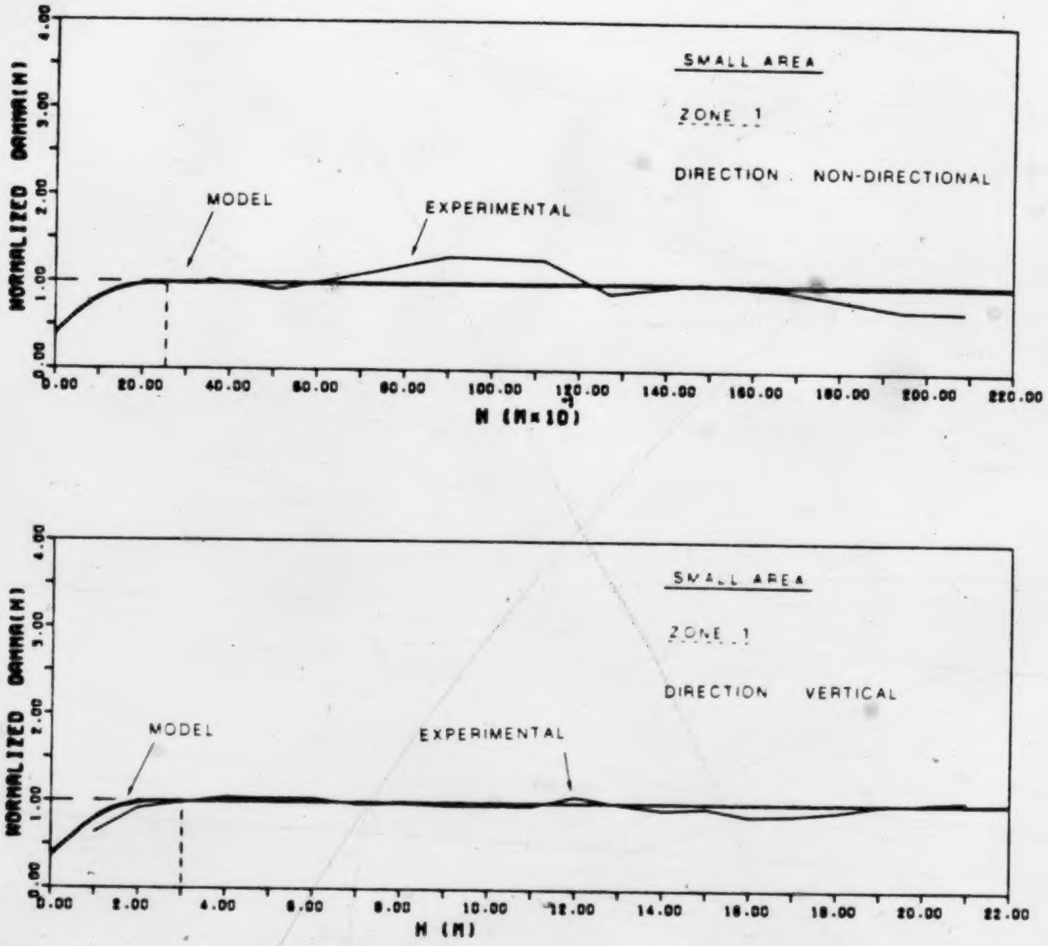

Figure 5.22 Experimental and model variograms of oil saturation in zone 1, small area; average horizontal (top) and vertical (bottom).

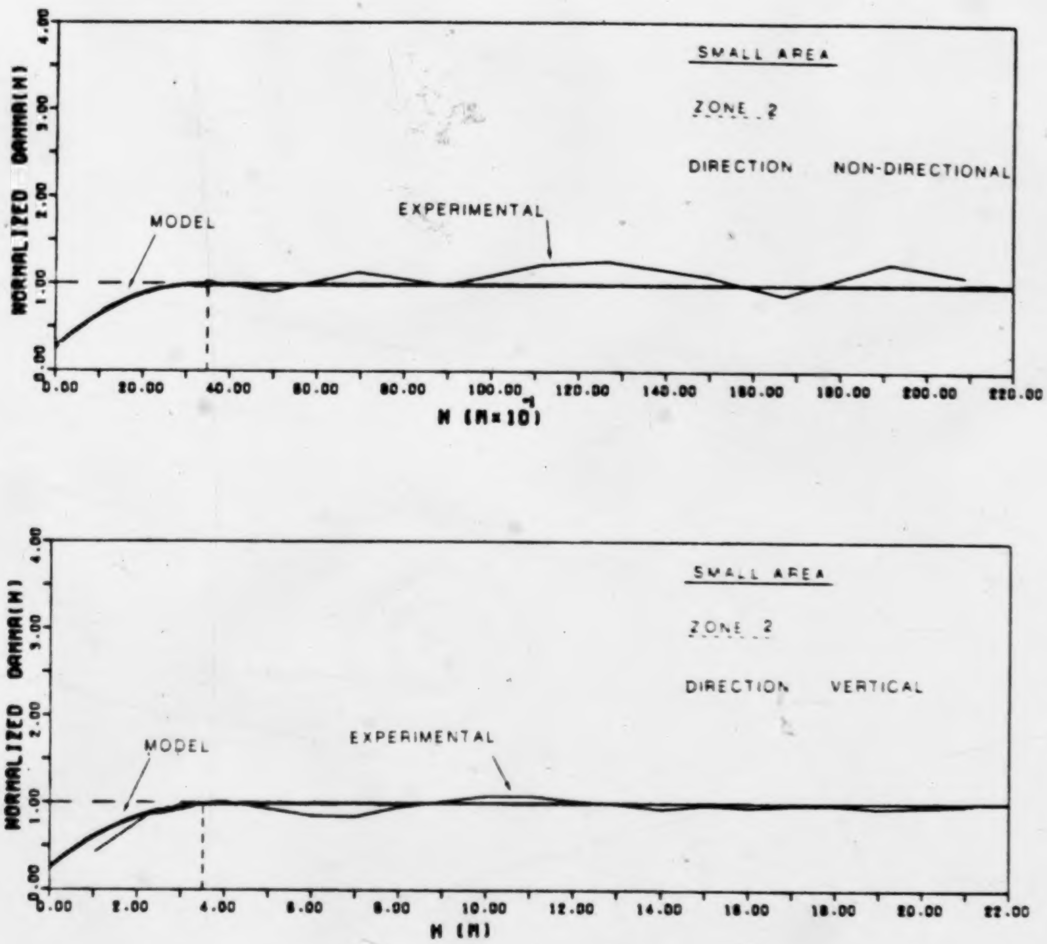

Figure 5.23 Experimental and model variograms of oil saturation in zone 2, small area; average horizontal (top) and vertical (bottom).

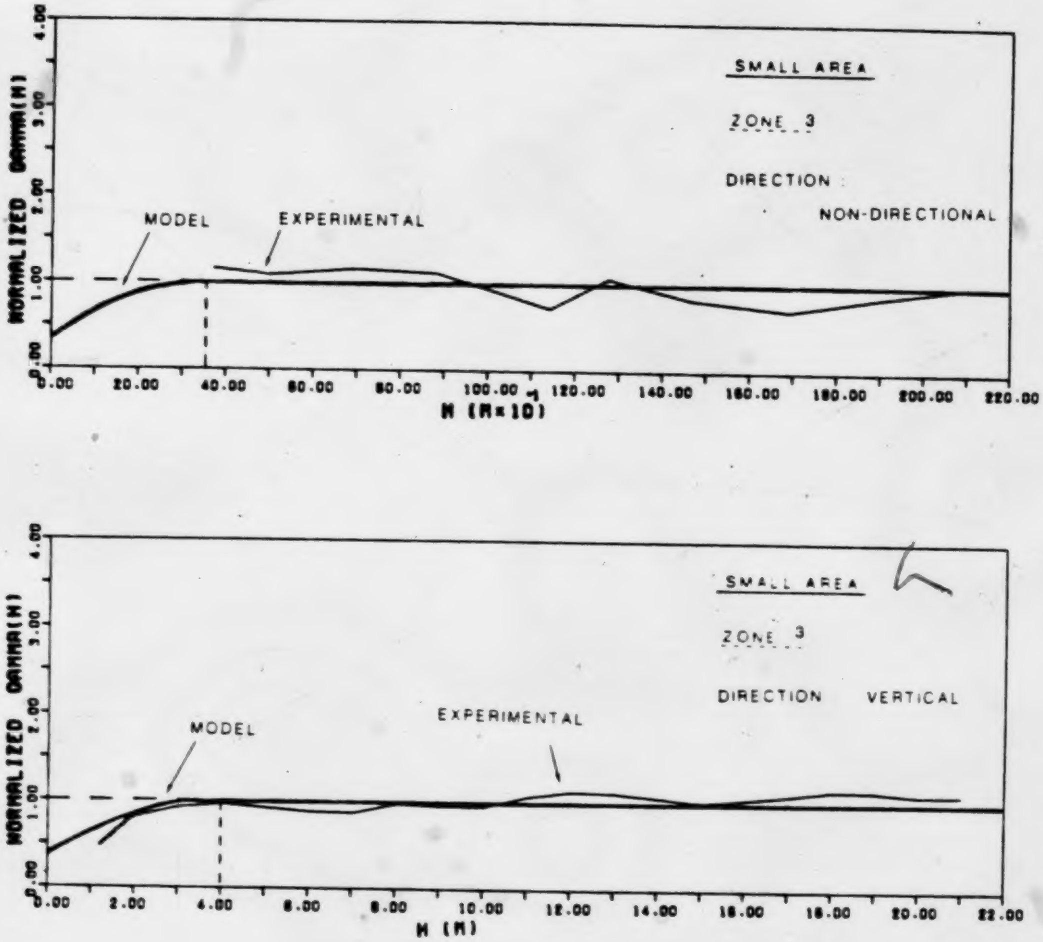

Figure 5.24 Experimental and model variograms of oil saturation in zone 3, small area; average horizontal (top) and vertical (bottom).

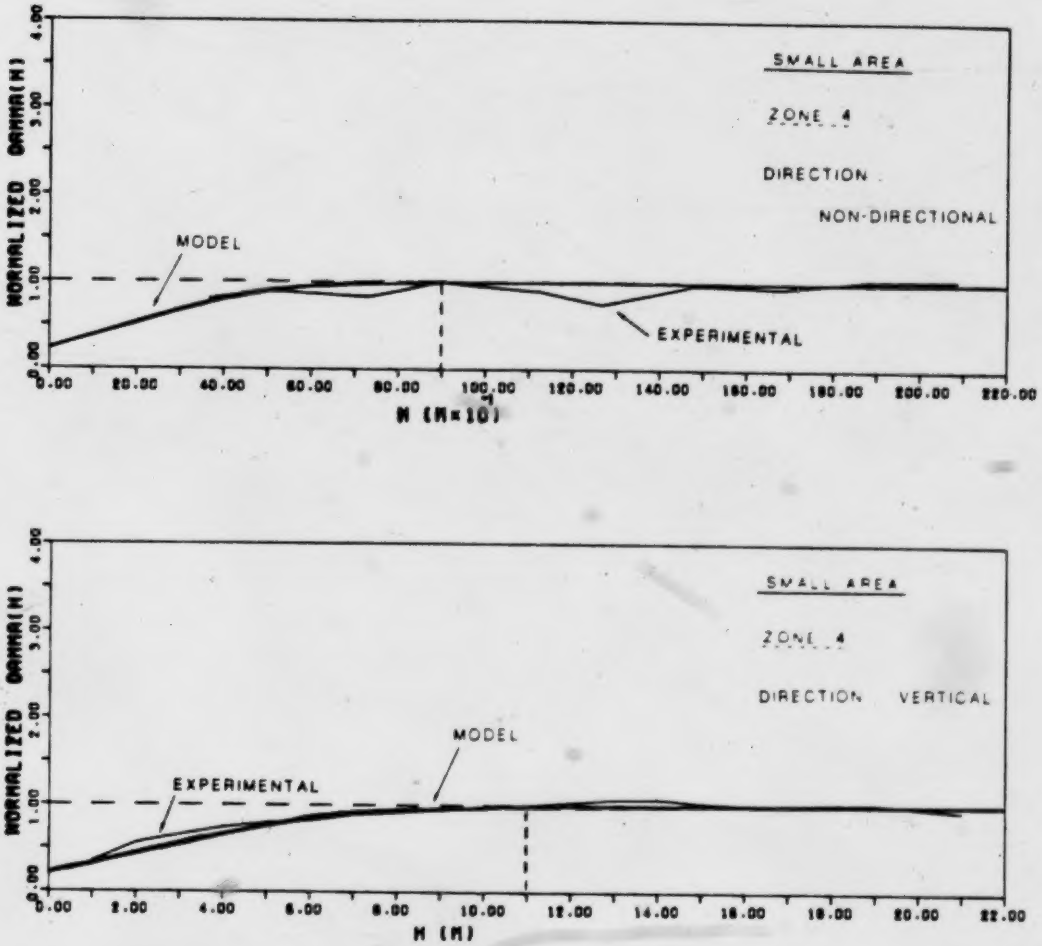

Figure 5.25 Experimental and model variograms of oil saturation in zone 4, small area; average horizontal (top) vertical (bottom).

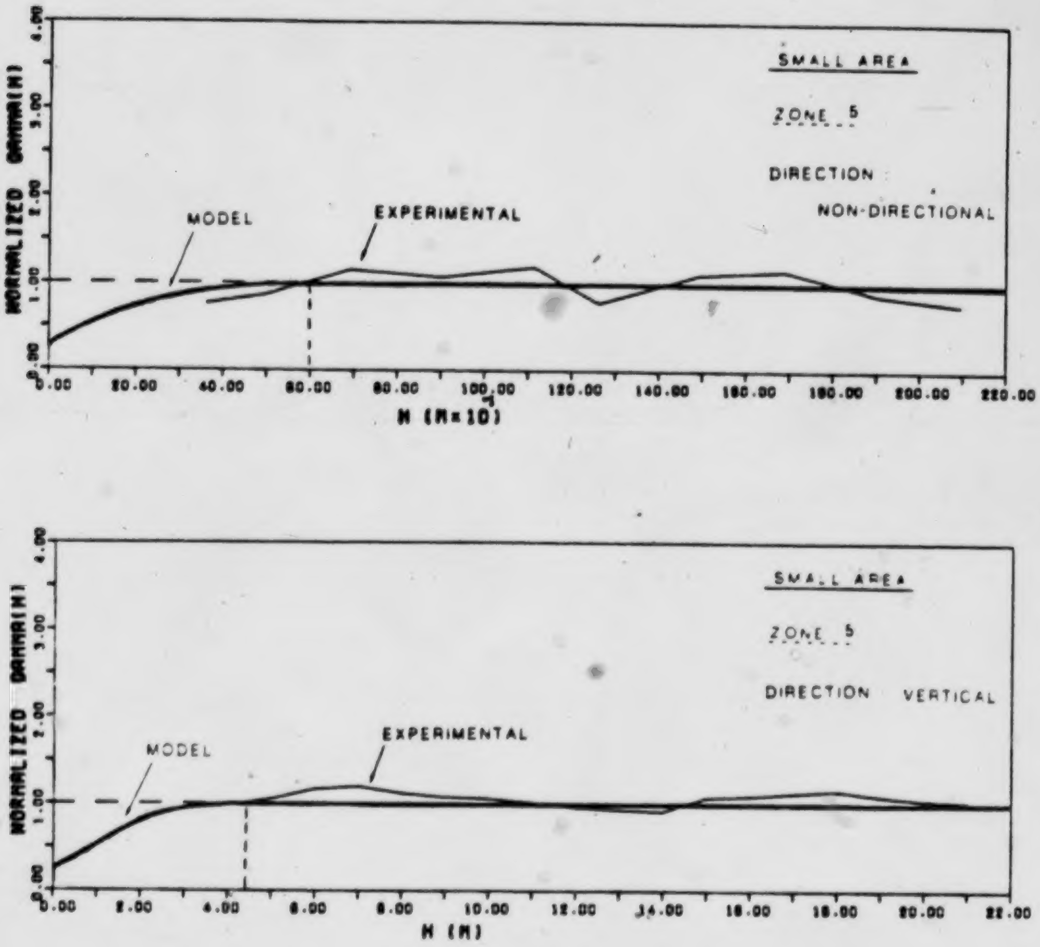

Figure 5.26 Experimental and model variograms of oil saturation zone 5, small area; average horizontal (top) and vertical (bottom).

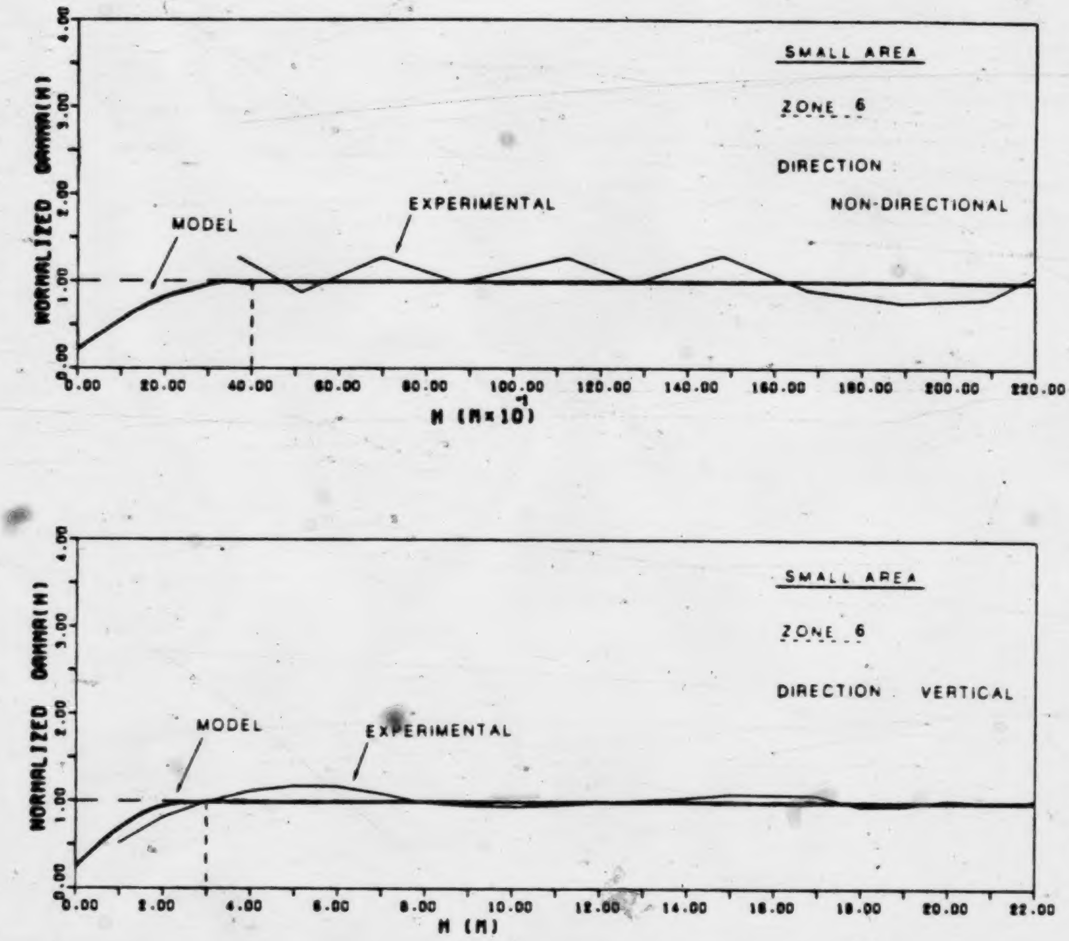

Figure 5.27 Experimental and model variograms of oil saturation in zone 6, small area; average horizontal (top) and vertical (bottom).

As in the large area, zones 4 and 6 represent the main 'ore'-bodies. These are relatively continuous with little variations in their oil content.

The experimental variograms of the 7 zones in the small area are depicted in figures 5.22, 5.23, 5.24, 5.25, 5.26, 5.27.

5.2.1 Geological evaluation of the experimental variograms

It is impossible to evaluate most of the variograms of oil saturation in the small area. Apparently, the oil-sands exhibit smaller variations in their bitumen content (at least in zones 4 and 6) than in the large area. This may be one explanation for the smaller ranges of the experimental variograms in both horizontal and vertical directions.

Another explanation, from a geological perspective, may be the following. In large areas (like the total study area), main paleo-channels are easily distinguished from their tributaries. This results in variograms whose ranges represent on an average, the dimensions of the main channels. On the contrary, in a small area (such as the control area) where parts of the main paleo-channels co-exist with a number of tributaries, variograms will not show any particular structures, or if they detect any, they may differ from the ones in a much larger area.

5.2.2 Fitting the variogram models

The lack of apparent structures in most of the experimental average horizontal variograms of the 7 zones in the small area created a problem in fitting variogram models.

The solution adopted was that of fitting models using the ranges of variograms from Grasley (1982). The variograms adopted from Grasley's study were calculated in a small area with an average drillhole spacing of 50 metres. This dense spacing allows the detection of small structures in the different zones.

The model variograms are:

in zone 1, the average horizontal model was:

$$\gamma_1(h_i)=0.4+0.6[1.5(h_i/250)-0.5(h_i/250)^3] \ , \forall \ h_i<250 \text{ m}$$

and

$$\gamma_1(h_i)=1.0 \ , \forall \ h_i\geq 250 \text{ m}$$

The vertical was:

$$\gamma_1(h_t)=0.4+0.6[1.5(h_t/3)-0.5(h_t/3)^3] \ , \forall \ h_t<3 \text{ m}$$

and

$$\gamma_1(h_t)=1.0 \ , \forall \ h_t\geq 3 \text{ m}$$

In zone 2, the average horizontal model was:

$$\gamma_2(h_i)=0.3+0.7[1.5(h_i/350)-0.5(h_i/350)^3] \ , \forall \ h_i<350 \text{ m}$$

and

$$\gamma_2(h_i)=1.0 \ , \forall \ h_i\geq 350 \text{ m}$$

The vertical was:

$$\gamma_2(h_t)=0.3+0.7[1.5(h_t/12)-0.5(h_t/12)^3] \ , \forall \ h_t<3.5 \text{ m}$$

and

TABLE 5.3 Summary of the weight % oil saturation average horizontal model variograms in the small area.

Zone	Normalized nugget effect (weight %)^2	Range (m)	*A priori* variance (weight %)^2
1	0.40	250	4.83
2	0.30	350	6.06
3	0.30	350	2.86
4	0.25	900	9.98
5	0.25	600	13.92
6	0.25	400	5.38
7	----	---	---

TABLE 5.4 Summary of the weight % oil saturation vertical model variograms in the small area.

Zone	Nugget effect (weight %)^2	Range (m)	*A priori* variance (weight %)^2
1	0.40	3.00	4.83
2	0.30	3.50	6.06
3	0.30	4.00	2.86
4	0.25	11.00	9.98
5	0.25	4.5	13.92
6	0.25	3.00	5.38
7	----	----	----

$\gamma_2(h_t)=1.0 \ , \forall \ h_t \geq 3.5$ m

In zone 3, the average horizontal model was:

$\gamma_3(h_i)=0.3+0.7[1.5(h_i/350)-0.5(h_i/350)^3] \ , \forall \ h_i<350$ m

and

$\gamma_3(h_i)=1.0 \ , \forall \ h_i \geq 350$m

The vertical was:

$\gamma_3(h_t)=0.3+0.7[1.5(h_t/4)-0.5(h_t/4)^3] \ , \forall \ h_t<4$ m

and

$\gamma_3(h_t)=1.0 \ , \forall \ h_t \geq 4$ m

In zone 4, the average horizontal model was:

$\gamma_4(h_i)=0.25+0.75[1.5(h_i/900)-0.5(h_i/900)^3] \ , \forall \ h_i<900$ m

and

$\gamma_4(h_i)=1.0 \ , \forall \ h_i \geq 900$ m

The vertical was:

$\gamma_4(h_t)=0.25+0.75[1.5(h_t/11)-0.5(h_t/11)^3] \ , \forall \ h_t<11$ m

and

$\gamma_4(h_t)=1.0 \ , \forall \ h_t \geq 11$ m

In zone 5, the average horizontal model was:

$\gamma_5(h_i)=0.25+0.75[1.5(h_i/600)-0.5(h_i/600)^3] \ , \forall \ h_i<600$ m

and

$\gamma_5(h_i)=1.0 \ , \forall \ h_i \geq 600$ m

The vertical was:

$\gamma_5(h_t)=0.25+0.75[1.5(h_t/4.5)-0.5(h_t/4.5)^3] \ , \forall \ h_t<4.5$ m

and

$\gamma_5(h_t)=1.0 \ , \forall \ h_t \geq 4.5$ m

In zone 6, the average horizontal model was:

$$\gamma_6(h_i)=0.25+0.75[1.5(h_i/400)-0.5(h_i/400)^3] \text{ , } \forall\ h_i<400 \text{ m}$$

and

$$\gamma_6(h_i)=1.0 \text{ , } \forall\ h_i\geq 400 \text{ m}$$

The vertical was:

$$\gamma_6(h_t)=0.25+0.75[1.5(h_t/3)-0.5(h_t/3)^3] \text{ , } \forall\ h_t<3 \text{ m}$$

and

$$\gamma_6(h_t)=1.0 \text{ , } \forall\ h_t\geq 3 \text{ m}$$

The characteristics of the fitted variogram models in the small area are summarized in Tables 5.3 and 5.4.

5.2.3 Surface variograms in the small area

Average experimental variograms were constructed for the elevations of the topographic surface, the tops of the seven zones and the top of the Devonian limestones (bottom of zone 7) by grouping the data. The basic lag was 200 m and the distance of tolerance 100 m. The number of pairs for the experimental points ranged from 28 to 49. Directional variograms were not calculated because of the small number of the available drillholes. To the experimental curves, simple circular variogram models were fitted (Figures 5.28 to 5.32).

The model variograms fitted are listed below.

The variogram of the surface topography was:

$$\gamma_s(h)=(2/\pi 1670^2)\ [h\sqrt{1670^2-h^2}+1670^2\text{Arcsin}(h/1670)] \text{ ,}$$

$$\forall\ h\leq 1670 \text{ m}$$

and $\gamma_s(h)=1.0$, $\forall\ h\geq 1670$ m

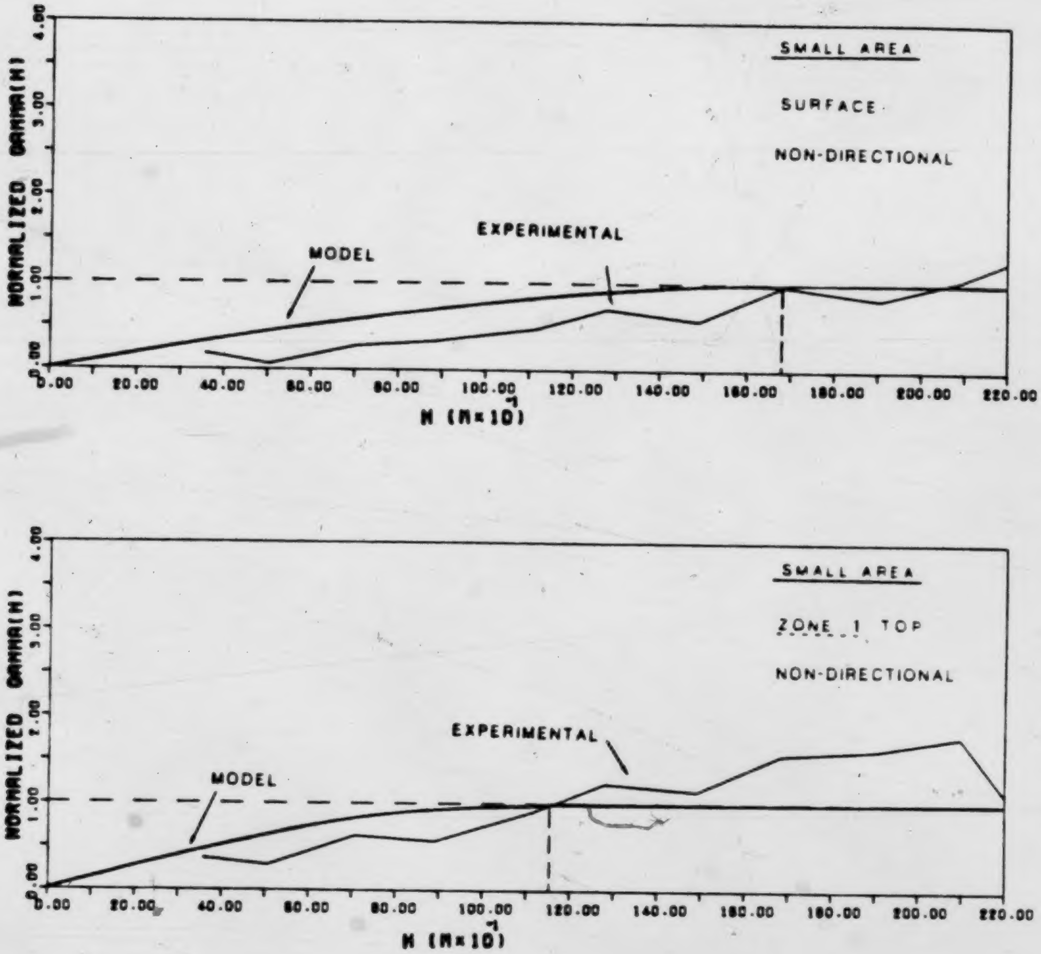

Figure 5.28 Experimental and model variograms of the topographic surface (top) and top of zone 1 (bottom).

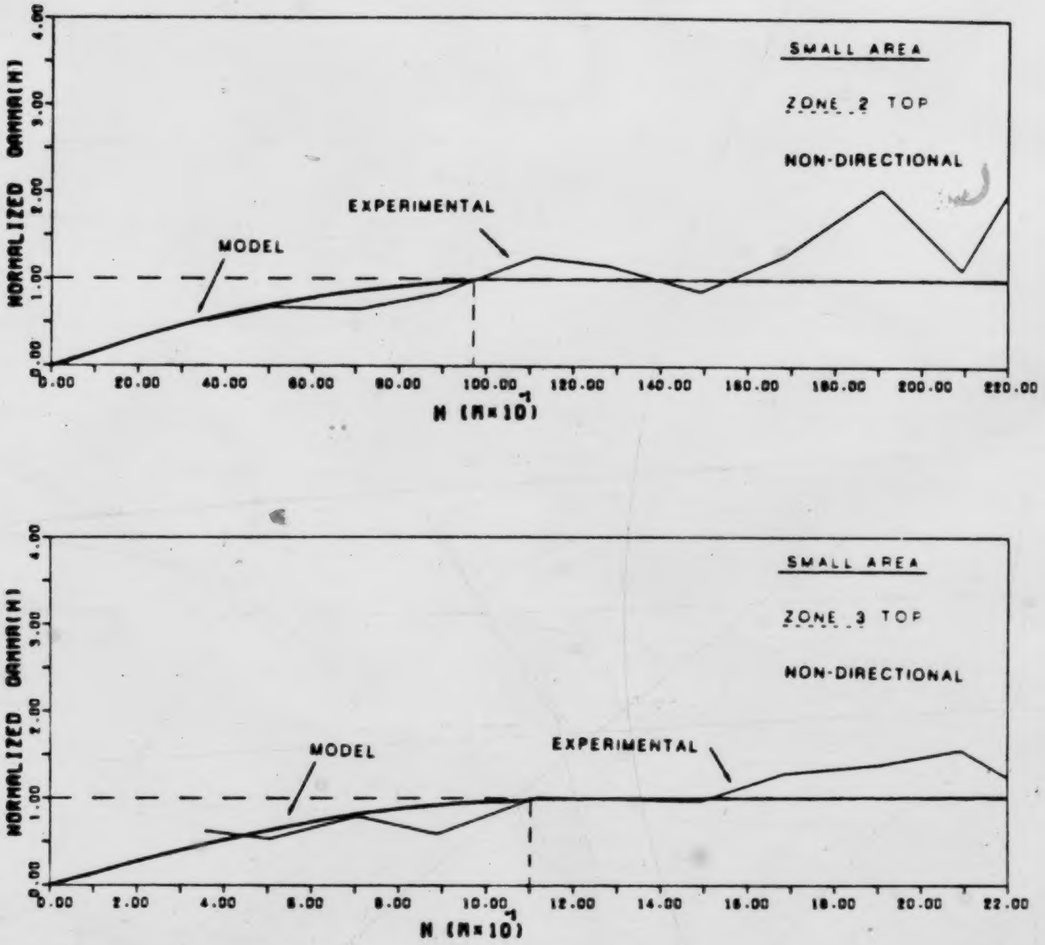

Figure 5.29 Experimental and model variograms of the top of zone 2 (top) and top of zone 3 (bottom).

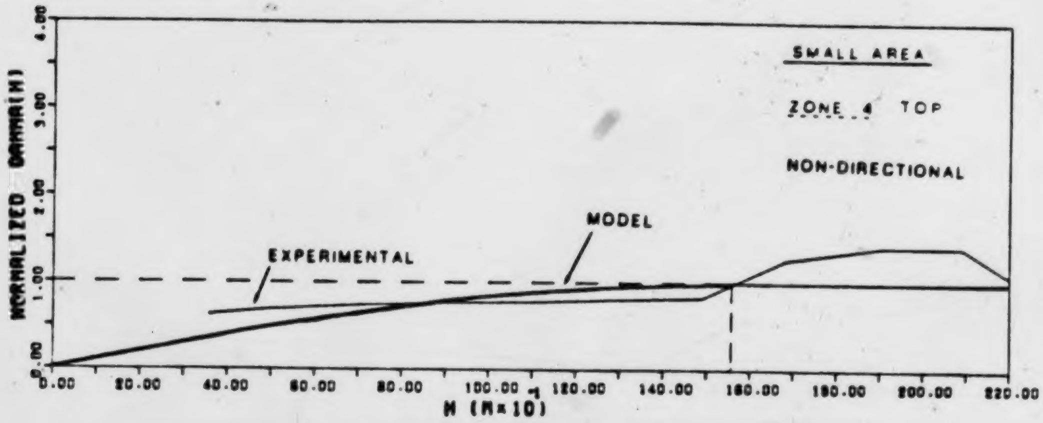

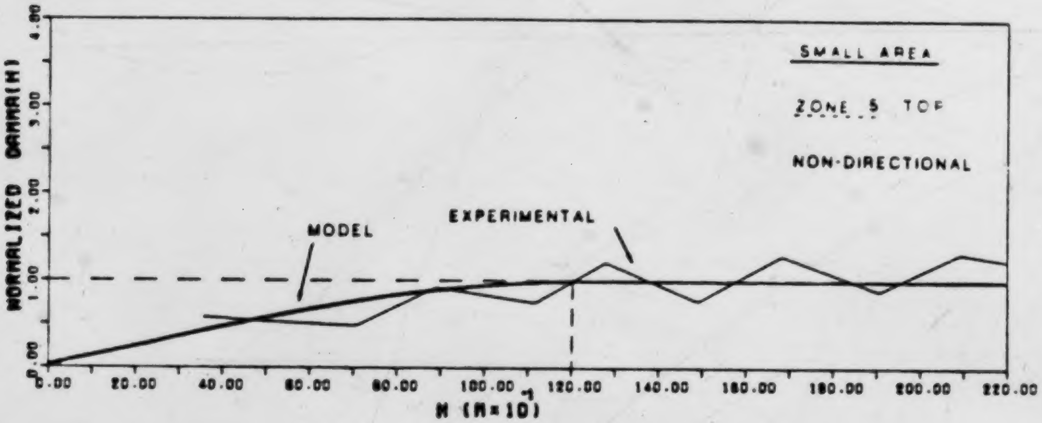

Figure 5.30 Experimental and model variograms of the top of zone 4 (top) and top of zone 5 (bottom).

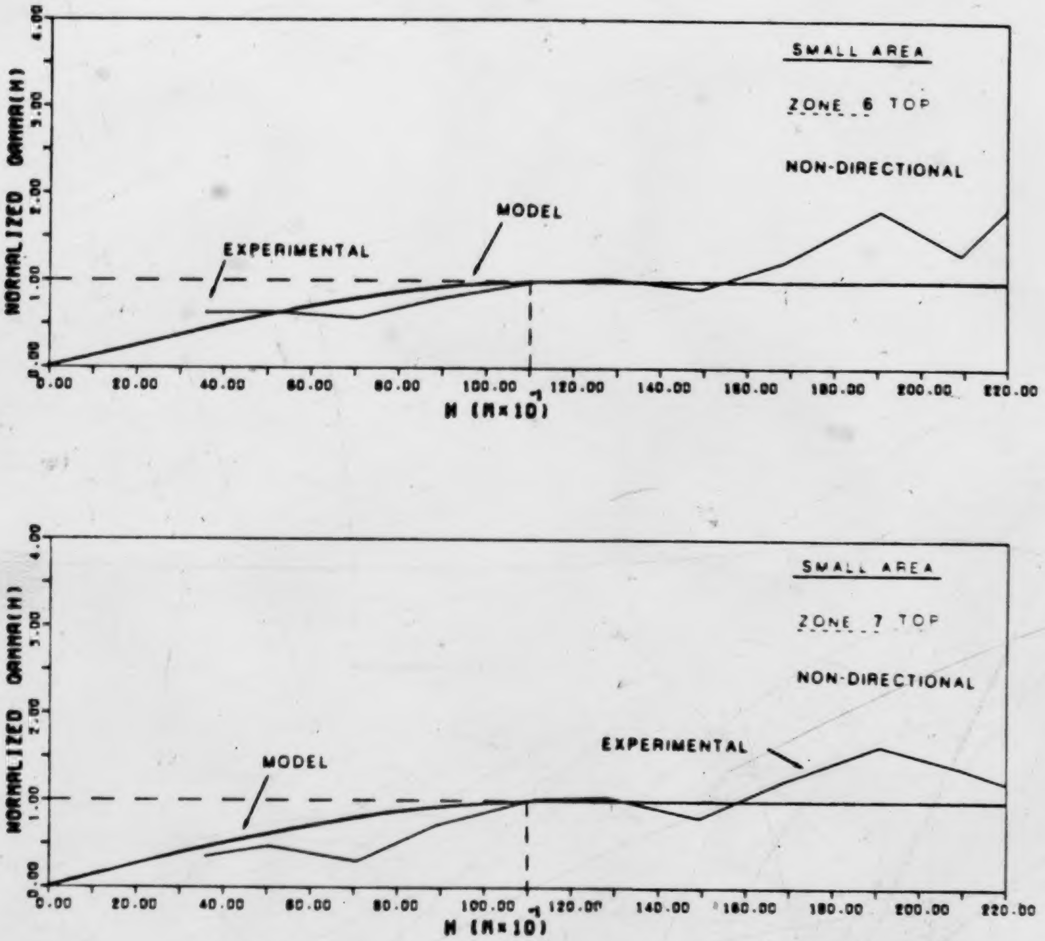

Figure 5.31 Experimental and model variograms of the top of zone 6 (top) and top of zone 7 (bottom).

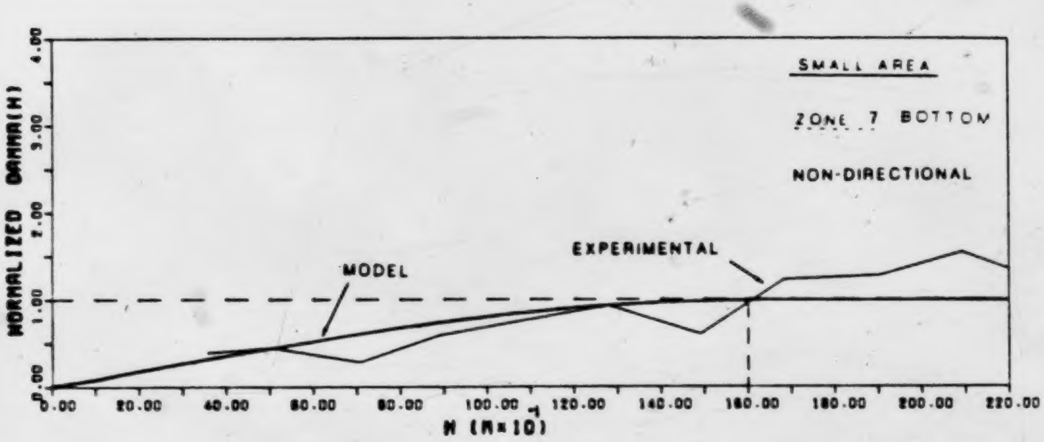

Figure 5.32 . Experimental and model variograms of the bottom of zone 7.

TABLE 5.5 Summary of the zones tops and bottoms model variograms in the small area.

Zone	Nugget effect	Range (m)	*A priori* variance $(m)^2$
Surface	0.00	1670	67.08
1-top	0.00	1150	40.52
2-top	0.00	970	50.96
3-top	0.00	1100	109.50
4-top	0.00	1570	150.30
5-top	0.00	1200	178.70
6-top	0.00	1100	150.80
7-top	0.00	1100	118.20
7-bottom	0.00	1600	85.19

The variogram of the top of zone 1 was:

$$\gamma_1(h)=(2/\pi 1150^2)\ [h\sqrt{1150^2-h^2}+1150^2\mathrm{Arcsin}(h/1150)]\ ,\quad \forall\ h\le 1150\ \mathrm{m}$$

and $\gamma_1(h)=1.0$, $\forall\ h\ge 1150$ m

The variogram of the top of zone 2 was:

$$\gamma_2(h)=(2/\pi 970^2)\ [h\sqrt{970^2-h^2}+970^2\mathrm{Arcsin}(h/970)]\ ,\quad \forall\ h\le 970\ \mathrm{m}$$

and $\gamma_2(h)=1.0$, $\forall\ h\ge 970$ m

The variogram of the top of zone 3 was:

$$\gamma_3(h)=(2/\pi 1100^2)\ [h\sqrt{1100^2-h^2}+1100^2\mathrm{Arcsin}(h/1100)]\ ,\quad \forall\ h\le 1100\ \mathrm{m}$$

and $\gamma_3(h)=1.0$, $\forall\ h\ge 1100$ m

The variogram of the top of zone 4 was:

$$\gamma_4(h)=(2/\pi 1570^2)\ [h\sqrt{1570^2-h^2}+1570^2\mathrm{Arcsin}(h/1570)]\ ,\quad \forall\ h\le 1570\ \mathrm{m}$$

and $\gamma_4(h)=1.0$, $\forall\ h\ge 1570$ m

The variogram of the top of zone 5 was:

$$\gamma_5(h)=(2/\pi 1200^2)\ [h\sqrt{1200^2-h^2}+1200^2\mathrm{Arcsin}(h/1200)]\ ,\quad \forall\ h\le 1200\ \mathrm{m}$$

and $\gamma_5(h)=1.0$, $\forall\ h\ge 1200$ m

The variogram of the top of zone 6 was:

$$\gamma_6(h)=(2/\pi 1100^2)\ [h\sqrt{1100^2-h^2}+1100^2\mathrm{Arcsin}(h/1100)]\ ,\quad \forall\ h\le 1100\ \mathrm{m}$$

and $\gamma_6(h)=1.0$, $\forall\ h\ge 1100$ m

The variogram of the top of zone 7 was:

$$\gamma_7(h)=(2/\pi 1100^2)\ [h\sqrt{1100^2-h^2}+1100^2\mathrm{Arcsin}(h/1100)]\ ,\quad \forall\ h\le 1100\ \mathrm{m}$$

and $\gamma_7(h)=1.0 \ , \ \forall \ h \geq 1100$ m

The variogram of the bottom of zone 7 was:

$$\gamma_8(h)=(2/\pi 1600^2)\ [h\sqrt{1600^2-h^2}+1600^2 \mathrm{Arcsin}(h/1600)] \ , \quad \forall \ h \leq 1600 \text{ m}$$

and $\gamma_8(h)=1.0 \ , \ \forall \ h \geq 1600$ m

The characteristics of the variogram models of the zones tops and bottoms are summarized in Table 5.5.

5.3 Comparison of the Fitted Variograms to Known Models

It was difficult to compare variograms of oil saturation calculated in this study with the variograms of other geostatistical studies on the Athabasca oil sands. This was because of the different approaches of the different investigators in defining the domains within which variograms are constructed (see paragraph 1.2, p. 6-8). A comparison could only be made, to an extent, with some of the variograms calculated by Grasley (1982).

The variograms of zones 4 and 6 corresponded to the 'estuarine' and 'fluvial' zones, respectively, of Grasley's study. In Grasleys's 'fluvial' zone, the variograms calculated over an area of approximately the size of the large area in this study had ranges of 1100 m, 900 m, 2000 m and 1700 m in the directions E-W, NE-SW, N-S and NW-SE respectively. These ranges do not significantly differ from the ranges of the equivalent variograms of zones 6 in the large area (1200 m, 1000 m, 1600 m and 2000 m, in the same directions). The apparent difference was that the range of

Grasley's variogram in the N-S direction was larger than in the NW-SE, while the opposite was evident in the variograms of zone 6. This was considered as a consequence of the fact that the variograms of the two studies were constructed over different parts of the Athabasca deposit and the existing paleo-channels differ slightly in trend and average size. The vertical variograms of the 'fluvial' zone and zone 6 also had approximately the same ranges (12 m and 13 m respectively).

Grasley's 'estuarine' zone corresponded roughly to zone 4. The main difference between the two zones was that the first included not only the channel system of the middle McMurray, but the also overlying shales and possibly parts of the upper McMurray. The directional variograms in the two zones were slightly different. In particular, the ranges in the 'estuarine' zone were 1200 m, 1500 m, 1700 m and 1400 m in the directions E-W, NE-SW, N-S, and NW-SE respectively. The equivalent ranges in zone 4 were 1200 m, 1200 m, 1600 m and 2000 m. The differences were obviously due to the different geological models used. The vertical variograms had almost the same ranges (12 m and 14 m).

6. MINIMUM VARIANCE MODELS

Grade models of the deposit in both total (large area) and control (small area) areas were constructed using ordinary punctual kriging. The grade estimation and assocated error calculations were based on the results of the structural analyses (paragraph 5.2). The process followed was:

a) interpolation of the boundaries of the identified zones,

b) three-dimensional gridding of the area modelled and coding of the grid points with respect to the zone to which they belonged, and

c) grade estimation and error calculation by zone using the samples within the zone only.

The details are discussed in the following two paragraphs.

6.1 Modelling of the Large Area

In the large area, the topographic, and Devonian surfaces as well as the tops of the seven identified zones were interpolated on a regular grid of 27 x 37 points at 600 x 600 meters grid spacing. This spacing was approximately half the average spacing of the wells in the area. The surfaces were modelled in a three-dimensional manner so that no crossing between them was possible. The method used was that of minimum curvature (Briggs, 1974; Swain, 1976).

Minimum curvature is the deterministic interpolation technique which not only fits polynomials to a set of data points but also forces them to produce surface models with minimum total curvature. The method also reproduces the data points which coincide with grid points.

The creation of the minimum variance weight percent oil saturation block model of the deposit was initiated with the gridding of the large area using a regular three-dimensional grid of 27 x 37 x 41 points with 600 x 600 x 3 meters resolution. The vertical grid spacing of 3 meters was considered as optimum, taking into account the ranges of the vertical grade variograms (at least 4 times less than the range of the vertical variograms of the three main oil saturated zones) and the horizontal grid spacing. The grid set-up was followed by the identification of the zone to which each grid point belonged, on the basis of the position in space of the interpolated surfaces.

The grade block model was completed as the oil saturations were kriged. In the estimation procedure, the fitted variogram models of each zone were used. As discussed in the previous chapter (paragraph 5.1.2), the regionalized variable weight percent oil saturation was geometrically anisotropic in two dimensions, with the nugget effect being the same in both horizontal and vertical variograms of each zone. Since the anisotropy and the coordinate axes were coincident, the horizontal variogram model used for kriging in each zone and the distance

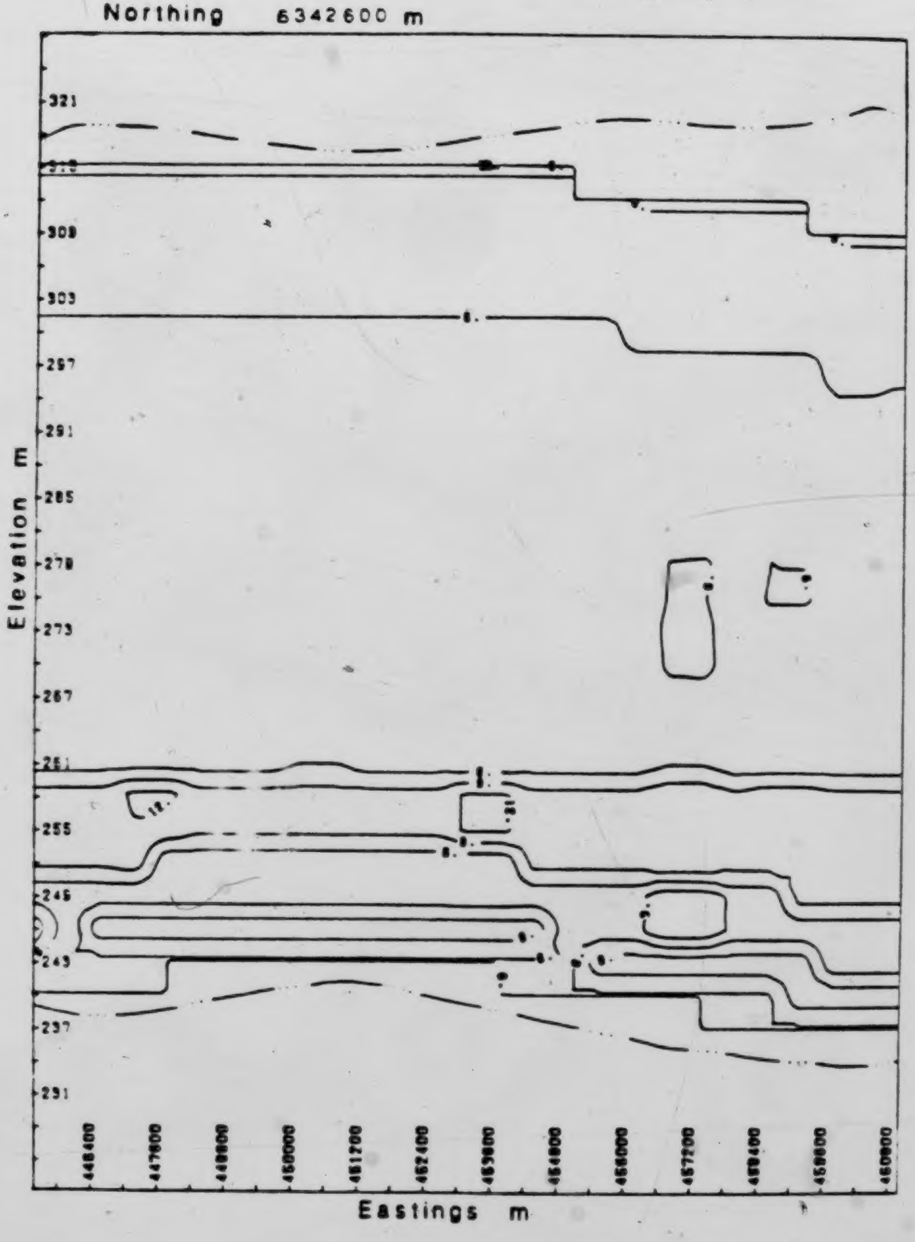

Figure 6.1 First cross-section of the grade model of the large area. The contour interval is 3% weight oil. – contours; – ··· – topographic (top) and unconformity (bottom) surfaces.

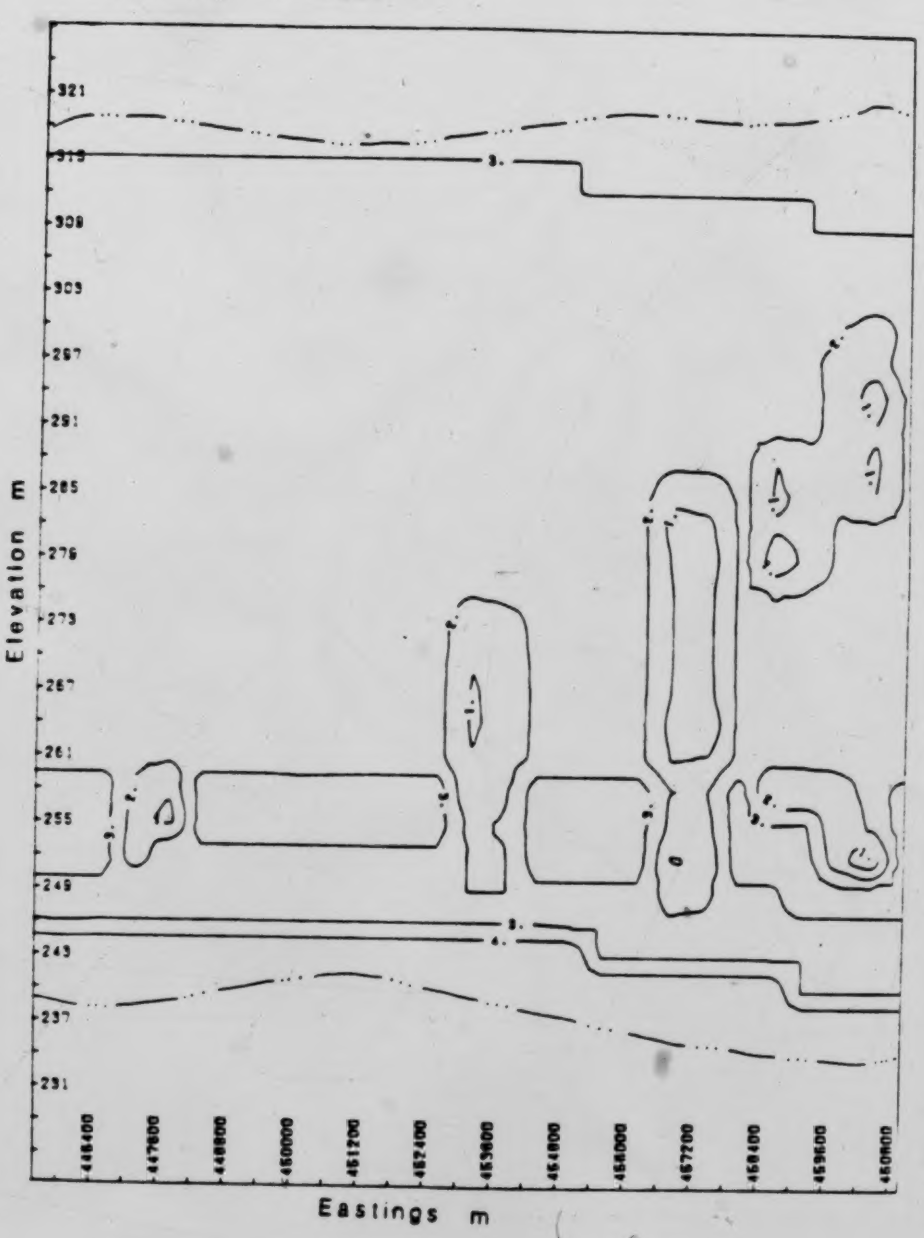

Figure 6.2 Error map of the first cross-section. The contour interval is 1 standard deviation. – contours; – ::: – topographic (top) and unconformity (bottom) surfaces.

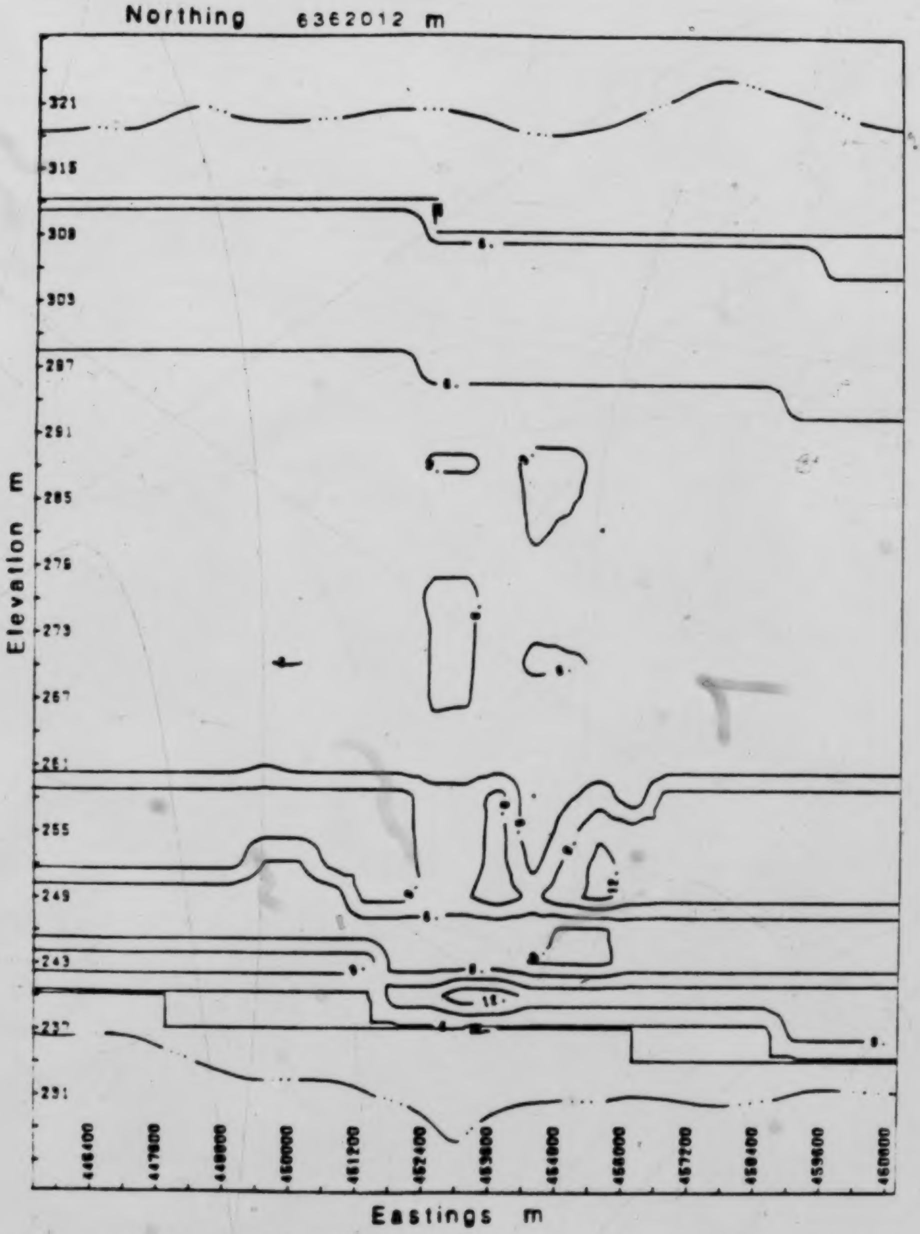

Figure 6.3 Second cross-section of the grade model of the large area. The contour interval is 3% weight oil. – contours; – ··· – topographic (top) and unconformity (bottom) surfaces.

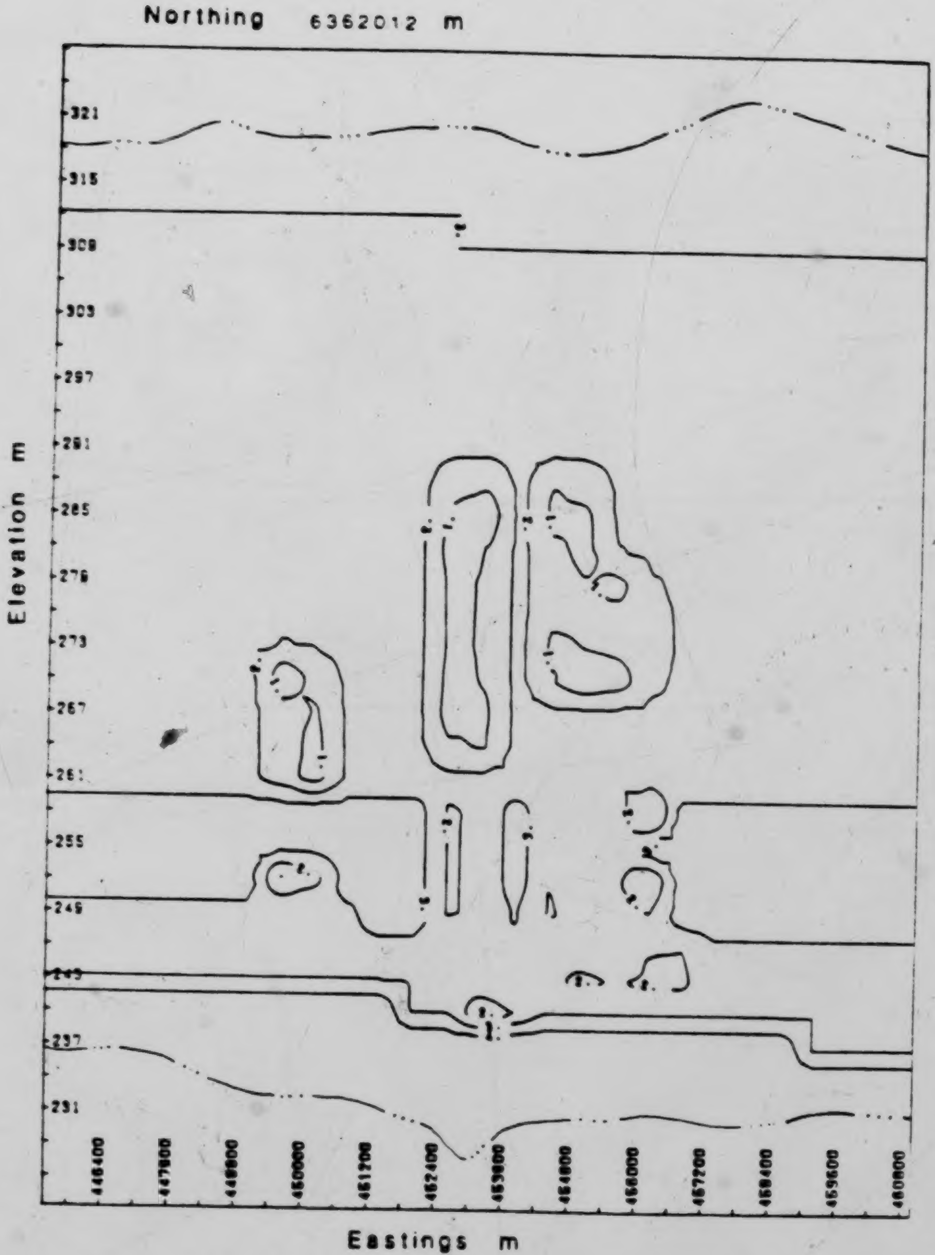

Figure 6.4 Error map of the second cross-section. The contour interval is 1 standard deviation. — contours; — ··· — topographic (top) and unconformity (bottom) surfaces.

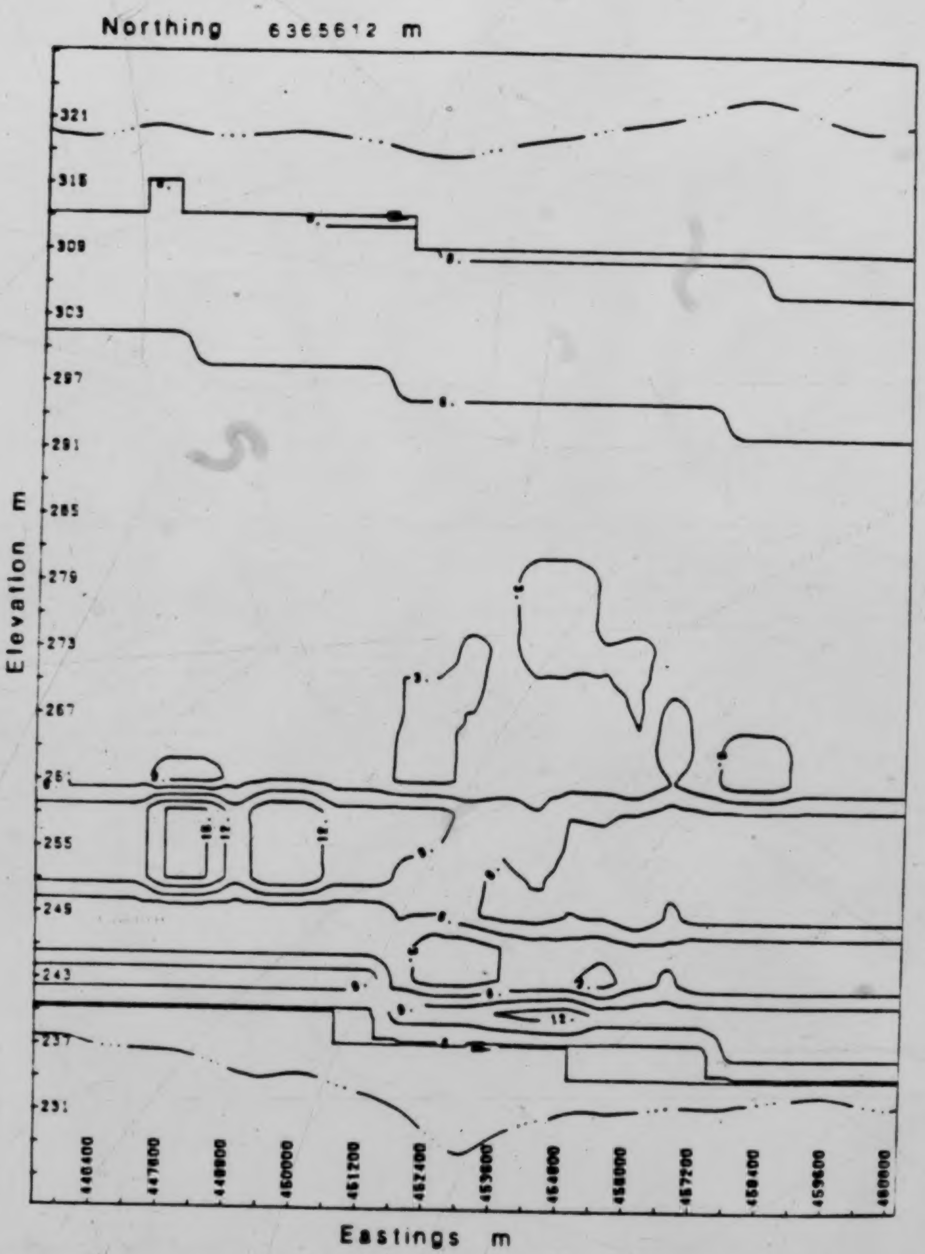

Figure 6.5 Third cross-section of the grade model of the large area. The contour interval is 3% weight oil. – contours; – ··· – topographic (top) and unconformity (bottom) surfaces.

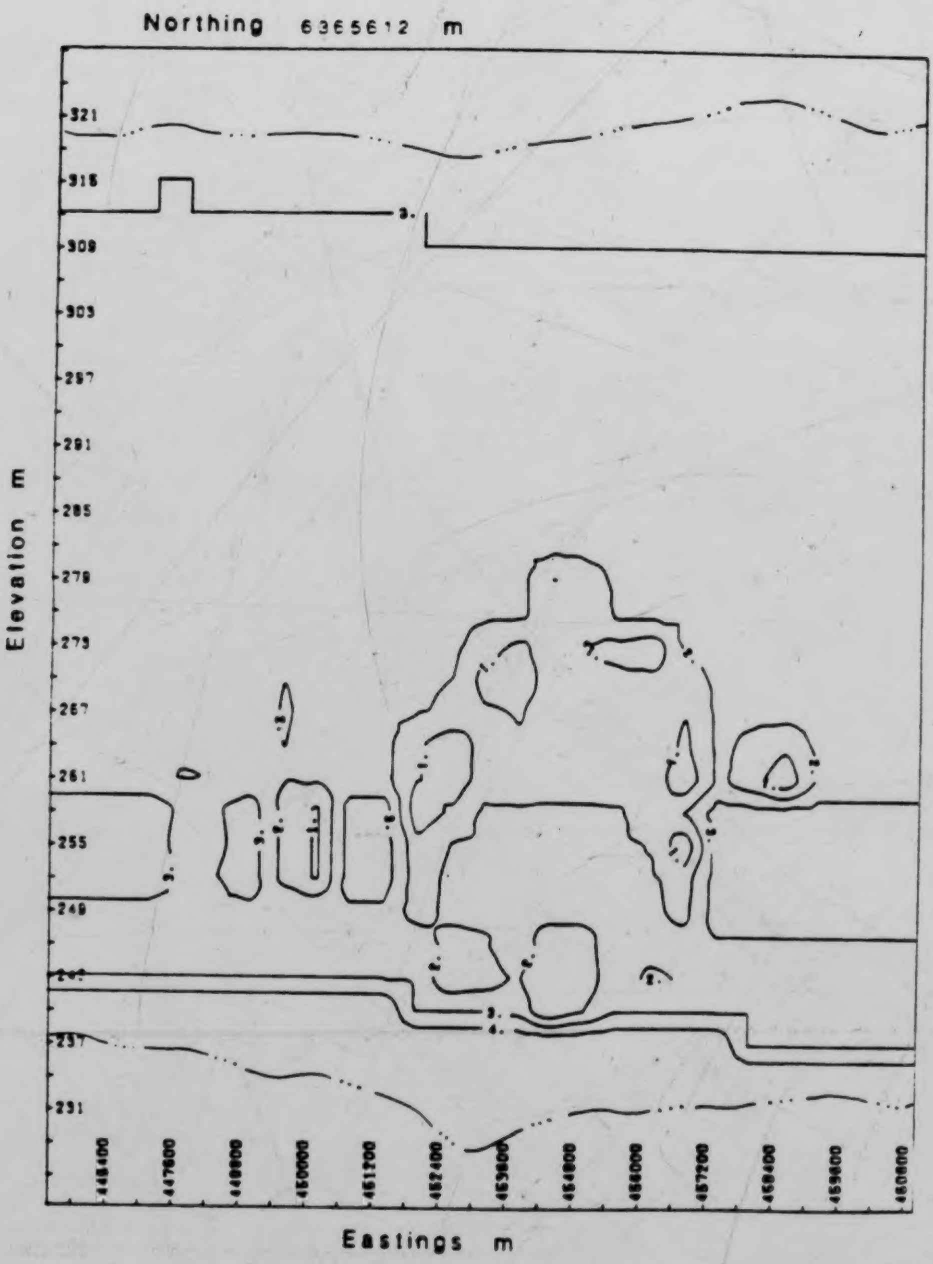

Figure 6.6 Error map of the third cross-section. The contour interval is 1 standard deviation. – contours; – ··· – topographic (top) and unconformity (bottom) surfaces.

between two points was calculated by the formula:

$$d=\sqrt{(x_1-x_2)^2+k^2(y_1-y_2)^2}$$

where k is the anisotropy ratio, equal to the ratio of the range of the horizontal to the range of the vertical variogram.

The estimation was local, using the 20 closest samples (with respect to distance d) to every grid point. In addition, grid points of a zone were estimated using samples within the same zone only. If no samples were within range, then the mean grade and standard deviation of the zone were assigned to the grid point.

Cross-sections of the constructed weight percent oil saturation model are depicted in Figures 6.1, 6.3 and 6.5. The error maps associated to the cross-sections are presented in Figures 6.2, 6.4 and 6.6. Note that the error is expressed in units of standard deviation.

6.2 Modelling of the Small Area

In the small area, the topographic and Devonian surfaces as well as the tops of the identified zones were interpolated in a three-dimensional sense using a grid of 152 x 43 points with 30 x 30 metres resolution. The grid spacing was approximately 13 times smaller than the average well spacing. The method used was ordinary punctual kriging, utilizing the variogram models derived in structural analysis (paragraph 5.2.3). Due to the fact that the ranges of the variogram models were relatively large with respect to the size of the area, no mean values were assigned to any control points.

The grade model of the deposit within the small area was constructed differently from that of the large area. Only the three main oil saturated zones, namely pay zone one (zone two), pay zone two (zone four) and pay zone three (zone six) were modelled.

The total area was again gridded (152 x 43 x 139 points), but with a higher resolution grid of 30 x 30 x 1 metres. The grid points were coded with respect to the zone to which they belonged, using the kriged surfaces as the boundaries of each zone. Each pay zone was then kriged separately using the variogram models fitted in structural analysis of the small area (paragraph 5.2.2).

A minimum variance model of the weight percent oil saturation was constructed. Cross-sections of the grade models of each zone are presented in Figures 6.7, 6.9, 6.11, 6.13, 6.15 and 6.17. The associated estimation error is given in Figures 6.8, 6.10, 6.12, 6.14, 6.16 and 6.18.

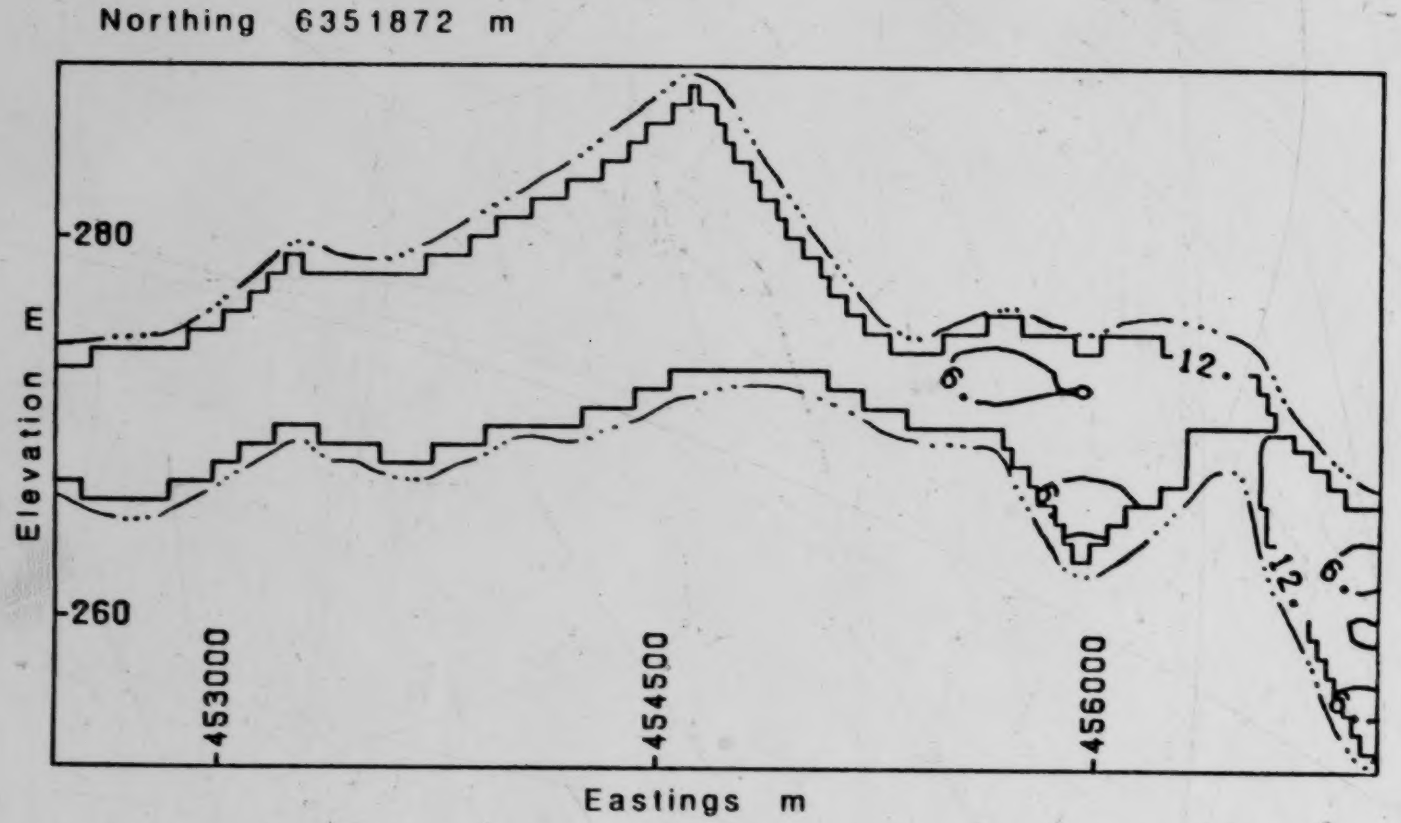

Figure 6.7 First cross-section of the grade model of pay zone 1 in the small area. The contour interval is 6% weight oil. – contours; – ··· – kriged boundaries of the zone.

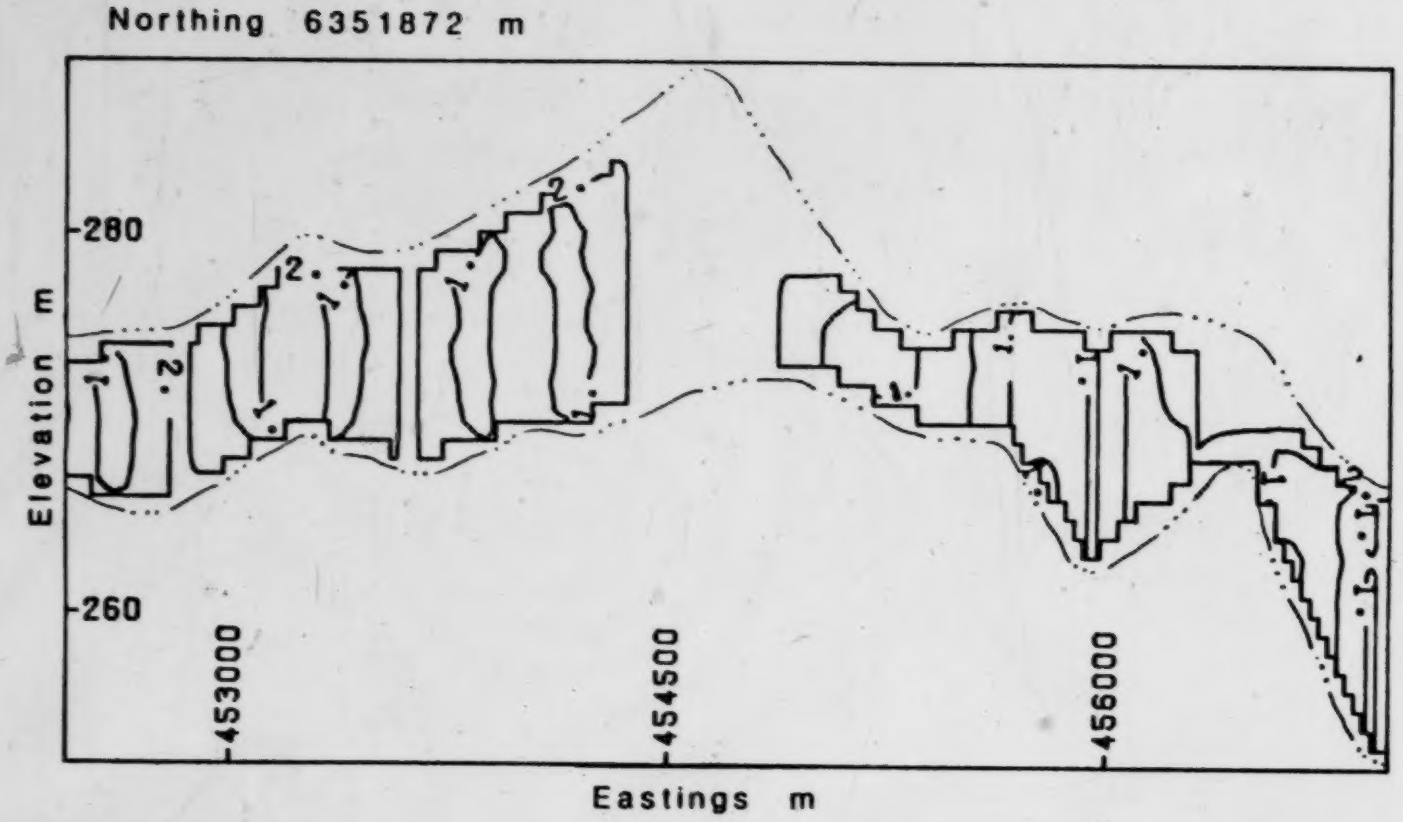

Figure 6.8 Error map of the first cross-section of pay zone 1. The contour interval is 1 standard deviation. – contours; – ··· – kriged boundaries of the zone.

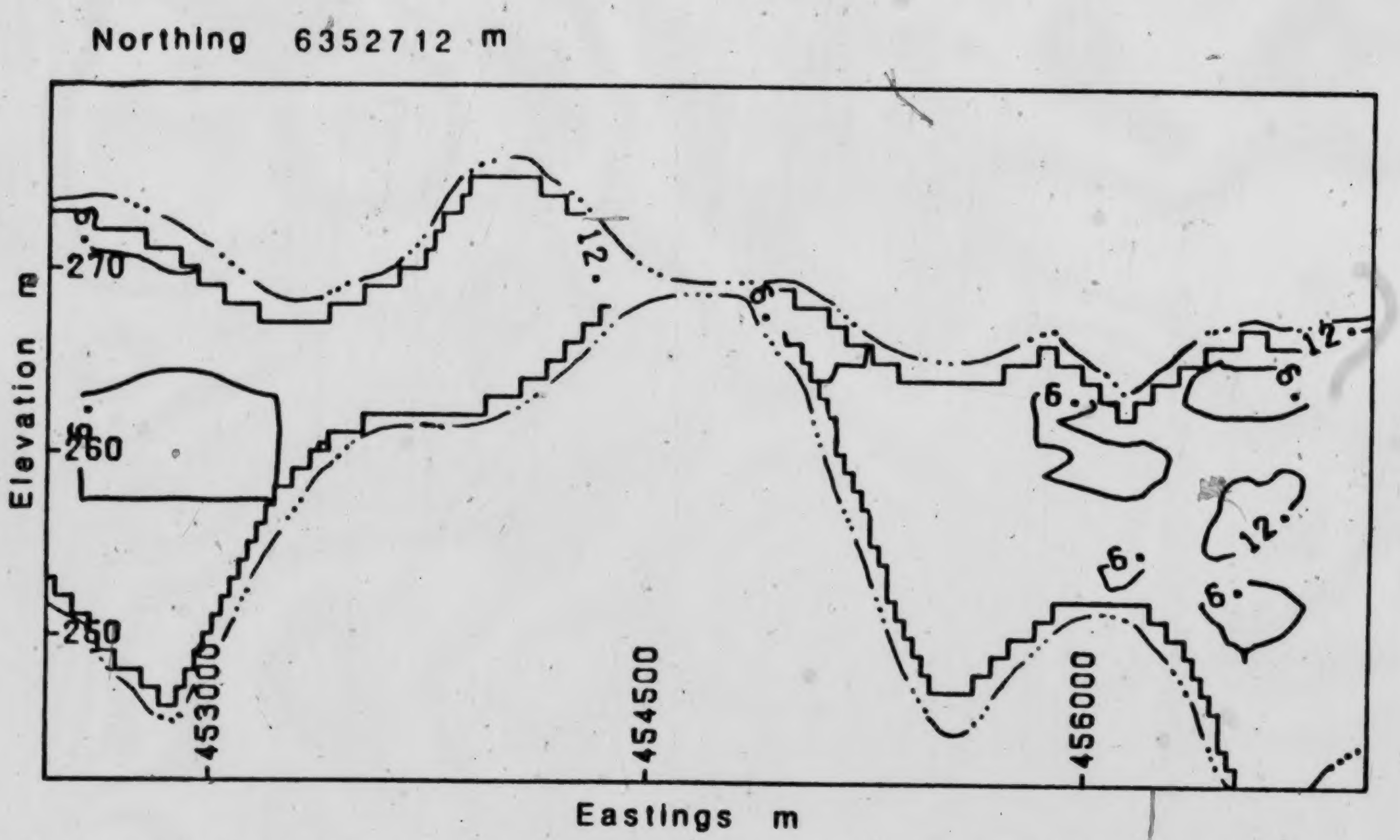

Figure 6.9 Second cross-section of the grade model of pay zone 1 in the small area. The contour interval is 6% weight oil. – contours; – ··· – kriged boundaries of the zone.

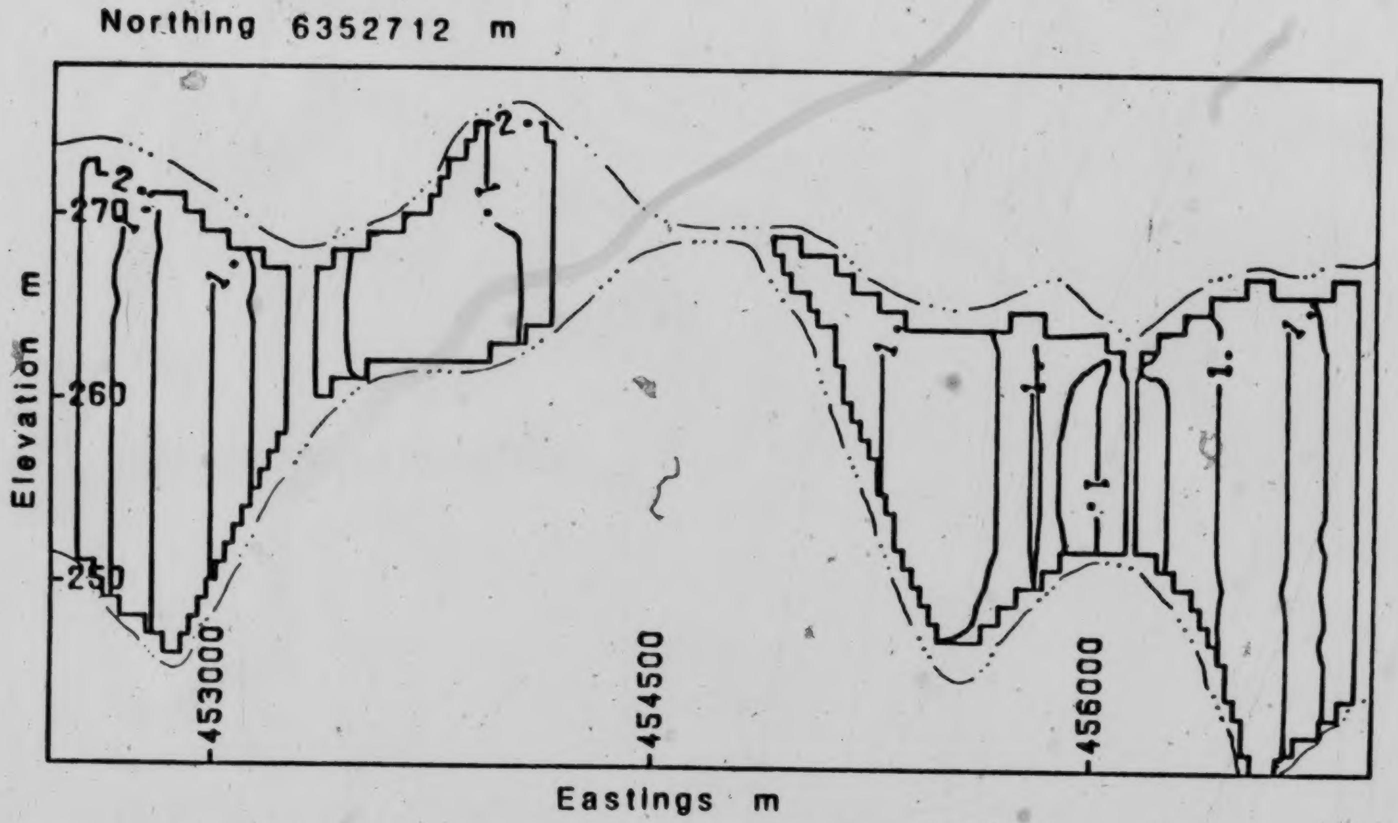

Figure 6.10 Error map of the second cross-section of pay zone 1. The contour interval is 1 standard deviation. – contours; – ··· – kriged boundaries of the zone.

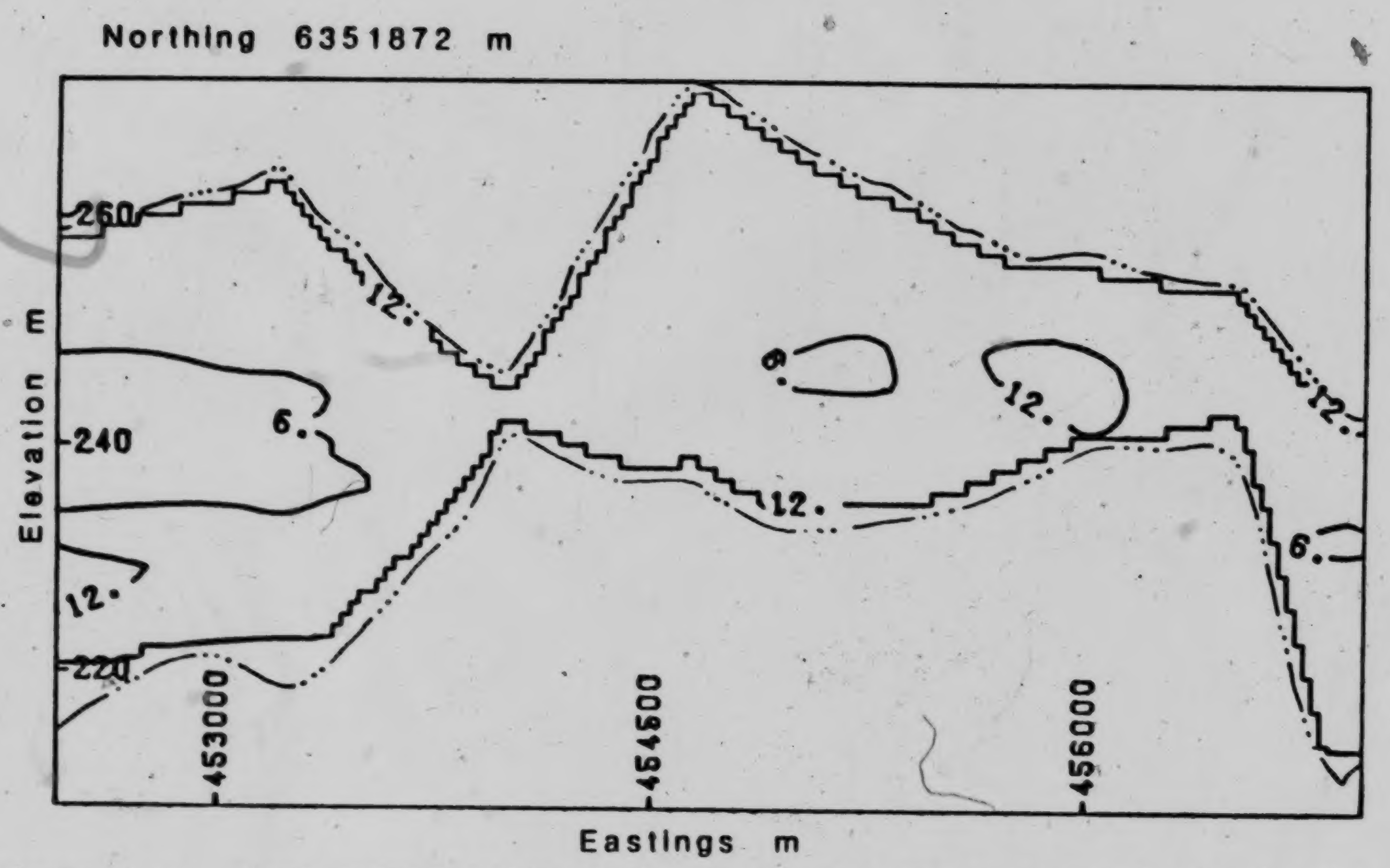

Figure 6.11 First cross-section of the grade model of pay zone 2 in the small area. The contour interval is 6% weight oil. – contours; – ··· – kriged boundaries of the zone.

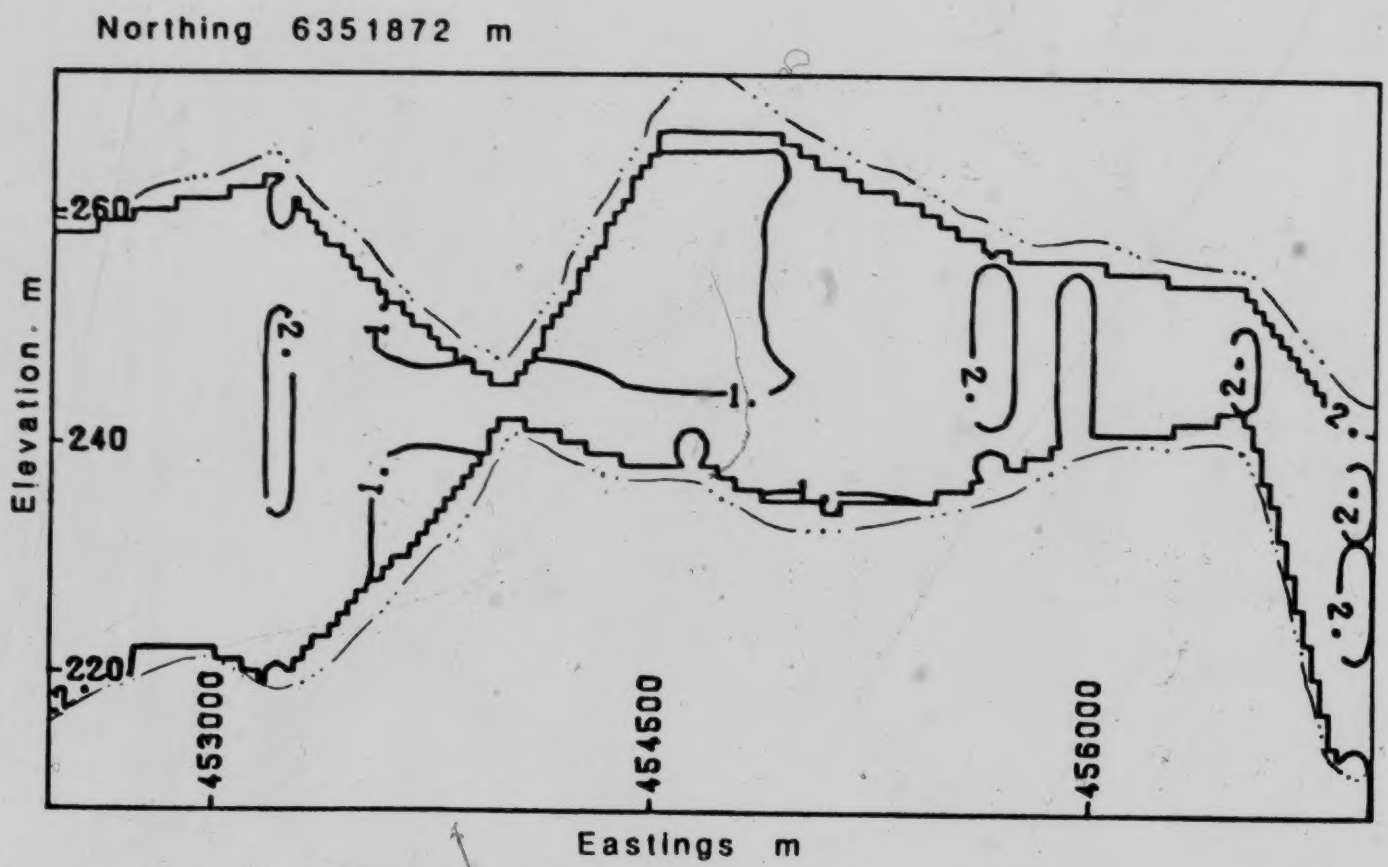

Figure 6.12 Error map of the first cross-section of pay zone 2. The contour interval is 1 standard deviation. – contours; – ··· – kriged boundaries of the zone.

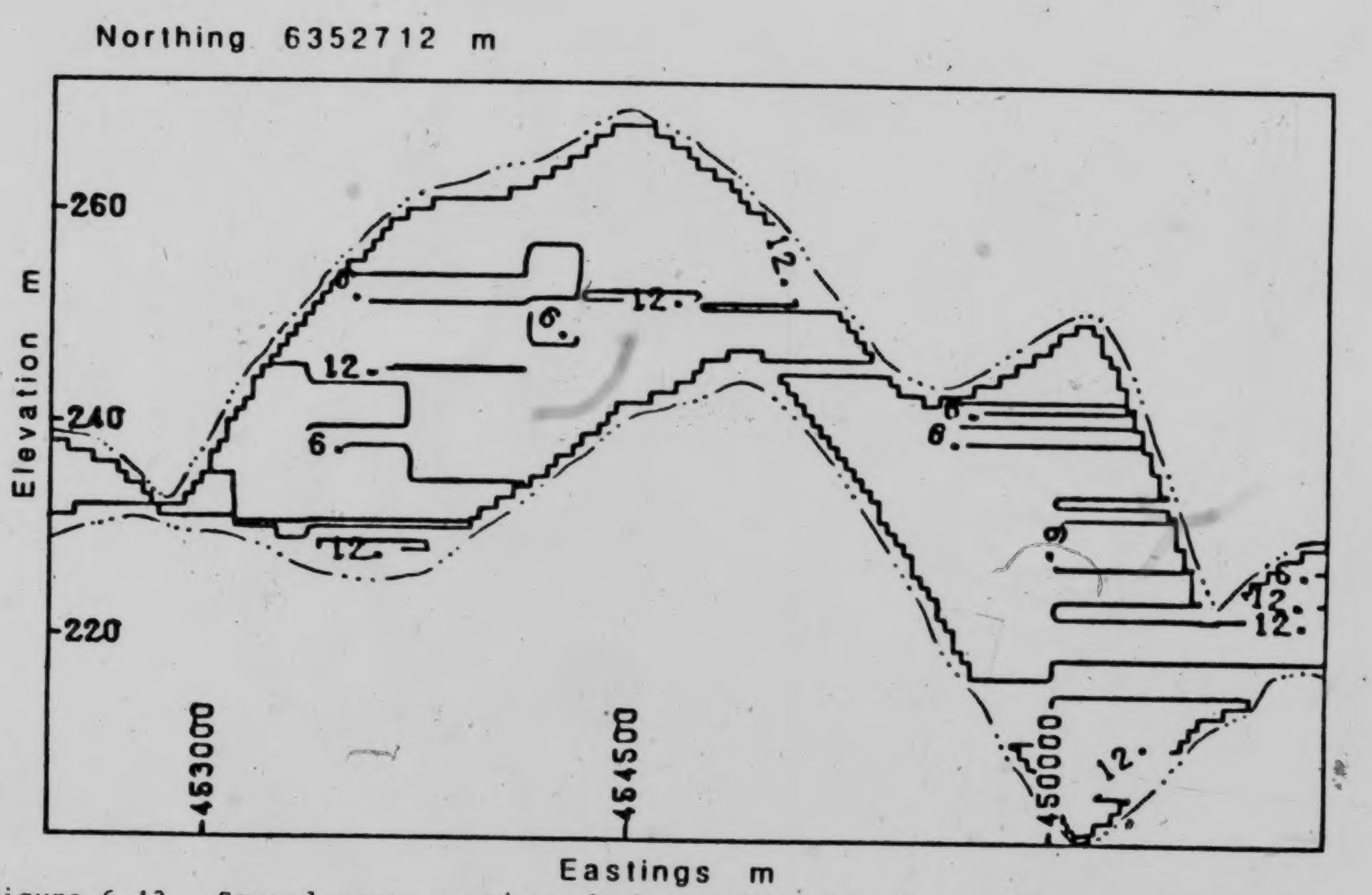

Figure 6.13 Second cross-section of the grade model of pay zone 2 in the small area. The contour interval is 6% weight oil. – contours; – ··· – kriged boundaries of the zone.

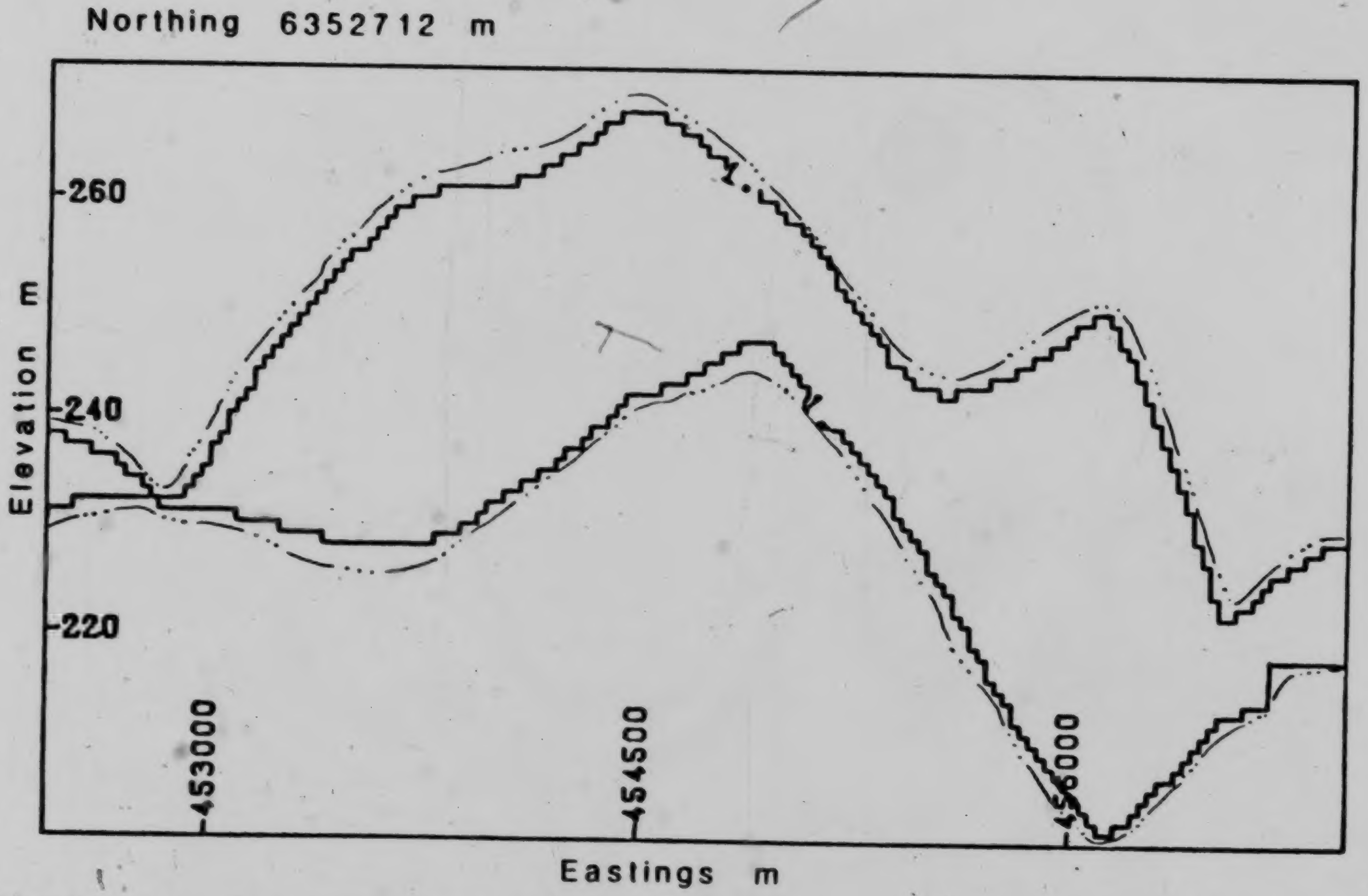

Figure 6.14 Error map of the second cross-section of pay zone 2. The contour interval is 1 standard deviation. – contours; – ··· – kriged boundaries of the zone.

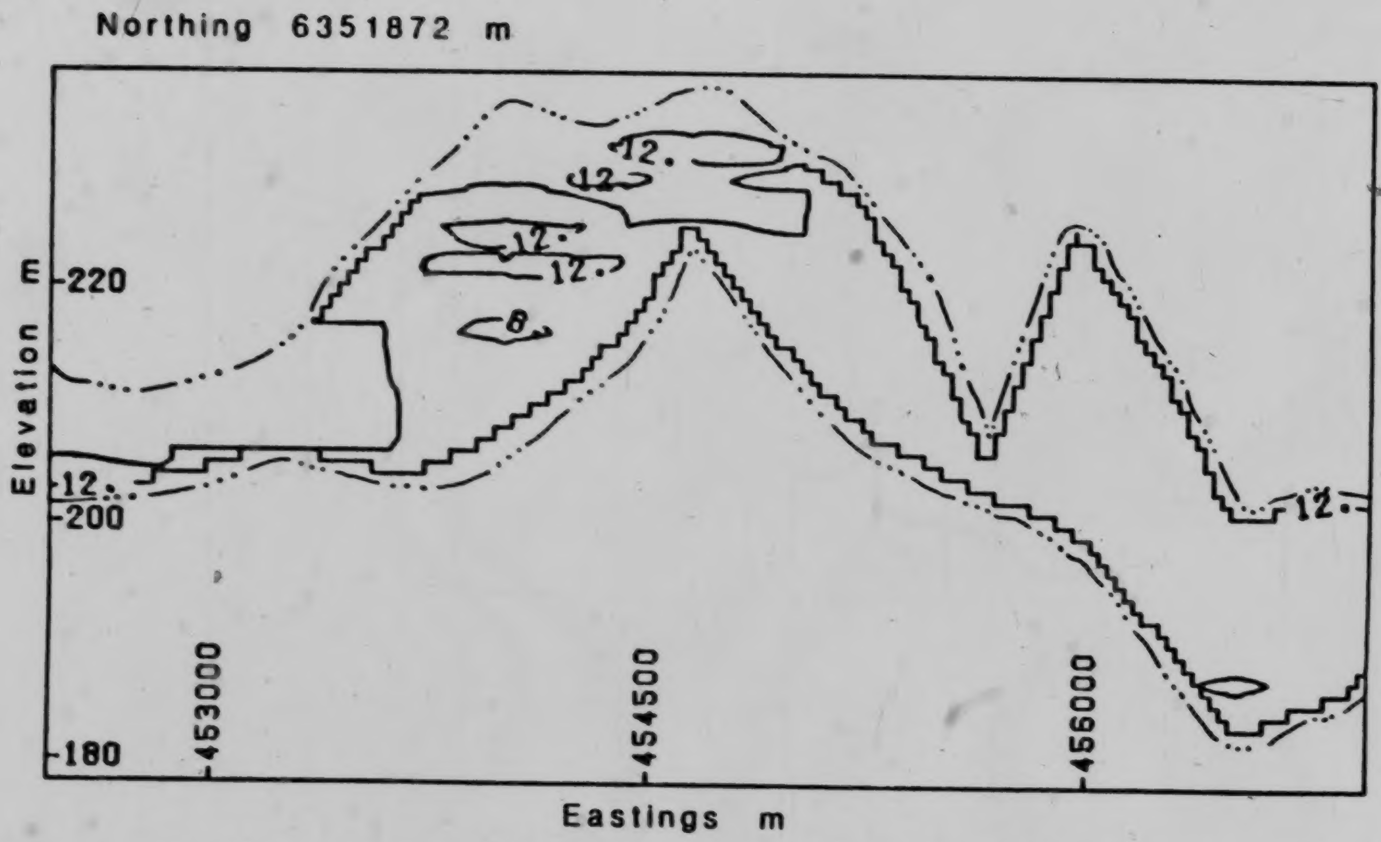

Figure 6.15 First cross-section of the grade model of pay zone 3 in the small area. The contour interval is 6% weight oil. – contours; – ··· – kriged boundaries of the zone.

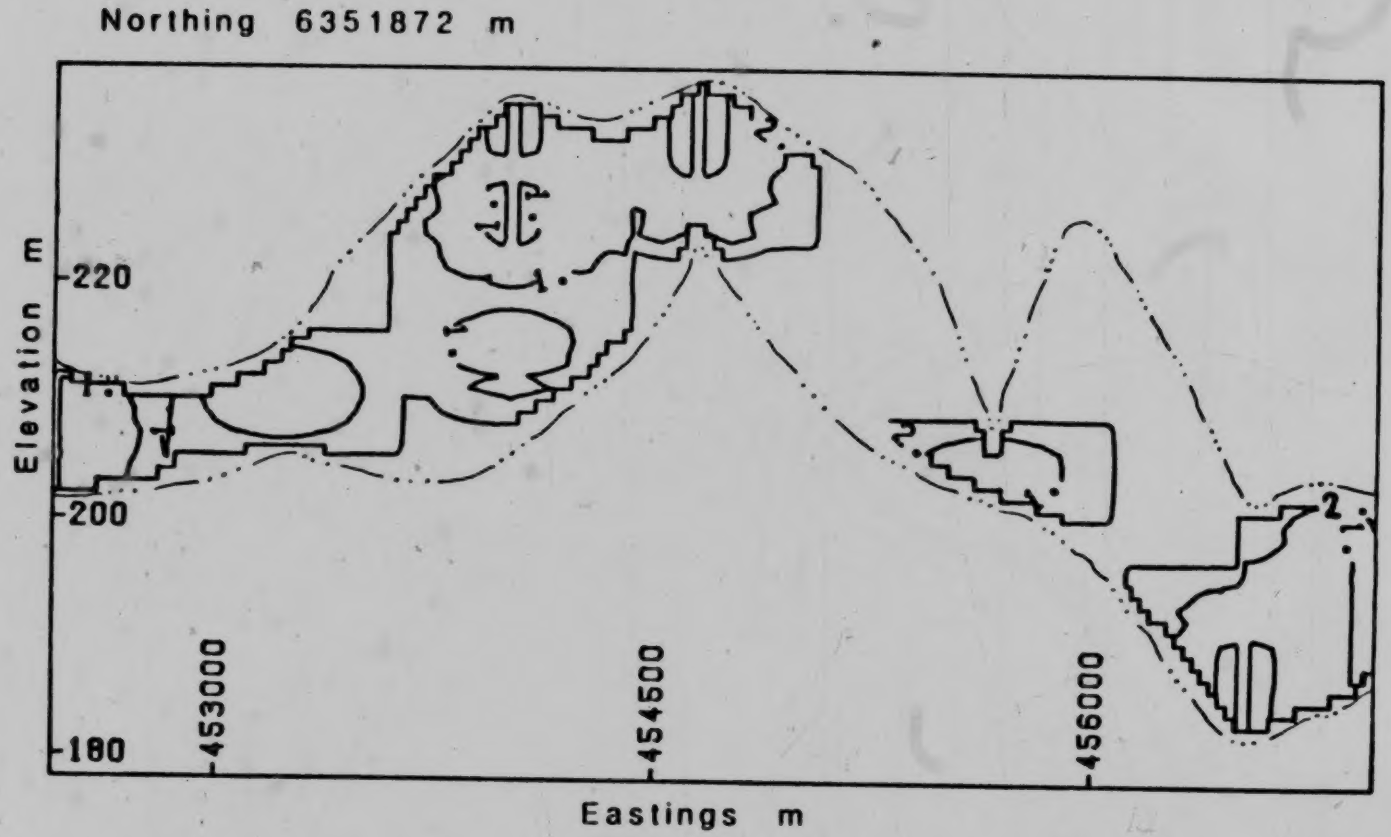

Figure 6.16 Error map of the first cross-section of pay zone 3. The contour interval is 1 standard deviation. – contours; – ··· – kriged boundaries of the zone.

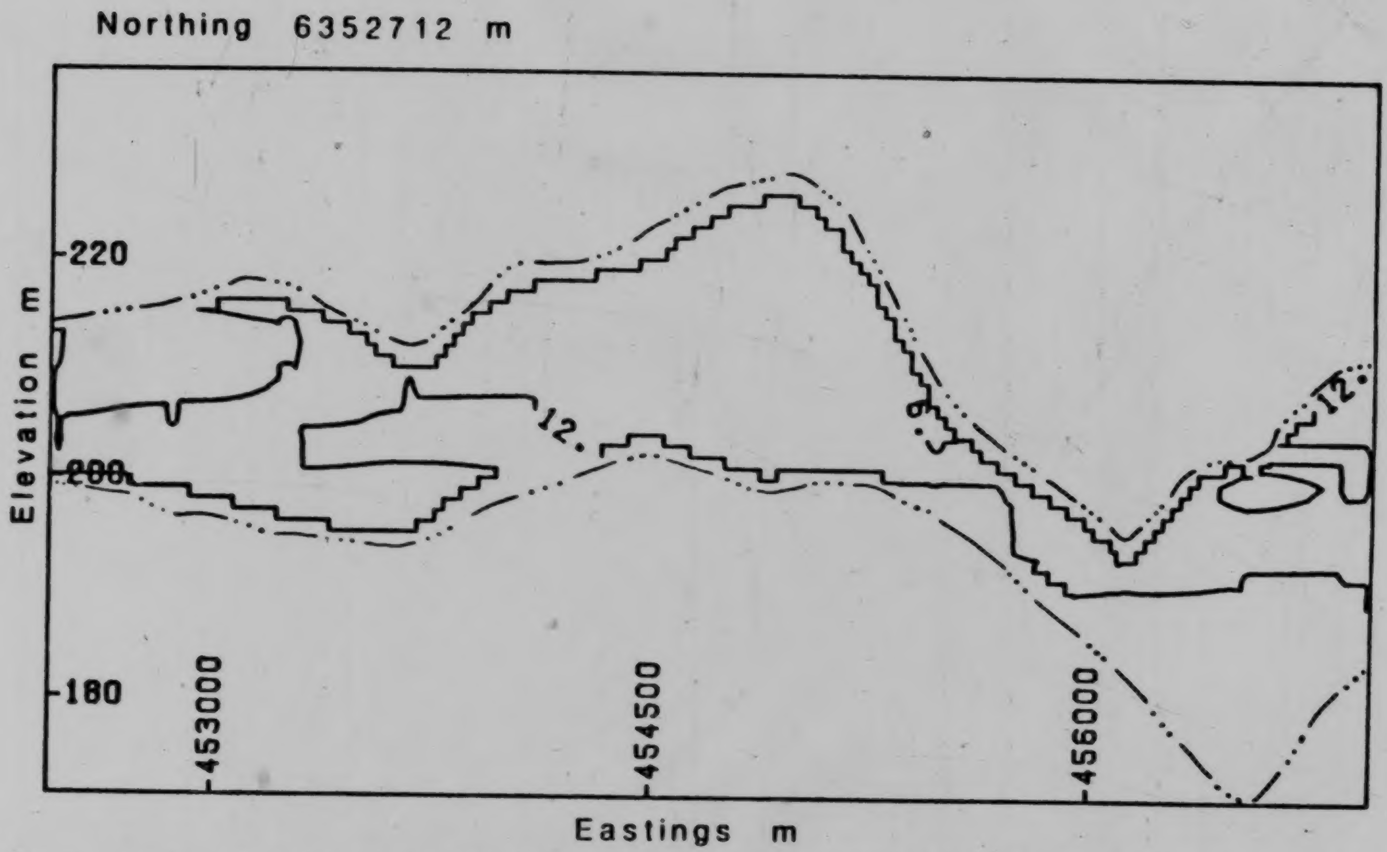

Figure 6.17 Second cross-section of the grade model of pay zone 3 in the small area. The contour interval is 6% weight oil. – contours; – ··· – kriged boundaries of the zone.

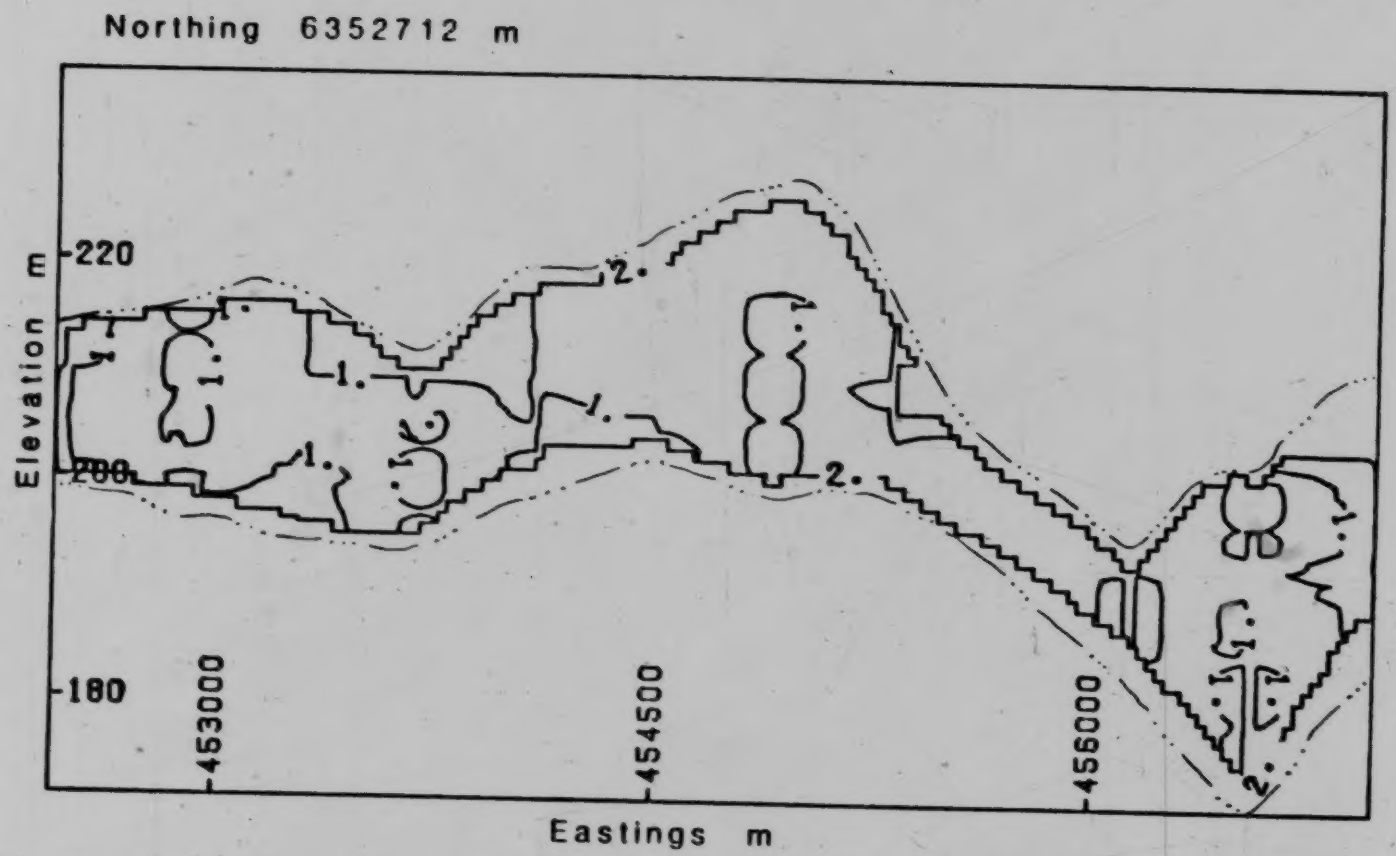

Figure 6.18 Error map of the second cross-section of pay zone 3. The contour interval is 1 standard deviation. – contours; – ··· – kriged boundaries of the zone.

7. CONDITIONALLY SIMULATED MODELS

The variability of the boundaries and the weight percent oil of each pay zone within the small area were reconstructed using the conditional simulation technique. The conditional simulation process involved the following four steps:

a) simulation of a random field, which consisted of a regular grid of simulated values with the same mean, variance and variogram as the data points,

b) kriging of the grid points using the original data,

c) kriging of the grid points using the simulated values at the sample points, and

d) summation on each grid point of the corresponding values from steps b and c and subtraction of the value from step a.

Note that for the conditioning process (steps b, c and d) each of the available samples was slightly moved from their original locations in order to coincide with the nearest grid point.

7.1 Simulation of the Surfaces

One standarized two-dimensional random field of 400 x 400 points was non-conditionally simulated on a regular grid of 30 x 30 metres resolution. The input variogram model for the simulation was circular and isotropic with a range of 1200 metres and a nugget effect of 0.0. Part of the simulated field (152 x 43 points) was selected, standarized and used for the construction of the non-conditionally simulated models of the boundaries of all zones. This was done by simply de-standarizing the simulated field so that each time it was in conformity with the mean and variance of the respective surface. The variogram (same for all) of the simulated surfaces is presented in Figure 7.1.

The use of the same random field ensured that the crossing between tops and bottoms of the same or successive zones would be a minimum. Thus, both the corrections imposed to restore the conformability as well as the distortion of the variogram of the non-conditionally simulated surfaces were minimal.

The characteristics of the input to the simulation variogram model were conformable to the results of the structural analysis (paragraph 5.2.3) with the exception of the range which was approximately the average of all ranges.

The reason that a large field was simulated and then a part of it selected, is as follows. As a consequence of the ergodic theorem, the larger the size of the field to be simulated is with respect to the range of the input variogram, the closer the output variogram is to the input model. Satisfactory reproduction is accomplished if the size of the simulated field is about 10 times the size of the range of the input variogram model.

For the conditioning of the simulated tops and bottoms to the data points, the drill holes were moved from their original locations to the closest grid points. The maximum distance of relocation was 15 metres. This distance was half the expected error in the given locations of the boreholes. Thus the relocation of the data points did not have any effect on the models produced.

The variograms of the conditionally simulated surfaces are depicted in Figures 7.1, 7.2, 7.3, 7.4 and 7.5. The summary statistics are given in Table 7.1.

Figure 7.6, depicts the simulated model of the surface topography in the small area. The conditionally simulated model of the same surface is presented in Figure 7.7. For visual comparison of the differences between simulated realities and estimated-interpolated models, the minimum variance and minimum curvature models of the same surface are also given in Figures 7.8 and 7.9 respectively.

7.2 Non-Conditional Simulation of the Pay Zones

The deposit in the small area was gridded in three-dimensions. The conditionally simulated boundaries of the zones were used to code each grid point with respect to the zone to which it belongs. The grid points belonging to each pay zone were separated and simulation was performed separately. The variogram models used for the simulations were the ones fitted in the structural analysis (paragraph 5.2.2).

The variograms of all pay zones are a combination of two nested structures, one pure nugget effect and a

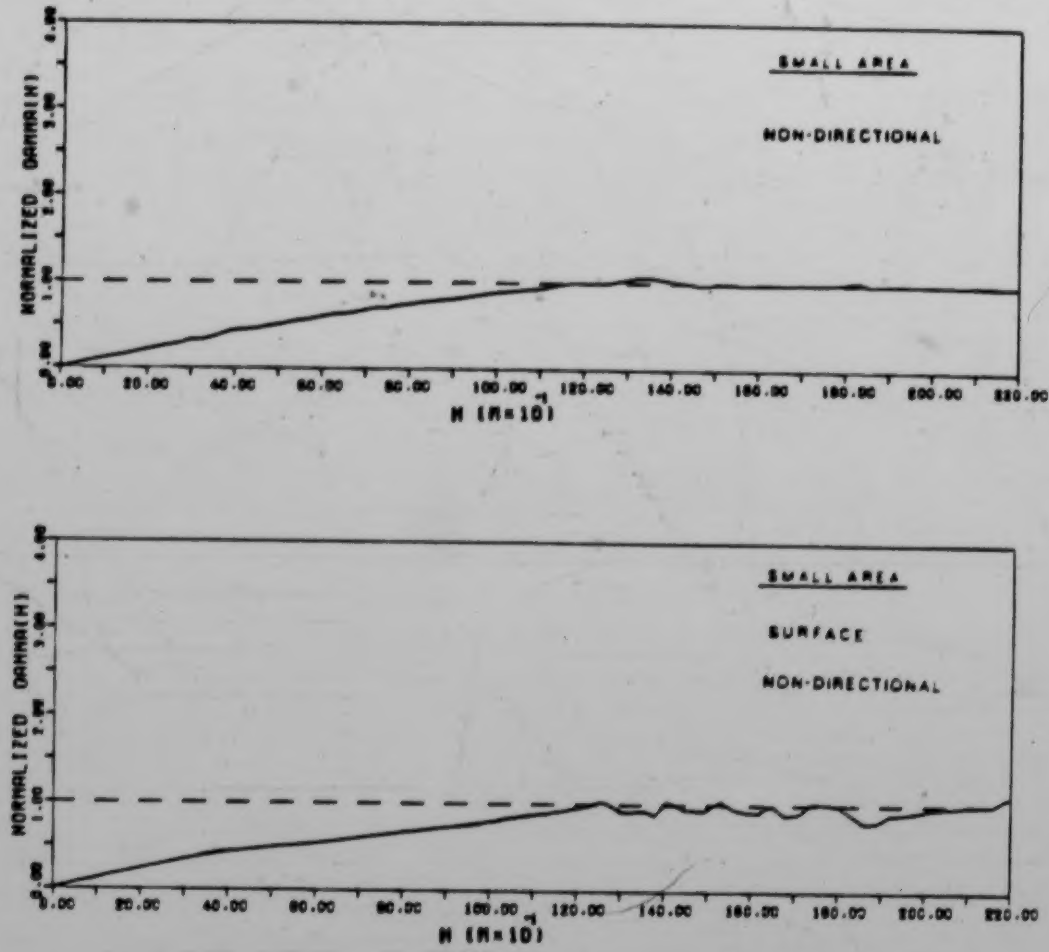

Figure 7.1 Variograms of the two-dimensional simulated field (top) and conditionally simulated surface topography (bottom).

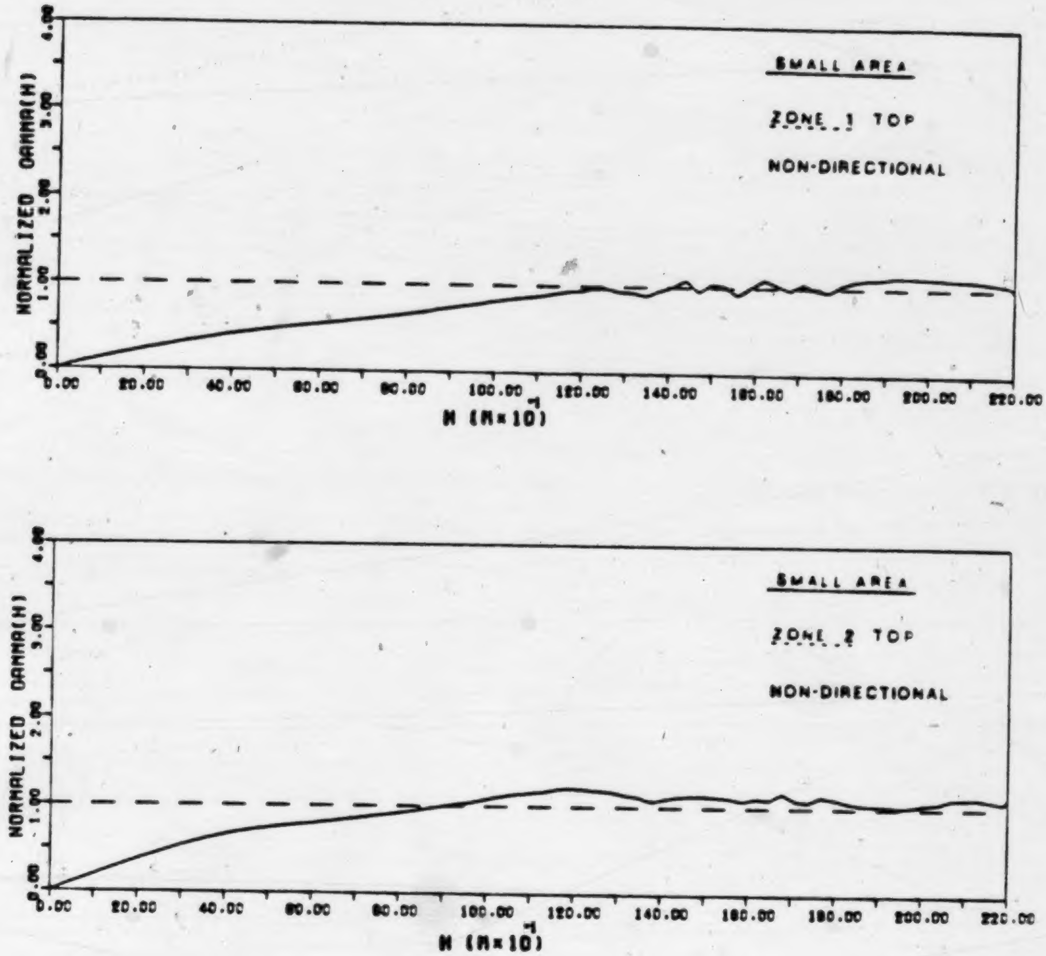

Figure 7.2 Variograms of the conditionally simulated tops of zone 1 (top) and zone 2 (bottom).

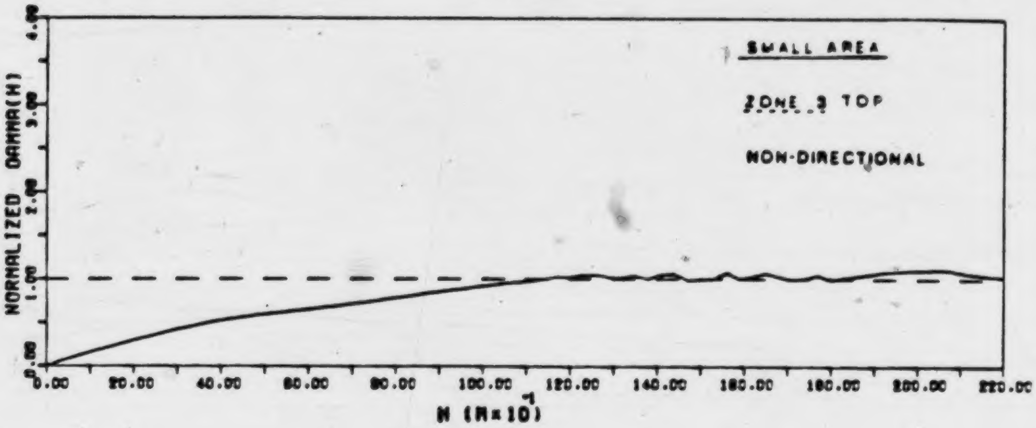

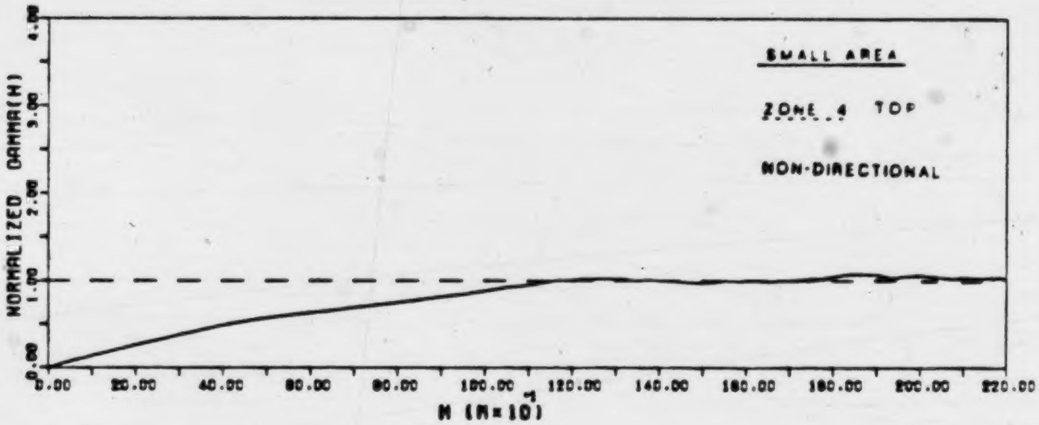

Figure 7.3 Variograms of the conditionally simulated tops of zone 3 (top) and zone 4 (bottom).

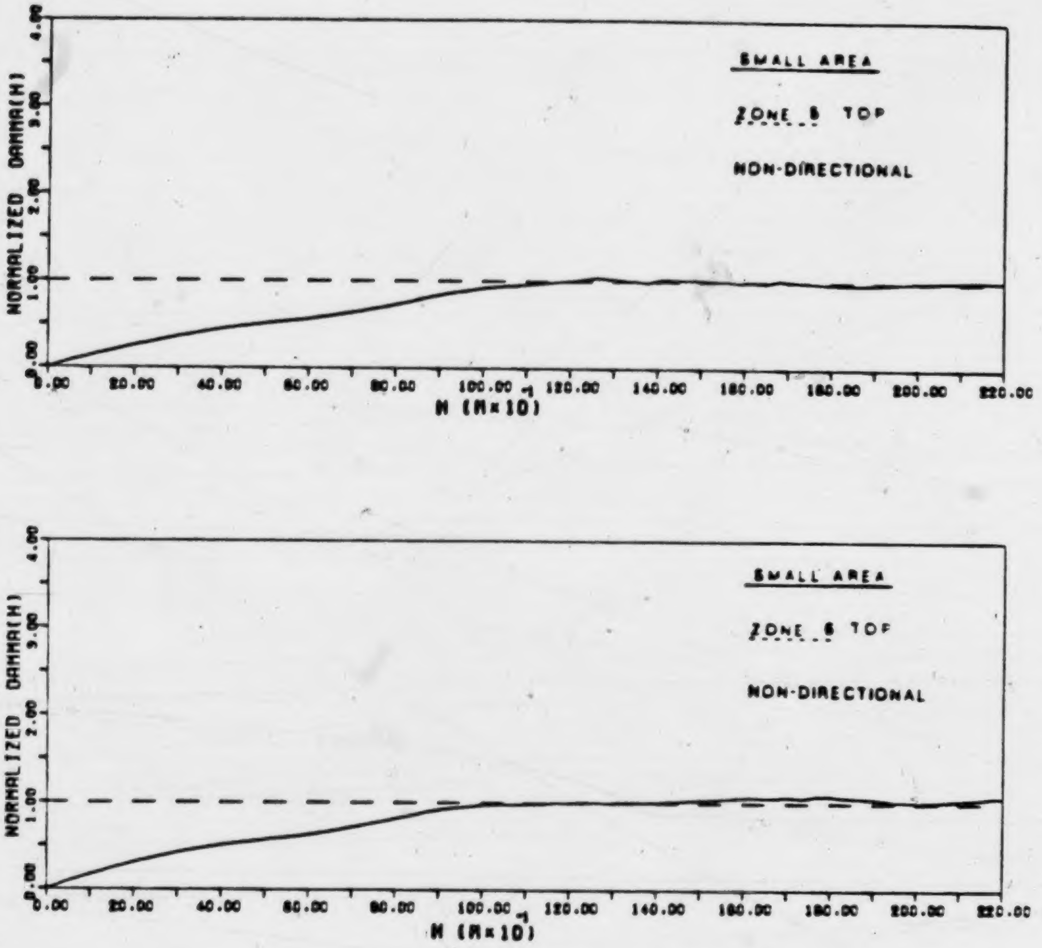

Figure 7.4 Variograms of the conditionally simulated tops of zone 5 (top) and zone 6 (bottom).

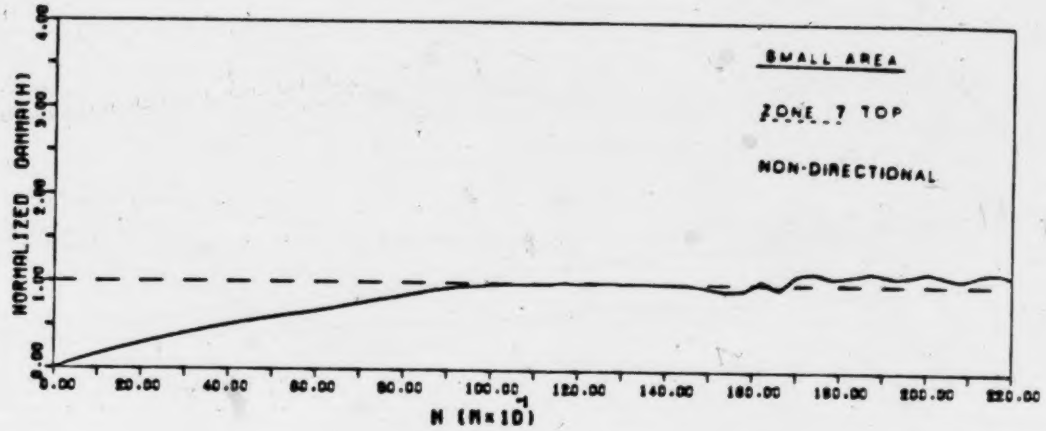

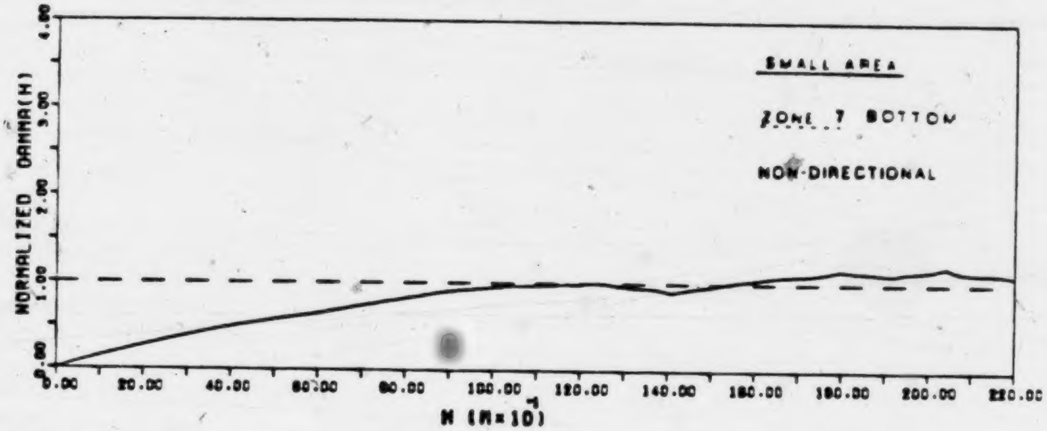

Figure 7.5 Variograms of the conditionally simulated top of zone 7 (top) and bottom of zone 7 (bottom).

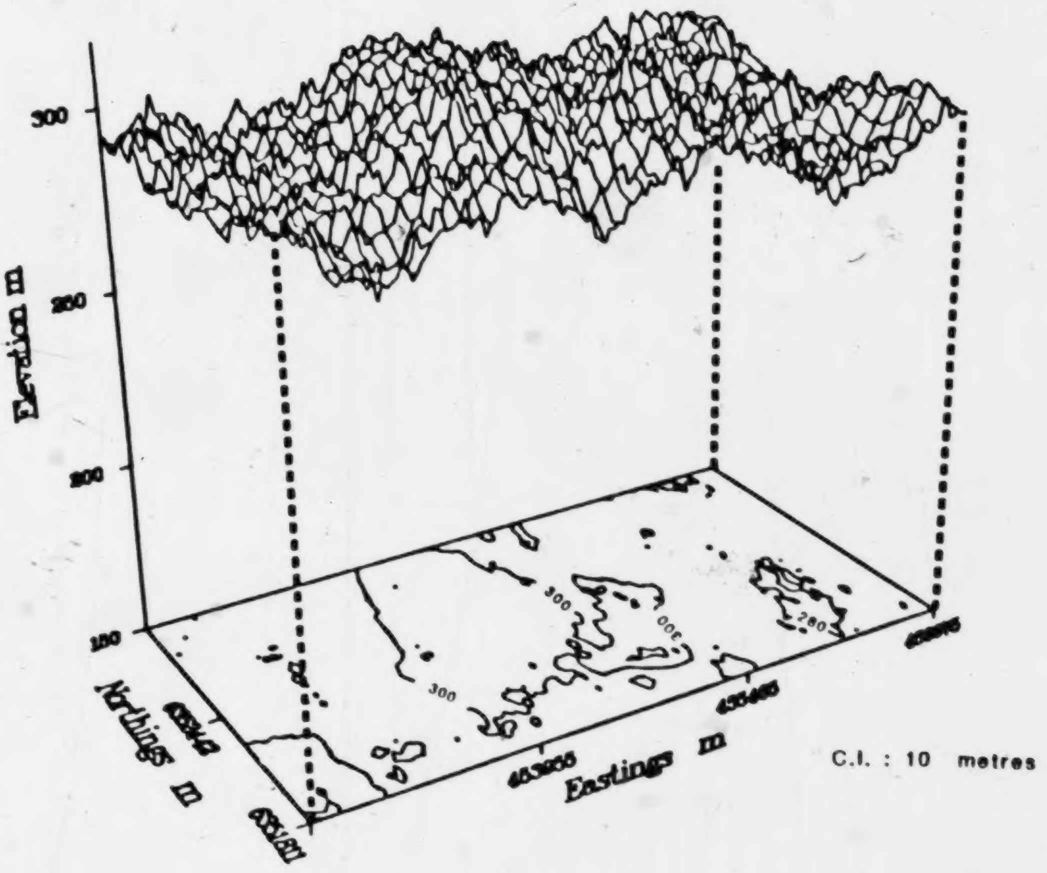
300
250
200
150
Elevation m
Northings m
Eastings m
300
300
300
280
C.I. : 10 metres

Figure 7.6 Simulated model of the topographic surface in the small area.

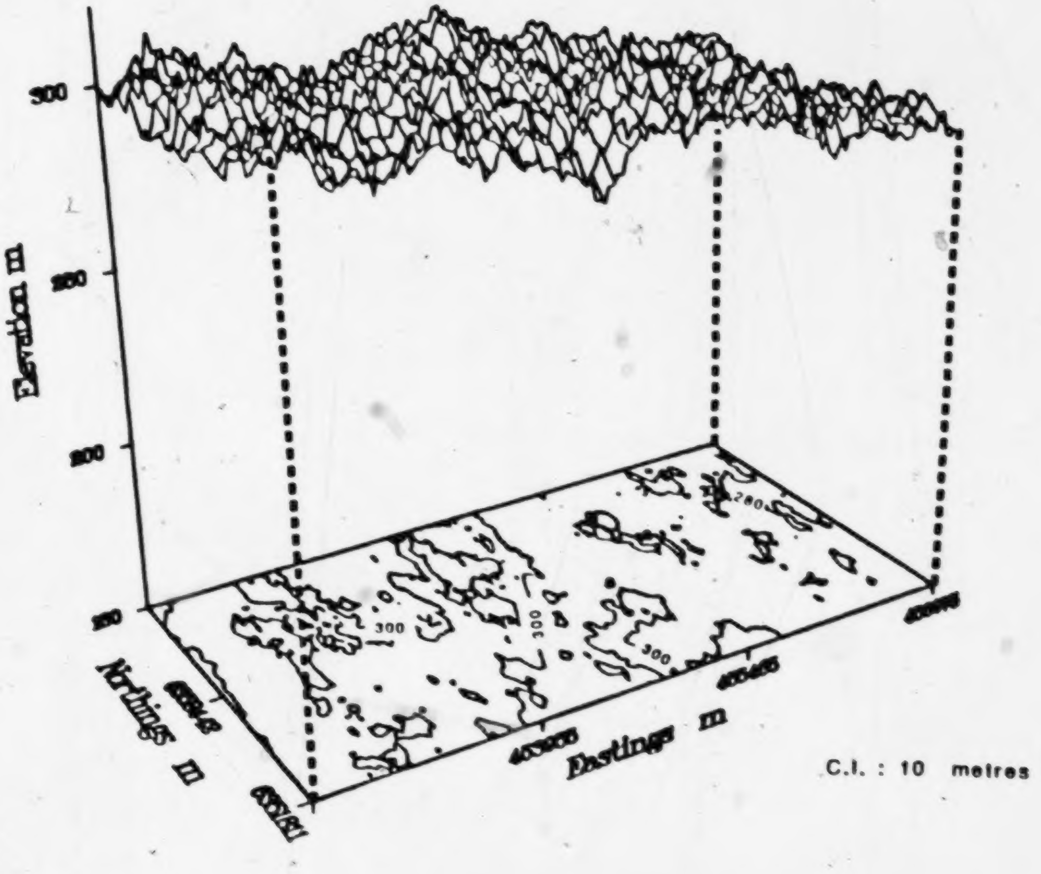

Figure 7.7 Conditionally simulated model of the topographic surface in the small area.

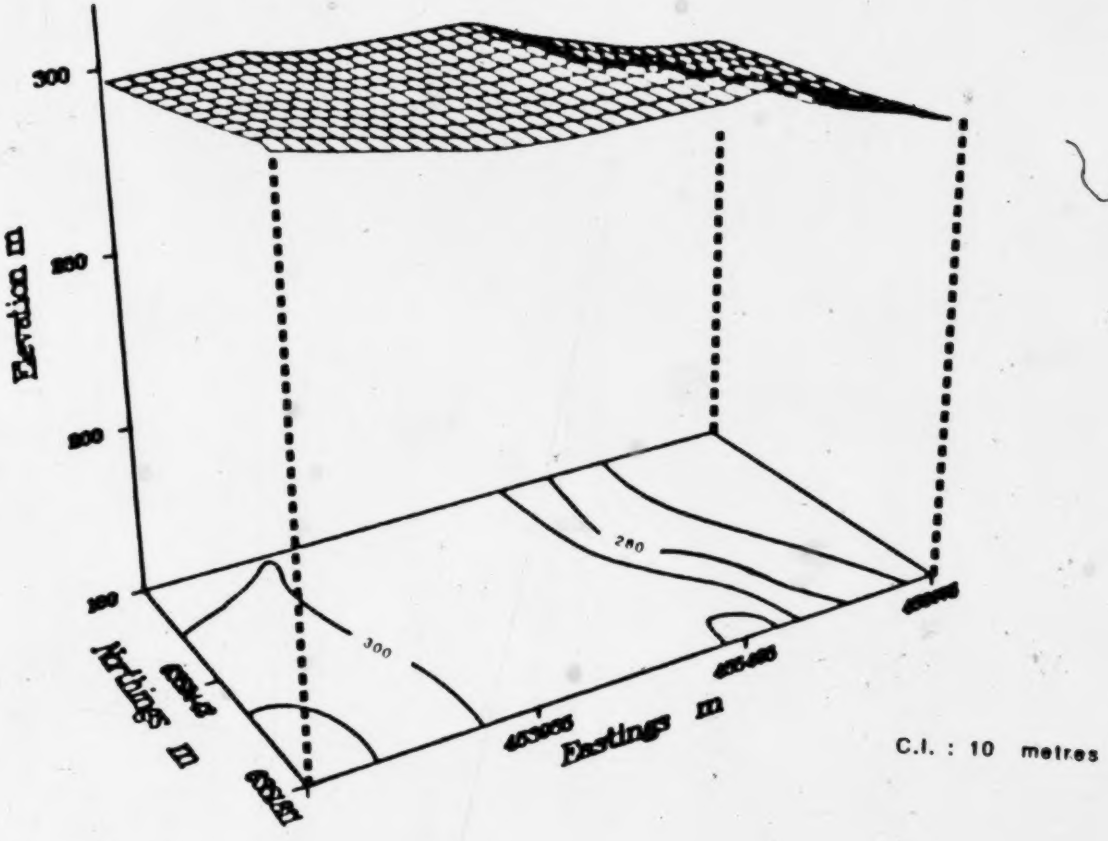

Figure 7.8 Minimum variance model of the topographic surface in the small area.

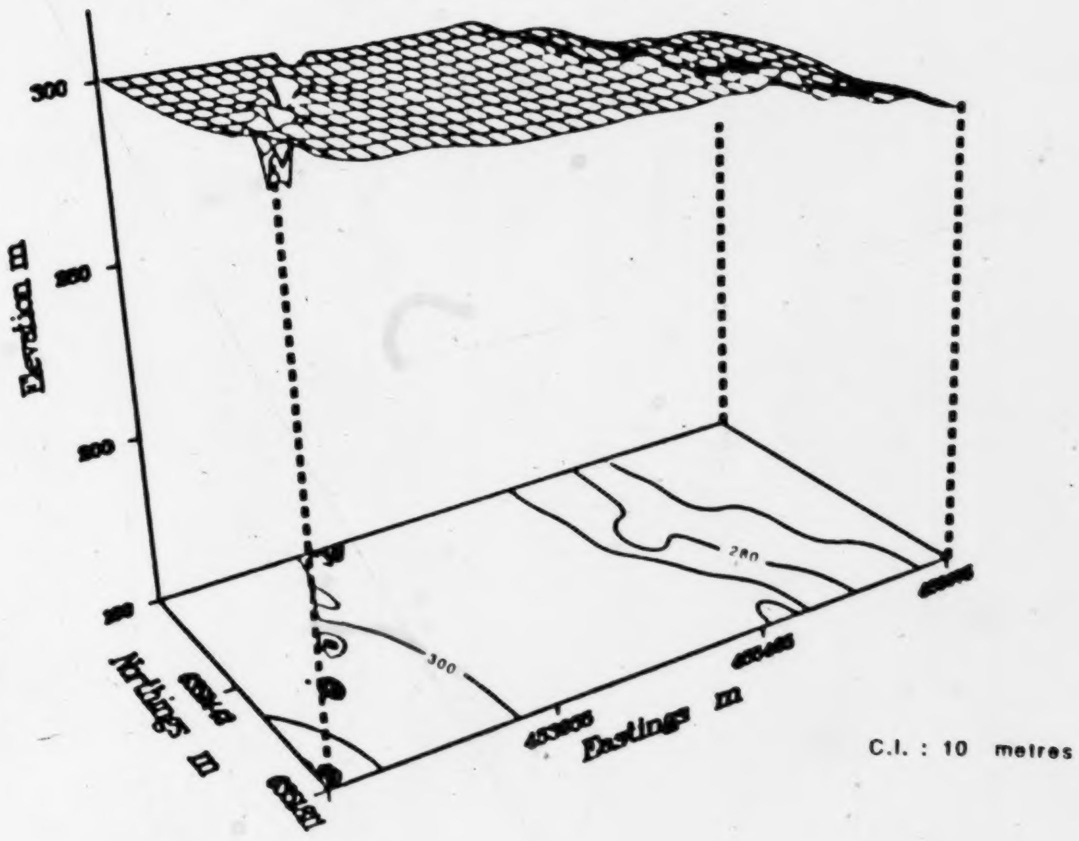
300
250
200
Elevation m
Northings m
Eastings m
280
300

C.I. : 10 metres

Figure 7.9 Minimum curvature model of the topographic surface in the small area.

TABLE 7.1 Summary statistics of the conditionally simulated elevations of the zones tops and bottoms in the large area.

Zone	Number of points	Mean (m)	Variance (m)^2
Surface	6536	293.9	66.86
1-top	6536	286.3	40.46
2-top	6536	272.0	50.87
3-top	6536	260.7	109.31
4-top	6536	251.6	150.03
5-top	6536	226.4	178.38
6-top	6536	215.7	150.55
7-top	6536	196.6	117.99
7-bottom	6536	193.9	85.04

geometrically anisotropic spherical model. The structures of each field were simulated separately. The mean of each simulation was 0.0 and the variance was adjusted to its proper relative value based on a total variance of one. For example, if the nugget effect was 25% of the sill, the variances of the field with the pure nugget effect and the spherical model were 0.25 and 0.75 respectively. The two simulated values at each point were summed and the field was de-standarized to conform the mean and variance of the grade in the zone.

The fields with a pure nugget effect were simulated by using a standard random number generator (IMSL Library subroutines). The fields with geometric anisotropies were simulated using the turning bands method. The anisotropies were reduced to isotropies by transforming the coordinate system by multiplying the values of the vertical axis by the corresponding anisotropy ratio and then using the horizontal variogram model as input for the simulation. For example, in pay zone one, the field had a grid spacing of 30 x 30 x 1 metres and a geometric anisotropy (anisotropy ratio $k=350/3.5=100$). Instead of an anisotropic, an isotropic field with resolution 30 metres horizontal and 100 metres vertical (1 metre grid spacing multiplied by $k=100$) was simulated using as input a spherical model with 350 metres range. Then the vertical distances were divided by k producing a field with the desired vertical resolution and geometric anisotropy.

The final simulation model of pay zone one was on a grid of 152 x 43 x 65 points with a resolution of 30 x 30 x 1 metres. The mean and variance of the simulated grade were 8.68 %bitumen and 6.19 $(\%\text{bitumen})^2$ respectively. The horizontal and vertical variograms of pay zone one are given in Figure 7.10.

The non-conditionally simulated grade model of pay zone two was on a grid of 152 x 43 x 95 points with the same resolution as in pay zone one. The mean of the simulated field was 10.06 %bitumen and the variance 9.94 $(\%\text{bitumen})^2$. The variograms both vertical and horizontal are presented in Figure 7.11.

Pay zone three was simulated on a grid of 152 x 43 x 85 points with the same resolution as in the previous two zones. The final de-standarized mean was 11.51 %bitumen and the variance 5.43 $(\%\text{bitumen})^2$. Both horizontal and vertical variograms are depicted in Figure 7.12.

7.2.1 Evaluation of the simulated fields

The distribution functions of the simulated fields are approximately normal because the random numbers generated on the 15 evenly-spaced lines (paragraph 3.5.3) are derived from a normal distribution. The normality of the simulated fields is in conformity with the actual distributions of the percent weight oil of the actual pay zones. The mean and variances

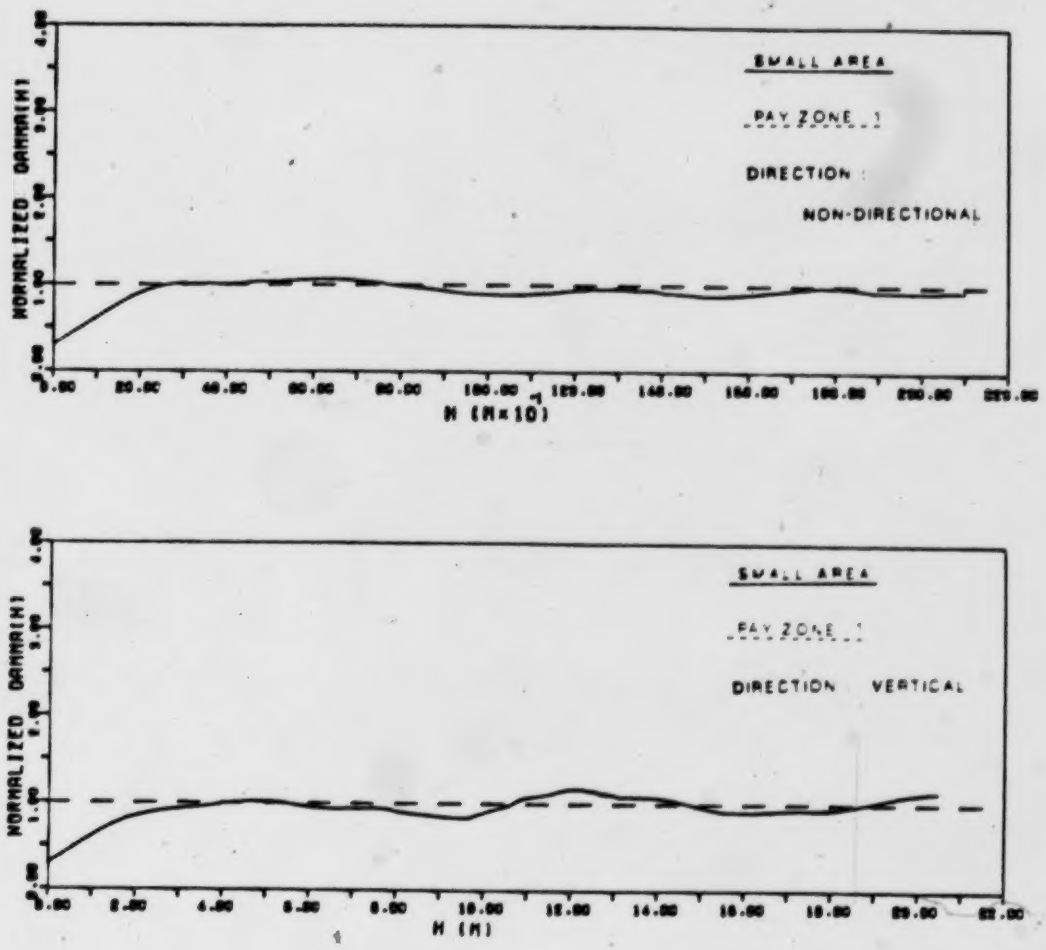

Figure 7.10 Horizontal (top) and vertical (bottom) variograms of the simulated oil saturation in pay zone 1.

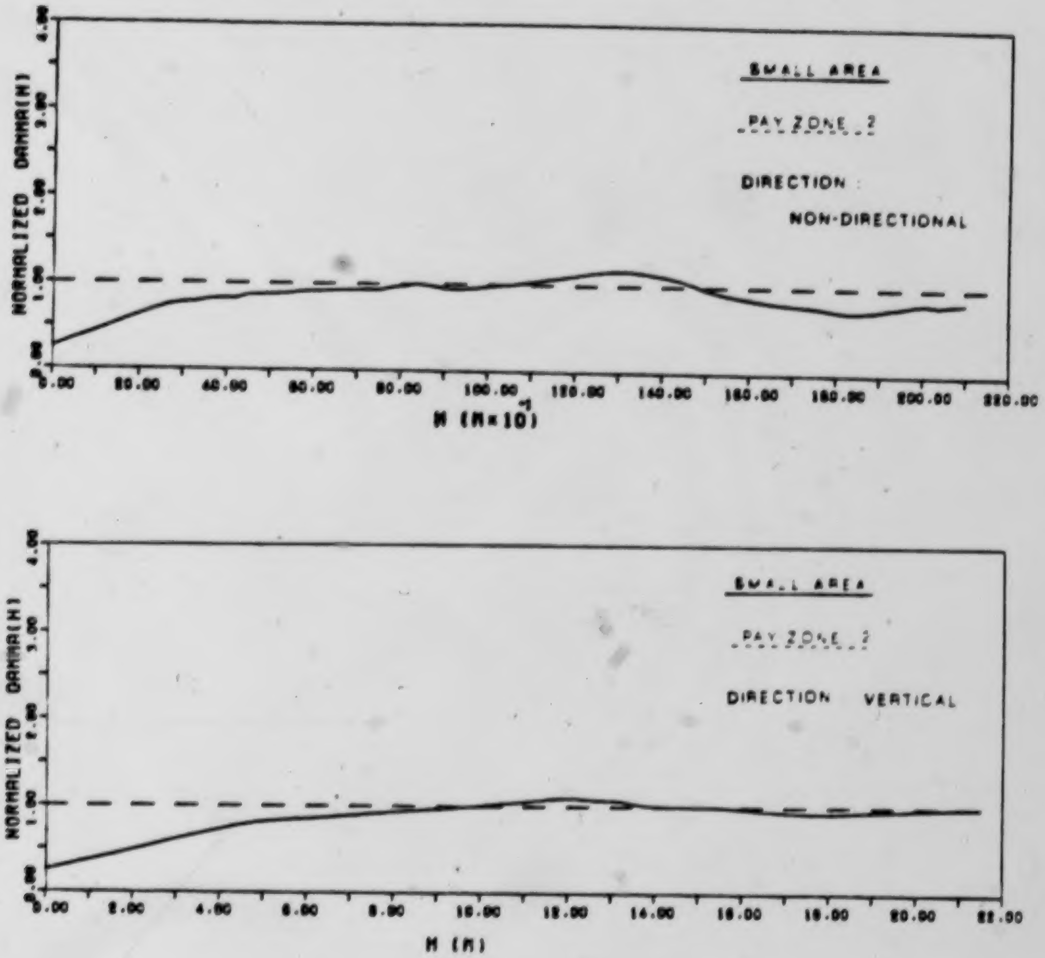

Figure 7.11 Horizontal (top) and vertical (bottom) variograms of the simulated oil saturation in pay zone 2.

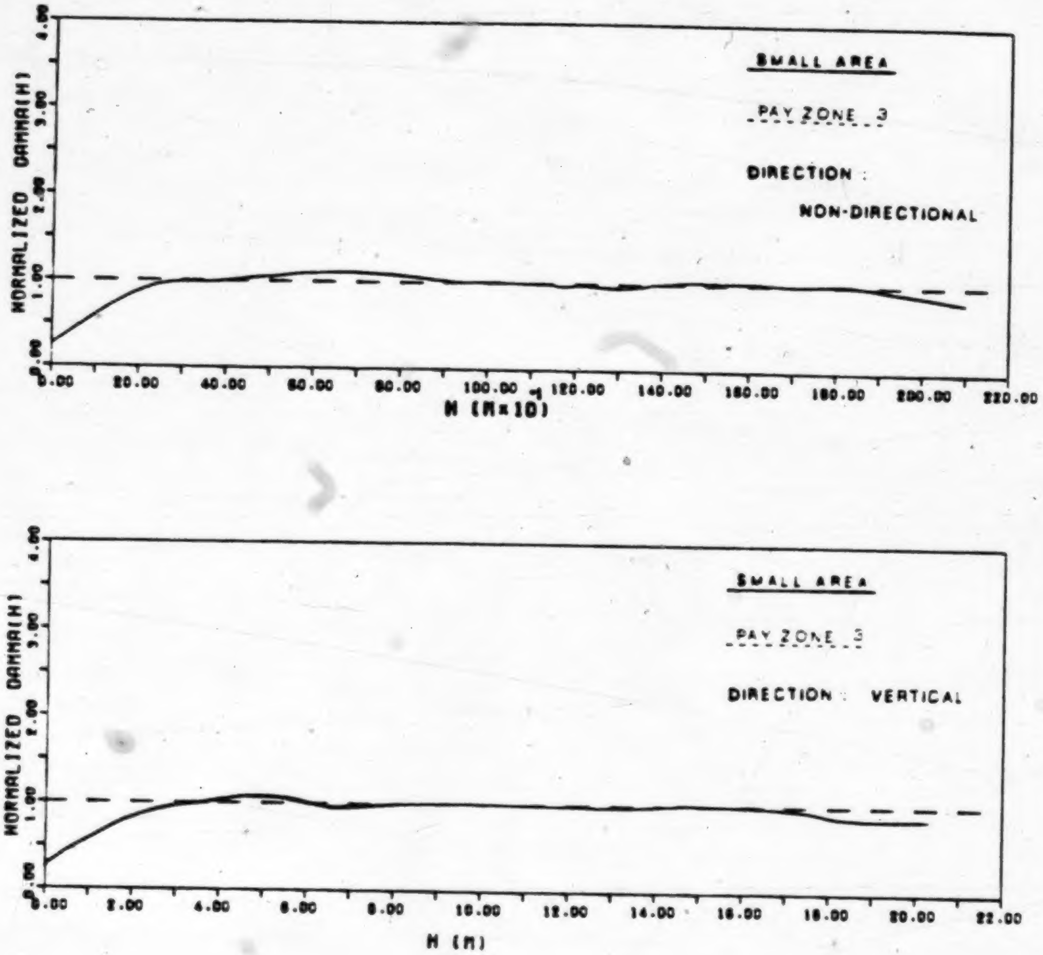

Figure 7.12 Horizontal (top) and vertical (bottom) variograms of the simulated oil saturation in pay zone 3.

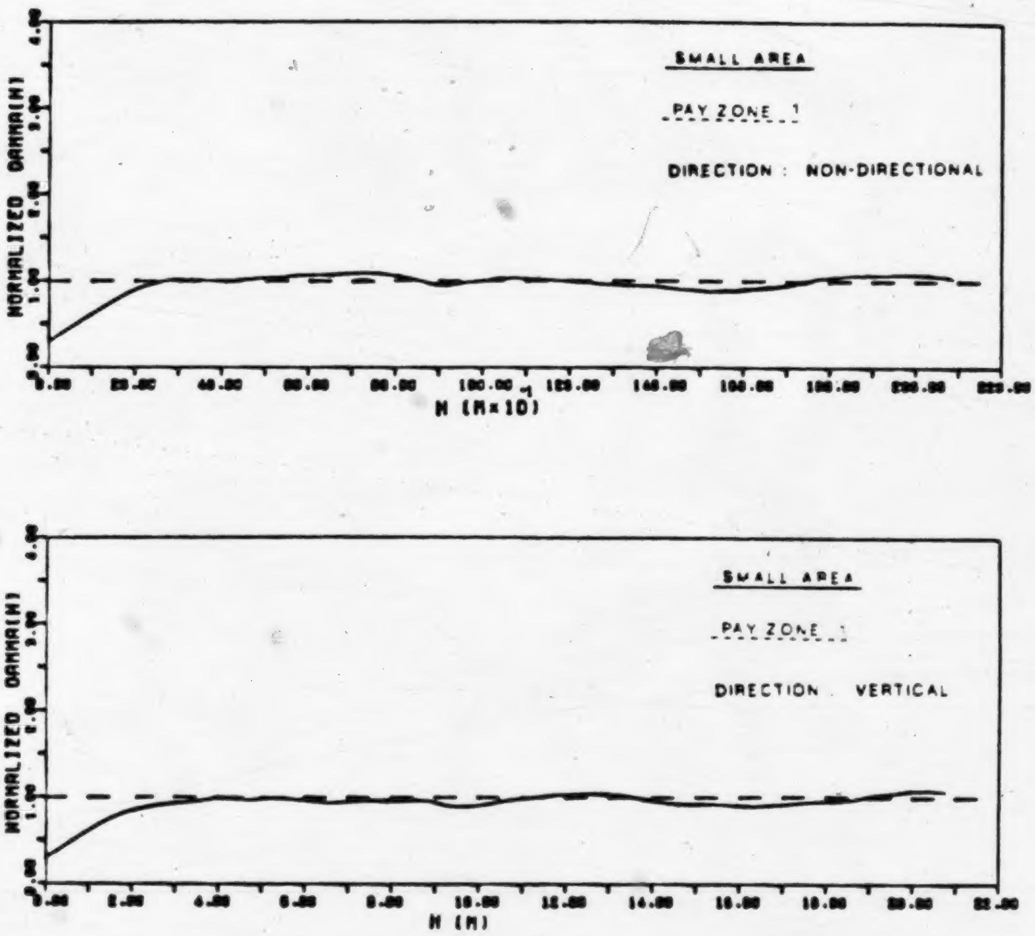

Figure 7.13 Horizontal (top) and vertical (bottom) variograms of the conditionally simulated oil saturation in pay zone 1.

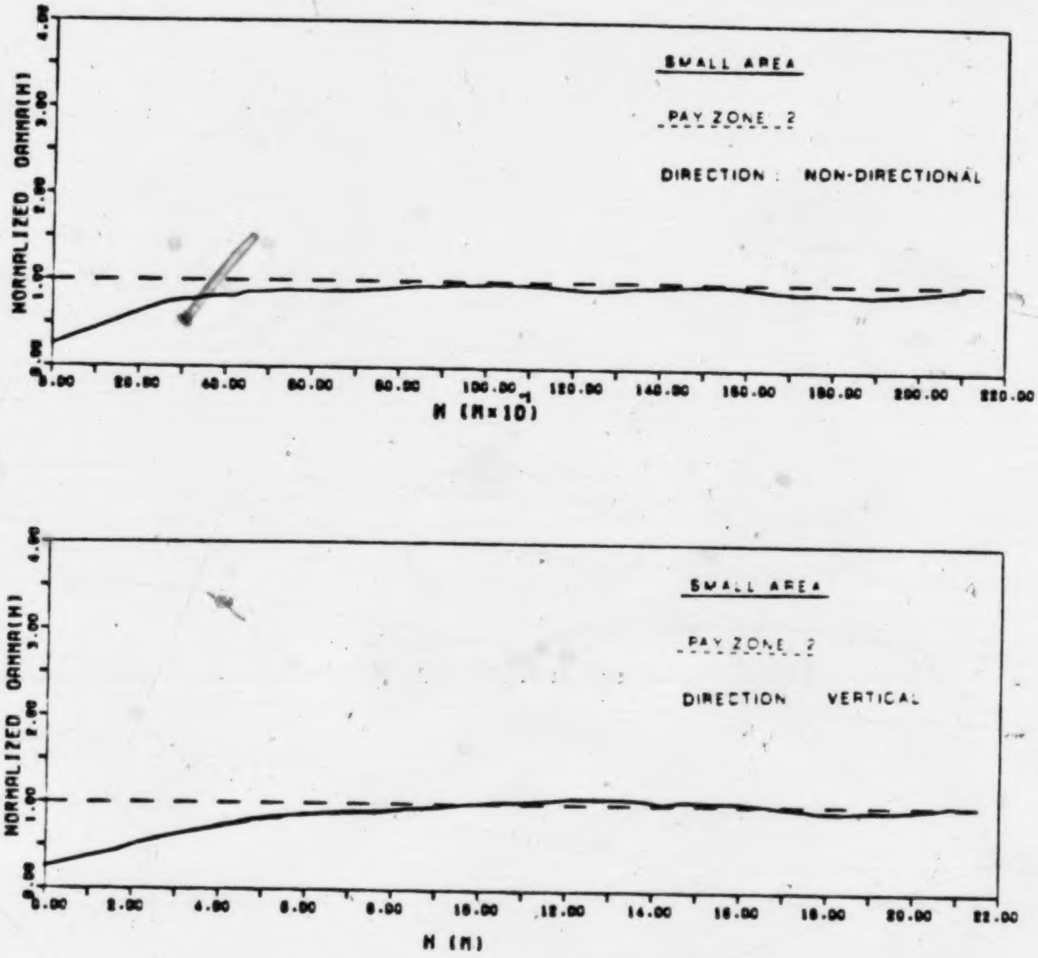

Figure 7.14 Horizontal (top) and vertical (bottom) variograms of the conditionally simulated oil saturation in pay zone 2.

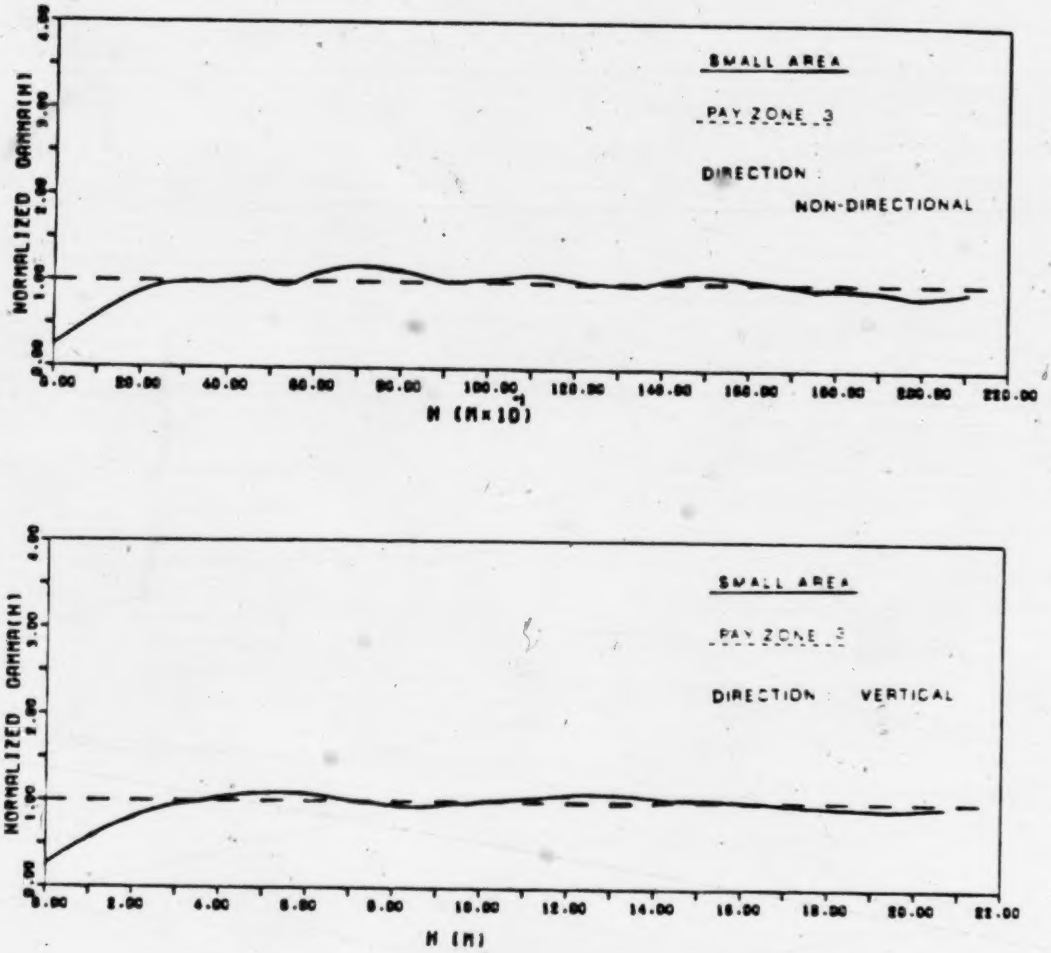

Figure 7.15 Horizontal (top) and vertical (bottom) variograms of the conditionally simulated oil saturation in pay zone 3.

are also accurately reproduced.

The variogram models of the actual pay zones are well reproduced, but are not exact duplicates of the input models because of problems in numerical analyses and computational limitations. These problems occur because of the following reasons.

The generated by the computer random numbers on the 15 lines (paragraph 3.5.3) are not strictly random. Usually some unintended correlation between the numbers exists which is expressed by oscilliations of the correlation structure around a pure nugget effect. Such undesired patterns are minimized by the weighting system within the range of the input variogram but not at distances larger than the range.

The thickness of the bands (paragraph 3.5.2) along the 15 lines is not infinitesimal as theoretically assumed. Implementation, in both computational and economical means, dictate that the bands have some thickness. This also is a cause of variation of the variogram of the field around the input model. In practice, band thickness of about or slightly less than 1/40 of the range of the model variogram is considered as a good approximation. The thicknesses of the bands of the three simulations in this study were 1/47, 1/58 and 1/53 of the respective ranges of the input variogram models.

Finally, the size of a simulated field is not infinite. The limited size affects the smoothness and characteristics of the output variogram. In practice, if the size of the field is about 10 times larger than the range of the input variogram, the model is sufficiently well reproduced. This rule of thumb was followed as much as possible in this study.

The three simulated fields satisfactorily reproduced the first and second order moments of the actual pay zones.

7.3 Conditioning of the Simulated Pay Zones

The 33 boreholes available in the small area were already relocated to the nearest grid point (paragraph 7.1), and the samples in each pay zone were also vertically moved to a maximum of 0.5 metres in order to coincide with the grid points in the vertical direction.

The conditioning of the three simulated fields to the actual data was performed using the variogram models derived from structural analysis (paragraph 5.2.2).

The final conditionally simulated model of pay zone one was on a grid of 152 x 43 x 65 points with a resolution of 30 metres horizontal and 1 metre vertical. The mean of the field was 8.47 %bitumen and the variance 6.36 (% bitumen)^2. The variograms of the field reproduced the input models and are presented in Figure 7.13. Cross-sections of the conditionally simulated models of pay zone one are depicted in Figures 7.16 and 7.18.

The simulated model of pay zone two was conditioned on a grid of 152 x 43 x 95 points with the same resolution as pay zone one. The mean was 9.98 %bitumen and the variance

9.72 (%bitumen)^2. The horizontal and vertical variograms of the grade of the constructed model are given in Figure 7.14. Cross-sections of the conditionally simulated pay zone two are depicted in Figure 7.20 and 7.22.

The simulated oil saturation of pay zone one was conditioned to the available data on a grid of 152 x 43 x 85 points with the same resolution as the grids of the previous two zones. The mean was 11.63 %bitumen and the variance was 5.91 (%bitumen)^2. The variograms of the produced model are given in Figure 7.15. Cross-sections of the conditionally simulated zone are given in Figures 7.24 and 7.25.

For comparison, the oil saturations in the three pay zones were also kriged using the conditionally simulated boundaries rather than the estimated ones as in Chapter 6. Accordingly, 'mixed' models were constructed. Cross-sections of these models are given in Figures 7.17, 7.19, 7.21, 7.23, 7.25 and 7.27.

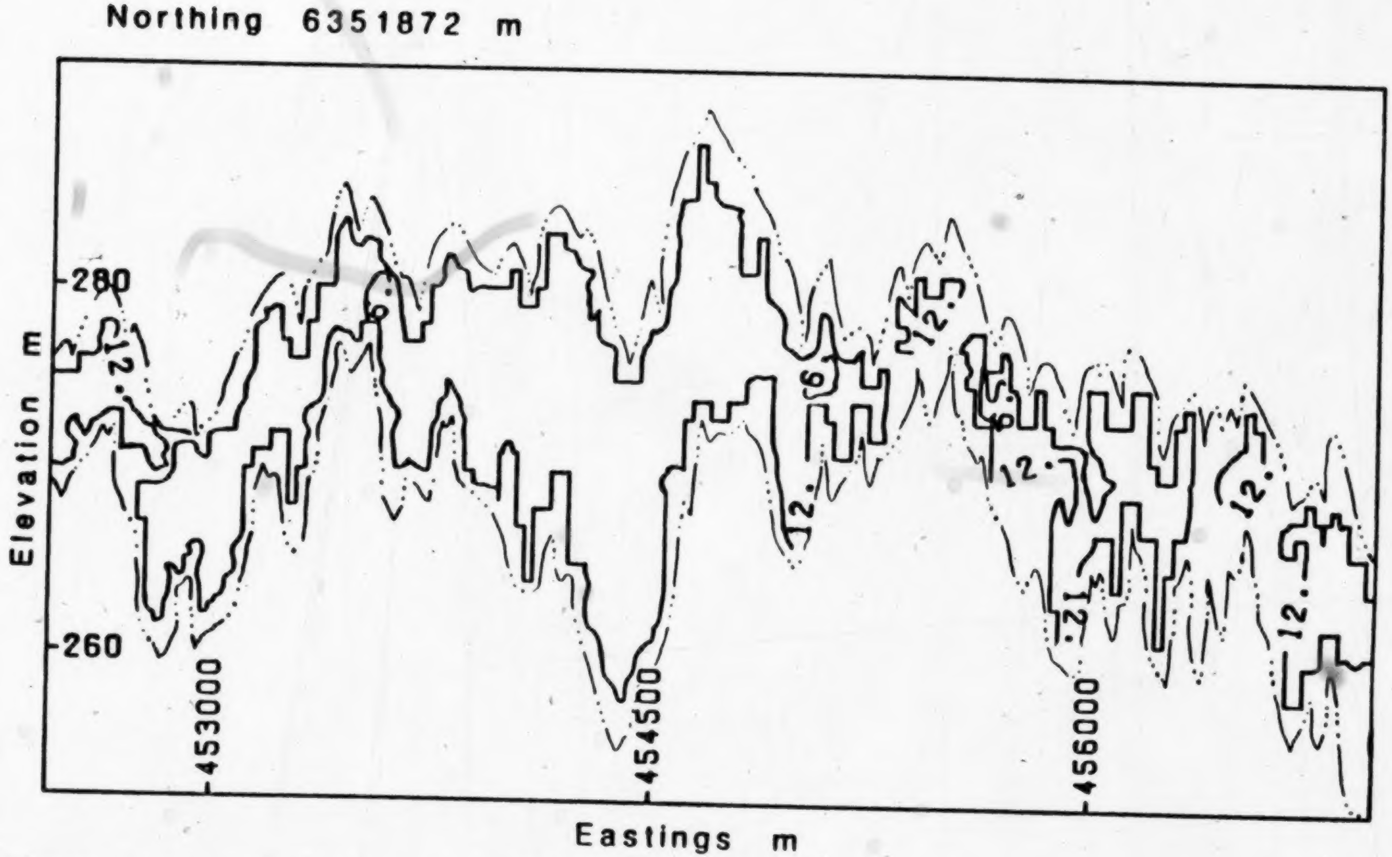

Figure 7.16 First cross-section of the conditionally simulated pay zone 1. The contour interval is 6% weight oil. – contours; – ··· – top and bottom boundaries of the pay zone.

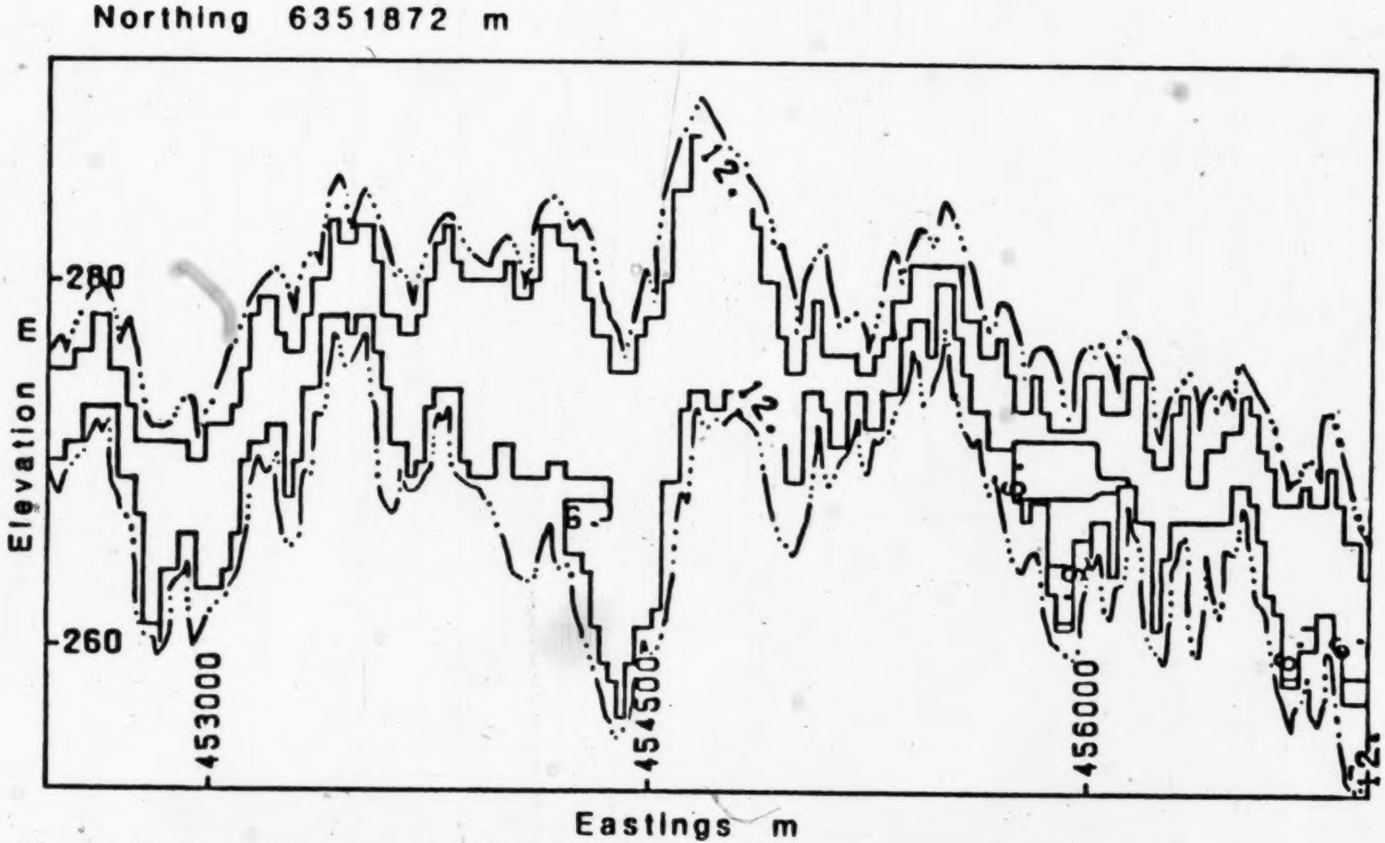

Figure 7.17 Pay zone 1. First cross-section of the small area model using conditionally simulated boundaries and kriged grades. The contour interval is 6% weight oil. – contours; – ··· – top and bottom boundaries of the pay zone.

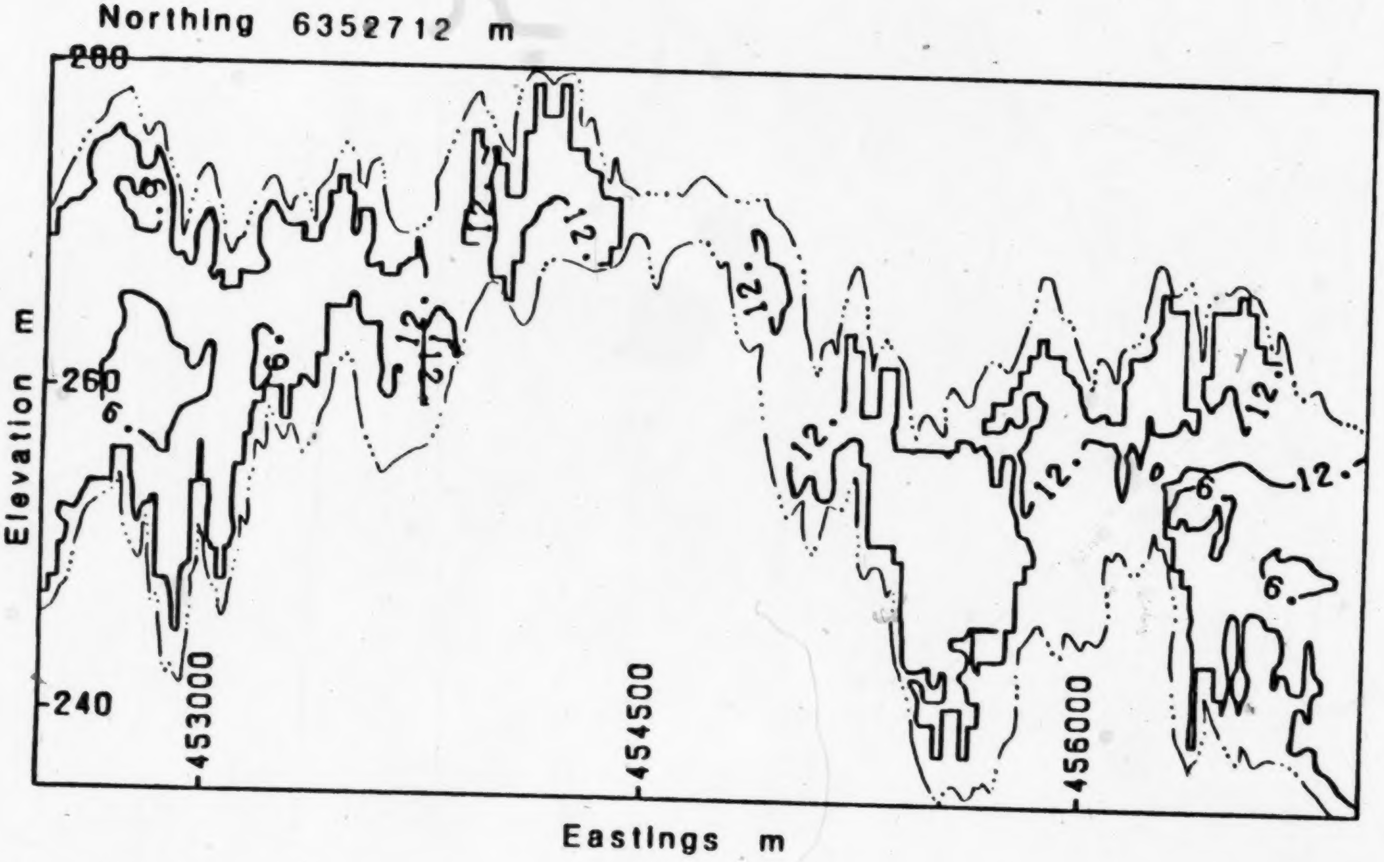

Figure 7.18 Second cross-section of the conditionally simulated pay zone 1. The contour interval is 6% weight oil. – contours; – ··· – top and bottom boundaries of the pay zone.

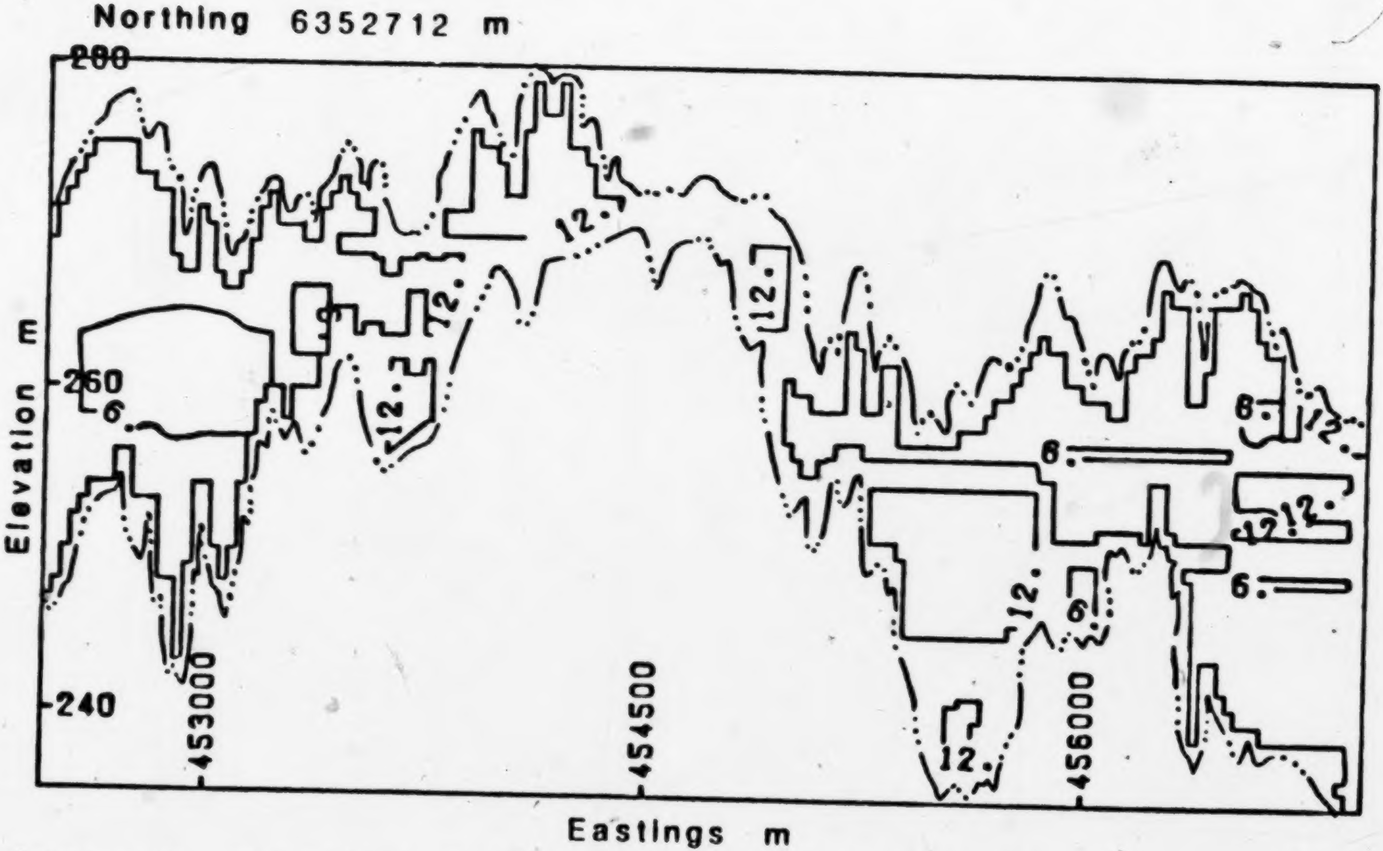

Figure 7.19 Pay zone 1. Second cross-section of the small area model using conditionally simulated boundaries and kriged grades. The contour interval is 6% weight oil. – contours; – ··· – top and bottom boundaries of the pay zone.

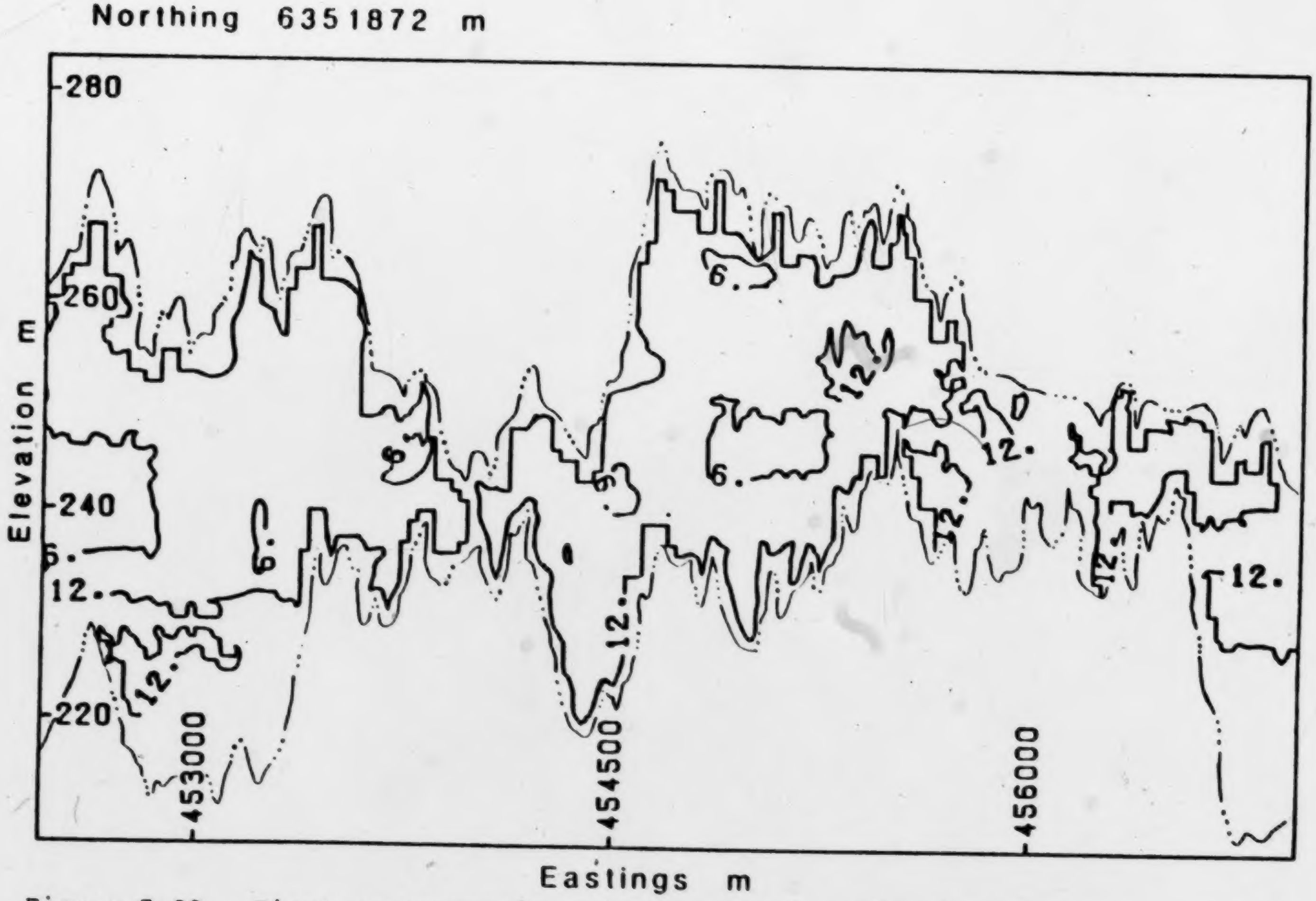

Figure 7.20 First cross-section of the conditionally simulated pay zone 2. – contours; – ··· – top and bottom boundaries of the pay zone.

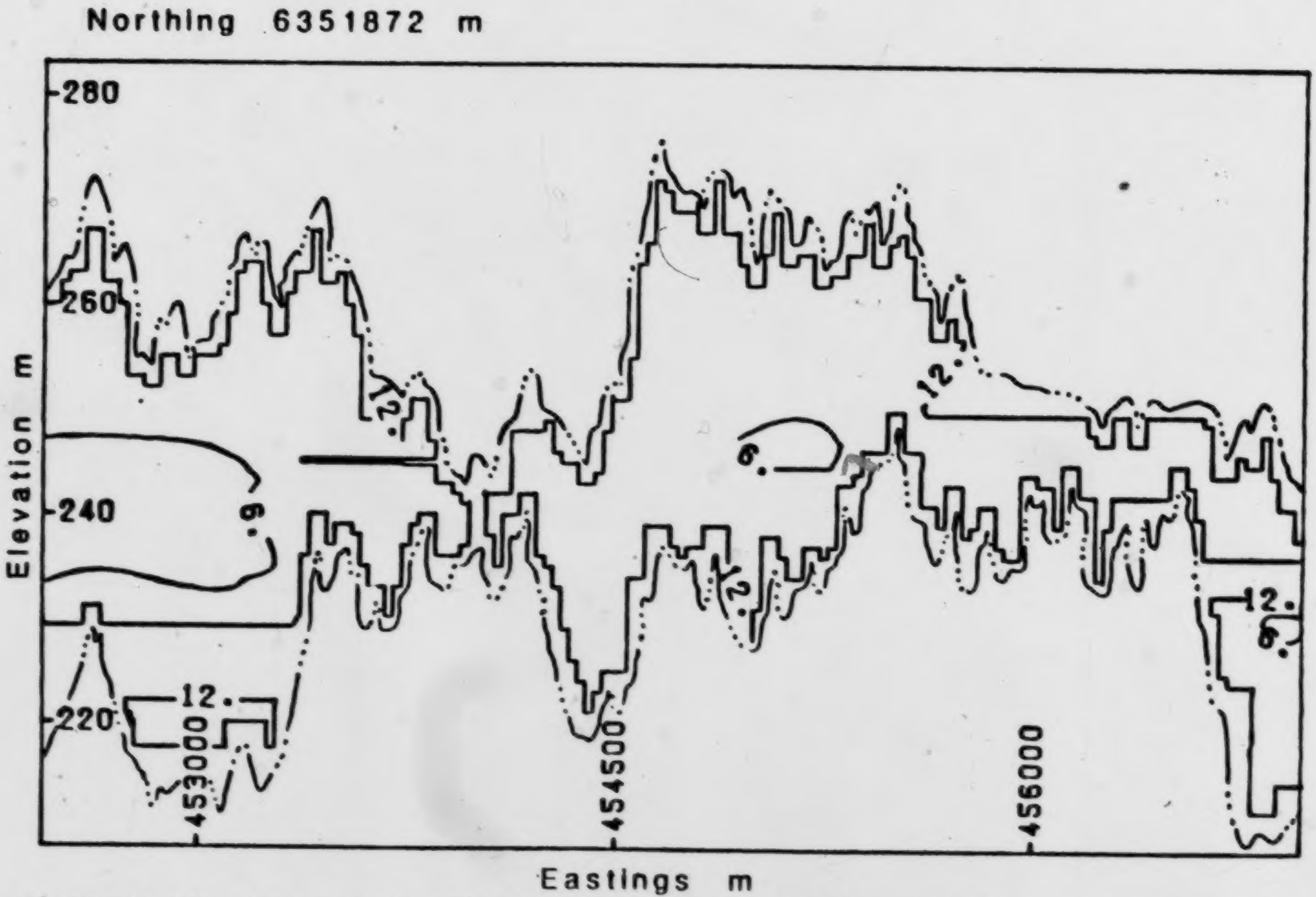

Figure 7.21 Pay zone 2. First cross-section of the small area model using conditionally simulated boundaries and kriged grades. – contours; – ··· – boundaries.

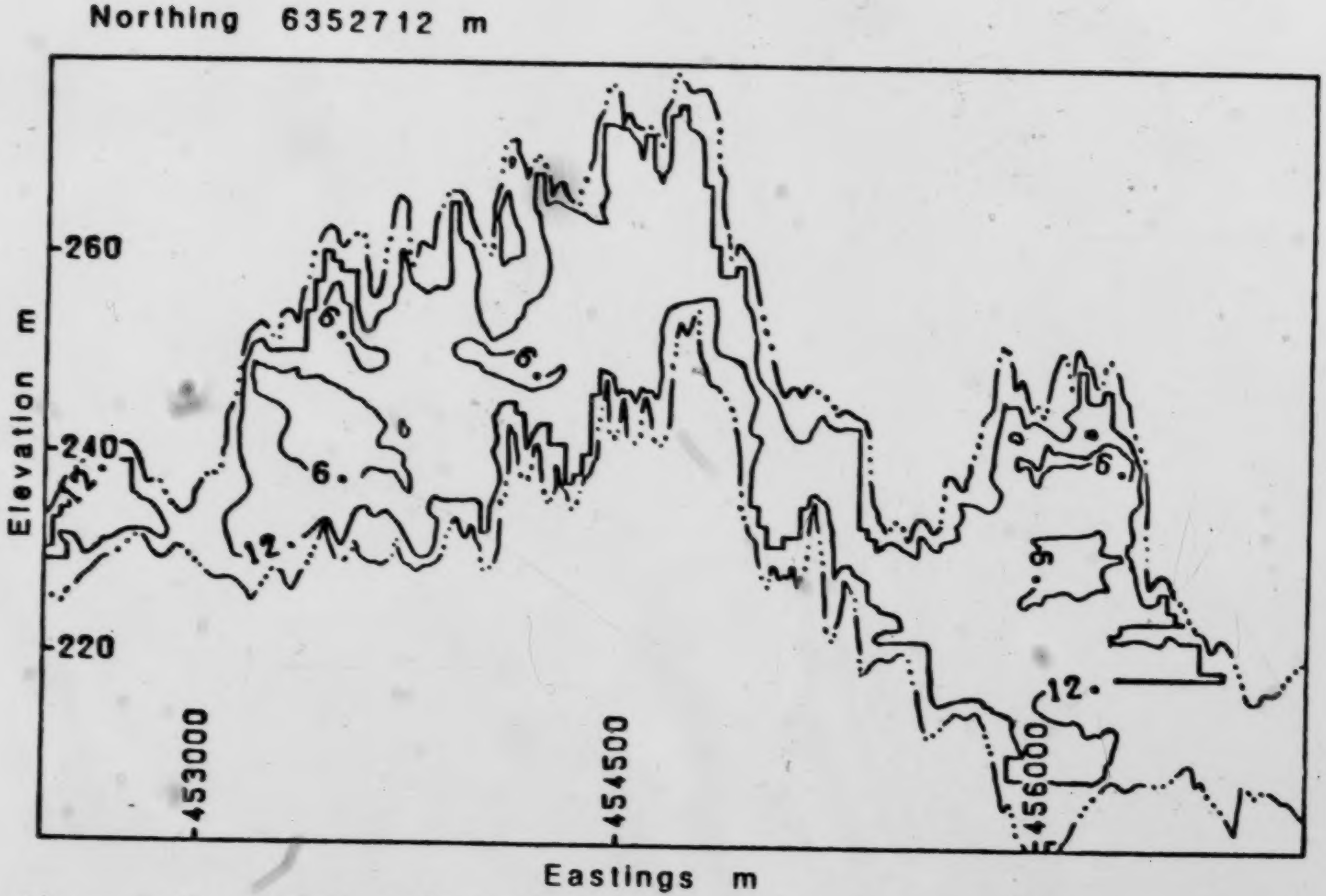

Figure 7.22 Second cross-section of the conditionally simulated pay zone 2. – contours; – ··· – top and bottom boundaries of the pay zone.

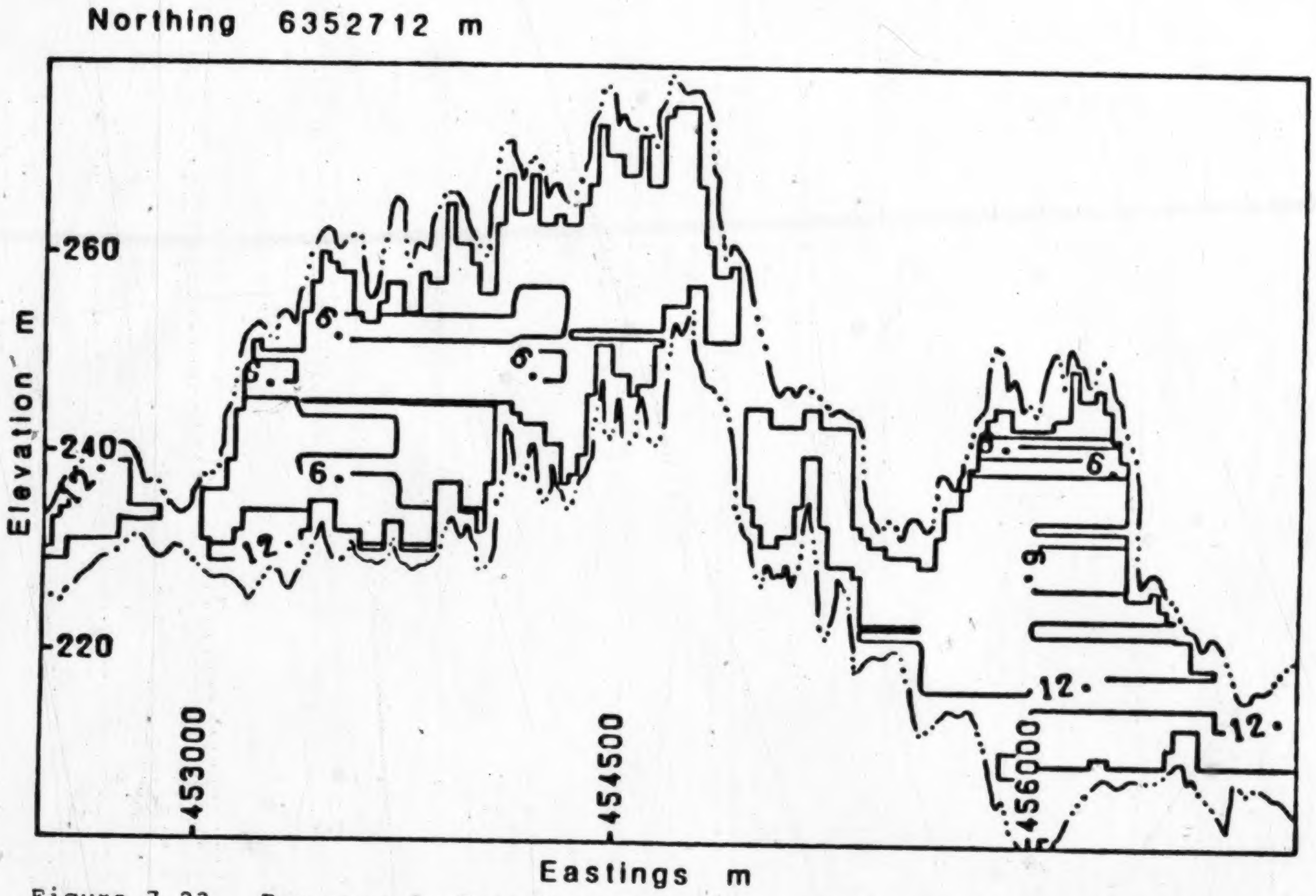

Figure 7.23 Pay zone 2. Second cross-section of the small area model using conditionally simulated boundaries and kriged grades. – contours; – ::: – boundaries.

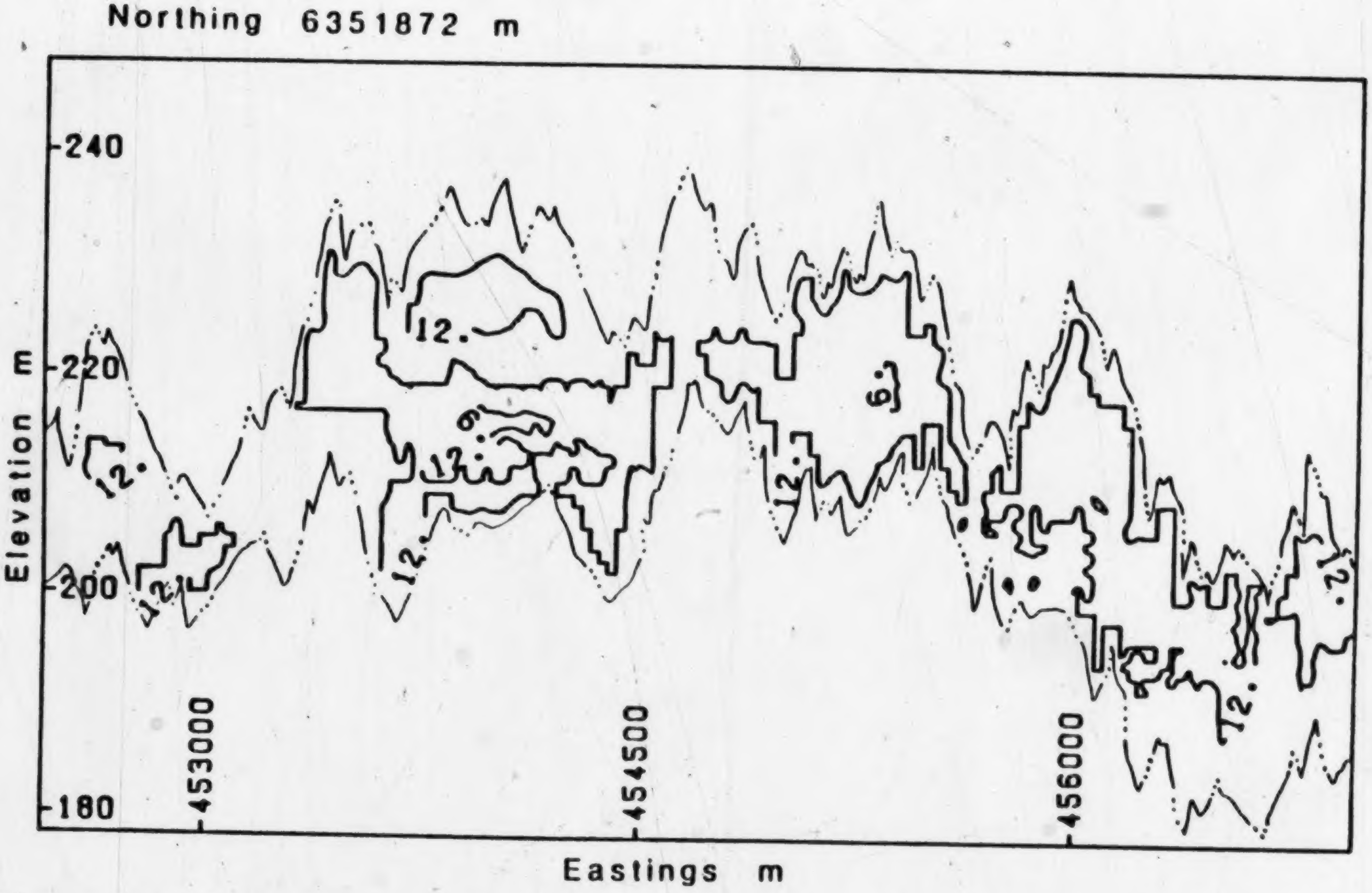

Figure 7.24 First cross-section of the conditionally simulated pay zone 3. – contours; – ··· – top and bottom boundaries of the pay zone.

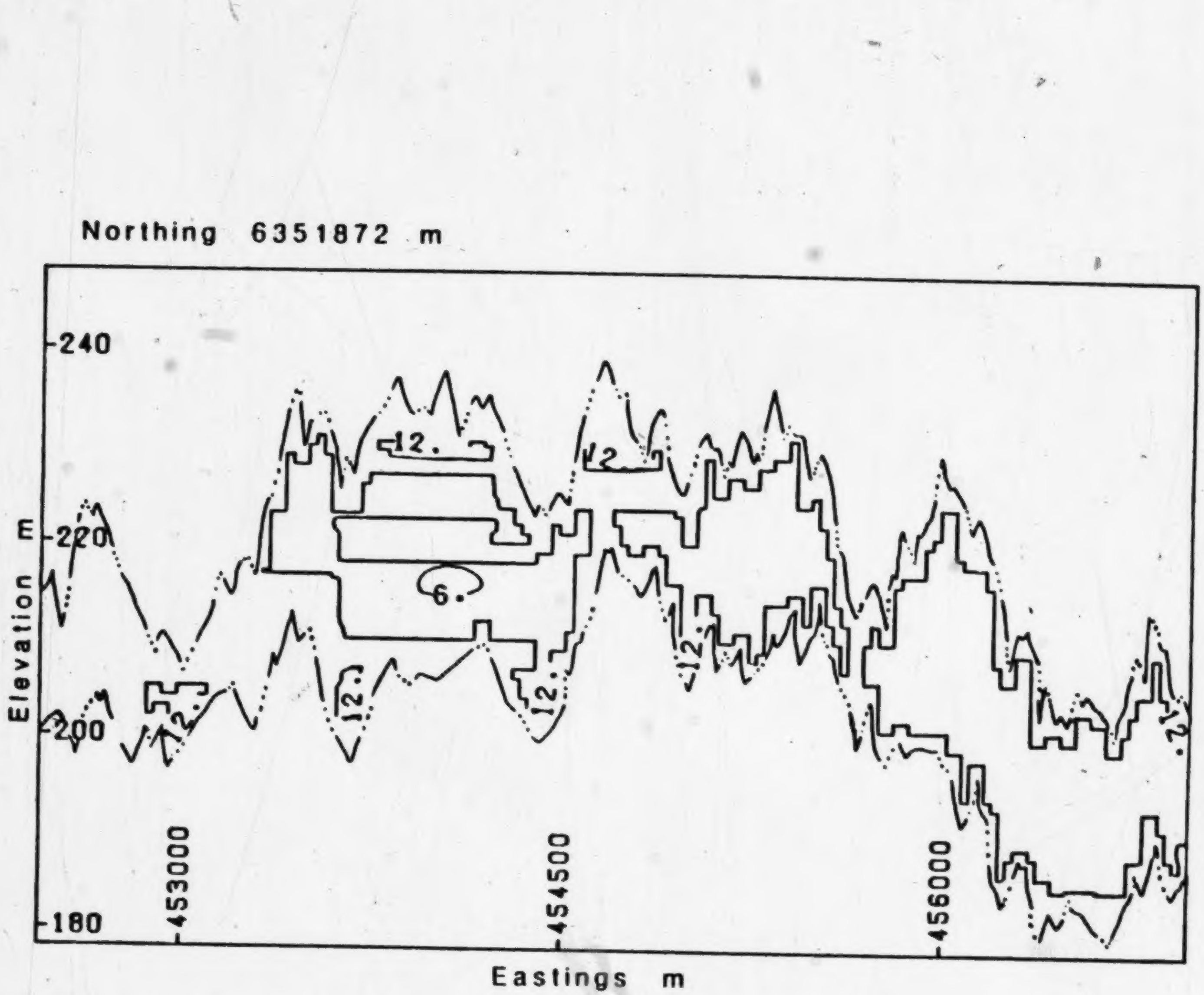

Figure 7.25 Pay zone 3. First cross-section of the small area model using conditionally simulated boundaries and kriged grades. - contours; - ··· -boundaries.

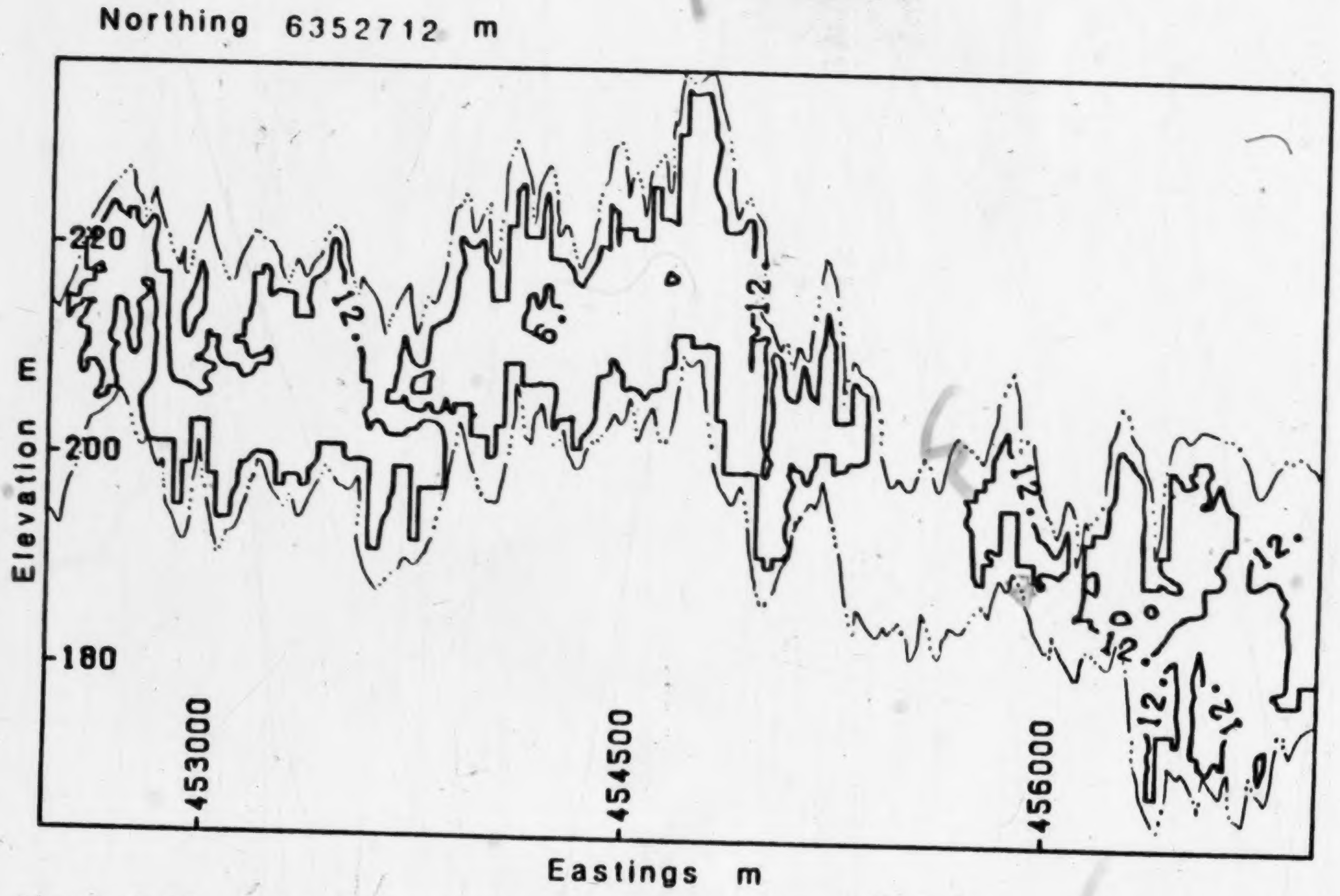

Figure 7.26 Second cross-section of the conditionally simulated pay zone 3. – contours; – ··· – top and bottom boundaries of the pay zone.

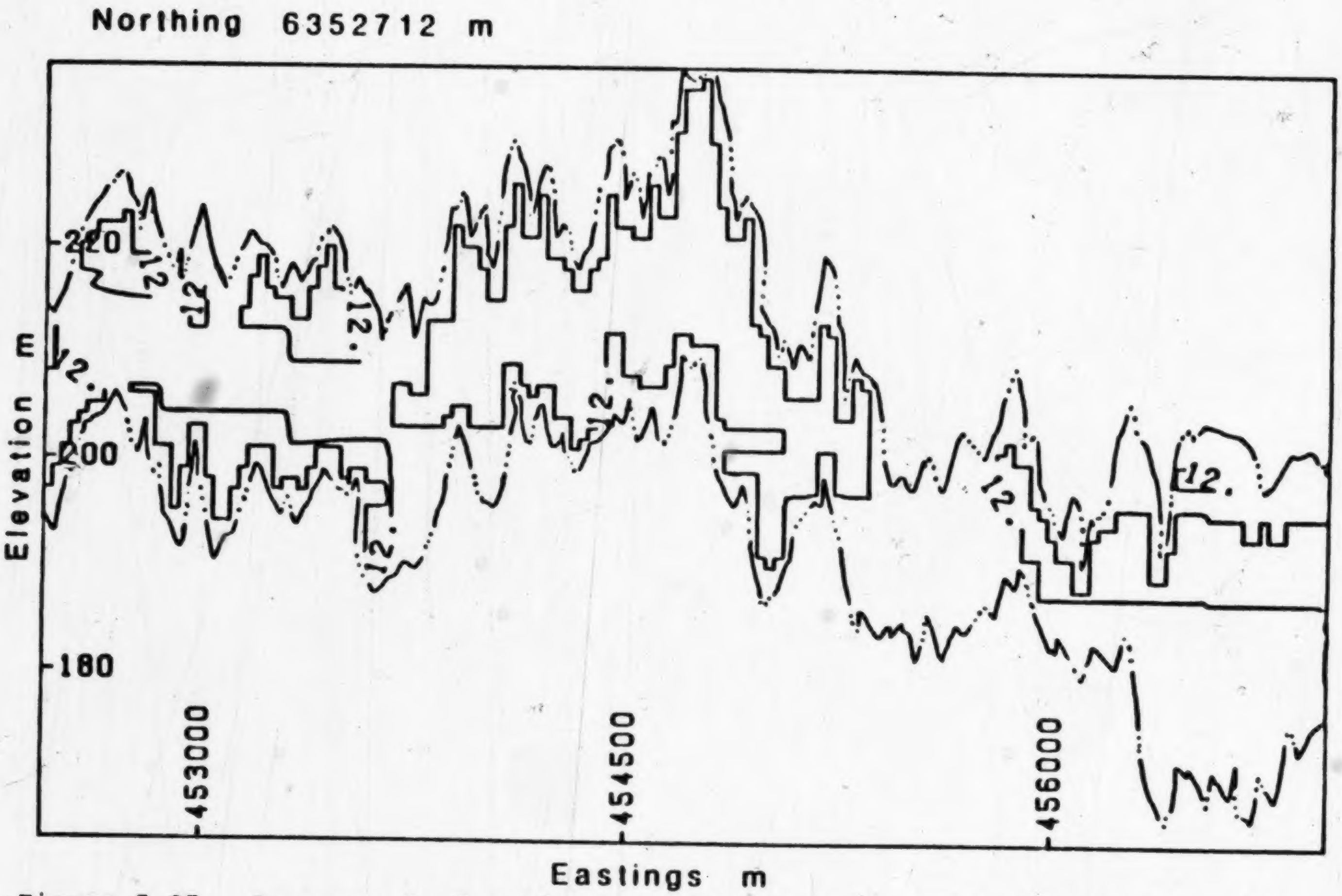

Figure 7.27 Pay zone 3. Second cross-section of the small area model using conditionally simulated boundaries and kriged grades. - contours; – ··· – boundaries.

8. PRELIMINARY EVALUATION OF THE IN-PLACE RESERVES

On the basis of the models constructed, a preliminary evaluation of the in-place reserves was carried out in the study area.

"... ore reserve estimation is not a matter of mere calculation but a procedure which involves, explicitly or implicitly, judgement and assumptions about geological, operational and investigational factors" (King et al. , 1982, p.1). In this sense, the evaluations and calculations to be presented in this chapter are predictions based upon the available data, geology and geostatistical techniques used. Further assessment of the in-place reserves and their economic potential is a function of a detailed mining plan, extraction method, available equipment etc., and should be based on the models derived, but is beyoned the scope of this study.

8.1 Definitions

The two engineering-economic parameters used here and which require definition are the in-place bitumen and the stripping (strip) ratio.

The in-place bitumen (IPB) is given by the formula:

$$IPB = V \times G \times M / D$$

where V is the volume of the extracted material, G is the *in-situ* density of the tar sand (2.082 tonnes/m^3), M is the weight percent bitumen of volume V and D is the specific gravity of the bitumen (1.008 tonnes/m^3)

The stripping ratio (S) of a pay zone is defined as:

S = volume of overburden / volume of pay zone

and indicates how much waste material must be removed before a volume of ore can be mined. Thus it is used as an indicator of whether or not surface mining is economical.

Note that in the case of two (or more) pay zones, the strip ratio of the second (third, etc.) pay zone is the ratio of the volume of all material to be removed down to the pay zone to the volume of the second (third, etc.) pay zone plus the volume of all pay zones already removed.

8.2 Evaluation of the Large Area

The volumes of the overburden, pay zones one (zone 2), barren zone one (zone three), pay zone two (zone four), barren zone two (zone five) and pay zone three (zone six) were calculated using the interpolated surfaces in the large area (paragraph 6.1). The volumes of the above zones, together with the area, perimeter and average thickness of each zone, is given in Table 8.1. The isopachs of the same zones are depicted in Figures 8.1 to 8.6 respectively.

The estimated in-place bitumen was 0.75, 0.80 and 0.26 billion m^3 for pay zones one, two and three respectively. The corresponding stripping ratios were 0.82, 2.50 and 2.82. The above figures are summarized in Table 8.2.

TABLE 8.1 Area, perimeter, volume, and average thickness of the zones in the large area.

Zone	Area (km^2)	Perimeter (km)	Volume (m^3 x 10^9)	Average thickness (m)
Overburden	336.96	74.4	3.433	12.30
Pay 1	336.96	74.4	4.138	14.07
Barren 1	336.96	74.4	12.381	36.83
Pay 2	336.96	74.4	3.811	13.42
Barren 2	336.96	74.4	1.953	6.56
Pay 3	336.96	74.4	1.160	4.08

TABLE 8.2 Volumes, in-place bitumen and stripping ratios of the pay zones in the large area.

Pay zone	Volume ($m^3 \times 10^9$)	Mean grade (weight %)	In-place bitumen ($m^3 \times 10^9$)	Stripping ratio
1	4.138	8.73	0.75	0.82
2	3.811	10.15	0.80	2.50
3	1.160	10.97	0.26	2.82

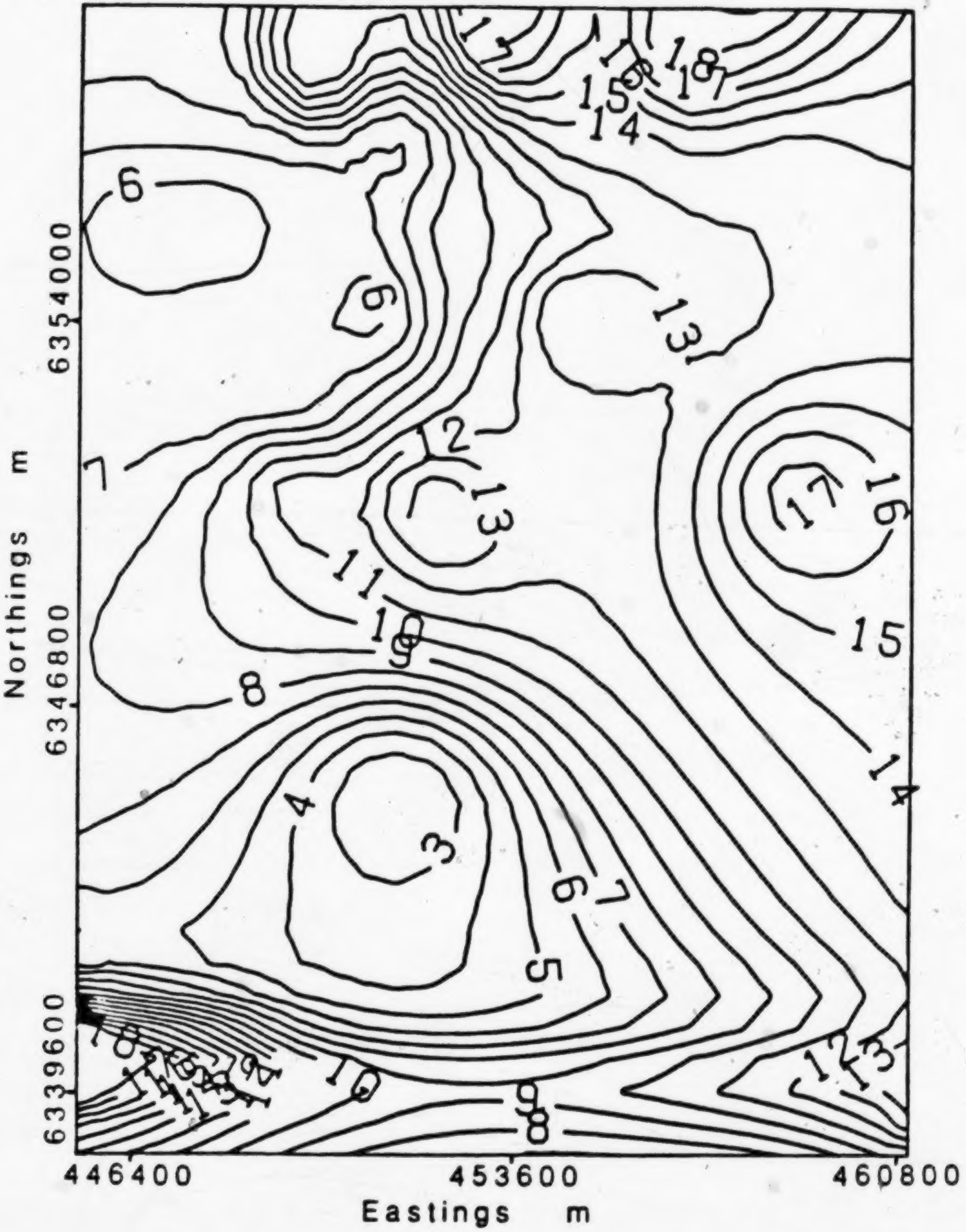
Northings m
6354000
6346800
6339600
Eastings m
446400
453600
460800
3
4
5
6
7
8
9
10
11
12
13
14
15
16
17
18

Figure 8.1 . Isopach of the overburden in the large area. The contour interval is 1 metre.

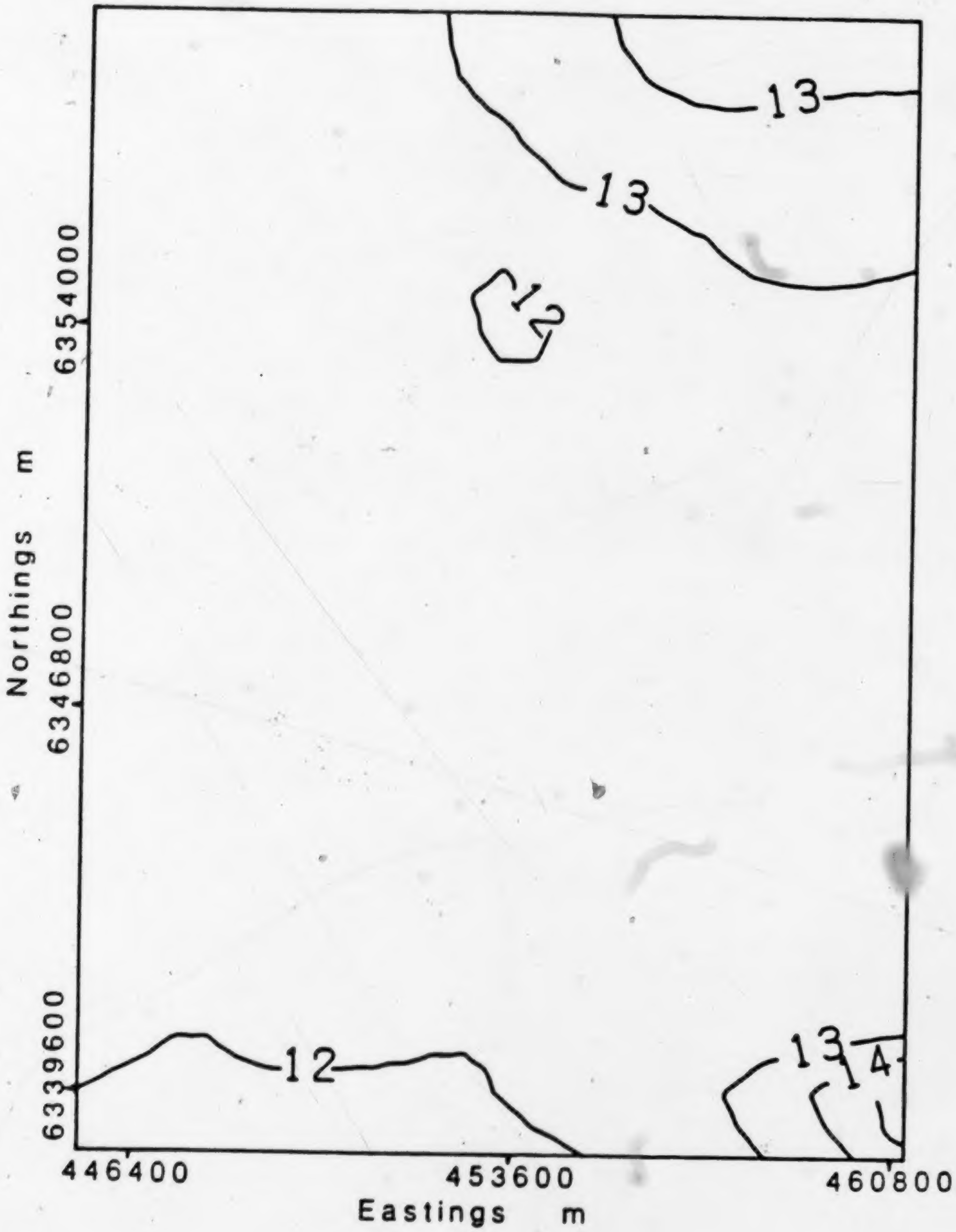
13
13
12
12
13
14
Northings m
6339600
6346800
6354000
Eastings m
446400
453600
460800

Figure 8.2 . Isopach of pay zone 1 in the large area. The contour interval is 1 metre.

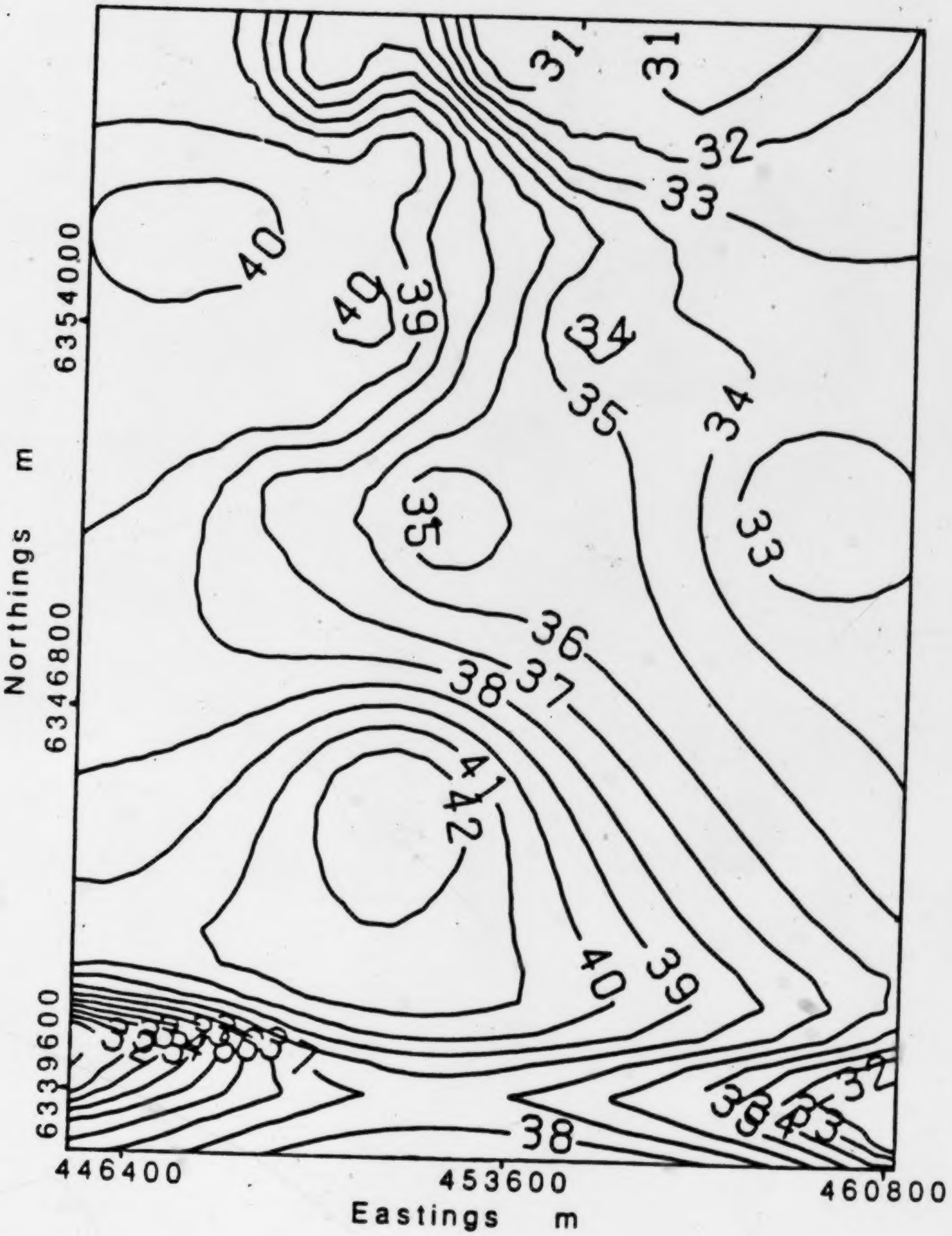
31
31
32
33
40
40
39
34
34
35
35
33
36
38
37
41
42
40
39
38
Northings m
6354000
6346800
6339600
Eastings m
446400
453600
460800

Figure 8.3 Isopach of barren zone 1 in the large area. The contour interval is 1 metre.

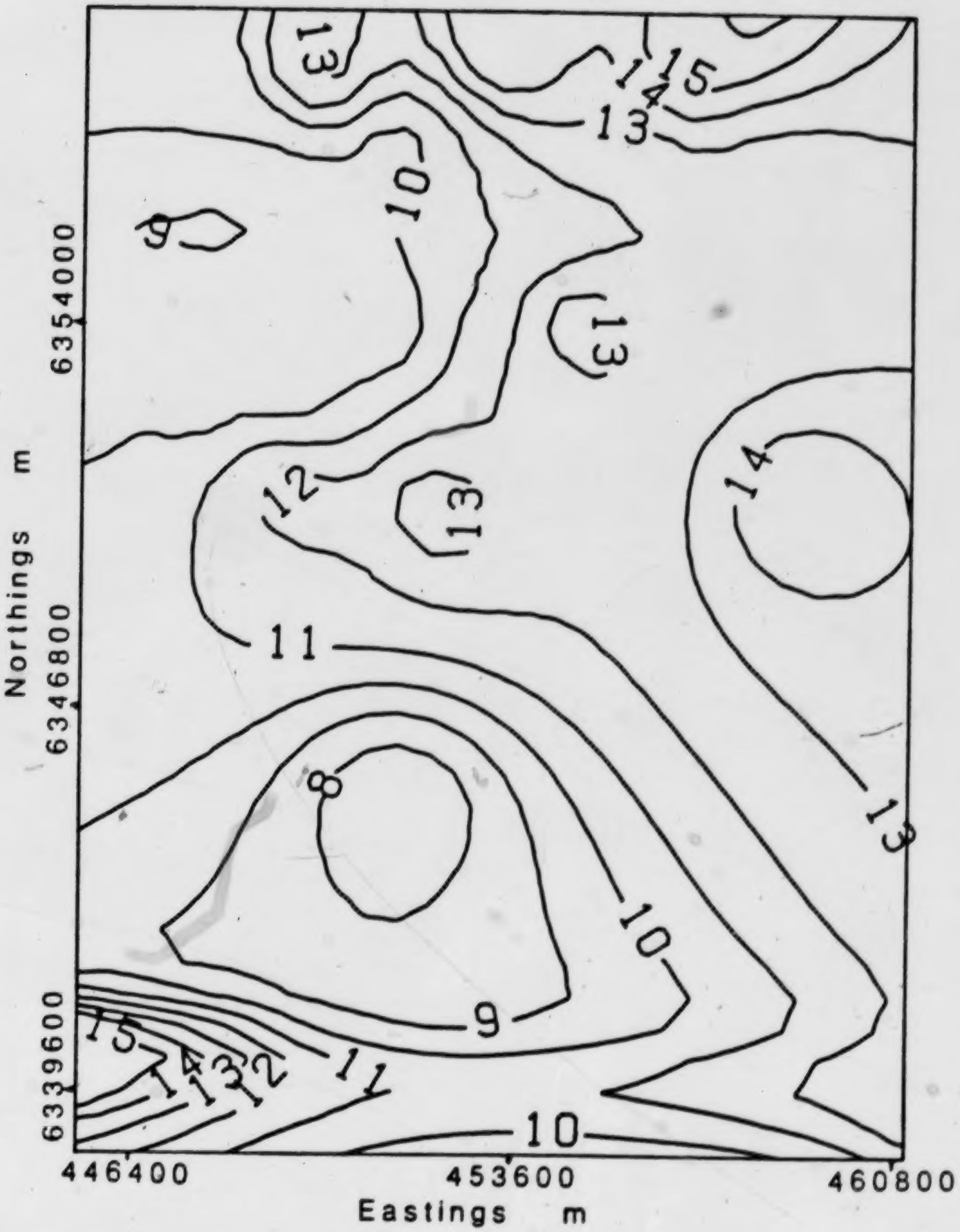
13
15
14
13
10
9
13
14
12
13
11
13
8
10
9
15
14
13
12
11
10
Northings m
6354000
6346800
6339600
446400
453600
460800
Eastings m

Figure 8.4 Isopach of pay zone 2 in the large area. The contour interval is 1 metre.

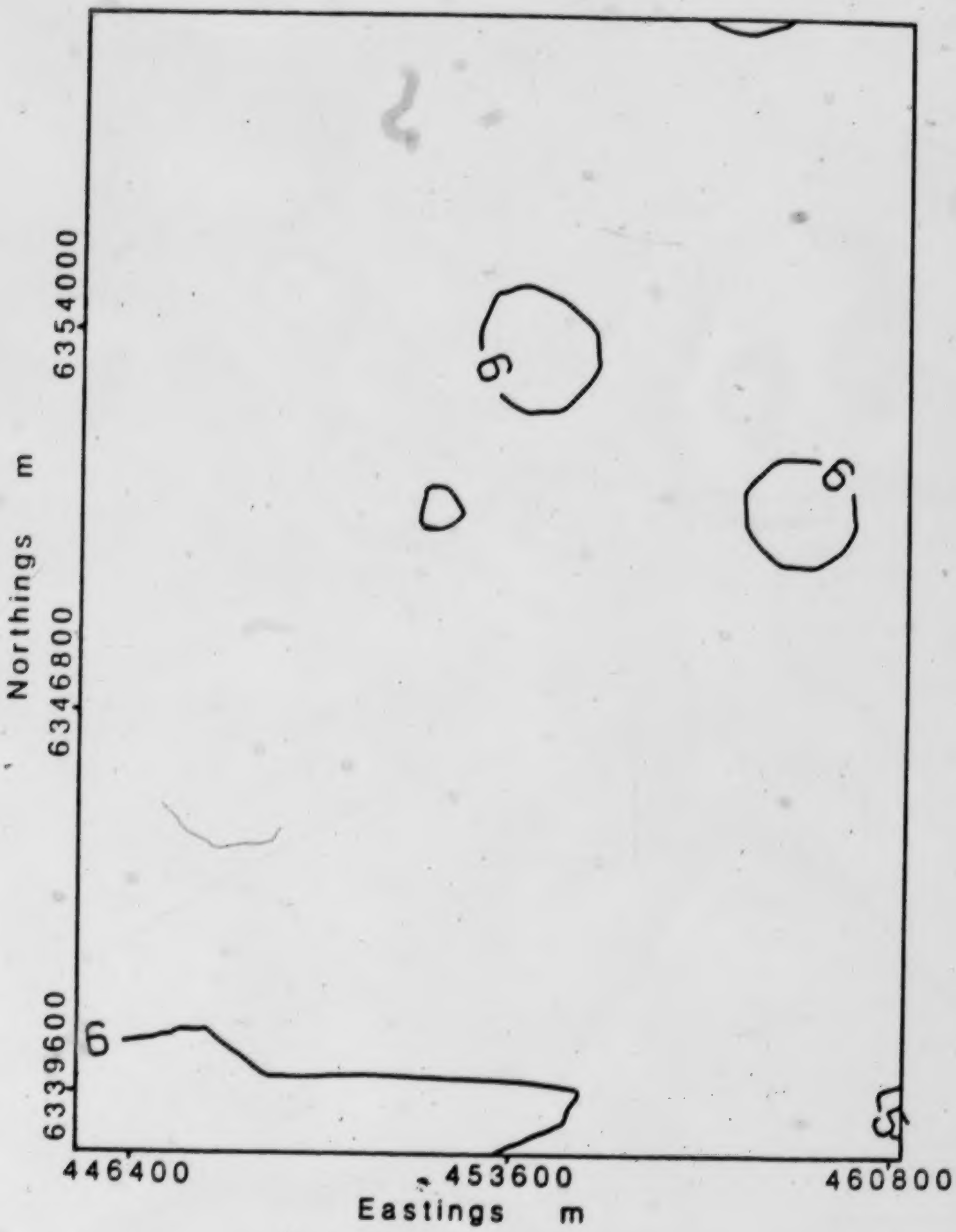
Northings m
6354000
6346800
6339600
Eastings m
446400
453600
460800
6
6
6
5

Figure 8.5 Isopach of barren zone 2 in the large area. The contour interval is 1 metre.

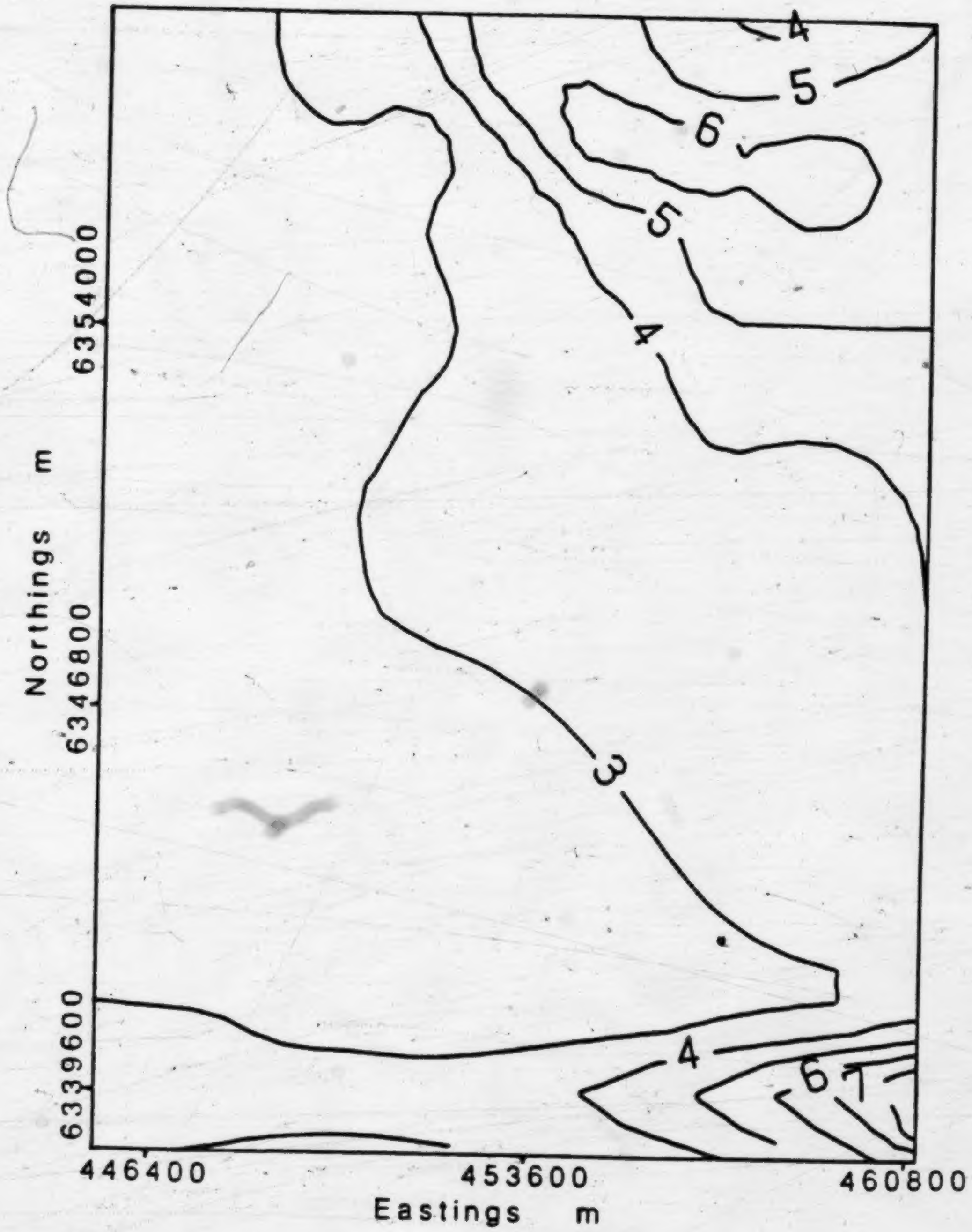
4
5
6
5
4
3
4
6
7
Northings m
6354000
6346800
6339600
446400
453600
460800
Eastings m

Figure 8.6 Isopach of pay zone 3 in the large area. The contour interval is 1 metre.

6

The large area has estimated in-place resources of 1.82 billion m^3 (11.36 billion bbl or 33.71 million bbl/km^2 or 0.34 bbl/m^3).

8.3 Evaluation of the Small Area

Volume calculations were carried out by zone as in the case of the large area. The volumes were calculated using the kriged grid models of the tops and bottoms of each zone (paragraph 6.2).

The volume calculations, as well as the area, perimeter and average thickness of each zone are given in Table 8.3. The kriged isopachs are presented in Figures 8.7, 8.9, 8.11, 8.13, 8.15 and 8.17.

Isopachs, using the conditionally simulated surfaces in the small area (paragraph 7.1), were also constructed and are depicted in Figures 8.8, 8.10, 8.12, 8.14, 8.16 and 8.18. Comparing the kriged and conditionally simulated isopachs, one can visualize the difference between a minimum variance, unbiased linear estimates and a simulated reality. Volume calculations are not based on the simulated isopachs because different realizations of the same isopachs would give different volume estimates which would vary around the volume calculated using the kriged surfaces.

The estimated in-place bitumen of pay zones one, two and three in the small area were 12.02, 28.28 and 25.96 million m^3 respectively. The calculated strip ratio of the

TABLE 8.3 Area, perimeter, volume and average thickness of the zones in the small area.

Zone	Area (km^2)	Perimeter (km)	Volume (m^3 x 10^8)	Average thickness (m)
Overburden	5.707	11.58	1.306	21.6
Pay 1	5.707	11.58	0.664	11.3
Barren 1	5.707	11.58	0.513	9.1
Pay 2	5.707	11.58	1.351	25.9
Barren 2	5.707	11.58	0.634	10.7
Pay 3	5.707	11.58	1.082	19.1

TABLE 8.4 Volumes, in-place bitumem and stripping ratios of the pay zone in the small area.

Pay zone	Volume ($m^3 \times 10^8$)	Mean grade (weight %)	In-place bitumen ($m^3 \times 10^6$)	Stripping ratio
1	0.664	8.68	12.02	1.96
2	1.351	10.05	28.28	1.14
3	1.082	11.52	25.96	1.44

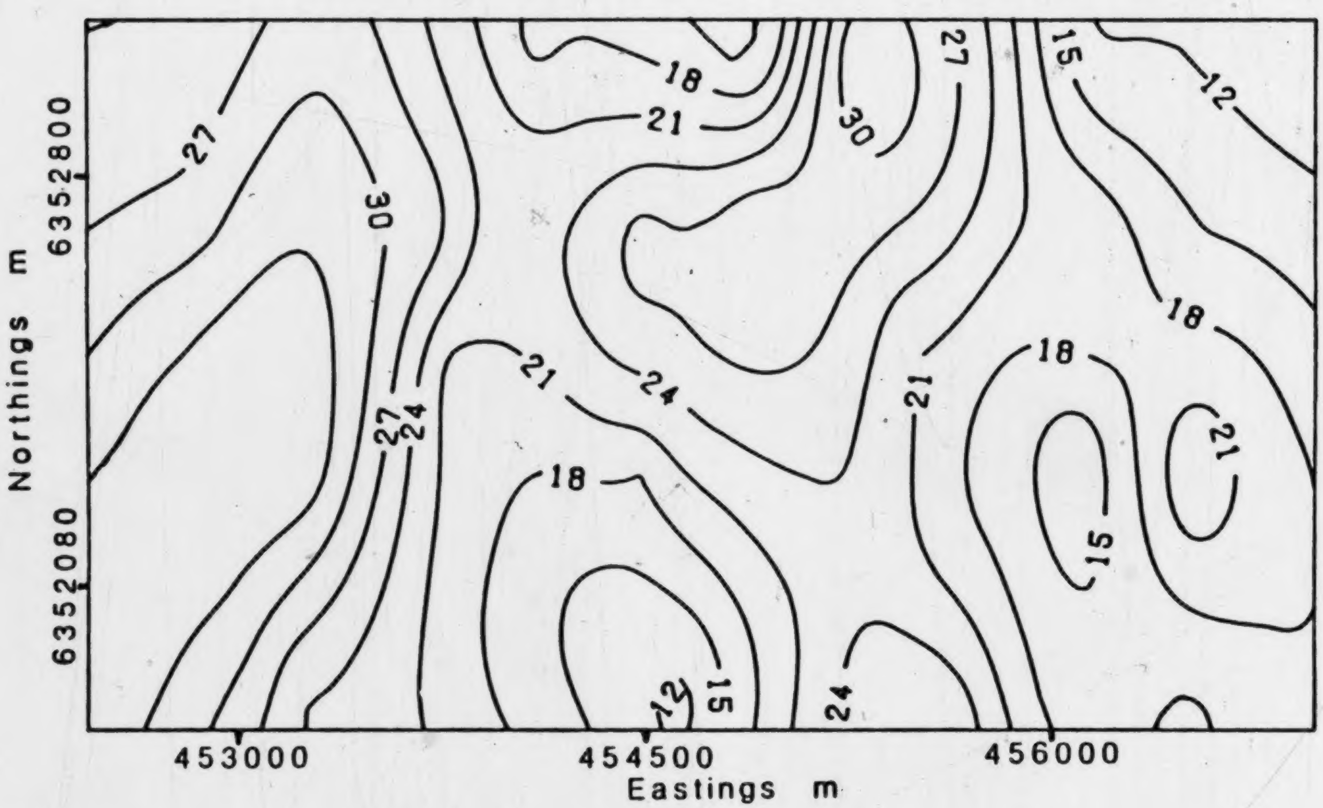
12
15
18
21
24
27
30
6352800
6352080
Northings m
453000
454500
456000
Eastings m

Figure 8.7 Minimum variance isopach of the overburden in the small area. The contour interval is 3 metres.

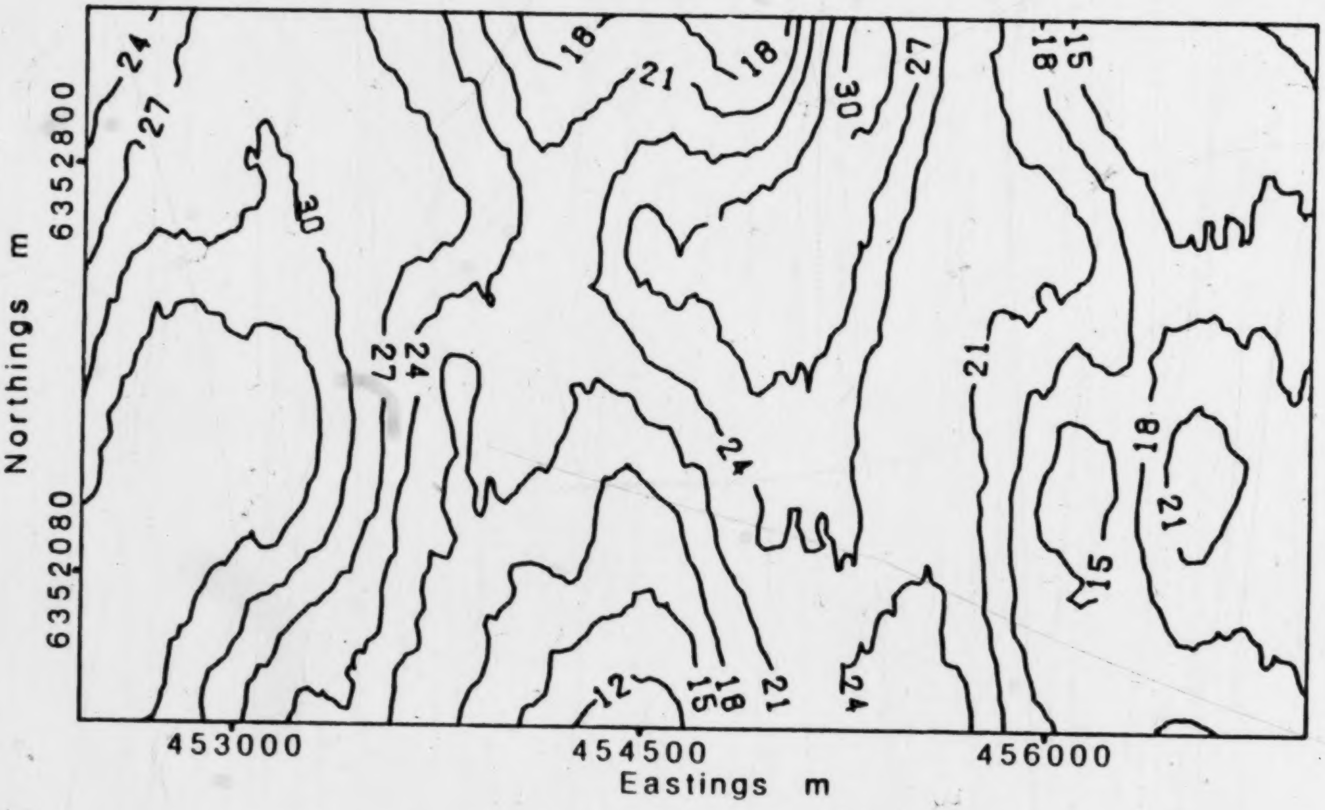
24
27
30
18
21
18
30
27
15
18
24
27
24
21
18
21
15
12
15
18
21
24
6352800
6352080
Northings m
453000
454500
456000
Eastings m

Figure 8.8 Conditionally simulated isopach of the overburden in the small area. The contour interval is 3 metres.

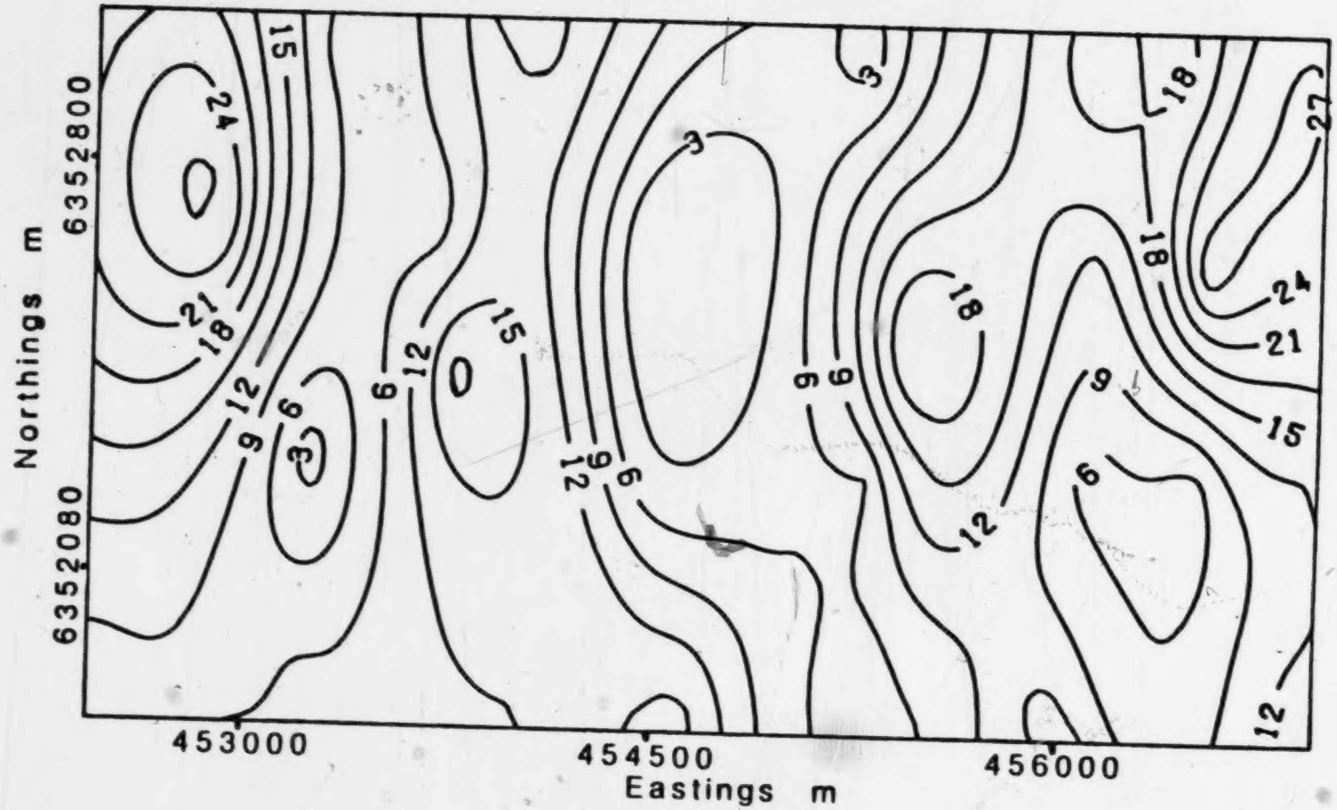
Northings m
6352800
6352080
453000
454500
456000
Eastings m
27
24
21
18
15
12
9
6
3

Figure 8.9 Minimum variance isopach of pay zone 1 in the small area. The contour interval is 3 metres.

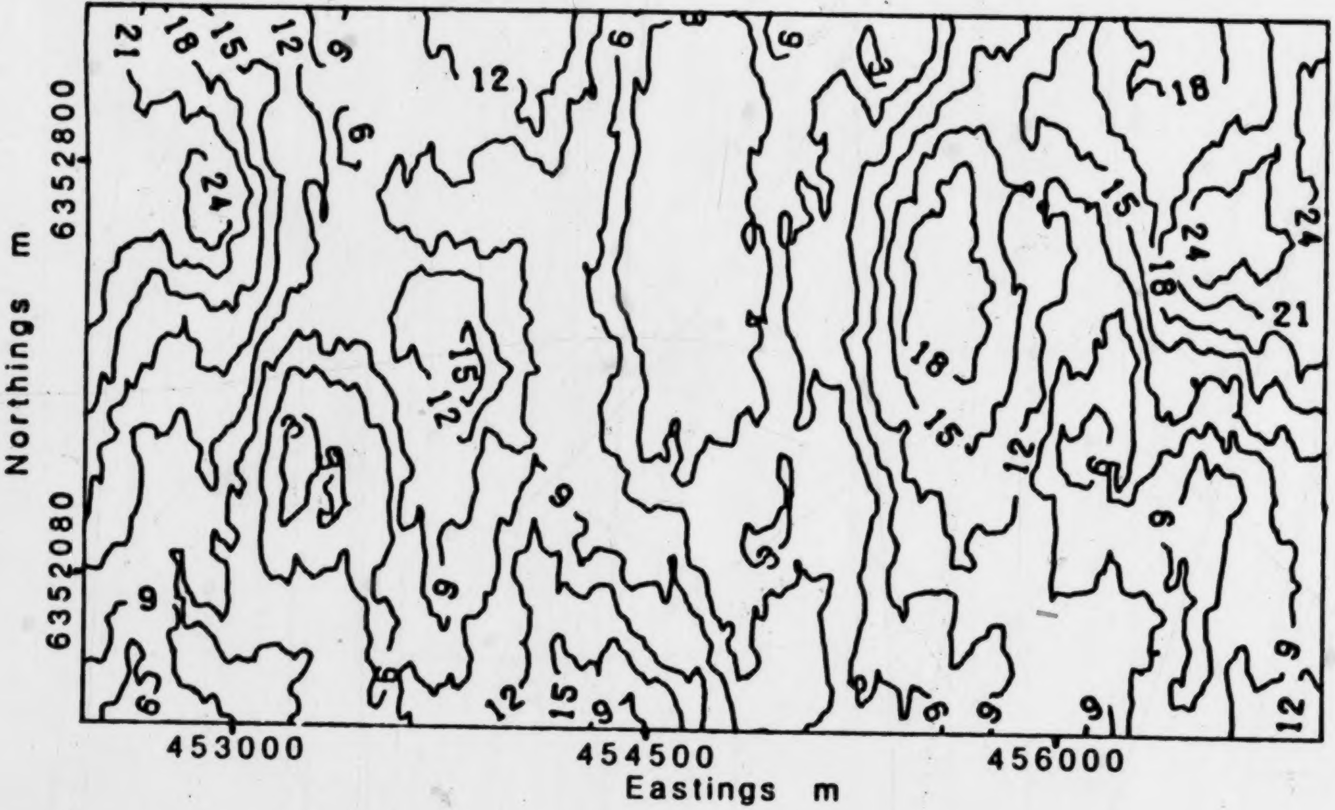
21
18
15
12
9
12
6
9
8
9
3
18
15
24
24
18
21
24
15
12
18
15
12
5
9
9
6
9
9
12
15
9
12
6
9
6
6
9
6352800
6352080
Northings m
453000
454500
456000
Eastings m

Figure 8.10 Conditionally simulated isopach of pay zone 1 in the small area. The contour interval is 3 metres.

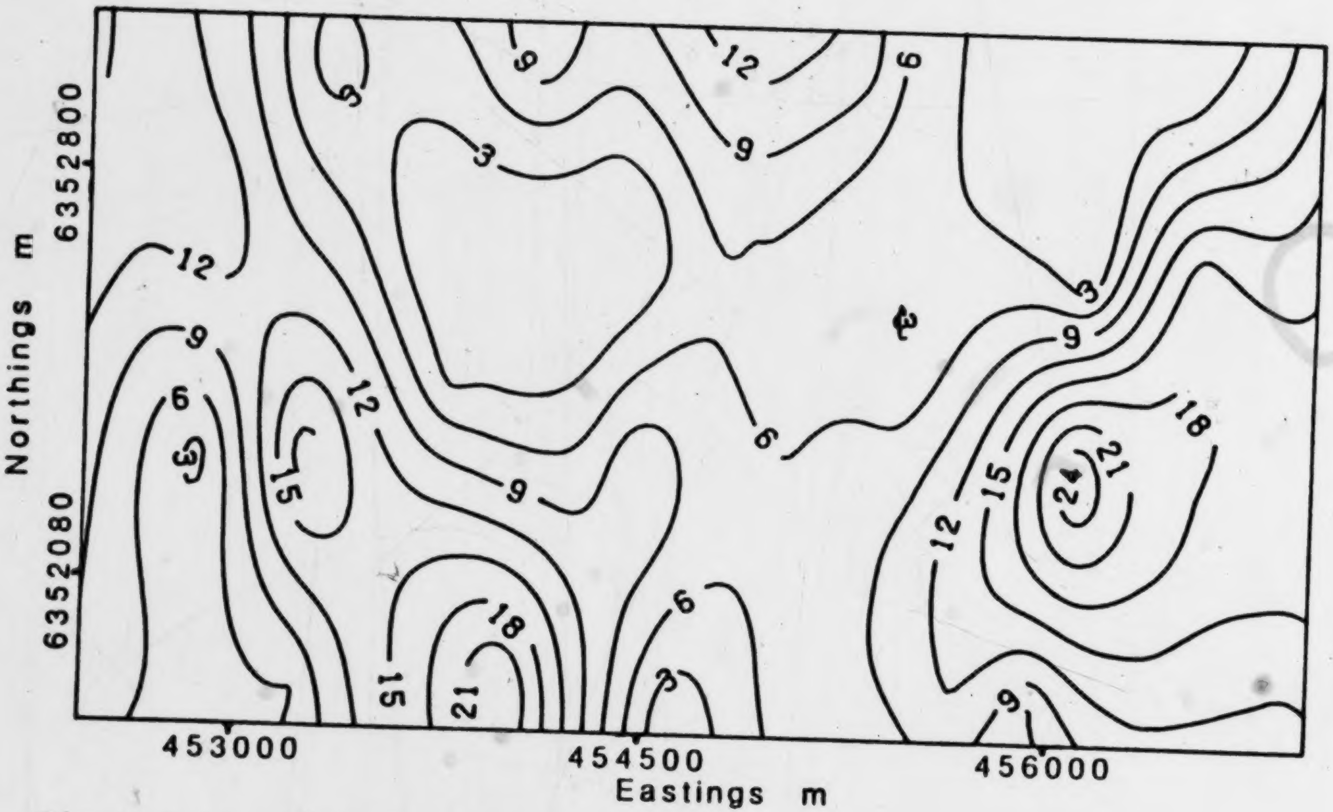
6352800
6352080
Northings m
453000
454500
456000
Eastings m
3
6
9
12
15
18
21
24

Figure 8.11 Minimum variance isopach of barren zone 1 in the small area. The contour interval is 3 metres.

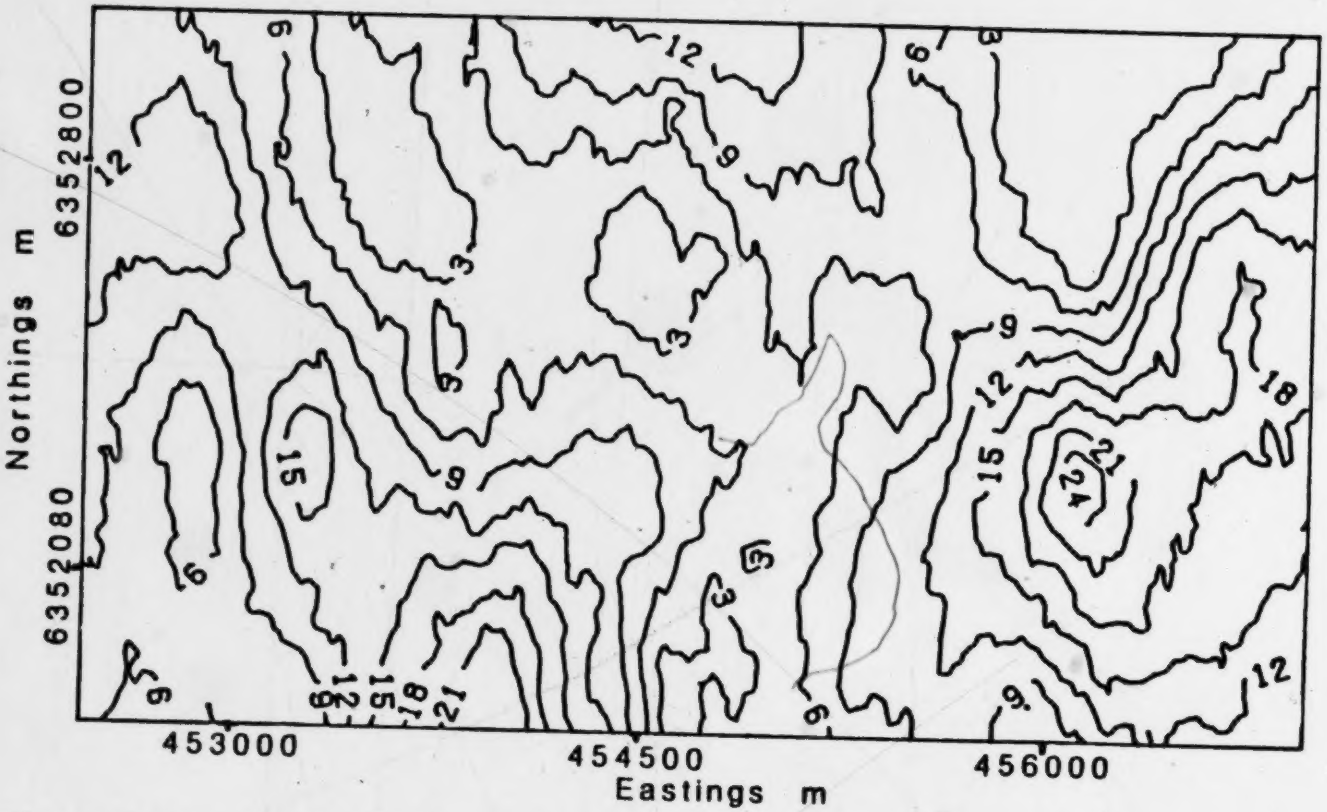
Northings m
6352800
6352080
453000
454500
456000
Eastings m
3
6
9
12
15
18
21
24

Figure 8.12 Conditionally simulated isopach of barren zone 1 in the small area. The contour interval is 3 metres.

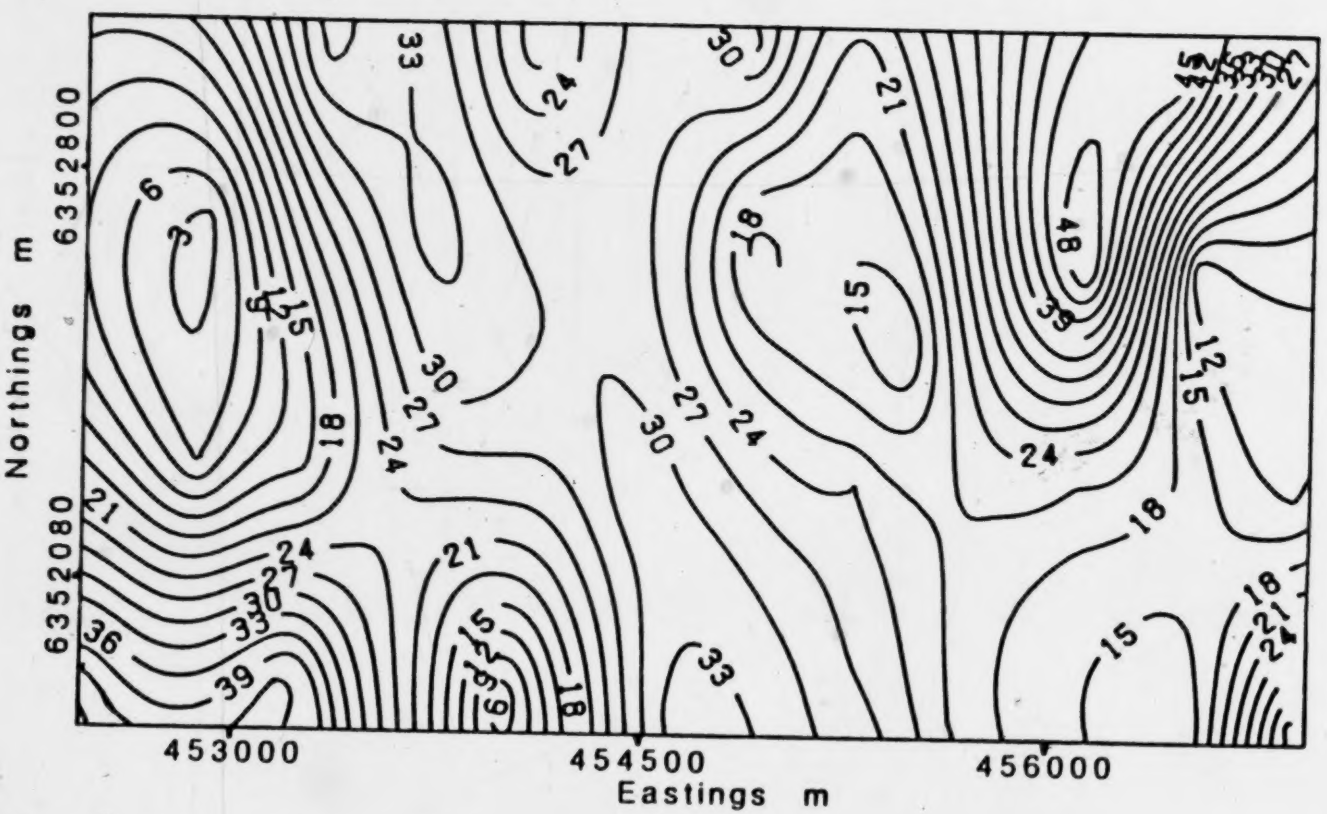
6352800
6352080
Northings m
453000
454500
456000
Eastings m
3
6
9
12
15
18
21
24
27
30
33
36
39
48
45
42
39
36
33
30
27
24
21
18
15
12
9
6

Figure 8.13 Minimum variance isopach of pay zone 2 in the small area. The contour interval is 3 metres.

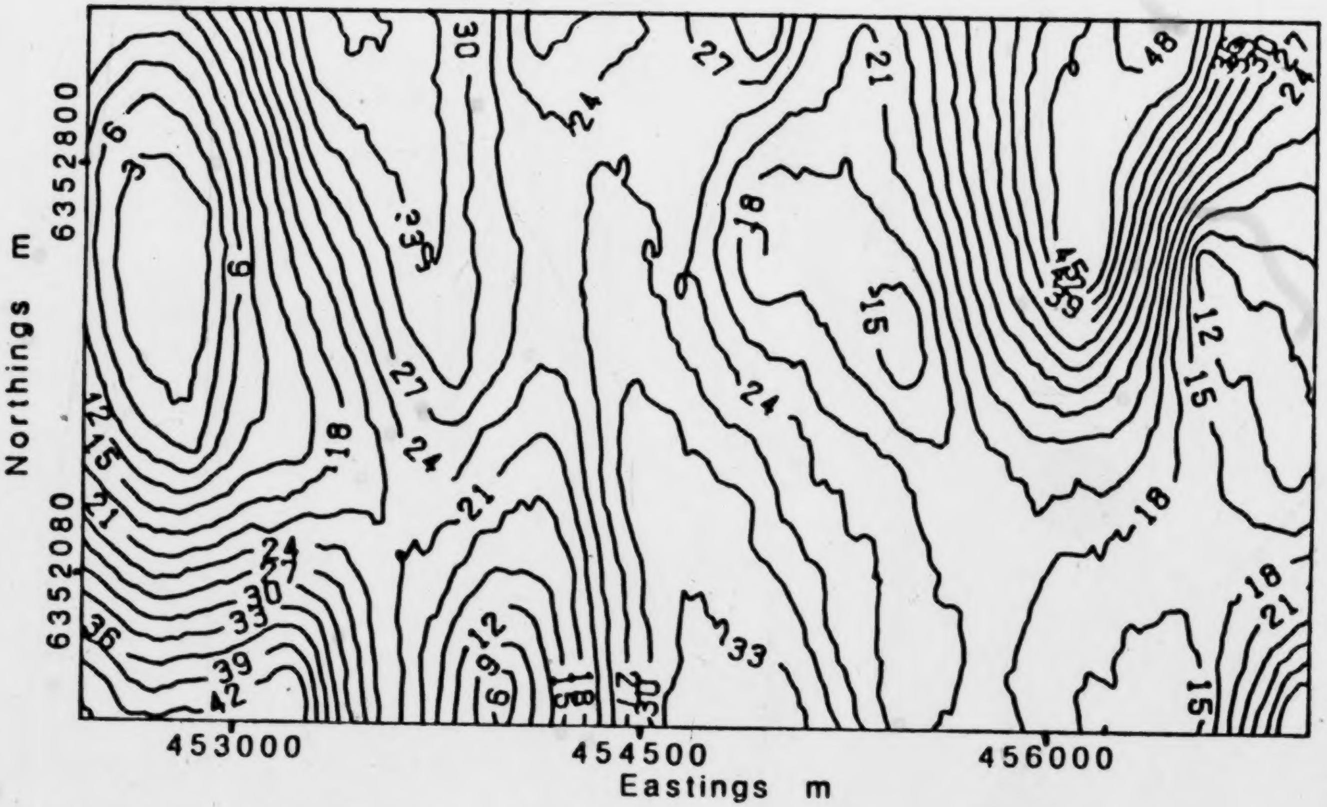
Northings m
6352800
6352080
Eastings m
453000
454500
456000
3
6
9
12
15
18
21
24
27
30
33
36
39
42
45
48

Figure 8.14 Conditionally simulated isopach of pay zone 2 in the small area. The contour interval is 3 metres.

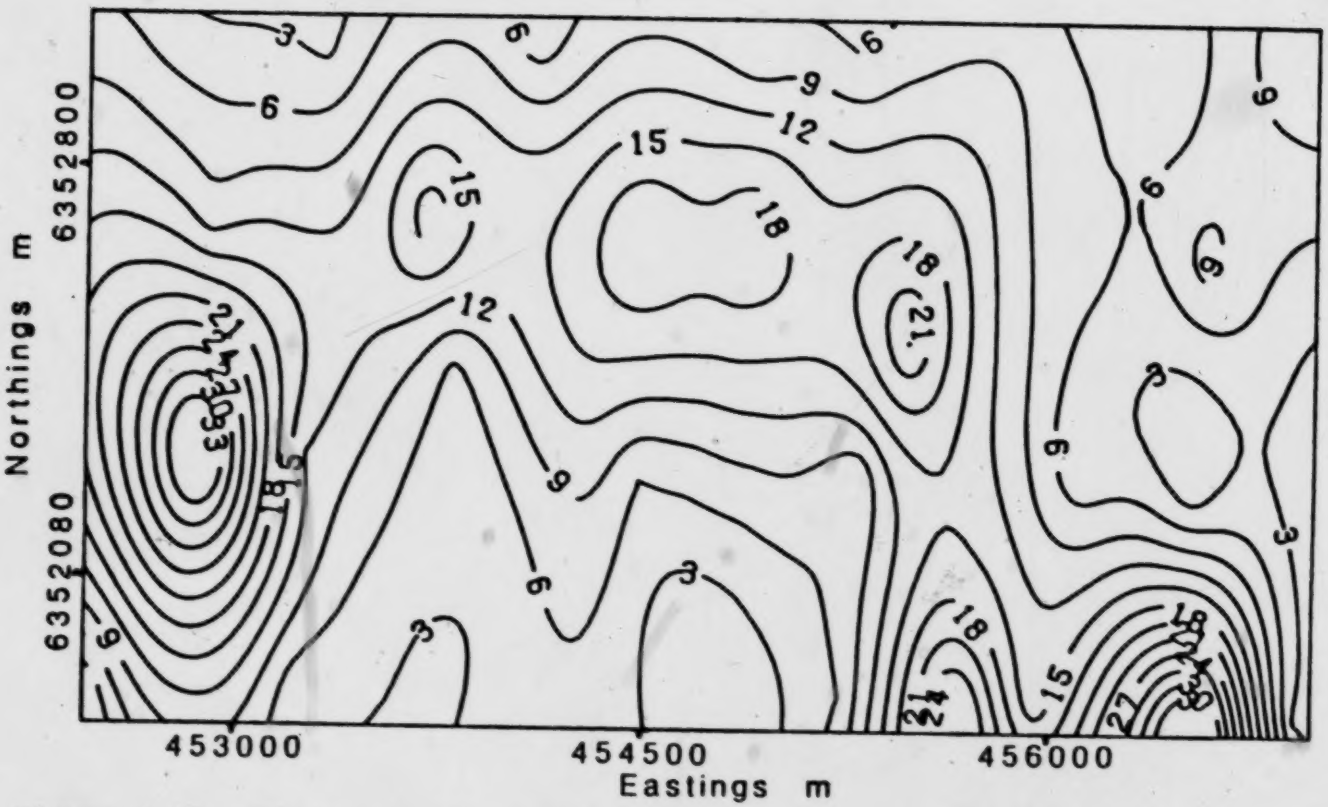
Northings m
6352800
6352080
Eastings m
453000
454500
456000
3
6
9
12
15
18
21
24
27
30
33

Figure 8.15 Minimum variance isopach of barren zone 2 in the small area. The contour interval is 3 metres.

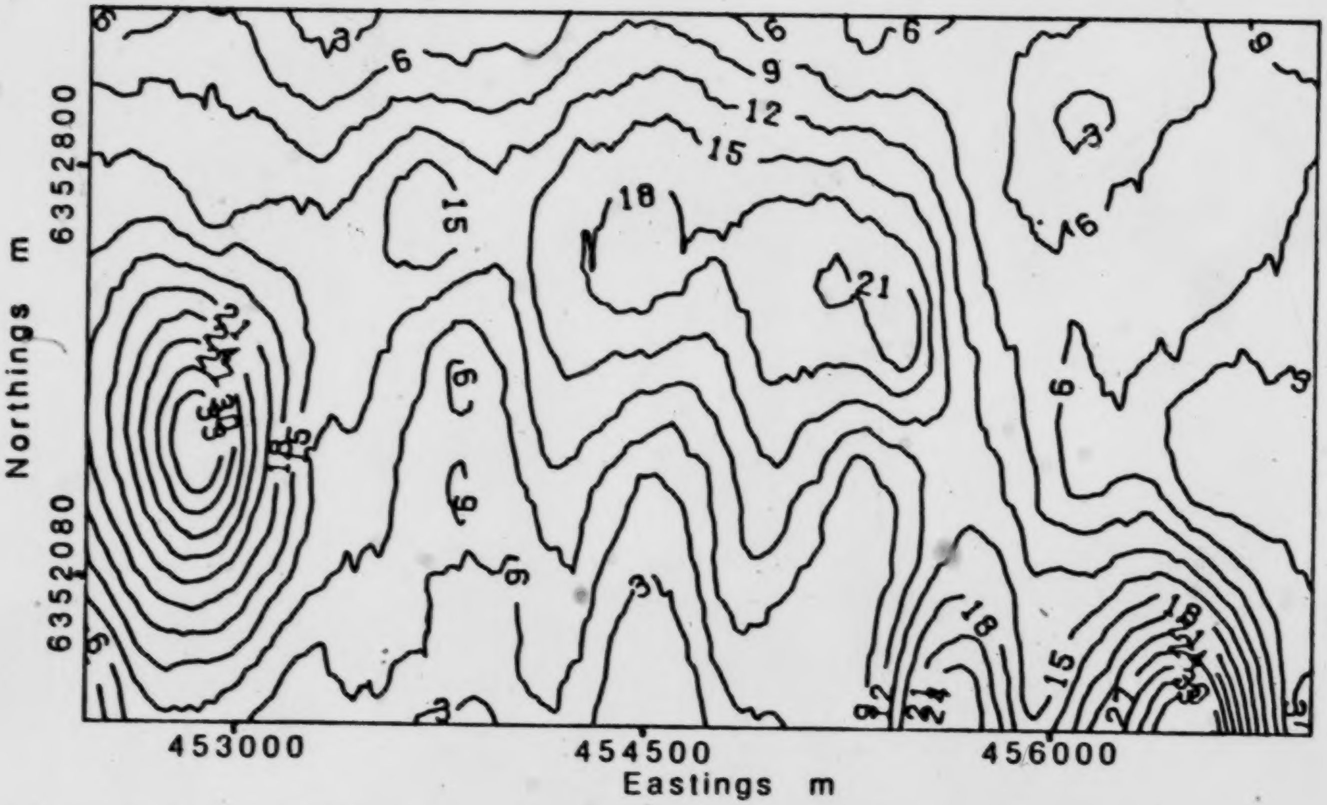
Northings m
6352800
6352080
Eastings m
453000
454500
456000
3
6
9
12
15
18
21
24
27
30
33

Figure 8.16 Conditionally simulated isopach of barren zone 2 in the small area. The contour interval is 3 metres.

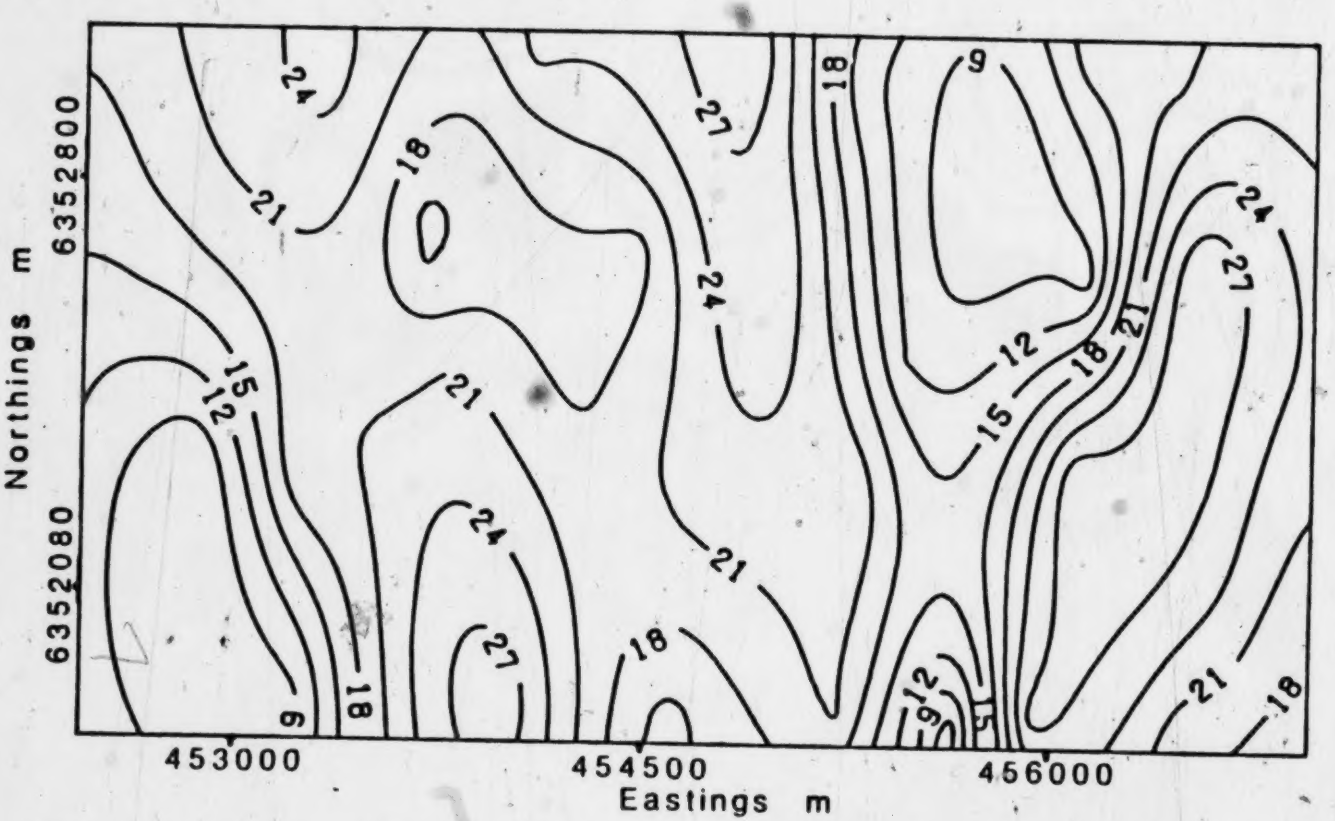
6352800
6352080
Northings m
453000
454500
456000
Eastings m
24
21
15
12
9
18
27
24
21
18
24
27
21
18
9
12
15
18
21
24
27
21
18
12
9
15

Figure 8.17 Minimum variance isopach of pay zone 3 in the small area. The contour interval is 3 metres.

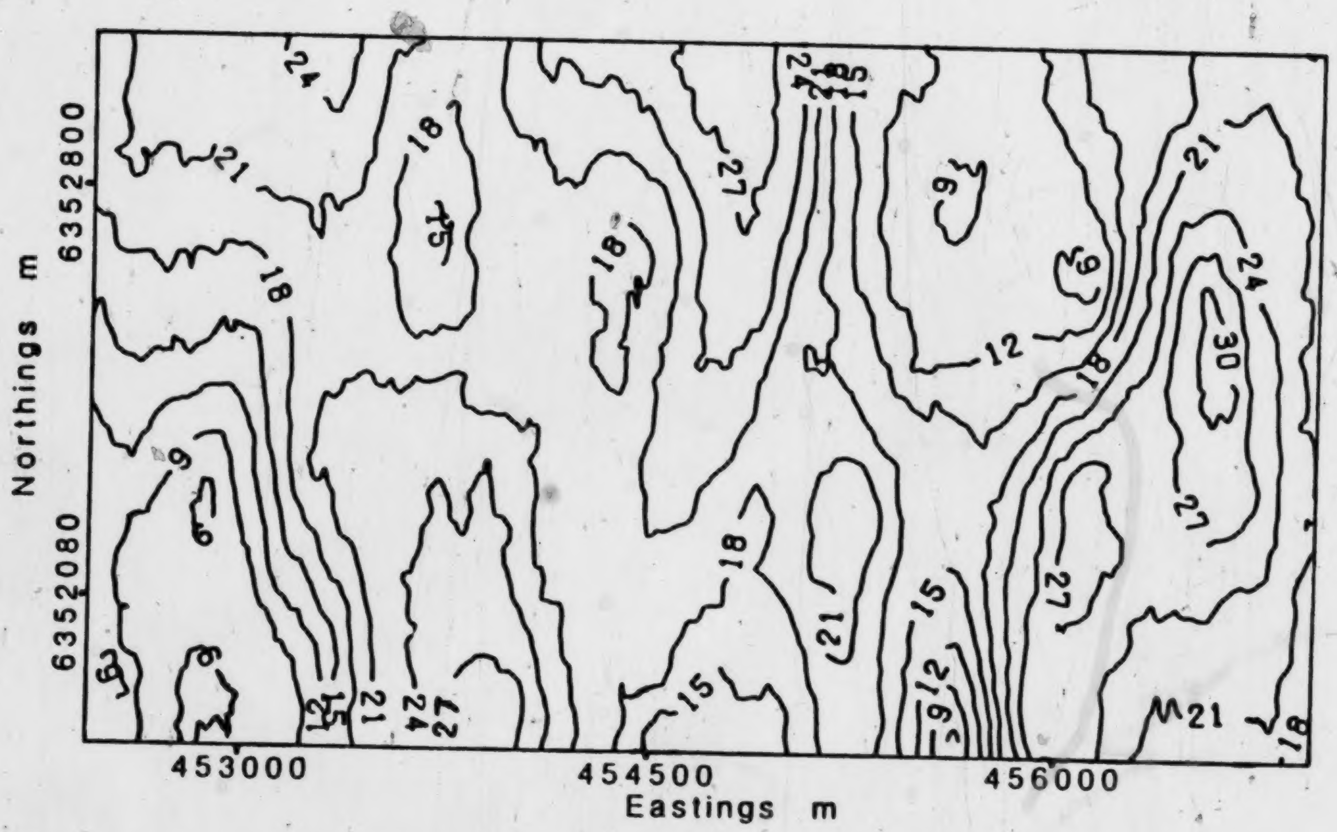
Northings m
6352800
6352080
Eastings m
453000
454500
456000
24
21
18
15
12
9
27
30

Figure 8.18 Conditionally simulated isopach of pay zone 3 in the small area. The contour interval is 3 metres.

pay zones, in the same order as above, were 1.96, 1.14 and 1.44. All relevant figures are summarized in Table 8.4.

The small area has estimated in-place resources of 65.72 million m³ (413.40 million bbl or 72.42 million bbl/km² or 0.72 bbl/m³). The resources per unit volume or area of the small area are almost double than of the total study area.

8.4 Remarks on the Reserves Estimation

The in-place reserves estimations presented in the previous paragraphs were based on the average grade of each pay zone, not on the constructed minimum variance grade models of the deposit. This was because the grade models must be used in conjunction with an extraction method, and the selection of an extraction method was beyoned of the scope of this study. If the extraction method is ignored, the more time-consuming calculations required to use the grade models in the reserves estimation would have only produced meaningless numbers.

An hypothetical example is given below to show how reserves should be estimated on the basis of interpolated sections of the grade models, provided that a mining method has been selected.

Consider the section along 6342600 meters Northing of the grade model in the large area. On the basis of a particular mining method, five polygons are drawn around the ore bodies to be extracted (Figure 8.19). Then the area of

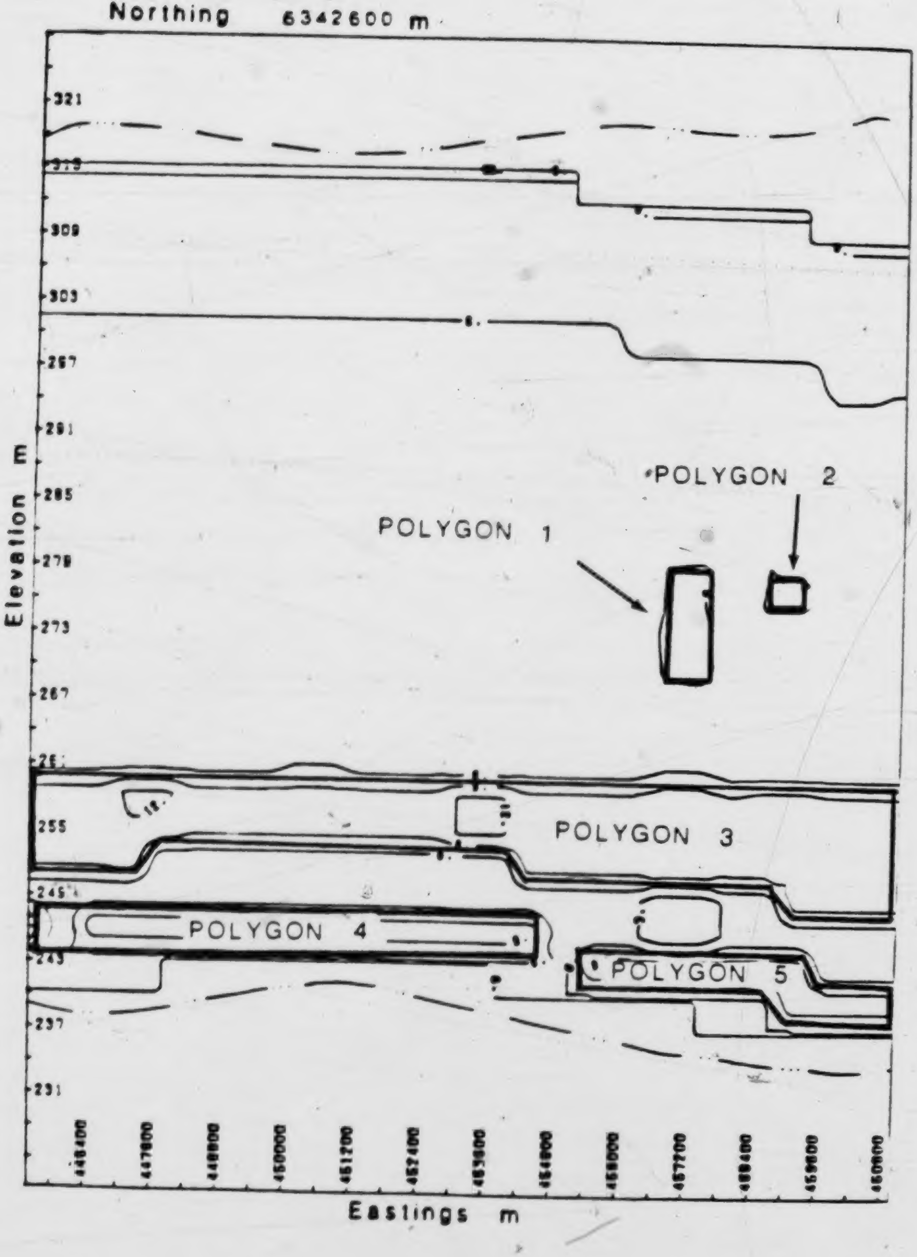
Northing 6342600 m
Elevation m
321
315
309
303
297
291
285
279
273
267
261
255
249
243
237
231
POLYGON 1
POLYGON 2
POLYGON 3
POLYGON 4
POLYGON 5
446400
447600
448800
450000
451200
452400
453600
454800
456000
457200
458400
459600
460800
Eastings m

Figure 8.19 Polygons drawn in section 6342600 m Northing.

each polygon, as well as grade and estimated error on each grid point within each polygon is integrated. The volume corresponding to each polygon is calculated by multiplying each integrated area by the horizontal grid spacing of the grade model (600 m) and finally the reserves corresponding to the section are estimated. The results are given in Table 8.5.

In the same way, the reserves corresponding to each section of the grade model, and eventually the total minable reserves can be calculated.

TABLE 8.5 Volume, grade and error integration using the polygons of section 6342600 m Northing.

Polygon	Area (m^2)	Volume (m^3x10^4)	Average grade (weight%)	Average error (weight%)	In-place bitumen (m^3x10^6)
1	7700	462	6.68	0.47	0.64±0.05
2	2400	144	6.53	1.73	0.20±0.05
3	114700	6882	10.58	2.54	15.16±3.73
4	36000	2160	10.88	3.11	4.89±1.39
5	27830	1670	10.87	3.62	3.78±1.25

9. CONCLUSIONS AND SUGGESTIONS

The major objective of this study was to develop conditionally simulated models of the boundaries and weight percent oil of the pay zones. These models capture the inherent *in-situ* variability of the deposit. Results of the validation of the models clearly indicate that the conditional simulation models correctly reproduced the mean, variance and stochastic structures (variograms) of the real deposit.

Both the kriged and simulated models were based upon an interpretive geological model of the depositional environments and facies of the McMurray Formation which was used to define geologically homogeneous domains in the deposit. Geostatistical analysis was then performed on each domain individually, incorporating thus the controlling the deposit geological features to the constructed numerical models.

9.1 The use of Conditional Simulation

Kriged models are aimed at the evaluation and estimation of the ore reserves and, to an extent, to the selection of the extraction method, whereas the conditionally simulated models, as simulated realities, have a different objective. Simulated models, such as the ones produced in this study, are to be used in the following areas:

a) To check the sensitivity of different estimation procedures (including kriging) versus the simulated deposit.

b) To study the sensitivity of the ore recovery to various parameters such as the size of the selected mining unit and ore dilution.

c) To determine the extraction method and required equipment.

d) To plan the blending of rich and poor ore from various areas as well as to determine the variability of run of the mining operation on a daily, monthly and yearly basis.

e) Finally, the total mining plan can be tested against different conditionally simulated realizations of the deposit, and the expected profitability and risk involved can be assessed. If the test indicates substantial differences, then additional data (e.g. from drilling) may be required. The drilling program could be carried out in the areas of highest uncertainty as suggested by the different simulated realizations.

9.2 The Improvement of Geostatistical Models

The models produced in this study could be improved by increasing the geological input as well as by using more advanced geostatistical techniques.

The geological input could be substantially improved by using all possible information from the core of the available wells, both in terms of data measurement and interpretation-definition of the sedimentary facies of the McMurray Formation. Geostatistically, the models could be improved by estimating volumes instead of points. In addition, techniques utilizing moments of the distribution functions of the analysed regionalized variables higher than second order (non-linear geostatistics), could improve the numerical accuracy of the constructed models.

Finally, geostatistical models are inferred from a set of data and consequently, there is no technique which will completely reproduce the uniqueness of the deposit. Thus, modelling is not a stationary operation, but a continuous and dynamic process which requires that the models be validated by the mining operation as well as improved by using all new information which the extraction procedure can provide.

9.3 Future Applications and Development of Geostatistics

The aim of this study was to demonstrate the potential of geostatistical techniques in reconstructing the variability of space-dependent characteristics of an oil-sand deposit using data at specific locations.

Future applications involving these and other variables (permeability, porosity, % fines, thickness etc.) should be considered in other oil sand deposits. These applications could assist surface or underground mining operations or *in-situ* recovery schemes by increasing their accuracy, efficiency and most importantly, profitability.

The applications should also be extended and adopted to the character of conventional oil reservoirs, particularly in the area of modelling reservoir parameters prior to enhanced recovery operations. For example, different recovery methods could be tested on conditionally simulated reservoir models. Another example could be the use of a simulated model of permeabilities over the area of the reservoir as an input to a fluid-flow simulator. Theoretical problems do exist however, particularly with parameters such as permeability. The problem of modelling a non-additive parameter such as permeability can be overcome with proper developments of the geostatistical theory.

The development of geostatistical methodology in the last few years is certainly in the direction of non-linear space. However, the complexity of the geostatistical techniques remains the main problem in the slow invasion of geostatistics in routine modelling procedures. The use of artificial intelligence techniques and expert systems will assist the non-expert in carrying out valid and accurate modelling operations.

REFERENCES

Bally, A.W., 1975. A geodynamic scenario for hydrocarbon occurrances. In Proc. 9th World Petrol. Cong., 2, Applied Science Publications Ltd., p.33-44.

Benthin, H.L. and Orgnero, U.J., 1977. Geology and heavy oil reserves of the Gregoire Lake area. Bull. Can. Petroleum Geology, 25, p.367-377.

Briggs, I.C., 1974. Machine contouring using minimum curvature. Geophysics, 39, no.1, p.39-84.

Carlier, A., 1958. Uranium-bearing shale deposits at St. Hippolyte (Haut-Rhin): An example of a study by statistical calculation. In Proc. 2nd United Nations International Conference on the peaceful uses of atomic energy, Geneva, 3, p.87-94.

Carrigy, M.A., 1959a. Geology of the McMurray Formation, Part III, General geology of the McMurray area. Alberta Res. Council, Mem. 1.

Carrigy, M.A., 1959b. The significance of a grain size classification of the sands of the McMurray Formation, Alberta. Fifth World Petroleum Cong., Sec. 1, Paper 31, p.1-14.

Carrigy, M.A., 1962a. Bibliography of the Athabasca oil sands, Alberta. Alberta Res. Council, Prer. Pep. 62-7.

Carrigy, M.A., 1962b. Effect of texture on the distribution of oil in the Athabasca oil sands, Alberta, Canada. Journal of Sedimentary Petrology, 32, no.2, p.312-325.

Carrigy, M.A., 1963a. Petrology of coarse-grained sands in the lower part of the McMurray Formation. Alberta Res. Council, Inform. Ser., no.45, p.43-54.

Carrigy, M.A., 1963b. Criteria for differentiating the McMurray and Clearwater Formations in the Athabasca oil sands. Alberta Res. Council Bull., 14, p.1-32.

Carrigy, M.A., 1963c. Paleocurrent directions from the McMurray Formation. Bull. Can. Petroleum Geology, 11, no.1, p.389-395.

Carrigy, M.A., 1966. Lithology of the Athabasca oil sands. Alberta Res. Council, Bull., 18.

Carrigy, M.A., 1967. Some sedimentary features of the

Athabasc oil sands. Sedimentary Geology, 1, p.327-332.

Carrigy, M.A., 1971. Deltaic sedimentation in Athabasca tar sands. Am. Assoc. Petroleum Geology Bull., 55, no.8, p.1155-1169.

Carrigy, M.A., 1973. Mesozoic geology of the Fort McMurray area. In Guide to the Athabasca oil sands area (ed. M.A Carrigy). Alberta Res. Council, Inform. Ser., no.65, p.77-101.

Conybeare, C.E.B., 1966. Origin of the Athabasca oil sands: a review. Bull. Can. Petroleum Geology, 14, no.1, p.145-163.

Corbett, G.S., 1955. In-situ origin of McMurray oil of northeastern Alberta and its relevance to general problem of origin of oil. Am. Assoc. Petroleum Geology Bull., 39, no.8, p.1601-1649.

David, M., 1977. Geostatistical ore reserve estimation. Elsevier, Amsterdam.

David, M., 1984. Applied advanced geostatistical ore reserve estimation. Gamma Geostat International, Montreal.

Demaison, G.J. 1977. Tar sands and supergiant oil fields. In, The Oil Sands of Canada-Venezuela, 1977 (eds. D.A. Redford and A.G. Winestock). CIM Special Volume 17, p.9-16.

Deroo, G., Tissot, B., McCrossan, R.G. and Der, F., 1974. Geochemistlry of the heavy oils of Alberta. In Oil Sands Fuel of the Future (ed. L.V. Hill). Can. Soc. Petroleum Geology, Mem. 3, p.148-167.

Deroo, G., Powell, T.G., Tissot, B. and McCrossan, R.G., with contributions from P.A. Hacquebard, 1977. The origin and migration of petroleum in the Western Canadian sedimentary basis, Alberta: A geochemical and thermal maturation study. Geological Surv. Can. Bull., 262.

Doob, J.L., 1953. Stochastic processes. Wiley and Sons, New York.

Dowd, P.A. 1984. Conditional simulation of inter-related beds in an oil deposit. In Geostatistics for Natural Resources Characterization (eds. G. Verly, *et al*.). D. Reidel Publishing Company, part 2, p.1031-1043.

Dowd, P.A. and Royle, A.G., 1977. Geostatistical applications in the Athabasca tar sands. In Proc.

15th APCOM Symposium, Brisbane, Australia, p.235-242.

Dutta, I. and Rao, S.V.L.N., 1977. Variograms and their role in interpretation of soft ore types. Mathematical Geology, 9, no.1, p.99-111.

Flach, P.D., 1977. A lithofacies analysis of the McMurray Formation, Lower Steepbank River, Alberta. MSc. Thesis, University of Alberta.

Flach, P.D. and Mossop, G.D., 1985. Depositional environments and paleohydrology of the Lower Cretaceous McMurray Formation, Athabasca Oil Sands, Alberta. Am. Assoc. Petroleum Geology Bull., 69, no.8, p.1195-1207.

Franklin, J., 1828. Narrative of a second expedition to the shores of the Polar Sea in the years 1825, 1826 and 1827, including an account of the progress of a detachment to the eastward by John Richardson. John Murray, London.

Gandin, L.S., 1963. Objective analysis of meterological fields GIMIZ Leningrad. Translated in 1965 by the Israel Program for Scientific Translations, Jerusalem.

Grasley, W., 1982. Grade model project: Phase 1, structural study, milestone report. Personal communication.

Gussow, W.C., 1956. Athabasca bituminus sands. In Symposium sobre yacimientos de petroleoy gas. 20th International Geological Cong. Mexico, 3, p.68-70.

Halbouty, M.T., King, R.E., Klemme, H.D., Dott, R.H. and Shabad,T. 1970. Factors affecting formation of giant gas fields and basin classification; Am. Assoc. Petroleum Geology, Memoir 14, p.534-540.

Hitchon, B., 1963. Composition and movement of formation fluids in strata above and below the pre-Cretaceous unconformity in relation to the Athabasca oil sands. In Athabasca Oil Sands, Alberta Res. Council, Inform. Ser., no.45, K.A. Clark Volume, p.63-74.

Hodgson, G.W. and Hitchon, B., 1965. Research trends in petroleum genesis. Alberta Res. Council, Contrib. no.270.

Hume, G.S., 1951. Possible Lower Cretaceous origin of bitumen in bituminus sands of Alberta. In Proc. Athabasca Oil Sands Conf., Coverment of Alberta, Edmonton, p.66-75.

James, D.P., 1977. The sedimentology of the McMurray Formation, east Athabasca. MSc. Thesis, University of Calgary.

James, D.P. and Oliver, T.A., 1978. The sedimentology of the McMurray Formation, east Athabasca. In the Oil Sands of Canada-Venezuela (eds. D.A. Redford and A.D. Winestock). CIM Special Volume 17, p.17-26.

Jardine, D., 1974. Cretaceous oil sands of western Canada. In Oil Sands Fuel of the Future (ed. L.V. Hills). Can. Soc. Petroleum Geology, Mem. 3, p. 50-67.

Jenkins, G.M. and Watts, D.G., 1968. Spectral analyses and its applications. San Francisco, Holden-Day.

Journel, A., 1974a. Geostatistics for conditional simulation of ore bodies. Economic Geology, 69, p.673-689.

Journel, A., 1974b. Simulations conditionelles-theorie et practique. Doctoral thesis, CG Fontainebleau.

Journel, A. and Huijbregts, C.J., 1978. Mining geostatistics. Academic Press, London.

Kim, Y.C., Medhi, P.K. and Arik, A., 1979. Investigation of in-pit ore-waste selection proseadures usinw conditionally simulated orebodies. In 17th APCOM Symposium (eds. T.B. Johnson and R.J. Barnes), p.121-192.

Khinchin, A.Y., 1934. Korrelationstheorie der stationaren stochastischen Prozesse. Mathematische Annalen, 109, p.604-615.

King, H.P., McMahon, D.W. and Bujtor, G.J., 1982. A guide to the understanding of ore reserve estimation. In Proc. Australasian Inst. Min. Metall., no.281.

Klemme, H.D., 1975. Giant oil fields related to their geological setting: a possible guide to exploration. Bull. Can. Petroleum Geology, 23, no.1, p.30-66.

Knudsen, H.P., 1981. Development of a conditional simulation model of a coal deposit. PhD. Thesis, The University of Arizona.

Kolmogorov, A.N., 1931. Uber die analytischen Methoden der Wahrschecnlichkeitsrechnung. Mathematische Annalen, 104, p.415-432.

Krige, D.G., 1976. Some basic considerations in the application of geostatistics to the valuation of ore in South African gold mines. Journal of the South

African Institute of Mining and Metallurgy, p.383-390.

Link, T.A., 1951. Sources of oil in 'tar sands' of Athabasca River, Alberta, Canada. Am. Assoc. Petroleum Geology Bull., 35, p.854-864.

Martin, R. and Jamin, F.G.S., 1963. Paleogeomorphology of the buried Devonian landscape in Northern Alberta. In Athabasca Oil Sands, Alberta Res. Council, Inform. Ser., no.45, K.A. Clark Volume, p.31-32.

Matern, B., 1960. Spatial variation. Meddelanden Fran Statens Skogsforskningsinstetut, 49, no.5.

Matheron, G., 1963a. Principles of geostatistics. Economic Geology, 58, p.1246-1266.

Matheron, G., 1963b. Traite de geostatistique appliquee. Technip, Paris.

Matheron, G., 1965. Les variables regionalisees et leur estimation. Masson, Paris.

Matheron, G., 1967. Kriging or plynomial interpolation procedures. CIM Transactions, 70, p.240-244.

Matheron, G., 1969. Le krigeage universel. Les Cahiers du Centre de Morphologie Mathematique, Fasc.1, CG, Fontainebleau.

Matheron, G., 1972. The theory of regionalized variables and its applications. Les Cahiers due Centre du Morphologie Mathematique, Fasc.5, CG, Fontainebleau.

Matheron, G., 1973. The intrinsic random functions and their applications. Advances in Applied Probability, 5, p.439-468.

McLearn, F.H., 1917. Athabasca River section, Alberta. Geol. Surv. Can. Summ. Rept. 1916, p.145-151.

Mejia, J.M. and Rodrigues-Itrube, I.R., 1974. On the synthesis of random field sampling for the spectrum: an application to the generation of hydrologic spatial process. Water Resources Research, 10, no.4, p.705-711.

Mellon, G.B. and Wall, J.H., 1956. Geology of the McMurray Formation. Alberta Res. Council, Rept.72, p.1-29.

Montgomery, D.S., Clugston, D.M., George, A.E., Smiley, G.T. and Sawatzky, H., 1974. Investigation of oils in the Western Canada tar belt. In Oil Sands Fuel of the

Future (ed. L.V. Hills). Can. Soc. Petroleum Geology, Mem. 3, p.168-183.

Mossop, G.D., 1976. Sedimentology of high grade oil sands, south Athabasca (abs.). Geol. Assoc. of Canada. Annual Mtg., 1976. Program with abstracts, 1, p.66.

Mossop, G.D., 1978a. Epsilon cross-strata in the Athabasca oil sands (abs.). In Fluvial Sedimentology (ed. A. Miall). Can. Soc. Petroleum Geology, Mem. 5, p.854-855.

Mossop, G.D., 1978b. Geological controls on reservoir heterogeneity, Athabasca Oil Sands. In AOSTRA Seminar on underground excavation in oil sands, Edmonton, University of Alberta, Item 5, Paper no.1.

Mossop, G.D., 1980a. Geology of the Athabasca oil sands. Science, 207, p.145-152.

Mossop, G.D., 1980b. Facies control on Bitumen saturation in the Athabasca oil sands. In Facts and Principles of World Petroleum Occurance (ed. A. Miall). Can. Soc. Petroleum Geology, Mem. 6, p.609-632.

Mossop, G.D. and Flach, P.D., 1978. Deep sinous channels and giant cross-beds in the Athabasca Oil Sands (abs.). Am. Assoc. Petroleum Geology Bull., 62, p.547.

Mossop, G.D. and Flach, P.D., 1983. Deep channel sedimentation in the Lower Cretaceous McMurray Formation, Athabasca Oil Sands, Alberta. Sedimentology, 30, p.493-509.

Nelson, H.W. and Glaister, R.P., 1978. Subsurface environmental facies and reservoir relationships of the McMurray oil sands, northeastern Alberta. Bull. Can. Petroleum Geology, 26, p.177-207.

Olea, R.A., 1975. Optimum mapping techniques using regionalized variable theory. Series on Spatial Analyses, no.2. Kansas Geological Survey, Lawrence, Kansas.

Outtrim, C.P. and Evans, R.G., 1978. Alberta's oil sands reserves and their evaluation, In th Oil Sands of Canada-Venezuela (eds. D.A. Redford and A.G. Winestock). CIM Special Volume 17, p.36-66.

Pemberton, G., Flach, P.D. and Mossop, G.D. 1983. Trace fossils from the Athabasca oil sands, Alberta, Canada. Science, 217, p.825-827.

Pow, J.R., Fairbanks, G.H. and Zamora, W.J., 1963.

Descriptions and reserve estimates of the oil sands of Alberta. In Athabasca Oil Sands, Alberta Res. Council Inform. Ser. no.45, K.A. Clark Volume, p.1-14.

Raymond, G.F., 1982. Geostatistical production grades estimates Mount Isa's copper orebodies. In Proc. Australasian Inst. Min. Metall., no.284, p.17-39.

Rendu, J-M., 1978. An introduction to geostatistical methods of mineral evaluation. South African Institute of Mining and Metallurgy, Johannesburg.

Rendu, J-M. and Readdy, L., 1982. Geology and the semivariogram - A critical relationship. In Proc. 17th Annual APCOM Symposium (eds. T.B. Johnson and R.J. Barnes). Soc. of Mining Engineers, New York, p.771-783.

Rennie, J.A., 1983. Applied geology - key to mining the Athabasca oil sands. CIM First District Five Meeting, paper 42.

Rennie, J.A., 1985. Sedimentology of the McMurray Formation on the Sandalta project study area, Northern Alberta, and implications for oil sand development. Reservoir Sedimentology (eds. R.W. Tillman and K. Weber). SEPM Special Publication no.36, (in press).

Rodriguez-Itrube, I.R. and Mejia, J.M., 1974a. The design of rainfall networks in time and space. Water Resources Research, 10, No.4, p.713-728.

Rodriguez-Itrube, I.R. and Mejia, J.M., 1974b. On the transformation of point rainfall to a real rainfall. Water Resources Research, 10, No.4, p.729-735.

Rudkin, R.A., 1964. Lower Cretaceous. In Geological History of Western Canada (eds. R.G. McGrossan and R.P. Glaister), Alberta Soc. Petroleum Geology, p.156-168.

Slutski, E.E., 1960. Selected works: Probability theory, mathematical statistics. Izv. Akademy. Nauk SSSR. Moscow.

Sproule, J.C., 1951. The McMurray Formation in its relation to oil occurrance. In Proc. Athabasca Oil Sands Conf., Goverment of Alberta, Edmonton, p.6-25.

Steinmetz, R., 1976. Application of Monte Carlo method for estimating reserves in Gregoire Lake Area, Athabasca tar deposits, Alberta (abstract). Am. Assoc. Petroleum Geology Bull., 60, no.4, p.726.

Stelck, C.R., 1975. Basement control of Cretaceous sand sequences in western Canada. In The Cretaceous System in the Western Interior of North America. (ed. W.G.E. Caldwell) Geol. Assoc. Canada, Special Paper 13, p.427-440.

Stewart, G.A., 1963. Geological controls of the distribution of Athabasca oil sands reserves. In Athabasca Oil Sands, Alberta Res. Council, Inform. Ser. no.45, K.A. Clark Volume, p.15.26.

Stewart, G.A., 1981. Athabasca oil sands in the future of heavy crude and tar sands. (eds. R.F. Meyer and C.T. Steele). McGraw-Hill, New York, p.208-222.

Stewart, G.A. and MacCallum, G.T., 1978. Athabasca oil sands guide book. Can. Soc. Petroleum Geology.

Swain, C.I., 1976. A Fortran IV program for interpolating irregularly spaced data using the difference equations for minimum curvature. Computers and Geosciences, 1, p.231-240.

Vigrass, L.W., 1968. Geology of the Canadian heavy oil sands. Am. Assoc. Petrol. Geol. Bull., 52, no.10, p.1984-1999.

Wiener, N., 1950. Extraploation, interpolation and smoothing of stationary time series. MIT Technology Press and John Wiley and Sons, New York.

Williams, G.D., 1960. The Mannville Group, Central Alberta. PhD. Thesis, University of Alberta.

Williams, G.D., 1963. The Mannville Group (Lower Cretaceous) of Central Alberta. Bull. Can. Petrleum Geology, 11, no.4, p.350-368.

Williams, G.D. and Stelck, C.R., 1975. Speculations on the Cretaceous paleogeography of North America. In The Cretaceous System of the Western Interior of North American (eds. W.G.E. Caldwell). Geol. Assoc. Canada, Special Paper no.13, p.1-20.

Whitten, E.H.T., 1977. Stochastic models in geology. Journal of Geology, 85, p.321-330.

Yaglom, A.M., 1962. Stationary random functions. Translated from Russian by R.A. Silverman, Prentice-Hall, Inc.

Zwicky, R.W., 1977. Preliminary geostatistical investigation of tar-bearing sands, lease-13 Athabasca tar sands, Canada. Journal of Canadian Petroleum Technology, 16, no.4, p.25-30.

Zwicky, R.W., 1979. Significance of the variogram with some examples from the Athabasca tar sands. Journal of Canadian Petroleum Technology, 18, no. 4, p.41-46.

APPENDIX 1

REGULARIZATION OF SAMPLE SIZE

Data such as the weight percent oil saturation, are measured over samples with a certain size and geometry. It is most common that the geometry and size of different samples are not the same.

Geostatistical techniques require that the volume of all samples be the same. This requirement rises from the fact that the larger the volume is, the smoother the spatial variability of the analysed characteristics becomes. This is also expressed by the fact that the larger the support of the sample is, the less the sill of the variogram becomes, with respect to the *a priori* variance. In most of the cases, the width of the samples (borehole diameter) is constant but the length is not. Accordingly, the available samples must be regularized over constant length. The method used here was that of weighting the sample grades by their respective length (Journel and Huijbregts, 1978, p.203).

For example, if the grade of three successive samples was Z_1, Z_2 and Z_3 and the lengths l_1, l_2 and l_3, the average grade Z over a length $l=l_1+l_2+l_3$ was :

$$Z = l_1Z_1+l_2Z_2+l_3Z_3 \ / \ l$$

Regularization smooths the data but as long as the selected length of regularization is close to the mean length of the samples no bias is introduced.

The percent weight oil samples of this study were regularized as shown above over a length equal to 1 m. This length is approximately the mean length (0.96 m) of the available samples. The relative frequency curve of the lengths of the original data is presented in Figure 1.1.

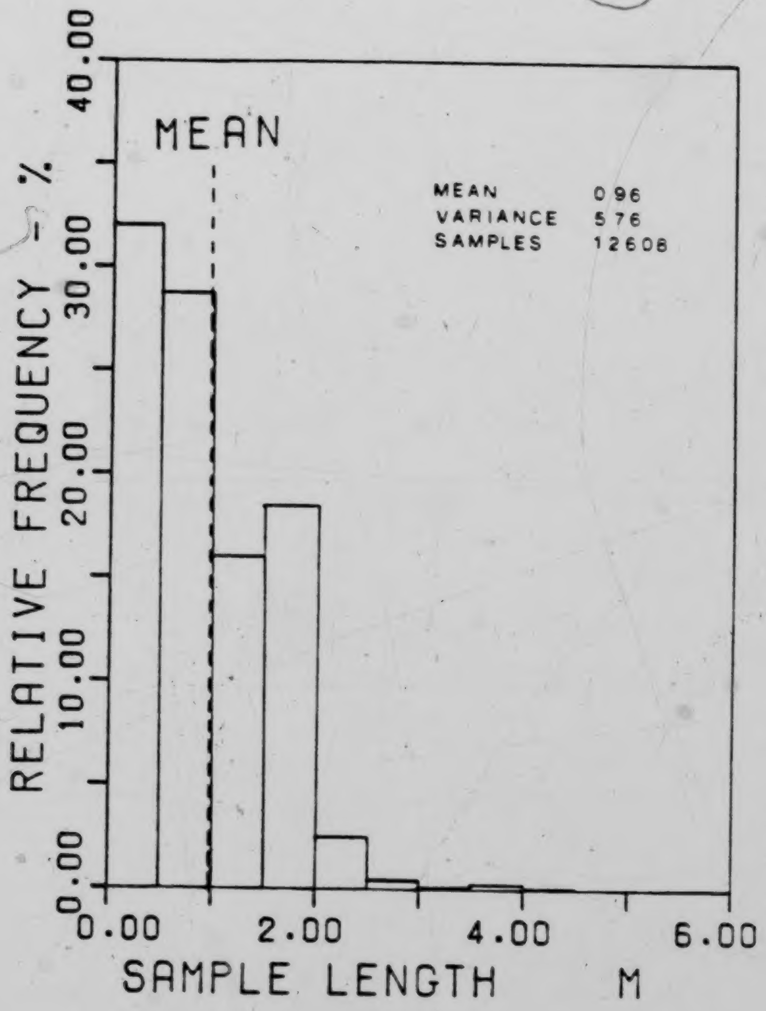

Figure 1 Histogram of the lengths of the original % weight oil samples.

APPENDIX 2

THE OILSAND SYSTEM

OILSAND (OS) is a set of FORTRAN programs developed to an extent, tested and used in this study. The programs are capable of performing all steps required for the geostatistical modelling, display and preliminary evaluation of the *in-situ* reserves.

The OILSAND system (Figure 2.1) consists of 5 main programs (OS.1 to OS.5), 3 display programs (OS.D1 to OS.D3) and 2 utility programs (OS.U1 and OS.U2). These programs are briefly described below.

OS.1 - This program generates grids of interpolated and/or conditionally simulated, rationalized vertically complete surfaces. For interpolation, options for using ordinary punctual kriging or minimum curvature exist.

OS.1a - This program calculates histograms and variograms of the input data to the OILSAND system or the simulated output fields.

OS.2 - This program codes the drill hole samples with respect to the domain to which they belong. It also performs the regularization over constant lengths.

OS.3 - This program performs the three dimensional gridding of the deposit and the coding of the grid points with respect to the domain to which they belong.

OS.4 - This program performs the three-dimensional grade estimation and/or conditional simulation as well as the calculation of the estimation error.

OS.5 - This program intergrates the area, grade and, if required, estimation error within one or more given polygons from one or more estimated or simulated grid sections.

The utility programs of the OILSAND system are described below:

OS.U1 - This utility program selects the interpolated or conditionally simulated top and bottom of a desired domain from the output of OS.1 program.

OS.U2 - This program selects the regularized samples of a desired domain from the output of program OS.2

The display programs of the OILSAND system are listed and briefly described below:

OS.D1 - This program displays histograms and variograms. It uses standard *PLOTLIB subroutines.

OS.D2 - This program displays two-dimensional or three-dimensional contour maps. It uses *PLOTLIB and *DISSPLA subroutines. This program also calculates volumes of selected domains.

OS.D3 - This program displays formation-controlled interpolated or conditionally simulated grid sections (or part of a section) using the output of program OS.4. It uses standard *PLOTLIB subroutines.

The OILSAND system is available at the Mineral Engineering (W. Griffin) and Geology (R. Dimitrakopoulos) Departments of the University of Alberta.

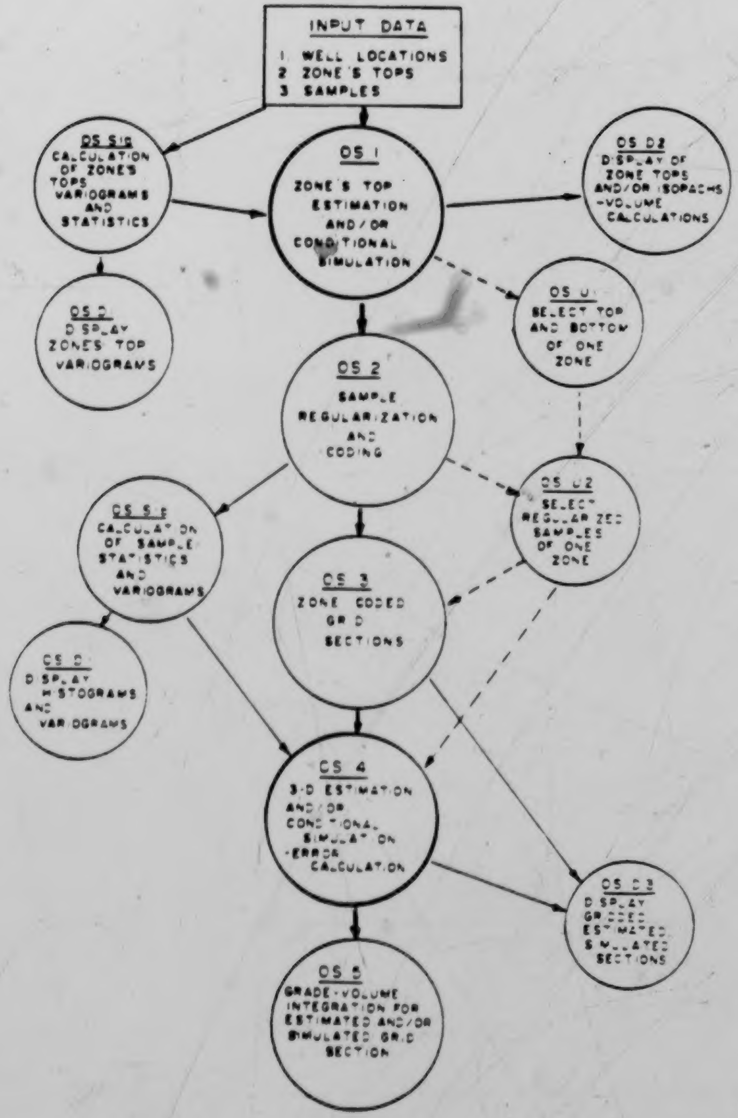
INPUT DATA
1 WELL LOCATIONS
2 ZONE'S TOPS
3 SAMPLES
OS S1a
CALCULATION OF ZONE'S TOPS VARIOGRAMS AND STATISTICS
OS 1
ZONE'S TOP ESTIMATION AND/OR CONDITIONAL SIMULATION
OS D2
DISPLAY OF ZONE TOPS AND/OR ISOPACHS -VOLUME CALCULATIONS
OS D1
DISPLAY ZONES TOP VARIOGRAMS
OS U1
SELECT TOP AND BOTTOM OF ONE ZONE
OS 2
SAMPLE REGULARIZATION AND CODING
OS U2
SELECT REGULARIZED SAMPLES OF ONE ZONE
OS S1b
CALCULATION OF SAMPLE STATISTICS AND VARIOGRAMS
OS 3
ZONE CODED GRID SECTIONS
OS D1
DISPLAY HISTOGRAMS AND VARIOGRAMS
OS 4
3-D ESTIMATION AND/OR CONDITIONAL SIMULATION -ERROR CALCULATION
OS D3
DISPLAY GRIDDED ESTIMATED SIMULATED SECTIONS
OS 5
GRADE-VOLUME INTEGRATION FOR ESTIMATED AND/OR SIMULATED GRID SECTION

Figure 2 Flow-diagram of OILSAND (OS) system.